Alma Mater Studiorum – Università di Bologna

DOTTORATO DI RICERCA IN

Scienze e tecnologie agrarie, ambientali e alimentari

Ciclo XXIX

Settore Concorsuale di afferenza: **07/F1**

Settore Scientifico disciplinare: **AGR/15**

TITOLO TESI

Optimization of Innovative non-thermal Technologies for Fruit and Vegetables Processing

Presentata da: **Nicolò Dellarosa**

Coordinatore Dottorato

Prof. Giovanni Dinelli

Relatore

Prof. Marco Dalla Rosa

Correlatore

Dr. Urszula Tylewicz

Esame finale anno 2017

Abstract

Pulsed electric fields, ultrasound, osmotic dehydration and high pressure homogenization are innovative non-thermal technologies which are attracting a growing interest in the fruit and vegetables sector because they allow processing of foodstuff with minimal drawbacks on their quality. In the present PhD thesis, these technologies were investigated from microstructural and metabolic point of view to provide evidence of the induced changes which could lead to potential benefits or disadvantages for different industrial purposes. Novel methods were developed and tested to assess the impact of the technologies on plant tissue and to provide tools for the optimization of the relevant parameters on industrial scale.

Microstructural modifications produced by ultrasound and pulsed electric fields treatments were studied by observing the subcellular water redistribution which was found to be correlated with mass transfer kinetics. Both reversible and irreversible electroporation upon high electric fields enhanced the water and solute migrations when combined with osmotic dehydration in apple and strawberry tissues. Similarly, the addition of calcium and ascorbic salts to a sucrose osmotic solution led to the alteration of the membranes permeability with the consequent increase of water removal and solutes entrance in the plant tissue.

The metabolic response induced by non-thermal technologies was evaluated in terms of cell viability, metabolic heat production and respiration rate while a metabolomic approach was adopted to finely explore their impact on specific metabolic pathways. High concentrations of ascorbic acid or high voltages applied to apple tissue markedly dropped the cell viability. Moreover, high electric field strengths affected both the anaerobic respiration pathways and the gamma-aminobutyric acid metabolism. High pressure homogenization, applied to a mandarin juice, influenced the microbial degradation pathways as a function of the applied pressure level.

Keywords: Pulsed electric fields; Ultrasound; Osmotic dehydration; High pressure homogenization; Microstructure; Metabolism; Plant tissue; Mass transfer; Nuclear magnetic resonance; Isothermal calorimetry.

Abstract [Italiano]

Tecnologie innovative non-termiche come campi elettrici pulsati, ultrasuoni, disidratazione osmotica e alte pressione di omogeneizzazione stanno attirando un forte interesse nel settore ortofrutticolo perché permettono il trattamento di frutta e verdura con minimi effetti negativi sulla qualità dei prodotti. La tesi di dottorato aveva come scopo lo studio dei cambiamenti microstrutturali e metabolici che possono portare vantaggi o svantaggi per diversi fini industriali. Nuovi metodi d'analisi sono stati sviluppati e testati per la valutazione dell'impatto delle tecnologie su matrici vegetali e per fornire strumenti di misura per l'ottimizzazione ed il controllo di possibili applicazioni industriali.

Le modifiche microstrutturali a seguito di trattamenti con ultrasuoni e campi elettrici pulsati sono state studiate misurando la redistribuzione dell'acqua nei compartimenti cellulari che è risultata correlata con le cinetiche di trasferimento di massa. L'elettroporazione sia reversibile sia irreversibile dovuta all'applicazione di campi elettrici ad alto voltaggio ha permesso di accelerare, in combinazione con trattamenti osmotici, la migrazione di acqua e soluti nei tessuti di fragola e mela. Analogamente, l'aggiunta di sali di calcio e acido ascorbico ad una soluzione di saccarosio ha alterato la permeabilità delle membrane con conseguente aumento della rimozione di acqua e dell'entrata dei soluti nei tessuti.

La risposta metabolica indotta dalle tecnologie non-termiche è stata valutata in termini di vitalità cellulare, produzione di calore metabolico e tasso di respirazione mentre il loro impatto su specifiche vie metaboliche è stato studiato attraverso un approccio metabolomico. Alte concentrazione di acido ascorbico o l'applicazione di alti voltaggi a tessuti di mela hanno diminuito sensibilmente la vitalità cellulare. Inoltre, campi elettrici ad alta intensità hanno influenzato la respirazione anaerobia e il metabolismo dell'acido gamma-amminobutirrico. Alte pressioni di omogeneizzazione, applicate ad un succo di mandarino, hanno modificato vie metaboliche degradative microbiologiche in funzione della pressione raggiunta.

Parole chiave: Campi elettrici pulsati; Ultrasuoni; Disidratazione osmotica; Alte pressione di omogeneizzazione; Microstruttura; Metabolismo; Tessuto vegetale; Trasferimento di massa; Risonanza magnetica nucleare; Calorimetria in isoterma.

Table of Contents

List of Papers

The present PhD thesis is based on the following peer-reviewed papers, which are attached to the manuscript:

I. Trimigno, A., Marincola, F. C., **Dellarosa**, **N.**, Picone, G., & Laghi, L. (2015). Definition of food quality by NMR-based foodomics. *Current Opinion in Food Science*, *4*, 99-104.

II. **Dellarosa**, **N.**, Ragni, L., Laghi, L., Tylewicz, U., Rocculi, P., & Dalla Rosa, M. (2015). Effect of Pulsed Electric Fields on Water Distribution in Apple Tissue as Monitored by NMR Relaxometry. In: *1st World Congress on Electroporation and Pulsed Electric Fields in Biology, Medicine and Food & Environmental Technologies* (pp. 355-358), Springer.

III. Mauro, M. A., **Dellarosa**, **N.**, Tylewicz, U., Tappi, S., Laghi, L., Rocculi, P., & Dalla Rosa, M. (2016). Calcium and ascorbic acid affect cellular structure and water mobility in apple tissue during osmotic dehydration in sucrose solutions. *Food chemistry*, *195*, 19-28.

IV. **Dellarosa**, **N.**, Ragni, L., Laghi, L., Tylewicz, U., Rocculi, P., & Dalla Rosa, M. (2016). Time domain nuclear magnetic resonance to monitor mass transfer mechanisms in apple tissue promoted by osmotic dehydration combined with pulsed electric fields. *Innovative Food Science & Emerging Technologies, 37*(C), 345–351.

V. **Dellarosa**, **N.**, Tappi, S., Ragni, L., Laghi, L., Rocculi, P., & Dalla Rosa, M. (2016). Metabolic response of fresh-cut apples induced by pulsed electric fields. *Innovative Food Science & Emerging Technologies*, *38*, 356-364.

VI. Betoret, E., Mannozzi, C., **Dellarosa**, **N.**, Laghi, L., Rocculi, P., & Dalla Rosa, M. (2017). Metabolomic studies after high pressure homogenization processed low pulp mandarin juice with trehalose addition. Functional and technological properties. *Journal of Food Engineering, 200*, 22-28.

VII. Tappi, S., Mauro, M. A., Tylewicz, U., **Dellarosa**, **N.**, & Dalla Rosa, M., & Rocculi, P. (2017). Effects of calcium lactate and ascorbic acid on osmotic dehydration kinetics and metabolic profile of apples. *Food and Bioproducts Processing, 103,* 1-9.

VIII. **Dellarosa**, **N.**, Frontuto, D., Laghi, L., Dalla Rosa, M., & Lyng, J. G. (2017). The impact of pulsed electric fields and ultrasound on water distribution and loss in mushrooms stalks. *Food chemistry*, In press.

IX. Tylewicz, U., Tappi, S., Mannozzi, C., Romani, S., **Dellarosa**, **N.**, Laghi, L., Ragni, L., Rocculi, P., & Dalla Rosa, M. (2017). Effect of pulsed electric field (PEF) pre-treatment coupled with osmotic dehydration on physico-chemical characteristics of organic strawberries. *Journal of Food Engineering*, Under review.

X. **Dellarosa**, **N.**, Laghi, L., Ragni, L., Dalla Rosa, M., Alecci, M., Florio, T. M., & Galante, A. (2017). Pulsed electric fields processing of apple tissue: spatial distribution of electroporation. *Innovative Food Science & Emerging Technologies*, Under review.

1. Introduction and objectives

Innovative non-thermal technologies are attracting a growing interest in food industries because they enable improving the effectiveness of several manufacturing processes with minimal or no drawbacks on the overall food quality. Historically, non-thermal treatments were initially focused on the replacement of heat-based processes to reduce microbial contaminations and, simultaneously, to preserve the sensorial and nutritional values typical of the raw materials (Raso & Barbosa-Cánovas, 2003). In the recent years, they are gaining importance for other purposes, including for instance the formulation of novel food products or the enhancement of the process yields (Knorr et al., 2011).

In this respect, non-thermal technologies able to affect mass transfer in fruit and vegetables tissues were the main target of the present PhD thesis. Namely osmotic dehydration (OD), pulsed electric fields (PEF), ultrasound (US) and high pressure homogenization (HPH) were considered for different potential industrial purposes. Moreover, specific studies were carried out to evaluate the feasible combination of the innovative technologies to improve the overall effectiveness of the processes.

Despite the different mechanisms of action, the potential industrial applications of novel technologies for fruit and vegetables processing are commonly limited by the lack of knowledge related to the complex microstructural and metabolic changes induced by the new processes. Those modifications require reliable tools for their assessment, therefore, the present PhD thesis introduced also the employment of innovative methodologies developed and tailored to advance the understanding of the process-product relationship.

The present PhD project resulted in the publication of ten peer-reviewed papers which were aimed at studying:

- Microstructural modifications in: apple tissue promoted by osmotic dehydration with binary and tertiary solutions (**Paper III**), pulsed electric fields applied alone (**Papers II**, **X**) or in combination with osmotic dehydration (**Paper IV**); strawberry tissue processed with pulsed electric fields and osmotic treatments (**Paper IX**); mushroom by-products treated with pulsed electric fields and/or ultrasound (**Paper VIII**);
- Metabolic response in: apple tissue upon pulsed electric fields (**Paper V**) or osmotically dehydrated (**Paper VII**); mandarin juice enriched with trehalose which underwent high pressure homogenization treatments (**Paper VI**); moreover, a novel approach for the assessment of metabolite changes in foodstuffs was described in a review (**Paper I**).

These papers can also be clustered, according to the applied food process technology or their combination in:

- Osmotic dehydration (**Papers III**, **IV**, **VII**, **IX**)
- Pulsed electric fields (**Papers II**, **IV**, **V**, **VIII**, **IX**, **X**)
- Ultrasound (**Paper VIII**)
- High pressure homogenization (**Paper VI**)

The following sections of the manuscript are aimed at highlighting the main findings with a special focus on their industrial relevance, including beneficial effects of the novel technologies and potential drawbacks which can limit their industrial applications. Chapter 2 briefly describes the most relevant microstructural and metabolic features of the plant tissues generally influenced by the application of food technologies. Novel methods, tailored to be employed for the evaluation of the biological effects of the applied technologies, are summarized in chapter 3. Finally, chapter 4 is dedicated to the introduction of the main results of the experimental trials published in the papers, sorted by studied technology.

2. Overview of food plant tissue

2.1 Microstructure

Cell microstructure of plant food is often described as a multi-compartmental structure where several organelles serve physical and metabolic functions. Fig. 1 illustrates a simplified model of plant cells. Plasma membrane and tonoplast respectively delimit cytoplasmic and vacuole spaces. Vacuoles are multifunctional organelles which play a strategic role in plant development. For instance, vacuoles store ions, metabolites, pigments and they are lytic compartments with a fundamental role in detoxification and homeostasis processes (Marty, 1999). Food processing operations frequently influence the integrity of vacuoles by altering the tonoplast or their content that indirectly affect their functionality (Hills & Remigereau, 1997; Santagapita et al., 2013).

Vacuole contains the largest amount of water and solutes within a plant cell, reaching up to 90 % of the cell volume while the remaining cell inner space is composed by cytoplasm (Hedrich & Neher, 1987). However, scientific literature reports that the highest amount of metabolic activities occur within the cytoplasmic space (Matile, 2012). Among them, transports of sugars, organic acids, ions across tonoplast and plasma membrane are basic metabolic functions commonly altered by food processing. Cell homeostasis and viability depend on the concentration of solutes which, in turn, is dependent on the proper functionality of the transport mechanisms (Aguilera, Chiralt, & Fito, 2003).

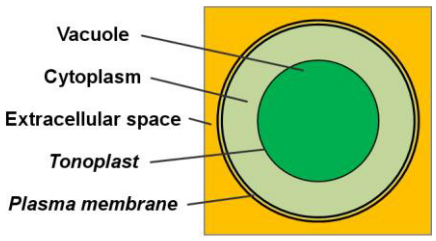

Fig. 1 Simplified model of apple parenchyma cells

Externally to the plasma membrane, three networks, which include cellulose/hemicelluloses, pectin polymers and structural proteins, characterized the cell wall. Chemical modifications of these structural constituents can result in macroscopic changes of the technological features, for instance textural behaviour, of the derived plant products. However, water occupies the largest volume, it plays a role in the interaction between wall components and, consequentially, regulates the cell structure preservation and functionality (Jackman & Stanley, 1995).

In general, modifications in microstructure related to interactions water-water, water-solute, water-macromolecules and solute-macromolecules, influence fruit proprieties and consumer perception (Nieto, Vicente, Hodara, Castro, & Alzamora, 2013). These modifications include changes in water content, mobility, distribution or biopolymer composition and arrangement as a function of different technology treatments.

2.2 Metabolism

Plant tissue metabolism involves many metabolic pathways which in turns are influenced by several endogenous and exogenous factors. Plant food quality mainly depends on endogenous postharvest metabolism and process technologies which can trigger, inhibit or alter metabolic pathways. Generally, conversion of starch and organic acids to sugars, production of volatile compounds, modifications of cell wall are the key changes of the postharvest ripening (MacRae, Quick, Benker, & Stitt, 1992). In the last decades, several non-thermal techniques, such as osmotic or vacuum treatments, were employed to prevent or reduce the ripening and senescence of fruit and vegetables. Modified atmosphere packaging and dipping treatments are becoming more popular in food industries to lower the respiration rate of plant food and delay the senescence effects (Rocculi, Cocci, Romani, Sacchetti, & Dalla Rosa, 2009).

Plant metabolism, including respiration, often requires molecular oxygen for a number of degradative and biosynthetic purposes. However, when plant tissue is subjected to lower concentration of oxygen, anaerobic pathways can be triggered. This typically occurs under certain storage conditions and may affect the entire fruit/vegetable or only a part of the plant. As a consequence of anaerobic conditions, increased concentrations of ethanol, lactate, alanine are usually verified along with the development of off-flavours (Ricard et al., 1994). Along with aerobic and anaerobic respiration metabolism, the development of secondary metabolites in plant tissue is an effect of the plant stress. Mechanical stress, minimal processing, abiotic responses can lead to the accumulation of secondary metabolites with potential bioactive effects on human health (Galindo, Sjöholm, Rasmusson, Widell, & Kaack, 2007).

Manufacturing steps, for instance cutting and peeling in fresh-cut productions, increase the respiration rate and simultaneously promote modifications on the secondary metabolites, generally quickening senescence phenomena with effects on texture, colour and flavour (Cortellino, Gobbi, Bianchi, & Rizzolo, 2015). In this context, novel technologies can drastically affect the postharvest metabolism and potentially trigger stress responses, with positive or negative implications for food quality. Examples are the positive effects on colour preservation obtained by applying atmospheric gas plasma in fresh-cut apples production. Enzymatic

browning of apples was significantly lowered due to the inhibition of the polyphenol oxidase activity upon gas plasma treatment (Tappi et al., 2014). Similarly, this technology enabled preventing blackening of potato by reducing both polyphenol oxidase and peroxidase activities (Bußler, Ehlbeck, & Schlüter, 2017).

Another innovative technology, i.e. pulsed electric fields, have been found to give rise to results strictly dependent on the treated plant product and the applied process parameters. In a case study, the oxidation of apple tissue was induced, leading to browning, textural changes along with a marked mass loss which might compromise the industrial application (Wiktor, Schulz, Voigt, Witrowa-Rajchert, & Knorr, 2015). Moreover, pulsed electric fields have been demonstrated to positively boost the development of several valuable secondary metabolites in juices, enhancing their nutritional features. For instance, tomato and watermelon juices showed a higher amount of antioxidant compounds, such as lycopene, β-carotene and vitamin C when subjected to high intensity pulsed electric fields (Odriozola-Serrano, Soliva-Fortuny, Hernández-Jover, & Martín-Belloso, 2009; Oms-Oliu, Odriozola-Serrano, Soliva-Fortuny, & Martín-Belloso, 2009).

3. Innovative tools for the quality assessment

3.1 Microstructural modifications

Optical or light microscopy has been widely used to study and characterize plant tissues and cell microstructure. The simple and immediate visualization of the tissue allows directly observing its native microstructure or the modifications caused by food processing. In recent years, microscopic evaluation was often improved by the employment of staining solutions aiming at discovering modifications in specific organelles. The use of neutral red highlights intact vacuoles and have been proposed for the microscopic investigation of heat treated tissue (Thebud & Santarius, 1982) or pulsed electric fields (Fincan & Dejmek, 2002). Optical microscopy has been also coupled with fluorescence lamps and dyes in order to visualize cell viability upon technological processes. Indeed, fluorescein diacetate allows estimating alive and dead cells for instance when plant tissue was desiccated or frozen (Halperin & Koster, 2006; Velickova et al., 2013). In **Paper III**, osmotic dehydration of apples was carried out by using sucrose in combination with calcium lactate and ascorbic acid. Both neutral red and fluorescein diacetate dyes were used along with light and fluorescence microscopy to investigate the integrity of tonoplast and plasma membranes when different concentrations of solutes were applied. Furthermore, fluorescence microscopy was similarly applied in **Paper IX**. The cell membrane integrity was studied in strawberries which underwent osmotic dehydration assisted with pulsed electric fields pre-treatment, at different electric field strengths.

Light microscopy provides a fast overview of the integrity of cells and their organelles, however, only qualitative evaluations can be carried out by using the abovementioned methods. Quantitative microstructural information, on the contrary, can be obtained by means of nuclear magnetic resonance relaxometry, also called time domain nuclear magnetic resonance (TD-NMR). The diverse interaction between proton pools located in different cell compartments gives rise to different relaxation times (Van Duynhoven, Voda, Witek, & Van As, 2010). This principle can be exploited to investigate the water distribution within the tissue and its redistribution as a function of the applied technologies. For instance, the technique was successfully employed to evaluate microstructural modifications of kiwifruit during osmotic dehydration (Santagapita et al., 2013) or ultrasound assisted treatments (Nowacka, Tylewicz, Laghi, Dalla Rosa, & Witrowa-Rajchert, 2014). In particular, transverse relaxation time (T_2) and water self-diffusion coefficients (D_w) have been found to be significantly affected by the process parameters resulting in a fast, non-destructive, quantitative monitor of the effect of novel technologies on product quality. This approach was adopted for the study of several food

processing operations described in **Papers II**, **III**, **IV**, **VIII**, **IX**. Water redistribution during osmotic dehydration of apples and strawberries with different solutions was successfully monitored with this technique. A reliable comparison between the effects of ultrasound and pulsed electric field on mushroom microstructure was also achieved. Furthermore, TD-NMR along with the employment of a contrast agent solution (Fig. 2) eased the detection of reversible or irreversible damages of cell membranes upon various pulsed electric fields treatments.

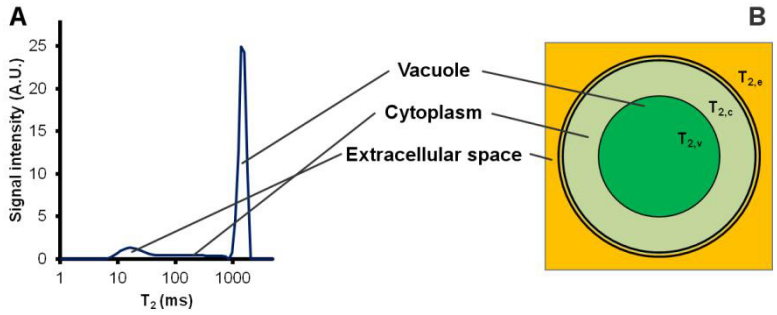

Fig. 2 Water distribution aided with a contrast agent: example of a spectrum (A) and cell model (B)

While TD-NMR enabled evaluating the extent of electroporation (i.e. cell damage caused by high voltage) in its reversible and irreversible form, it was not able to measure its spatial distribution through the plant tissue. However, multiparametric magnetic resonance imaging (MRI) can be used to overcome this drawback (Kranjc, Bajd, Serša, de Boevere, & Miklavčič, 2016). The method abovementioned based on TD-NMR with the addition of the contrast agent was adapted and tailored to MRI analysis to simultaneously measure the extent of electroporation and its spatial distribution through the apple tissue. **Paper X** was dedicated to the optimization of the MRI sequences which resulted in a generation of images based on both longitudinal (T_1) and transverse (T_2) relaxation time, within few minutes. Eventually, this led to the accurate description of the spatially distributed microstructural modifications promoted by pulsed electric fields as well as their kinetics.

3.2 Metabolic response

The application of external energy inputs during fruit and vegetables processing can promote metabolic stress responses which might limit the industrial application of novel technologies. Especially novel forms of energy delivery to plant food, such as atmospheric gas plasma or pulsed electric fields, can trigger unknown and uncommon metabolic pathways. In recent years, isothermal microcalorimetry has been introduced in the food technology field to gain insight into the overall metabolic response of plant tissue. In standardized experimental conditions, microcalorimetric results, often coupled with gas composition analysis, i.e. oxygen consumption and carbon dioxide production, have revealed to be able to reliably evaluate the nonspecific

gross response of plant tissues subjected to various treatments (Wadsö & Galindo, 2009). This technique was applied in **Papers V** and **VII** in which the metabolic heat profiles were studied to respectively optimize pulsed electric fields and osmotic treatments in fresh-cut apple tissue.

Alongside nonspecific methods, the measurement of the concentration changes of the metabolites aims at discovering which pathways are affected by the technological treatments. In this respect, specific experimental trials can be designed to separate and quantify metabolites belonging to known pathways where the metabolic effect of the studied technology is notorious. On the contrary, whether *a priori* selection of metabolites is not applicable, a non-targeted approach becomes unavoidable. Metabolomics can be employed to verify change in tens or hundreds of metabolites simultaneously, therefore without a prior knowledge about the expected metabolic changes (Laghi, Picone, & Capozzi, 2014). The metabolomic approach can be considered downstream to genomics, proteomics and transcriptomics. It aims at exploring the metabolic profiles by identifying and quantifying, in a wide range of concentrations, metabolites belonging to sugars, alcohols, organic acids, fatty acids, amino acids and other secondary metabolites. Advantages and drawbacks of this approach, including the latest applications for the food quality assessment, were explained in the review **Paper I**.

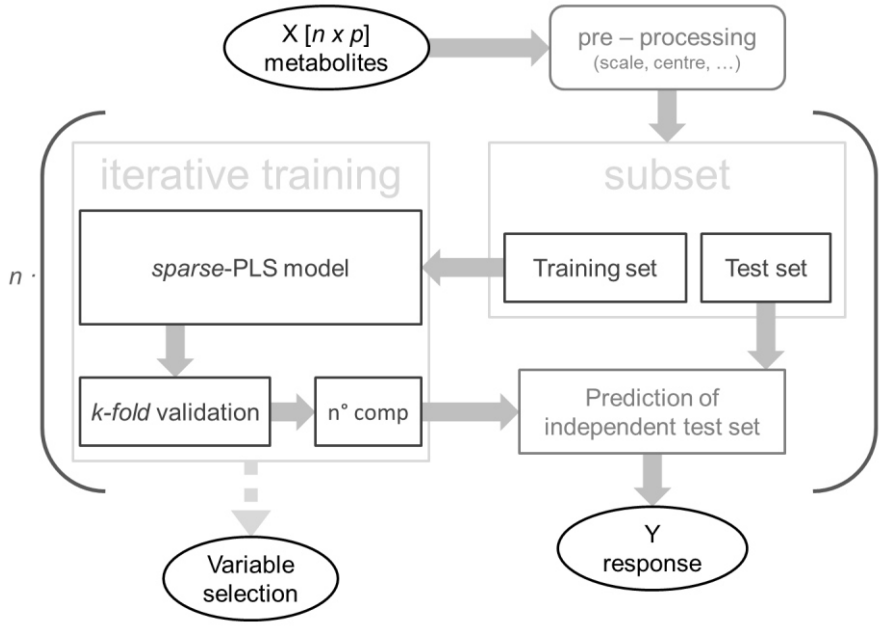

Fig. 3 Metabolomic approach: example of a sPLS based algorithm for data analysis

Metabolomic data are commonly acquired by means of high-throughput techniques, namely high resolution nuclear magnetic resonance, liquid and gas chromatography coupled with mass spectrometry. The generated datasets need reliable and robust statistical tools to be explored. To the purpose, proper statistical methods have been proposed in literature, based on both unsupervised and supervised data analysis. Among them, supervised methods which

simultaneously allow selecting the important metabolites seem to improve the accuracy and robustness of the analysis (Savorani, Rasmussen, Rinnan, & Engelsen, 2013). For instance, analytical tools based on orthogonal projections to latent structures were successfully employed to correlate metabolomic results with pulsed electric fields treatments in potatoes (Galindo et al., 2009). Fig. 3 displays an in-house developed algorithm based on sparse partial least square (sPLS) employed in **Papers V** and **VI**. In the former case, sPLS methodology led to differentiate the effects of pulsed electric fields processing at three electric field strengths in apple tissue. In the latter one, sPLS was used in its regression and discriminant analysis forms to investigate the metabolic changes provoked by the high pressure homogenization step at two pressure levels in mandarin juice processing.

4. Non-thermal technologies

4.1 Osmotic dehydration (OD)

Osmotic dehydration is a partial dewatering of plant tissue which allows reducing the a_w of the products without a phase change. The employment of a hypertonic solution leads to the removal of water and the counter migration of solutes into the plant tissue. The process is commonly applied in industry to obtain minimal processed plant food with intermediate moisture content or as pre-treatment for other processes such as drying or freezing (Dalla Rosa & Giroux, 2001). In fresh-cut production, the use of hypertonic sucrose solutions is often combined with calcium and ascorbic salts to prevent negative changes in terms of texture and colour, respectively (Barrera, Betoret, & Fito, 2004; Silva, Fernandes, & Mauro, 2014). The addition of a mixture of salts at different concentrations to a hypertonic sucrose solution, nevertheless, can result in an alteration of the mass transfer kinetics, i.e. water removal and solute entrance. Microstructure affects mass transport mechanisms, therefore, knowledge about its modifications during treatment is fundamental for the control of the process. Moreover, the composition of the hypertonic solution might have a not negligible effect on the metabolism of the fresh-cut tissue with possible drawbacks in terms of quality and shelf-life. This can restrict the industrial application of certain osmotic solutions. Evidence of the induced changes upon osmotic dehydration with sucrose solutions combined with ascorbic acid and calcium lactate in apple tissue, were provided in **Papers III** and **VII**.

These investigations highlighted the enhancement of mass transfer when sucrose solution was combined with ascorbic acid and calcium lactate. Both increased the water removal and the solid gain, however, as expected the simultaneous employment of the three solutes led to the highest influence on mass transfer kinetics. The lowest a_w of the tertiary solution played the major role on this finding, however, microstructural modifications were also suspected and therefore investigated. Calcium lactate and ascorbic acid, separately added to the sucrose solution, similarly improved the water migration rate. Nevertheless, it is worth observing that calcium lactate alone showed a lower entrance of solutes from the external solution toward the inner compartments of the tissue in comparison with ascorbic acid.

The interaction of calcium salts with the cell wall biopolymers promoted the release of water from the fixed structures, as monitored through TD-NMR, due to the influence of calcium on pectic acid polymers. Observations obtained by means of the same technique, showed a good agreement with mass transfer kinetics. Water redistribution through the compartments was a function of the applied external solution where sucrose alone was the less influent on water

migration from vacuole toward cytoplasm and extracellular spaces. Conversely, both calcium lactate and ascorbic acid boosted water redistribution, moreover, a synergistic effect of their combination was noticed throughout the dehydration process. The vacuole shrinkage led to the total redistribution of water 4 h from the beginning of the treatment confirming that the mass transfer kinetics observed macroscopically were a function of the microstructural modifications of the tissue. The water redistribution, however, did not alter the tonoplast and the vacuole integrity at every treatment conditions. Direct observation of cell microstructure was carried out using light microscopy combined with neutral red staining. This staining strategy confirmed that osmotic dehydration with binary and tertiary solutions induced changes among cell wall, vacuole, cytoplasm and extracellular spaces without the irreversible loss of compartmentalization.

Despite the positive effects on texture, colour and mass transfer, the mixture of ascorbic acid and calcium lactate was expected to play a role on the cell metabolism. Indeed, concentrations of ascorbic acid higher than 1 %, in sucrose solutions with concentrations ranging from 20 to 40 %, markedly reduced the cell viability as monitored through fluorescence microscopy. A further confirmation was gained using isothermal calorimetry which allowed measuring the endogenous metabolic heat upon osmotic dehydration processes with various treatment solutions. This technique, combined with O_2 and CO_2 gas analysis, highlighted a noteworthy heat production and O_2 consumption as a consequence of the stress metabolic reactions. In this respect, the low pH and a_w seemed to cause severe injuries in the cellular structure, although the mechanisms are still not clear. Conversely, the combination of sucrose solutions with calcium lactate contributed to extent cell viability along with the beneficial effect on the dehydration efficiency abovementioned. The reduction of metabolic activity together with the preservation of cell viability was attributed to several potential interactions of calcium with cell membranes and walls. Interestingly, those effects generally lead to positively slow down the ripening and senescence of fruit with a great potential benefit for the fresh-cut productions.

4.2 Pulsed electric fields (PEF)

The alteration of cell membrane permeability can also be promoted by the application of high electric fields strength to plant tissue. The breakage of membranes, known as electroporation, has been studied for both microbial inactivation and mass transfer enhancement. In the latter case, the increase of the extraction yields, including the release of specific intracellular compounds, or the improvement of combined dehydration processes have been achieved and described in the literature (Barba et al., 2015). Since the effects of PEF are strictly related to the

applied process parameters, namely pulse shape, number, duration, frequency and electric field strength, their accurate control is fundamental for the industrial implementation. Electroporation generally involves the polarization of membranes, the creation of pores and their expansion. In addition, whenever the applied PEF protocols did not exceed a certain critical energetic threshold, pores might reseal (Vorobiev & Lebovka, 2008). The process can lead to reversible or irreversible consequences on cell viability as a function of the applied PEF treatments (Fig. 4). Industrially, irreversible electroporation can be exploited to ease the extraction processes.

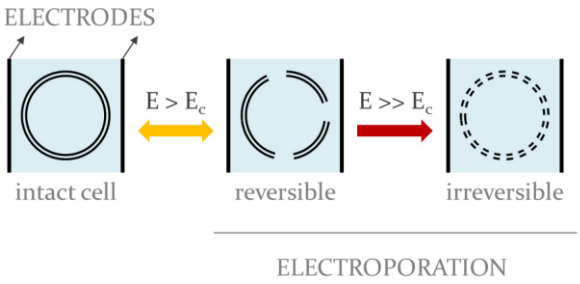

Fig. 4 Reversible and irreversible electroporation

Papers II, **X** and **V** were focused on the basic mechanisms of PEF processing of apple tissue. In order to obtain comparable results, similar PEF treatments were employed in all the investigations, with electric field strength ranging from 100 to 400 V/cm, 20 and 60 near-rectangular shape pulses, pulse width fixed at 10 µs and 10 ms of repetition time giving rise to a frequency of 100 Hz. The first investigation included the development of an innovative method to detect and quantify both reversible and irreversible modifications of the cell microstructure. The second investigated the spatial distribution of electroporation through the tissue by observing spatially distributed changes of cell microstructure. In the third study, the metabolic response caused by the exposition of apple tissue at high electric fields was evaluated.

In those studies, the threshold of irreversible electroporation was estimated around 150 V/cm. As shown in Fig. 5, the application of electric field strength higher than that value caused visible changes in the apple tissue. Those changes directly reflected the loss of compartmentalization highlighted through TD-NMR with the contrast agent. When irreversible electroporation occurred, the damage of tonoplast and plasma membranes eased the release of intracellular content, including enzymes, triggering degradation reactions. The observations were carried out through the analysis of the transverse relaxation time which was performed for several hours after the end of the treatments. It worth noticing that, even though the application of high voltage pulses lasted less than a second, the effects on tissue microstructure were seen during

2 h after the treatments. While treatments above the threshold of irreversibility completely redistributed water resulting a broad TD-NMR peak uniformly distributed through the compartments, a totally different behaviour was noticed for reversible treatments. A partial redistribution from vacuole toward cytoplasm and extracellular space was registered, however, the compartments were still distinguishable and their water content was measurable. In both cases, electric field strength and total number of delivered pulses had a significant effect on water distribution. Those results were correlated to macroscopic mass transfer phenomena, described in **Papers IV** and **IX**. In these papers, centred on the combined application of PEF with osmotic dehydration in apple and strawberry samples, the efficiency of water removal and solid gain was correlated to the water repartition through the compartments. Apart from the effects of PEF on the tissues, **Paper IV** introduced also the non-destructive measurement of water self-diffusion coefficient which resulted in an accurate screening method able to describe the dehydration process within minutes. It was, therefore, confirmed that tools capable to effectively monitor microstructural changes of plant tissues provide also useful information for possible industrial applications.

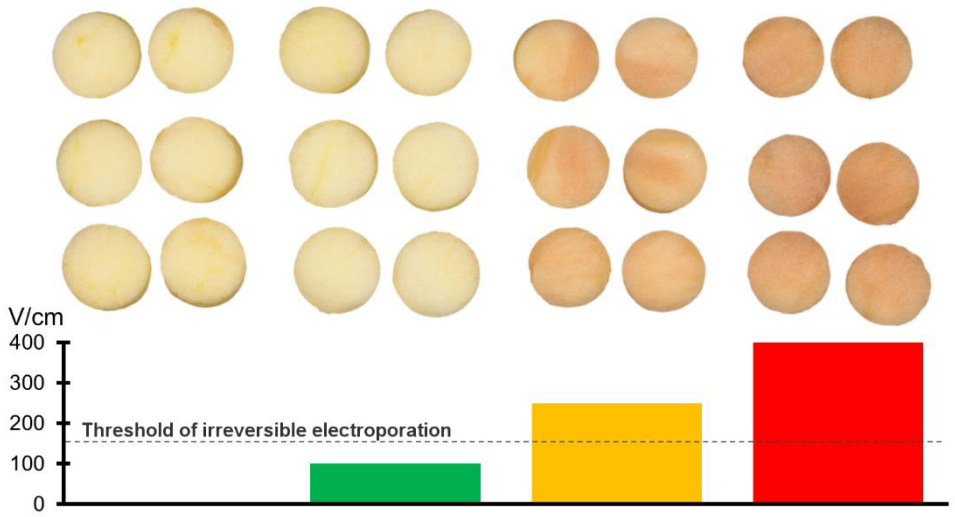

Fig. 5 Visual appearance of PEF treated apples at different electric field strength (60 pulses, 10 µs pulse width and 100 Hz), 60 minutes after treatments

The high sensitivity of magnetic resonance to water state was further exploited to verify whether the electroporation occurred homogeneously or not through the apple tissue, by means of magnetic resonance imaging. A different extent of electroporation in various areas of the tissue was found by analysing the decrease of the transverse relaxation time, as a consequence of the loss of compartmentalization. Due to the standardized conditions of the

experiments, the observed inhomogeneity was mainly attributed to the different local conductivity of the raw material. This led to local differences in the effective electric field strength and resulted in an inhomogeneous damage of the cell membranes through the tissue. Moreover, the use of another MRI sequence allowed a direct evaluation of the kinetics of shrinkage of the inner compartments during 1 h after the treatment. The percolation of the intracellular solutions was directly observed by combining a sequence based on longitudinal relaxation time with the use of a contrast agent.

The abovementioned modifications of microstructure were hypothesised to concurrently affect the metabolic behaviour of cells. In the experiments, isothermal calorimetry combined with gas analysis described a marked drop of metabolic heat production and O_2 consumption together with a lower CO_2 production, as a probable consequence of the loss of cell viability upon irreversible electroporation. Conversely, only a slight increase of heat production was noticed in the case of reversible treatments. Those trends were further confirmed by a metabolomic study which involved the use of a novel tailored statistical method for data analysis. Indeed, alterations of anaerobic respiration pathways and γ-aminobutyric acid metabolism were observed. However, the low impact of reversible electroporation on plant tissue metabolism and, as previously described, on tissue microstructure promoted the use of pulsed electric fields in reversible conditions for industrial applications where the overall food quality is fundamental.

Taking advantage of the specific membrane breakage induced by pulsed electric fields technology, innovative extraction processes can be designed to recovery valuable compounds from plant tissue. In particular, the effective recovery of valuable molecules from food waste streams can lead to improve the efficiency of food productions. In this respect, **Paper VIII** considered the impact of novel technologies, such as pulsed electric fields and ultrasound, on the microstructure of mushrooms stalks in order to optimize the cell disruption to ease the extraction. The main findings, including the comparison of pulsed electric fields with ultrasound, are described in the next section.

4.3 Ultrasound (US)

Ultrasound technology has been introduced in food industry because it can bring advantages in terms of yield increasing, selectivity of the extraction, processing time and cost reduction when compared to conventional extraction techniques. The application of high intensity ultrasound, usually ranging between 100 and 400 W, at 20-100 kHz, resulted in high recoveries of valuable compounds from various foodstuffs, leading to improve the efficiency of both

extraction and purification. The mechanism of action involved includes the generation of gas bubbles which collapse producing high energy shock waves and intense shear forces, which is known as cavitation effect (Chemat & Khan, 2011). This effect physically affects the structure of the treated tissue, generally increasing the mass transfer phenomena.

Paper VIII took into account microstructural changes of a quantitatively important by-product of the mushroom industry, i.e. the stalks, subjected to PEF, US and their combination, applied at both low and high temperatures. Being rich of various potential valuable compounds, the effect of these technologies applied to mushroom stalks was studied to provide evidence of the basic mechanisms of mass transfer enhancement. Combined analytical tools, generally based on the water state, were chosen to describe mass transport phenomena. Namely, changes of the electrical impedance, known as disintegration index, water distribution and water loss along with the qualitative UV/Vis analysis of the extracts were simultaneously evaluated. Results showed a good agreement among the methods which highlighted a different specific and selective target of the studied technologies. Pulsed electric fields led to the highest extent of cell disruption with a high efficiency in extracting intracellular water and scores comparable to high temperature treatments. Being non-thermal and less expensive in terms of energy input, this result encourages the use of PEF for the extraction of valuable thermolabile compounds. Interestingly, despite the higher energy input of ultrasound applications, a lower extent of cell disruption was noticed comparing US with PEF treatments. Moreover, no synergistic (neither additive) effects were observed due to the combination of PEF with US at both low and high temperatures. Ultrasound, on the other hand, might improve the extraction and purification of compounds located in the fixed structures of the cell wall such as polysaccharides.

4.4 High pressure homogenization (HPH)

High pressure homogenization is a non-thermal food process, mainly adopted to inactivate microorganisms and enzymes in liquid food with a low negative impact, or even a positive effect, on the nutritional and sensorial properties of the products. Different pressure levels, commonly spanning from few MPa to around 500 MPa, are applied in continuous to fluid products (Betoret, Betoret, Rocculi, & Dalla Rosa, 2015). When applied to freshly squeezed juices, the employment of this novel process is expected to improve the preservation and the availability of bioactive compounds, especially when compared to harsh heat treatments.

In **Paper VI** the impact of high pressure homogenization at 20 and 100 MPa was studied in mandarin juice enriched with trehalose, which is known to improve several technological proprieties. Alongside the expected changes, the juice was evaluated from a nutritional point of

view. A targeted analysis of the main microelements, namely flavonoids, and the overall antioxidant (antiradical) activity was performed. In parallel, a metabolomic based non-targeted approach was adopted to discovery possible simultaneous side effects of high pressures on tens of juice metabolites. As expected, high pressures treatments reduced the suspended pulp and maintain, together with the trehalose addition, the cloudiness of the juice. The physical changes of the juice led to a protective effect on hesperidin, the most abundant flavonoid of mandarin juice, during a 10-days refrigerated storage. The highest level of pressure seemed to negatively affect the initial content of the flavonoid. On the other hand, antioxidant capacity was particularly enhanced only when the juice samples were treated at 20 MPa. Moreover, metabolomics resulted in the detection of four important metabolites, among the 89 analysed signals, which were significantly affected by both high pressure homogenization treatments and storage time. Those compounds reflected possible solubilisation effects and residual microbial activities which were jointly modulated by the initial application of high pressure treatments.

5. Conclusions

The present PhD thesis provided evidence of microstructural and metabolic responses induced by the application of non-thermal technologies. The innovative analytical approaches proposed were developed to boost the adoption and optimization of novel potential industrial applications. The method based on time domain nuclear magnetic resonance with the contrast agent allowed the simultaneous measurement of the reversible and irreversible extent of electroporation. Water redistribution through the tissue compartments was found to be a function of the electric field strength and the total energy of the pulsed electric fields treatment. The loss of compartmentalization, observed when irreversible electroporation occurred, was exploited to develop a magnetic resonance imaging tool which was able to describe the spatial distribution of electroporation through the tissue. Results showed a marked inhomogeneity of the pulsed electric fields treatments and the migration of the intracellular content toward the external solution which led to the shrinkage of the apple tissue.

The application of pulsed electric fields in combination with osmotic dehydration eased the water removal from apple tissue and increased the solute concentration. The improvement of mass transfer phenomena confirmed that the alteration of the membrane permeability led to an enhancement of the overall efficiency of the process. The effect of pulsed electric fields was also compared to ultrasound treatments in mushroom stalks. Results highlighted the higher efficiency of high voltages in terms of both cell disintegration ability and quantitative extraction of the intracellular content. Similarly, the chemical alteration of plasma membranes, which was promoted by the simultaneous employment of sucrose, calcium and ascorbic salts, improved the dehydration performances.

Both pulsed electric fields pre-treatment and osmotic dehydration with binary and tertiary solutions affected the metabolic response of the treated tissue. Cell viability markedly dropped when either irreversible electroporation took place or high concentrations of ascorbic acid were experimented. The metabolomic approach, which was aimed at exploring the fine metabolic response as a function of pulsed electric fields and high pressure homogenization treatments, led to the identification of metabolic pathways triggered by these non-thermal processes. The observation of the concentrations changes of the metabolites in a mandarin juice highlighted the main impact of high pressure homogenization on microbial activities. Pulsed electric fields applied to apple tissue, conversely, seemed to influence the metabolic activities of plant cells lowering the anaerobic respiration pathways and activating the γ-aminobutyric acid metabolism.

6. References

Aguilera, J. M., Chiralt, A., & Fito, P. (2003). Food dehydration and product structure. *Trends in Food Science & Technology, 14*(10), 432-437.

Barba, F. J., Parniakov, O., Pereira, S. A., Wiktor, A., Grimi, N., Boussetta, N., Witrowa-Rajchert, D. (2015). Current applications and new opportunities for the use of pulsed electric fields in food science and industry. *Food Research International, 77*, 773-798.

Barrera, C., Betoret, N., & Fito, P. (2004). Ca^{2+} and Fe^{2+} influence on the osmotic dehydration kinetics of apple slices (var. Granny Smith). *Journal of Food Engineering, 65*(1), 9-14.

Betoret, E., Betoret, N., Rocculi, P., & Dalla Rosa, M. (2015). Strategies to improve food functionality: Structure–property relationships on high pressures homogenization, vacuum impregnation and drying technologies. *Trends in Food Science & Technology, 46*(1), 1-12.

Bußler, S., Ehlbeck, J., & Schlüter, O. K. (2017). Pre-drying treatment of plant related tissues using plasma processed air: Impact on enzyme activity and quality attributes of cut apple and potato. *Innovative Food Science & Emerging Technologies, 40*, 78-86.

Chemat, F., & Khan, M. K. (2011). Applications of ultrasound in food technology: processing, preservation and extraction. *Ultrasonics Sonochemistry, 18*(4), 813-835.

Cortellino, G., Gobbi, S., Bianchi, G., & Rizzolo, A. (2015). Modified atmosphere packaging for shelf life extension of fresh-cut apples. *Trends in Food Science & Technology, 46*(2), 320-330.

Dalla Rosa, M., & Giroux, F. (2001). Osmotic treatments (OT) and problems related to the solution management. *Journal of Food Engineering, 49*(2), 223-236.

Fincan, M., & Dejmek, P. (2002). In situ visualization of the effect of a pulsed electric field on plant tissue. *Journal of Food Engineering, 55*(3), 223-230.

Galindo, F. G., Dejmek, P., Lundgren, K., Rasmusson, A. G., Vicente, A., & Moritz, T. (2009). Metabolomic evaluation of pulsed electric field-induced stress on potato tissue. *Planta, 230*(3), 469-479.

Galindo, F. G., Sjöholm, I., Rasmusson, A. G., Widell, S., & Kaack, K. (2007). Plant stress physiology: opportunities and challenges for the food industry. *Critical reviews in food science and nutrition, 47*(8), 749-763.

Halperin, S. J., & Koster, K. L. (2006). Sugar effects on membrane damage during desiccation of pea embryo protoplasts. *Journal of experimental botany, 57*(10), 2303-2311.

Hedrich, R., & Neher, E. (1987). Cytoplasmic calcium regulates voltage-dependent ion channels in plant vacuoles. *Nature, 329*, 833-836.

Hills, B. P., & Remigereau, B. (1997). NMR studies of changes in subcellular water compartmentation in parenchyma apple tissue during drying and freezing. *International Journal of Food Science and Technology, 32*(1), 51-61.

Jackman, R. L., & Stanley, D. W. (1995). Perspectives in the textural evaluation of plant foods. *Trends in Food Science & Technology, 6*(6), 187-194.

Knorr, D., Froehling, A., Jaeger, H., Reineke, K., Schlueter, O., & Schoessler, K. (2011). Emerging technologies in food processing. *Annual review of food science and technology, 2*, 203-235.

Kranjc, M., Bajd, F., Serša, I., de Boevere, M., & Miklavčič, D. (2016). Electric field distribution in relation to cell membrane electroporation in potato tuber tissue studied by magnetic resonance techniques. *Innovative Food Science & Emerging Technologies, 37*, 384-390.

Laghi, L., Picone, G., & Capozzi, F. (2014). Nuclear magnetic resonance for foodomics beyond food analysis. *TrAC Trends in Analytical Chemistry, 59*, 93-102.

MacRae, E., Quick, W. P., Benker, C., & Stitt, M. (1992). Carbohydrate metabolism during postharvest ripening in kiwifruit. *Planta, 188*(3), 314-323.

Marty, F. (1999). Plant vacuoles. *The Plant Cell, 11*(4), 587-599.

Matile, P. (2012). *The lytic compartment of plant cells* (Vol. 1): Springer Science & Business Media.

Nieto, A. B., Vicente, S., Hodara, K., Castro, M. A., & Alzamora, S. M. (2013). Osmotic dehydration of apple: Influence of sugar and water activity on tissue structure, rheological properties and water mobility. *Journal of Food Engineering, 119*(1), 104-114.

Nowacka, M., Tylewicz, U., Laghi, L., Dalla Rosa, M., & Witrowa-Rajchert, D. (2014). Effect of ultrasound treatment on the water state in kiwifruit during osmotic dehydration. *Food Chemistry, 144*, 18-25.

Odriozola-Serrano, I., Soliva-Fortuny, R., Hernández-Jover, T., & Martín-Belloso, O. (2009). Carotenoid and phenolic profile of tomato juices processed by high intensity pulsed electric fields compared with conventional thermal treatments. *Food Chemistry, 112*(1), 258-266.

Oms-Oliu, G., Odriozola-Serrano, I., Soliva-Fortuny, R., & Martín-Belloso, O. (2009). Effects of high-intensity pulsed electric field processing conditions on lycopene, vitamin C and antioxidant capacity of watermelon juice. *Food Chemistry, 115*(4), 1312-1319.

Raso, J., & Barbosa-Cánovas, G. V. (2003). Nonthermal preservation of foods using combined processing techniques. *Critical Reviews in Food Science and Nutrition, 43*(3), 265-285.

Ricard, B., Couee, I., Raymond, P., Saglio, P. H., Saint-Ges, V., & Pradet, A. (1994). Plant metabolism under hypoxia and anoxia. *Plant Physiology and Biochemistry, 32*, 1-1.

Rocculi, P., Cocci, E., Romani, S., Sacchetti, G., & Dalla Rosa, M. (2009). Effect of 1-MCP treatment and N_2O MAP on physiological and quality changes of fresh-cut pineapple. *Postharvest Biology and Technology, 51*(3), 371-377.

Santagapita, P., Laghi, L., Panarese, V., Tylewicz, U., Rocculi, P., & Dalla Rosa, M. (2013). Modification of transverse NMR relaxation times and water diffusion coefficients of kiwifruit pericarp tissue subjected to osmotic dehydration. *Food and Bioprocess Technology, 6*(6), 1434-1443.

Savorani, F., Rasmussen, M. A., Rinnan, Å., & Engelsen, S. B. (2013). Interval based chemometric methods in NMR-foodomics *Chemometrics in Food Chemistry* (pp. 449-486): Elsevier Science.

Silva, K. S., Fernandes, M. A., & Mauro, M. A. (2014). Effect of calcium on the osmotic dehydration kinetics and quality of pineapple. *Journal of Food Engineering, 134*, 37-44.

Tappi, S., Berardinelli, A., Ragni, L., Dalla Rosa, M., Guarnieri, A., & Rocculi, P. (2014). Atmospheric gas plasma treatment of fresh-cut apples. *Innovative Food Science & Emerging Technologies, 21*, 114-122.

Thebud, R., & Santarius, K. A. (1982). Effects of high-temperature stress on various biomembranes of leaf cells in situ and in vitro. *Plant physiology, 70*(1), 200-205.

Van Duynhoven, J., Voda, A., Witek, M., & Van As, H. (2010). Time-domain NMR applied to food products. *Annual reports on NMR spectroscopy, 69*, 145-197.

Velickova, E., Tylewicz, U., Dalla Rosa, M., Winkelhausen, E., Kuzmanova, S., & Galindo, F. G. (2013). Effect of vacuum infused cryoprotectants on the freezing tolerance of strawberry tissues. *LWT-Food Science and Technology, 52*(2), 146-150.

Vorobiev, E., & Lebovka, N. (2008). Pulsed-electric-fields-induced effects in plant tissues: fundamental aspects and perspectives of applications *Electrotechnologies for extraction from food plants and biomaterials* (pp. 39-81): Springer.

Wadsö, L., & Galindo, F. G. (2009). Isothermal calorimetry for biological applications in food science and technology. *Food Control, 20*(10), 956-961.

Wiktor, A., Schulz, M., Voigt, E., Witrowa-Rajchert, D., & Knorr, D. (2015). The effect of pulsed electric field treatment on immersion freezing, thawing and selected properties of apple tissue. *Journal of Food Engineering, 146*, 8-16.

PAPERS

Paper I

Trimigno, A., Marincola, F. C., **Dellarosa**, **N.**, Picone, G., & Laghi, L. (2015)

Definition of food quality by NMR-based foodomics

Current Opinion in Food Science, *4*, 99-104

Available online at www.sciencedirect.com

ScienceDirect

Current Opinion in Food Science

Definition of food quality by NMR-based foodomics

Alessia Trimigno[1], Flaminia Cesare Marincola[2], Nicolò Dellarosa[1], Gianfranco Picone[1] and Luca Laghi[1]

Quality definition of food includes several complex factors like physical, compositional and microbial features, modifications induced by technological processes or storage, nutritional value and safety. Foodomics is a holistic approach applying omics technologies to observe food along the entire production/consumption chain. In the present review, we present key applications of nuclear magnetic resonance in foodomics described in the 2012–2015 period, in the quest for robust and thorough information required by the scientific community. In doing so, we summarize the issues connected to food traceability and authenticity, composition and physical characteristics, processing and storage and health, that mostly impact food quality.

Addresses
[1] Department of Agricultural and Food Sciences, University of Bologna, Piazza Goidanich 60, 47521 Cesena, Forl`Cesena, Italy
[2] Department of Chemical and Geological Sciences, University of Cagliari, Cittadella Universitaria, SS 554, km 4.5, Monserrato, 09042 Cagliari, Italy

Corresponding author: Laghi, Luca (l.laghi@unibo.it)

Current Opinion in Food Science 2015, **4**:99–104

This review comes from a themed issue on **Foodomics technologies**

Edited by **Alejandro Cifuentes**

http://dx.doi.org/10.1016/j.cofs.2015.06.008

2214-7993/© 2015 Elsevier Ltd. All rights reserved.

Introduction

Soon after the advent of genomics, transcriptomics, proteomics and metabolomics, aimed to a holistic understanding of the complex human biology and physiology, it has been natural to apply the same approaches to food. The information collected in this way at each step of the production/consumption chain has been enclosed into the single definition of foodomics, which now is defined as 'the discipline that studies the food and nutrition domains through the application and integration of advanced omics technologies to improve consumer's well-being, health, and confidence' [1]. Among the techniques used for this discipline, Nuclear Magnetic Resonance (NMR) has given a great boost to the new approach, thanks, in particular, to the high reproducibility of its observations [2•].

Goodacre [3], in a recent divertissement, has noted that the growth of the metabolomics literature reminded that of microorganisms. The lag phase is represented by a handful of papers, listed by Goodacre [3], which created the conceptual framework. A key element of the initial phase can be identified also in the development of software and algorithms (i.e. Projection on Latent Structures [4]) specifically tailored to highlight the useful features in the overwhelming information represented by large experimental datasets. The phase of rapid growth can be felt in the works focusing on the most diverse biofluids, foods and raw materials, aiming at verifying the applicability of the metabolomics approach. A common trait of these papers is some degree of failure in making each step of the investigation (i.e. experimental design, data generated and analytical tools) totally transparent. The stationary, desirable, phase is represented by works where experimental design, data generated and the means of analysis are made publicly available, and the level of metabolite identification is properly assigned [5], as well as the level of confidence of each key statement. Papers actively contribute to a generalized increase of quality, when they fulfill such requirements better than any other of their own field, by forcing the scientific community to adapt.

In the present review, we mainly focus on the literature of the 2012–2015 period and present key applications of NMR in foodomics, in the quest for robust and thorough information required by the scientific community. In doing that, we will run through the steps of the food production chain, from the origin of the raw material to the transformation that food undergoes during storage, that mostly affect food quality, as summarized in Figure 1.

Traceability, authenticity and safety of food

A relevant percentage of the commercial value of several foods and beverages relies on the ensemble of climate, land, cultural practices and history of the raw material, collectively enclosed in the term 'terroir'. NMR has been used from the eighties with the purpose of geographic characterization, by studying the distribution of stable isotopes of the bio-molecules [6]. A natural consequence of the advent of the 'omic' analytical techniques has been to consider the entire metabolome in the perspective of terroir characterization. This is generally observed in a non-targeted fashion [7], that is without focusing on specific molecules but letting features of the NMR spectra emerge from the entire spectrum profile, through the appropriate mathematical treatments. Examples of this

Figure 1

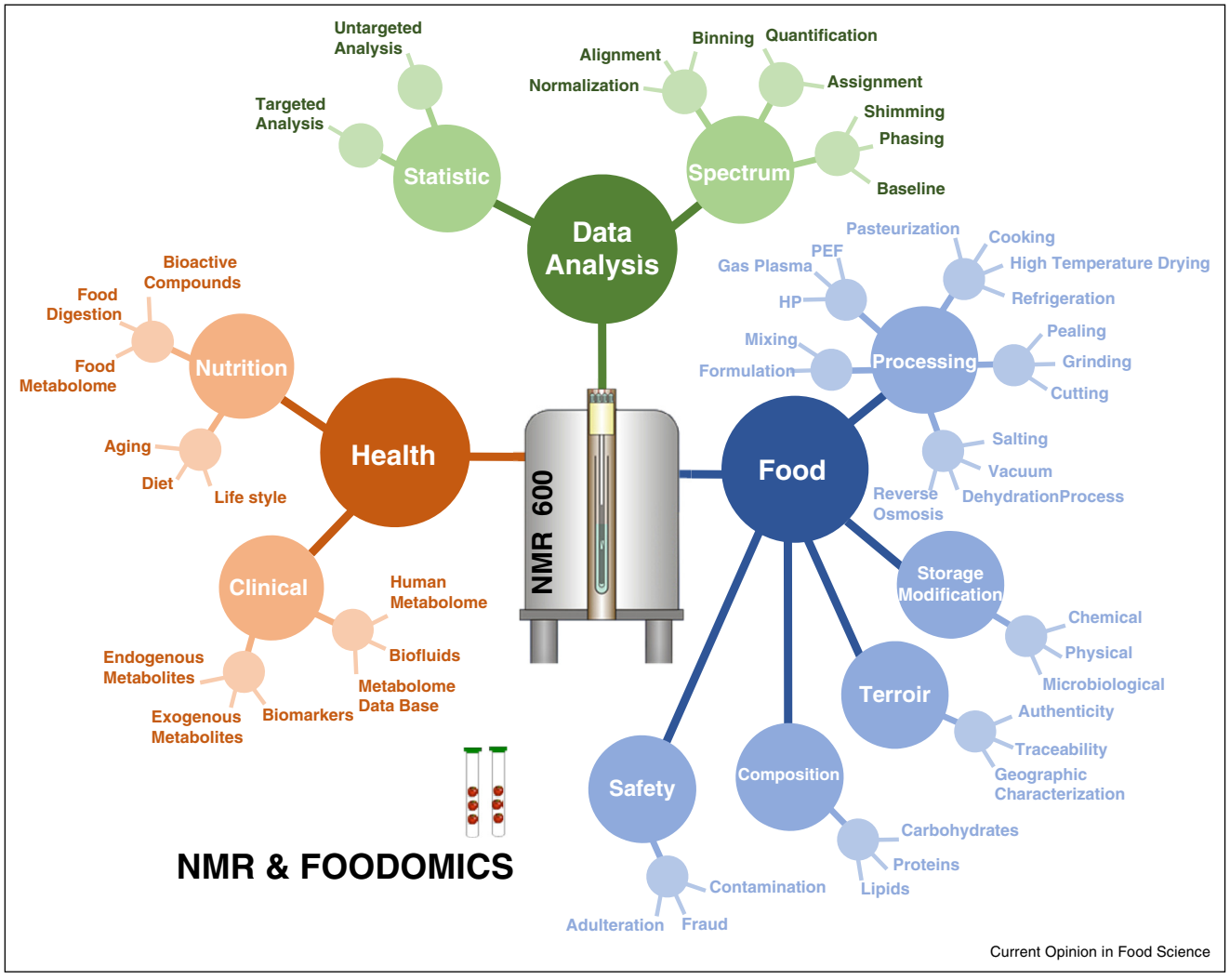

Infografic of the information that can be obtained along the food production/consumption chain by NMR, through a foodomic approach. For the spectra, processing steps see Ref. [2].

approach are the work by Gallo *et al.* [8] on table grape, and the work by Hohman *et al.* [9] about tomato.

Unfortunately, each aspect of a food terroir potentially affects the metabolome, so that general applicability represents the weak point of any mathematical model trying to relate features of an NMR spectrum with a single aspect of the origin of a food. This is probably why no method based on non-targeted fingerprinting has been accepted for food official controls [7]. The recently published work that can be considered a to-date benchmark in this respect is the one by Godelmann *et al.* [10••] testing wine screening method WineScreener™. The analysis of 600 German wine samples, produced during 2 years in 5 areas from 10 grape varieties, led to the maximum correct prediction of geographical origin, year of vintage and grape variety (89%, 97% and 95% respectively).

It has been suggested that the studies on food safety, similarly to those on terroir, would bring information to a higher level if including an omic-untargeted approach, because many features that raise concerns about the healthiness of food, as genetic modification [11] or micro-organisms development [12,13], are likely to influence large portions of food or raw material molecular profile [14].

The main challenge for scientists facing non-targeted analysis is to correctly define appropriate biomarkers from raw NMR spectra containing hundreds of metabolites. The rationale of this practice is that the inclusion of a

feature of a spectrum unrelated to a characteristic of interest leads to lower correct prediction rates or less parsimonious models. Consequentially, an increasing number of papers has been expressly focused on metabolites selection as the key part of mathematical data modeling [15•,16]. As a general trend, in the last decade data treatment has taken advantages of computer-aided multivariate analysis tools that allow the simultaneous model building and variable selection by associating to each metabolite a proper weight in the model. Examples are interval partial least square (*i*PLS), interval extended canonical variable analysis (*i*ECVA) [17] and sparse PLS [18]. Those models have largely replaced statistical methods based on Normal distributions, for example *t*-test or ANOVA, because less prone to false discoveries, that is, false positives or negatives, which typically affect univariate analysis [19]. Even though computer-aided methods have considerably improved the data analysis performance, their incorrect use, typically the lack of a proper validation step, can lead to false correlation between metabolites and the characteristic of interest.

There is consensus that a key step toward reliable non-targeted fingerprinting methods is the exchange and comparison of data between the stakeholders involved in foodomics observations, through databases dedicated to food, where standard format NMR spectra are enriched by metadata and powerful data mining engines [3]. The last few years have seen for the purpose the launch of MetaboLights by the European Bioinformatic Institute [20], the launch of NIH Metabolomics Workbench (http://www.metabolomicsworkbench.org), establishing similar data storage infrastructures, and the collection of huge amount of data on single food products [21,22].

Food composition and physical characteristics

The extensive implementation of automatic spectrometer setup procedures achieved in the last decades has made quantitative investigations on modern NMR instruments limitedly user dependent. In addition, the effects of suboptimal instrument setup can be accurately mapped [23]. The number of quantitative NMR (qNMR) applications targeted toward specific molecules is therefore increasing [24,25], and this is particularly useful when all the legal requirements of a food can be entirely assessed by means of NMR spectroscopy. This is the case of egg yolk based liqueurs [26], where total sugar and alcohol have been directly quantified, while the egg yolk content has been successfully estimated.

Targeted NMR based applications are particularly suitable for (semi-) automatized signals deconvolution procedures, fundamental in sight of the standardized/harmonized operating procedures [7]. Significant steps forward in this respect are represented by the software products like Chenomx, (Chenomx Inc., Edmonton, CA) merging automatic procedures and users guidance though a game-like interaction with the software, Batman [27••] R (www.R-project.org) package, with many pros among which being licenced under the GNU general public license, and MVPACK [28], promising to follow the entire pipeline of NMR spectra processing and data mining.

The quantitative applications targeted toward *a priori* selected molecules is stimulating (and is stimulated by) the marketing of cost-effective bench-top, air-cooled, medium field spectrometers. In these instruments, the problems of signal resolution, caused by the magnetic field lower than the one of the cryogenic-cooled counterparts, are partially solved by working on field homogeneity, with modifications of the permanent magnets arrangement originally described by Halbach [29•].

Mathematical relationships granting good rates of correct predictions have been established between NMR spectra and even physical characteristics of food, of key value for transformation. This is the case of meat, where tenderness [30] and water-holding capacity [31], the most important characteristics of meat, together with appearance [32], have been successfully modeled through NMR. This is the case also for milk, the coagulating properties of which have been successfully related to the metabolites profile, observed by ^{1}H NMR and Principal Component Analysis (PCA) [33].

Food processing and storage

The ideal food combines nutritional and sensorial quality, but the design of the appropriate manufacturing processes is still a considerable challenge [34]. Food processing technologies and modification phenomena occurring during storage have a general impact on the metabolic pathways of food cells and microorganisms and, in turn, on the food metabolome, making holistic analytical techniques invaluable for the characterization of food quality. Despite the great potential, their employment in investigations on the consequences of technological processes to the quality of food is erratic.

Great attention has been paid by the NMR community to chemical and microbiological evolution phenomena occurring during food storage, with particular emphasis on degradation processes. Observations are accumulating at a fast pace for fish [35,36], meat [12], vegetables [37] and spices [38], taking into consideration not just storage time, but also storage conditions, such as composition of modified atmospheres and temperature [35].

Mechanical treatments, such as peeling, chopping, shredding, and heat transfer treatments still appear to be investigated below their potentialities. Lopez-Sanchez [34] was able to follow the effects of different combinations of heating and blending on the phytochemical composition of tomato, broccoli and carrots purees. In

the review by Erikson *et al.* [39], effects of frying and boiling of different species of fish are described. Roasting effects have been observed for coffee [40] and laver product [41]. Freezing causes massive water migration among cell compartments and causes cell membranes breakage, due to the formation of ice crystals. This may allow freeze stored food to be distinguished from the refrigerated one. An example is represented by fish freezing, leading to the formation of dimethylamine [42], that instead can be found only in traces in refrigerated fish. Effects on fish molecular profile due to mass transfer have also already been noticed because of salting [35].

The request for minimally processed food is stimulating the research on non-thermal technological treatments for bacteria reduction or degradative enzymes inactivation, such as irradiation, use of high pressures or application of gas plasma [43]. NMR-based foodomics applications are emerging also in this field, as in the case of ground beef [44]. The high demand for functional food is increasing the research on mass transfer processings alternative to osmosis, such as vacuum impregnation [45]. We found no examples of foodomics investigation in literature, but such gap is likely to be soon filled.

The relationships between specific processes applied to food and the features of the NMR spectra profile must be considered with caution, due to the presence of confounding factors. During fish storage, for example, trimethylamine is produced by bacterial spoilage of proteins [39], but its concentration cannot be reliably used as an universal index for the correctness of fish conservation, because deeply influenced by fish breeding too.

Food and health

Today, we are witnessing an increasingly growing opinion that a proper nutrition, along with an adequate lifestyle, plays a key role in the prevention, onset and control of many diseases, among which metabolic syndrome, diabetes and cancer [46]. In order to gain insight into this issue, the knowledge of which food components influence the health status and their mechanisms of action is crucial. In this context, research in food science and nutrition has started to move in the direction of integrative analysis, finding in foodomics an holistic way to study the complex hierarchical structure (from genes to proteins to metabolites) linking food and health [47–49]. Indeed, the foodomics approach can help the investigation of both the food metabolome and the correlated human metabolome: the characterization of the whole metabolic fingerprint of food might greatly help the analysis of the mechanisms of nutrition at the molecular level, while, on the other side, the investigation of human metabolome in response to a specific diet can be useful to identify novel biomarkers of food intake not necessarily predictable by the sole food composition. This new methodology, giving insights on the effects of nutritional exposure, thus also on the nutritional status and nutritional impact on diseases, is proven to be particularly promising in the prospect of the development of tailored dietary and health recommendations.

The foodomics studies that have been setup to investigate the issues connected to nutrition, often collectively considered in the definition of nutri-metabonomics, can be grouped into three main categories. The first and more traditional is the nutritional intervention study, where a group of subjects is given a particular diet and the consequent metabolome changes are investigated. In this case the metabolic profile presents two kinds of metabolites, the exogenous, that can be considered as a marker of the specific food intake, and the endogenous, metabolites generated by our bodies as a consequence of the consumption of that food product. One example is the NMR study from Heinzmann [50] where subjects were followed after the acute ingestion of specific food products (fish, fruits, wine and grapes) and both the direct effects (presence of biomarkers) and indirect effects (metabolic pathway alterations) were observed on urine samples. Rasmussen *et al.* [51] investigated both the effects of the consumption of a high/low protein diet and of fiber and dietary glycemic index.

The second type of nutritional assessment is the one that analyses both dietary data and metabolome from biofluids of a selected population. In this case, dietary patterns and trends are observed in the population by the statistical analysis of the dietary information collected. Biomarkers are looked for in the human metabolome as a hint to the real consumption of the declared items. Savorani *et al.*, [52] performed this kind of observational study and assessed the presence of three distinct dietary patterns both with the employment of the food diaries and the urine and plasma metabolome. Similar work has been carried out by De Filippis *et al.*, [53] where NMR-based metabolomics was employed to extract the relevant dietary patterns of vegans, vegetarians and omnivores and then to find their impacts on the saliva metabolome.

The last type of nutri-metabonomic research is the one studying population with different health conditions. In this case, a nutritional intervention is usually employed, and dietary data might be collected in order to assess the compliance to the diet. Following the intervention, the metabolome is analyzed, in order to assess the specific metabolic profile and thus, identify the biomarkers, of the effect of food ingestion on health and metabolic pathways. Lehtonen [54] observed the modifications of post prandial fingerpirnts of human urine after consumption of lingonberries as a supplement to an oil-rich meal. Moazzami [55] investigated the effect of rye bread on postmenopausal women, showing that the dietary intervention leads to shifts in metabolic pathways that can have beneficial effects on the selected population.

Conclusions

In conclusion, foodomics has been proven a powerful tool for many different aspects of food quality definition. Its high-throughput approach can give insights on the whole metabolic profile of food products, helping the characterization and the definition of specific quality features that make certain foods unique. Contributions toward this direction have been provided in studies of food authentication or in investigations concerning processing and storage procedures. Furthermore, foodomics has been giving boost to new kind of nutritional studies, aimed at understanding how metabolites contained in food can influence human metabolism and health.

The Foodomics community foresees advancements in this new omic field through an intense networking activity. Indeed, there is an evident necessity to increase the level of collaboration within experts of different disciplines, such as bioinformatics, chemometrics, analytical chemistry, biochemistry or statistics [56]. This networking approach will help creating more accessible and reliable information through the employment of specific compounds databases and the definition of good operating procedures and standard protocols in order to generate a more common perspective and more robust data.

Conflict of interest statement

The authors declare no conflict of interest.

References and recommended reading

Papers of particular interest, published within the period of review, have been highlighted as:

- • of special interest
- •• of outstanding interest

1. Cifuentes A: **Special issue: advanced separation methods in food analysis**. *J Chromatogr A* 2009, **1216**:7109-7358.

2. • Laghi L, Picone G, Capozzi F: **Nuclear magnetic resonance for foodomics beyond food analysis**. *Trend Anal Chem* 2014, **59**:93-102.

This is one of the most recent reviews describing the technical issues which must be addressed in order to obtain valuable results in Foodomics investigations performed by NMR.

3. Goodacre R: **I spy with my little eye something beginning with … 'H'**. *Metabolomics* 2015, **11**:6-8.

4. Wold S, Sjöström M, Eriksson L: **PLS-regression: a basic tool of chemometrics**. *Chemometr Intell Lab* 2001, **58**:109-130.

5. Sumner LW, Amberg A, Barrett D, Beale MH, Beger R, Daykin CA, Fan TM, Fiehn O, Goodacre R, Griffin JL *et al.*: **Proposed minimum reporting standards for chemical analysis**. *Metabolomics* 2007, **3**:211-221.

6. Versari A, Laurie VF, Ricci A, Laghi L, Parpinello GP: **Progress in authentication, typification and traceability of grapes and wines by chemometric approaches**. *Food Res Int* 2014, **60**:2-18.

7. Esslinger S, Riedl J, Fauhl-Hassek C: **Potential and limitations of non-targeted fingerprinting for authentication of food in official control**. *Food Res Int* 2014, **60**:189-204.

8. Gallo V, Mastrorilli P, Cafagna I, Nitti GI, Latronico M, Longobardi F, Minoja AP, Napoli C, Romito VA, Schäfer H *et al.*: **Effects of agronomical practices on chemical composition of table grapes evaluated by NMR spectroscopy**. *J Food Compos Anal* 2014, **35**:44-52.

9. Hohmann M, Christoph N, Wachter H, Holzgrabe U: **^{1}H NMR profiling as an approach to differentiate conventionally and organically grown tomatoes**. *J Agric Food Chem* 2014, **62**:8530-8540.

10. •• Godelmann R, Fang F, Humpfer E, Schütz B, Bansbach M, Schäfer H, Spraul M: **Targeted and nontargeted wine analysis by ^{1}H NMR spectroscopy combined with multivariate statistical analysis. Differentiation of important parameters: grape variety, geographical origin, year of vintage**. *J Agric Food Chem* 2013, **61**:5610-5619.

Transparency of each investigation step is the most important characteristic in the description of a work dealing with foodomics. This paper represents a todate benchmark for the purpose.

11. Picone G, Mezzetti B, Babini E, Capocasa F, Placucci G, Capozzi F: **Unsupervised principal component analysis of NMR metabolic profiles for the assessment of substantial equivalence of transgenic grapes (*Vitis vinifera*)**. *J Agric Food Chem* 2011, **59**:9271-9279.

12. Ercolini D, Ferrocino I, Nasi A, Ndagijimana M, Vernocchi P, La Storia A, Laghi L, Mauriello G, Guerzoni ME, Villani F: **Monitoring of microbial metabolites and bacterial diversity in beef stored under different packaging conditions**. *Appl Environ Microbiol* 2011, **77**:7372-7381.

13. Picone G, Laghi L, Gardini F, Lanciotti R, Siroli L, Capozzi F: **Evaluation of the effect of carvacrol on the *Escherichia coli* 555 metabolome by using ^{1}H-NMR spectroscopy**. *Food Chem* 2013, **141**:4367-4374.

14. Davies H: **A role for ''omics'' technologies in food safety assessment**. *Food Control* 2010, **21**:1601-1610.

15. • Mehmood T, Liland KH, Snipen L, Sæbø S: **A review of variable selection methods in Partial Least Squares Regression**. *Chemometr Intell Lab* 2012, **118**:62-69.

This review offers a valuable overview of the methods for variables selection in PLS regression methods, granting the highest corrected prediction rates and parsimonious models.

16. Savorani F, Rasmussen MA, Rinnan Å, Engelsen SB: **Interval based chemometric methods in NMR-foodomics**. In *Chemometrics in Food Chemistry.* Edited by Marini F. Elsevier Science; 2013:449-486.

17. Savorani F, Picone G, Badiani A, Fagioli P, Capozzi F, Engelsen SB: **Metabolic profiling and aquaculture differentiation of gilthead sea bream by ^{1}H NMR metabonomics**. *Food Chem* 2010, **120**:907-914.

18. Jiang M, Wang C, Zhang Y, Feng Y, Wang Y, Zhu Y: **Sparse partial-least-squares discriminant analysis for different geographical origins of *Salvia miltiorrhiza* by ^{1}H NMR-based metabolomics**. *Phytochem Anal* 2014, **25**:50-58.

19. Broadhurst D, Kell D: **Statistical strategies for avoiding false discoveries in metabolomics and related experiments**. *Metabolomics* 2006, **2**:171-196.

20. Haug K, Salek RM, Conesa P, Hastings J, de Matos P, Rijnbeek M, Mahendraker T, Williams M, Neumann S, Rocca-Serra P *et al.*: **MetaboLights—an open-access general-purpose repository for metabolomics studies and associated meta-data**. *Nucleic Acids Res* 2012, **41**:D781-D786.

21. Longobardi F, Ventrella A, Napoli C, Humpfer E, Schütz B, Schäfer H, Kontominas MG, Sacco A: **Classification of olive oils according to geographical origin by using ^{1}H NMR fingerprinting combined with multivariate analysis**. *Food Chem* 2012, **130**:177-183.

22. Cagliani LR, Culeddu N, Chessa M, Consonni R: **NMR investigations for a quality assessment of Italian PDO saffron (*Crocus sativus* L.)**. *Food Control* 2015, **50**:342-348.

23. Giraudeau P, Silvestre V, Akoka S: **Optimizing water suppression for quantitative NMR-based metabolomics: a tutorial review**. *Metabolomics* 2015:1-15.

24. Li ZY, Welbeck E, Wang RF, Liu Q, Yang YB, Chou GX, Bi KS, Wang ZT: **A universal quantitative ^{1}H nuclear magnetic resonance (qNMR) method for assessing the purity of dammarane-type ginsenosides**. *Phytochem Anal* 2015, **26**:8-14.

25. Cao R, Nonaka A, Komura F, Matsui T: **Application of diffusion ordered-^{1}H-nuclear magnetic resonance spectroscopy to quantify sucrose in beverages**. *Food Chem* 2015, **171**:8-12.

26. Hohmann M, Koospal V, Bauer-Christoph C, Christoph N, Wachter H, Diehl B, Holzgrabe U: **Quantitative ^{1}H NMR analysis of egg yolk, alcohol, and total sugar content in egg liqueurs**. *J Agric Food Chem* 2015, **63**:4112-4119.

27. •• Hao J, Astle W, De Iorio M, Ebbels TMD: **BATMAN—an R package for the automated quantification of metabolites from nuclear magnetic resonance spectra using a Bayesian model**. *Bioinformatics* 2012, **28**:2088-2090.
BATMAN R package is one of the most advanced software products for NMR spectral profiling; it allows the complete automatization (thus standardization) of molecules quantification and it is free and open source, key characteristics in sight of transparency.

28. Worley B, Powers R: **MVAPACK: a complete data handling package for NMR metabolomics**. *ACS Chem Biol* 2014, **9**:1138-1144.

29. ↓ Armstrong-Smith I: **A briefcase full of NMR**. *Anal Sci* 2015:24-29.
The applications of NMR to Foodomics investigations are limited by the fantasy of the users. This paper gives an impression of the enormous spaces which can be explored by the scientific community in this regard.

30. D'Alessandro A, Zolla L: **Foodomics to investigate meat tenderness**. *Trend Anal Chem* 2013, **52**:47-53.

31. Bowker BC, Grant AL, Forrest JC, Gerrard DE: **Muscle metabolism and PSE pork**. *J Anim Sci* 2000, **79**:1-8.

32. Petracci M, Bianchi M, Mudalal S, Cavani C: **Functional ingredients for poultry meat products**. *Trends Food Sci Tech* 2013, **33**:27-39.

33. Sundekilde UK, Frederiksen PD, Clausen MR, Larsen LB, Bertram HC: **Relationship between the metabolite profile and technological properties of bovine milk from two dairy breeds elucidated by NMR-based metabolomics**. *J Agric Food Chem* 2011, **59**:7360-7367.

34. Lopez-Sanchez P, de Vos RCH, Jonker HH, Mumm R, Hall RD, Bialek L, Leenman R, Strassburg K, Vreeken R, Hankemeier T *et al.*: **Comprehensive metabolomics to evaluate the impact of industrial processing on the phytochemical composition of vegetable purees**. *Food Chem* 2015, **168**:348-355.

35. Piras C, Scano P, Locci E, Sanna R, Cesare Marincola F: **Analysing the effects of frozen storage and processing on the metabolite profile of raw mullet roes using ^{1}H NMR spectroscopy**. *Food Chem* 2014, **159**:71-79.

36. Shumilina E, Ciampa A, Capozzi F, Rustad T, Dikiy A: **NMR approach for monitoring post-mortem changes in Atlantic salmon fillets stored at 0 and 4 °C**. *Food Chem* 2015, **184**:12-22.

37. Kortesniemi M, Vuorinen AL, Sinkkonen J, Yang B, Rajala A, Kallio H: **NMR metabolomics of ripened and developing oilseed rape (*Brassica napus*) and turnip rape (*Brassica rapa*)**. *Food Chem* 2015, **172**:63-70.

38. Ordoudi SA, Cagliani LR, Lalou S, Naziri E, Tsimidou MZ, Consonni R: **^{1}H NMR-based metabolomics of saffron reveals markers for its quality deterioration**. *Food Res Int* 2015, **70**:1-6.

39. Erikson U, Standal IB, Aursand IG, Veliyulin E, Aursand M: **Use of NMR in fish processing optimization: a review of recent progress**. *Magn Reson Chem* 2012, **50**:471-480.

40. Wei F, Furihata K, Miyakawa T, Tanokura M: **A pilot study of NMR-based sensory prediction of roasted coffee bean extracts**. *Food Chem* 2014, **152**:363-369.

41. Ye Y, Yang R, Lou Y, Chen J, Yan X, Tang H: **Effects of food processing on the nutrient composition of *Pyropia yezoensis* products revealed by NMR-based metabolomic analysis**. *J Food Nutr Res* 2014, **2**:749-756.

42. Martinez I, Bathen T, Standal IB, Halvorsen J, Aursand M, Gribbestad IS, Axelson DE: **Bioactive compounds in cod (*Gadus morhua*) products and suitability of ^{1}H NMR metabolite profiling for classification of the products using multivariate data analyses**. *J Agric Food Chem* 2005, **53**:6889-6895.

43. Tappi S, Berardinelli A, Ragni L, Dalla Rosa M, Guarnieri A, Rocculi P: **Atmospheric gas plasma treatment of fresh-cut apples**. *Innov Food Sci Emerg* 2014, **21**:114-122.

44. Zanardi E, Caligiani A, Palla L, Mariani M, Ghidini S, Di Ciccio PA, Palla G, Ianieri A: **Metabolic profiling by ^{1}H NMR of ground beef irradiated at different irradiation doses**. *Meat Sci* 2015, **103**:83-89.

45. Panarese V, Dejmek P, Rocculi P, Gómez Galindo F: **Microscopic studies providing insight into the mechanisms of mass transfer in vacuum impregnation**. *Innov Food Sci Emerg* 2013, **18**:169-176.

46. Kumar PA, Chitra PS, Reddy GB: **Metabolic syndrome and associated chronic kidney diseases: nutritional interventions**. *Rev Endocr Metab Disord* 2013, **14**:273-286.

47. Ibáñez C, Valdés A, García-Cañas V, Simó C, Celebier M, Rocamora-Reverte L, Gómez-Martínez Á, Herrero M, Castro-Puyana M, Segura-Carretero A *et al.*: **Global foodomics strategy to investigate the health benefits of dietary constituents**. *J Chromatogr A* 2012, **1248**:139-153.

48. Valdés A, García-Cañas V, Simó C, Ibáñez C, Micol V, Ferragut JA, Cifuentes A: **Comprehensive foodomics study on the mechanisms operating at various molecular levels in cancer cells in response to individual rosemary polyphenols**. *Anal Chem* 2014, **86**:9807-9815.

49. Valdés A, Simó C, Ibáñez C, Rocamora-Reverte L, Ferragut JA, García-Cañas V, Cifuentes A: **Effect of dietary polyphenols on K562 leukemia cells: a foodomics approach**. *Electrophoresis* 2012, **33**:2314-2327.

50. Heinzmann SS, Merrifield CA, Rezzi S, Kochhar S, Lindon JC, Holmes E, Nicholson JK: **Stability and robustness of human metabolic phenotypes in response to sequential food challenges**. *J Proteome Res* 2012, **11**:643-655.

51. Rasmussen L, Winning H, Savorani F, Ritz C, Engelsen S, Astrup A, Larsen T, Dragsted L: **Assessment of dietary exposure related to dietary GI and fibre intake in a nutritional metabolomic study of human urine**. *Genes Nutr* 2012, **7**:281-293.

52. Savorani F, Rasmussen MA, Mikkelsen MS, Engelsen SB: **A primer to nutritional metabolomics by NMR spectroscopy and chemometrics**. *Food Res Int* 2013, **54**:1131-1145.

53. De Filippis F, Vannini L, La Storia A, Laghi L, Piombino P, Stellato G, Serrazanetti DI, Gozzi G, Turroni S, Ferrocino I *et al.*: **The same microbiota and a potentially discriminant metabolome in the saliva of omnivore, ovo-lacto-vegetarian and vegan individuals**. *PLoS One* 2014, **9**:1-9.

54. Lehtonen H-M, Lindstedt A, Järvinen R, Sinkkonen J, Graça G, Viitanen M, Kallio H, Gil AM: **^{1}H NMR-based metabolic fingerprinting of urine metabolites after consumption of lingonberries (*Vaccinium vitis-idaea*) with a high-fat meal**. *Food Chem* 2013, **138**:982-990.

55. Moazzami AA, Bondia-Pons I, Hanhineva K, Juntunen K, Antl N, Poutanen K, Mykkanen H: **Metabolomics reveals the metabolic shifts following an intervention with rye bread in postmenopausal women—a randomized control trial**. *Nutr J* 2012, **11**:88.

56. García-Cañas V, Simó C, Herrero M, Ibáñez E, Cifuentes A: **Present and future challenges in food analysis: foodomics**. *Anal Chem* 2012, **84**:10150-10159.

Paper II

Dellarosa, **N.**, Ragni, L., Laghi, L., Tylewicz, U., Rocculi, P., & Dalla Rosa, M. (2015)

Effect of Pulsed Electric Fields on Water Distribution in Apple Tissue as Monitored by NMR Relaxometry

In: *1st World Congress on Electroporation and Pulsed Electric Fields in Biology, Medicine and Food & Environmental Technologies* (pp. 355-358), Springer

Effect of Pulsed Electric Fields on Water Distribution in Apple Tissue as Monitored by NMR Relaxometry

N. Dellarosa[1], L. Ragni[1,2], L. Laghi[1,2], U. Tylewicz[1], P. Rocculi[1,2], and M. Dalla Rosa[1,2]

[1] Department of Agricultural and Food Science, University of Bologna, Cesena, Italy
[2] Interdepartmental Centre for Agri-Food Industrial Research, University of Bologna, Cesena, Italy

Abstract— **Pulsed electric fields (PEF) technology is a promising innovative non-thermal process to improve mass transfer in food sector. PEF treatments induce a partial cell membranes electroporation which extent depends on electric field strength, number, duration and shape of the pulses and application time. The present work aimed at highlighting the effect of the application of PEF on mass transfer phenomena in apple parenchyma tissue, by evaluating the water distribution across cell compartments by means of NMR relaxometry. Pulsed electric fields treatments were carried out using near-rectangular shaped pulses with fixed 100 µs pulse width and 10 ms repetition time at three different specific voltage (100, 250 and 400 V cm^{-1}) and two different pulse number series (n=20 and n=60).**

Results showed different trends according to the applied voltage. The lowest (100 V cm^{-1}) was not able to induce significant changes in plasma membranes, so that no water redistribution was achieved between cytoplasm and extracellular space. At the opposite, a marked redistribution was registered inside the cellular compartments, namely vacuole and cytoplasm, showing an alteration of the tonoplast. The total number of pulses was found to influence the amount of water migrating, from vacuole to cytoplasm, from 15 % with 20 pulses to 40 % with 60 pulses.

Medium and high voltage (250 and 400 V cm^{-1}, respectively) removed the possibility to distinguish the different cell compartments, probably due to intense damage of both plasma membrane and tonoplast. By observing water transverse relaxation time an additive effect of both voltage and total number of pulses was demonstrated. Interestingly, by considering water distribution during 120 minutes after PEF treatment time-dependent trends were found in the effects of each experimented protocol.

Keywords— **PEF, NMR, water distribution, contrast agent, apple tissue**

I. INTRODUCTION

The application of pulsed electric fields (PEF) is an innovative technology to induce the breakage of cellular membrane by the application of an electric treatment. The effect on membrane, known as electroporation, has been studied in foodstuff for two main aims: improving food safety through a microbial inactivation and enhance mass transfer in food tissue for extraction purposes.

Such effects can be regulated by adjusting strength of the applied electric field, total time of treatment and number, duration and shape of the pulses [1,2].

For mass transfer applications, the consequences of the treatments are generally evaluated from the entity of the desired effect: extraction yields and release of bioactive compounds from the cell structures [3]. Alternatively, possible side effects on food quality parameters can be evaluated, such as color and texture deterioration upon PEF treatment [4].

A limited number of methods have been set up to specifically evaluate the effect of PEF treatments focusing on cell membranes integrity. The most commonly applied among them are based on the indirect estimation of cell disintegration from electrical conductivity measurement [5] while others are focused on the electroporation related electrolytic leakage [6].

NMR relaxometry was recently applied to acquire transverse relaxation time (T_2) weighted curves able to give quantitative information about water spatial distribution among apple cell parenchyma compartments [7].

This has given rise to several applications to directly estimate the effects of technological process on different kinds of fruit [8,9].

The present work aimed at taking advantage of the same information to directly evaluate the effect of pulsed electric fields on apple cell plasma membrane and tonoplast integrity. The observation of specific compartments was eased by the use of the contrast agent $FeCl_3$, which paramagnetic ion Fe(III) selectively influences water T_2, not dissimilarly to what is typically exploited in magnetic resonance imaging. As $FeCl_3$ does not passively diffuse through intact membranes, it is able to selectively influence water T_2 of extracellular spaces only, upon dipping. In contrast, electroporation leads to water T_2 modifications of inner cell compartments, proportional to the membranes damage.

II. MATERIALS AND METHODS

A. Materials

*A*pples (*Malus sylvestris*), Cripps Pink variety, were purchased from a local market and stored at 2 ± 1 °C until

© Springer Science+Business Media Singapore 2016

T. Jarm and P. Kramar (eds.), *1st World Congress on Electroporation and Pulsed Electric Fields in Biology, Medicine and Food & Environmental Technologies (WC 2015)*, IFMBE Proceedings 53,
DOI: 10.1007/978-981-287-817-5_78

treatment. The refractometric index measured by a digital refractometer (PR1, Atago, Japan) was 14.5 ± 0.5 ° Brix and the moisture content was 83.5 ± 0.5 %. Cylindrical samples (8-mm diameter) were obtained from apple parenchyma with a manual cork borer and, afterwards, cut to a length of 10 mm using a manual cutter.

B. Pulsed Electric Fields Treatment

Twelve apple cylinders were placed, for each treatment, in a 20 x 20 x 30 mm treatment chamber and filled up with tap water which conductivity was 328 ± 15 μs cm^{-1} as measured by an electrical conductivity meter (Basic 30, Crison Instrument, Spain). Afterwards, samples were immediately removed and immersed in an isotonic sucrose solution containing 0.01 M iron (III) chloride as a contrast agent for nuclear magnetic resonance analysis. Near-rectangular shaped pulses, with fixed pulsed width (100 ± 2 μs) and repetition time (10 ± 1 ms) were applied in the present work. Three applied voltage (100, 250 and 400 V cm^{-1}) and two different pulses series (number of pulses 20 and 60) were tested.

C. Nuclear Magnetic Resonance Relaxometry

Protons T_2-weighted signals were acquired using the CPMG pulse sequence implemented on a Bruker 'The Minispec' NMR spectrometer operating at proton resonance frequency of 20 MHz. The echo time was set at 0.3 ms with 6000 acquisition points over 8 scans and a recycle delay time of 10 s. To evaluate the water redistribution as a consequence of the PEF treatments samples were collected at 15, 30, 60 and 120 minutes after the end of the treatment, directly placed in 10 mm diameter NMR tubes and immediately analyzed. The total time of analysis was approximately 90 seconds. The registered spectra were analyzed using UpenWin Software [10] to obtain a quasi-continuous T_2-weighted intensity distribution which showed a multiexponential signal decay as a consequence of the different relaxation time of the compartmental water protons pools. To achieve quantitative results describing the amount of water in each cell compartment, the signals were fitted using a non-linear curve fitting method based on Levenberg-Marquardt algorithm. All the experiments were repeated three times and significant differences were studied by ANOVA and Tukey's post-hoc test (the significant level was set at $p = 0.05$).

III. RESULTS

A. Peak Assignment

NMR signals of raw apple parenchyma showed a multiexponential decay which was assigned, according to the transverse relaxation time, to different cell compartment protons pools, namely vacuole (T_2 1391 ± 45 ms), cytoplasm (T_2 282 ± 25 ms) and cell wall (T_2 17 ± 3 ms) [7]. The average intensities of the three compartments, with the respect of the total signal, were 77.5 ± 1.7, 18.5 ± 1.5 and 4.0 ± 0.4 % for vacuole, cytoplasm and cell wall respectively.

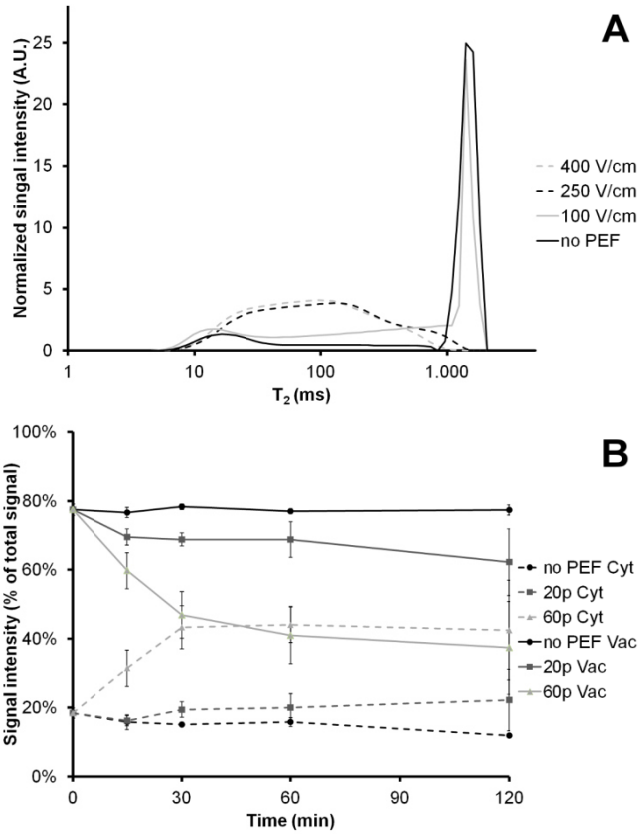

Fig. 1 Water distribution plot (A) of PEF treated samples at different voltage, observed after 120 min. Quantitative water redistribution (B) between cytoplasm and vacuole in samples treated at 100 V cm^{-1}.

In the present study the use of a paramagnet compound, the iron (III) chloride, into the isotonic solution allowed to highlight the mass transfer between the cellular water and the external solution. The concentration of $FeCl_3$ was chosen in order to give rise, in untreated samples, to a clear peak with a known T_2 set around 12 ms (Fig. 1A). The ability of the external solution to passively permeate through the cell membrane was tested by measuring T_2 and compartmental water distribution in apple cylinders immersed in the isotonic solution for 120 minutes. T_2 results (data not shown) presented no significant differences at any treatment time proving that the external solution was not able to cross the cell membrane layer. A slight but significant ($p < 0.05$) difference was achieved taking into account the water distribution (i.e. T_2-weighted intensity) after 120 minutes when

a partial dewatering of the cytoplasmatic compartment toward the extracellular space was observed. The total water protons which were redistributed accounted for 3.5 ± 0.3 % of the total amount.

B. Pulsed Electric Field Treatment

PEF treated samples showed two different trends in accordance to the input voltage (Fig. 1A). The three cell compartments, described in the previous section, were only visible when low voltage (100 V cm^{-1}) was applied. However, the application of pulsed electric field provoked a significant water redistribution within the cell, between vacuole and cytoplasm. It is interesting to notice that this effect strongly depended on the total number of pulses applied during the treatment. Figure 1B describes the effects of PEF treatment at 100 V cm^{-1} applying both 20 and 60 pulse series. The application of 60 pulses led to the highest degree of redistribution from 15 minutes after the treatment when the 18 % of the total cellular water migrated from the vacuole to the cytoplasm. This value increased up to the 40 % after 2 hours. Accordingly, the shortest pulse series, 20 pulses, led to a total redistribution of 8 % and 15 % after 15 and 120 minutes, respectively.

A totally different behavior was found when higher specific voltage (250 and 400 V cm^{-1}) was applied to apple tissue. The three compartments did not show consistent relaxation time which suggested that the paramagnetic solution was able to cross both the plasma membrane and the tonoplast and diffuse inside the cell. As shown in Figure 2, the redistribution process was a function of the time, the applied voltage and number of pulses. For example, the initial average transverse relaxation time of raw apple tissue (1131 ± 36 ms) dropped, after 15 minutes, to 526 ± 53 ms for the treatment which included 20 pulses at 250 V cm^{-1} and to 276 ± 32 ms when 60 pulses at 400 V cm^{-1} were applied. These values were considerately lower after 120 minutes when T_2 values showed average values of 171 ± 35 ms and 72 ± 6 ms, respectively.

IV. DISCUSSION

The proposed method, based on the application of NMR relaxometry combined with the use of a paramagnetic agent seemed to be a reliable non-destructive tool for the quantitative measurement of the effect of the application of pulsed electric field on vegetable tissues. In agreement with the preliminary test iron (III) chloride was not able to passively cross the membrane in the native form. As resulted by the significant decrease of the average relaxation time, when the cell membrane underwent to electroporation, it lost its selectivity and the external solution could diffuse into the cellular space.

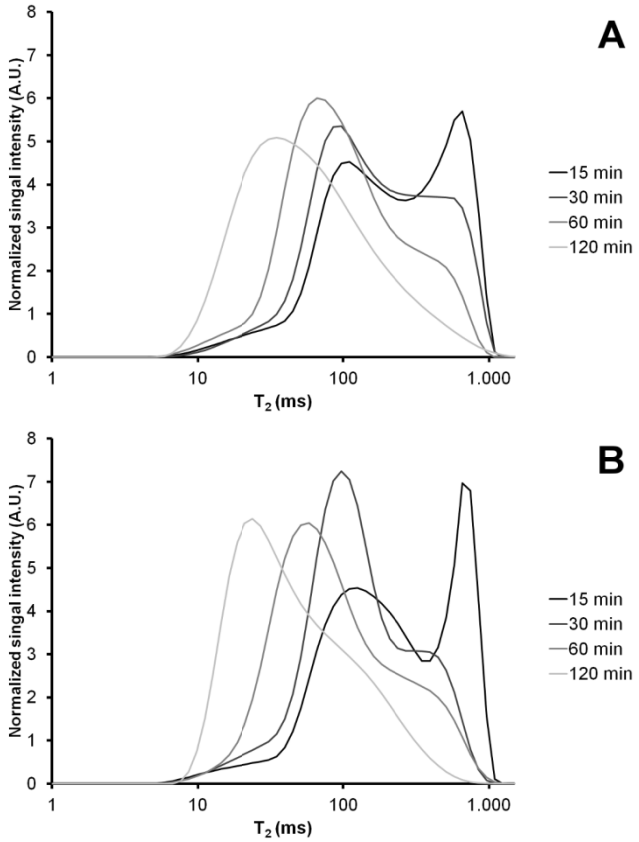

Fig. 2 Water distribution plot of PEF treated samples with 60 pulses at 250 (A) and 400 V cm^{-1} (B) at different sampling time.

The two highest voltage levels (250 and 400 V cm^{-1}) were both able to permeabilize the apple cell membrane while the lowest experimented voltage (100 V cm^{-1}) did not produce a significant change. Interestingly, at low voltage water protons were also redistributed between cell vacuole and cytoplasm. In this respect, the tonoplast, that surrounds the vacuole, showed a higher susceptibility to pulsed electric field when compared to plasma membrane. Beside the two different responses due to the specific applied voltage, water redistribution was also affected by both time and number of pulses. At 100 V cm^{-1} (Fig. 1B), 60 pulses, after 15 minutes, caused a higher redistribution, between vacuole and cytoplasm, than the one obtained by the application of 20 pulses throughout 120 minutes.

On the contrary, the model which includes three compartments could not be directly applied to vegetable tissues when plasma membrane is damaged, since the internal compartmental protons pools did not show a clear distinct relaxation time. Nevertheless, it is worth observing that the internal water redistribution rate depended on the applied energy, including both specific voltage and number of

pulses. As reported in a previous study [11] and confirmed by the present study, the average relaxation time could be a useful index of cell integrity even though a direct relationship with extraction yields was not investigated in the present work.

V. CONCLUSIONS

In conclusion, the proposed method, based on NMR relaxometry, provided useful information about cell compartmentalization and its changing due to the applied PEF treatment protocols. Water redistribution was demonstrated to be applicable also in case of low electric field strengths, able to selectively act only on tonoplast. The suggested method offers a direct observation of membrane damages so that it can be conveniently used to finely tune technological treatments which act on mass transfer, for example osmotic dehydration and vacuum impregnation.

CONFLICT OF INTEREST

The authors declare that they have no conflict of interest.

REFERENCES

1. Bazhal M I, Lebovka N I, & Vorobiev E (2001) Pulsed electric field treatment of apple tissue during compression for juice extraction. J Food Eng 50: 129-139
2. Heinz V, Alvarez I, Angersbach A, & Knorr D (2001) Preservation of liquid foods by high intensity pulsed electric fields—basic concepts for process design. Trends Food Sci Tech 12: 103-111
3. Soliva-Fortuny R, Balasa A, Knorr D, & Martín-Belloso O (2009) Effects of pulsed electric fields on bioactive compounds in foods: a review. Trends Food Sci Tech 20: 544-556
4. Ammar J B, Lanoisellé J L, Lebovka N I et al. (2010) Effect of a pulsed electric field and osmotic treatment on freezing of potato tissue. Food biophys 5: 247-254
5. Knorr D, & Angersbach A (1998) Impact of high-intensity electric field pulses on plant membrane permeabilization. Trends Food Sci Tech 9: 185-191
6. Ersus S, & Barrett D M (2010) Determination of membrane integrity in onion tissues treated by pulsed electric fields: use of microscopic images and ion leakage measurements. Innov. Food Sci Emerg 11: 598-603
7. Marigheto N, Venturi L, & Hills B (2008) Two-dimensional NMR relaxation studies of apple quality. Postharvest Biol Tec 48: 331-340.
8. Hills B P, & Remigereau B (1997) NMR studies of changes in subcellular water compartmentation in parenchyma apple tissue during drying and freezing. Int J Food Sci Technol 32: 51-61
9. Tylewicz U, Panarese V, Laghi L, et al. (2011) NMR and DSC water study during osmotic dehydration of Actinidia deliciosa and Actinidia chinensis kiwifruit. Food biophys 6: 327-333
10. Borgia G C, Brown R J S, & Fantazzini P. (1998) Uniform-penalty inversion of multiexponential decay data. J Magn Reson 132: 65-77
11. Ersus S, Oztop M H, McCarthy M J, & Barrett D M (2010) Disintegration Efficiency of Pulsed Electric Field Induced Effects on Onion (Allium cepa L.) Tissues as a Function of Pulse Protocol and Determination of Cell Integrity by 1H NMR Relaxometry. J Food Sci 75: E444-E452.

Author: Dellarosa Nicolò
Institute: Department of Agricultural and Food Science, University of Bologna
Street: P.za Goidanich 60
City: Cesena
Country: Italy
Email: nicolo.dellarosa@unibo.it

Paper III

Mauro, M. A., **Dellarosa**, **N.**, Tylewicz, U., Tappi, S., Laghi, L., Rocculi, P., & Dalla Rosa, M. (2016)

Calcium and ascorbic acid affect cellular structure and water mobility in apple tissue during osmotic dehydration in sucrose solutions

Food Chemistry, *195*, 19-28

Food Chemistry 195 (2016) 19–28

Contents lists available at ScienceDirect

Food Chemistry

journal homepage: www.elsevier.com/locate/foodchem

Calcium and ascorbic acid affect cellular structure and water mobility in apple tissue during osmotic dehydration in sucrose solutions

Maria A. Mauro [a,*], Nicolò Dellarosa [b], Urszula Tylewicz [c], Silvia Tappi [b], Luca Laghi [b,c], Pietro Rocculi [b,c], Marco Dalla Rosa [b,c]

[a] Department of Food Engineering and Technology, São Paulo State University (UNESP), São José do Rio Preto, Brazil
[b] Department of Agri-Food Science and Technology – University of Bologna, Cesena, Italy
[c] Interdepartmental Centre for Agri-Food Industrial Research, University of Bologna, Cesena, Italy

ARTICLE INFO

Article history:
Received 5 December 2014
Received in revised form 17 April 2015
Accepted 19 April 2015
Available online 23 April 2015

Chemical compounds studied in this article:
Ascorbic acid (PubChem CID: 54670067)
Calcium lactate (PubChem CID: 16211540)

Keywords:
Cell compartments
Mass transfer
Cell viability
Microscopy
NMR

ABSTRACT

The effects of the addition of calcium lactate and ascorbic acid to sucrose osmotic solutions on cell viability and microstructure of apple tissue were studied. In addition, water distribution and mobility modification of the different cellular compartments were observed. Fluorescence microscopy, light microscopy and time domain nuclear magnetic resonance (TD-NMR) were respectively used to evaluate cell viability and microstructural changes during osmotic dehydration. Tissues treated in a sucrose–calcium lactate–ascorbic acid solution did not show viability. Calcium lactate had some effects on cell walls and membranes. Sucrose solution visibly preserved the protoplast viability and slightly influenced the water distribution within the apple tissue, as highlighted by TD-NMR, which showed higher proton intensity in the vacuoles and lower intensity in cytoplasm-free spaces compared to other treatments. The presence of ascorbic acid enhanced calcium impregnation, which was associated with permeability changes of the cellular wall and membranes.

© 2015 Elsevier Ltd. All rights reserved.

1. Introduction

The concentration of plant foods by immersing solid food pieces in a hypertonic solution consisting of salt, sugar, glycerol, or other humectants is known as osmotic dehydration (OD) (Sereno, Moreira, & Martinez, 2001). This technique reduces the a_w of the product without a phase change because the flow of water from the product into the concentrated solution is compensated by the solutes migration from the solution into the product (Nieto, Vicente, Hodara, Castro, & Alzamora, 2013). This process permits the formulation of products with intermediate moisture content through dewatering and impregnation of desired solutes (Barrera, Betoret, & Fito, 2004). Because of its versatility, OD has a wide range of applications in the development of minimally processed plant foods or as pretreatment for other preservation methods such as freezing or drying (Alzamora, Cerrutti, Guerrero, & López-Malo, 1995; Garcia Loredo, Guerrero, Gomez, & Alzamora, 2013).

The addition of calcium in osmotic solutions has been widely used in plant foods as fortifier and to enhance firmness (Anino, Salvatori, & Alzamora, 2006; Barrera, Betoret, Corell, & Fito, 2009; Mavroudis, Gidley, & Sjöholm, 2012; Silva, Fernandes, & Mauro, 2014a). Fortification using combinations of substances such as calcium and iron (Barrera et al., 2004) or Ca and vitamin C (Silva, Fernandes, & Mauro, 2014b) has also been investigated.

OD causes physical modifications of cell membranes and cell walls, which affects the rheological properties and state of water (Nieto et al., 2013; Vicente, Nieto, Hodara, Castro, & Alzamora, 2012). Knowledge about the microstructure and mass transport in OD of plant tissues is fundamental for controlling production of foods fortified with vitamins and mineral salts. Mass transfer in cellular tissue is influenced by the osmotic pressure and structure properties such as permeability of the plasma membrane and vacuole membrane, cell wall porosity, or even intercellular porosity. The osmotic pressure, in turn, depends on the solute concentration and the salt and acid dissociation because each substance presents specific transport properties through plasma and vacuole membranes or cell wall pores. When the cellular structure is changed, the tissue selectivity is also modified, so that water mobility and distribution are affected.

Osmotic dehydration of plant foods is largely controlled by the cellular membranes, which have different permeabilities to different substances. Biological membranes are composed of phospholipid

* Corresponding author.
E-mail address: cidam@ibilce.unesp.br (M.A. Mauro).

http://dx.doi.org/10.1016/j.foodchem.2015.04.096
0308-8146/© 2015 Elsevier Ltd. All rights reserved.

bilayers with intrinsic proteins. Studies have shown that water can cross plant membranes through proteinaceous channels formed by members of the aquaporin superfamily, also called water channels (Weig, Deswarte, & Chrispeels, 1997). Aquaporins are hydrophobic proteins that enhance the biological membrane's permeability to water. They belong to a group of membrane proteins, the major intrinsic proteins (MIP) family of channels, with a molar mass in the range of 26 and 30 kDa (Tyerman, Niemietz, & Bramley, 2002; Weig et al., 1997). These channels increase the permeability of biological membranes to water compared to the lipid bilayers; they are detected by the low activation energy needed to transport water across water channels (Tyerman et al., 2002).

Calcium ions that occupy spaces outside the plasma membrane (apoplast) have a structural role in the cell wall because they interact with pectic acid polymers to form cross-bridges that reinforce the cell adhesion, thereby reducing cell separation, which is one of the major causes of plant tissue softening (Roy et al., 1994). Moreover, calcium can affect water channel activity; however, the significance of the inhibition of plant aquaporins by calcium is complex and has still not been clarified (Maurel, 2007). Conversely, calcium can also cross membranes through cation channels. A vacuolar non-selective Ca^{2+} channel (Peiter et al., 2005) has been identified as a plasma membrane non-selective cation channel (Tapken et al., 2013) in plant cells.

Ascorbic acid (AA) influences the cell physiology; however, little is known about its role in plant tissue. Exposure of *Arabidopsis thaliana* seedlings to ascorbic acid demonstrated that exogenous AA caused grow inhibition and damage in the cellular structure by increasing the ROS (reactive oxygen species) content (Qian et al., 2014). In addition, a very low pH (2–3) can increase the cell wall porosity (Zemke-White, Clements, & Harris, 2000), which increases diffusion of great molecules in the free spaces of the cellular tissue.

The complexity of osmotic dehydration of plant tissues rises when using a multicomponent solution because all the solutes and their respective concentrations affect the membrane permeability and cell wall. Consequently, monitoring the water distribution can be useful to clarify the behavior of the cellular microstructures as osmotic dehydration proceeds. Time domain nuclear magnetic resonance (TD-NMR) is an analytical method that allows the determination of the water content and its mobility in different cell compartments by proton relaxation times of water in foods (Hills & Duce, 1990). It is a non-invasive method suitable for large tissue samples that relates water content and water properties in different proton pools within the tissue with different transverse relaxation times (T_2) of water (Hills & Remigereau, 1997; Panarese et al., 2012; Tylewicz et al., 2011). In fruit samples, the higher the mobility of a proton bearing molecule, the higher the spin–spin (T_2) relaxation time is expected to be. The intensities of proton pools with different transverse relaxation times are a relative measure of the amount of water corresponding to a specific T_2. This technique has been used in OD of plants to evaluate water mobility and distribution within the cellular tissue (Cornillon, 2000; Panarese et al., 2012; Tylewicz et al., 2011). Microscopic techniques can also be important tools to clarify cell viability by using vital dyes. Protoplasts stained with fluorescein diacetate (FDA) allow the estimation of two types of plasma membrane injuries: lysis and the loss of semipermeability (Halperin & Koster, 2006; Koster, Reisdorph, & Ramsay, 2003). Vacuole membrane alterations can be evaluated by the capacity of intact tonoplasts to retain neutral red and provide contrast to vacuoles (Carpita, Sabularse, Montezinos, & Delmer, 1979; Thebud & Santarius, 1982).

A multianalytical approach that combines several techniques such as micro and ultrastructural microscopy, calorimetry and NMR have been successfully employed in investigations of plant foods subjected to mild processing conditions (Panarese et al., 2012; Rocculi et al., 2012; Tylewicz et al., 2011).

The main objective of this work was to investigate the effects of the addition of calcium lactate (CaLac) and ascorbic acid (AA) to sucrose (Suc) osmotic solutions on mass transfer, cell viability and structure of apple tissue, as well as the consequential water distribution and mobility modification among the different cellular compartments.

2. Materials and methods

2.1. Raw materials

Apples (*Malus domestica* Borkh) of the Cripps Pink variety, popularly known by the brand name Pink Lady (Castro, Barrett, Jobling & Mitcham, 2008), were provided by the local market and stored at 5 ± 1 °C for no longer than 2 weeks, during which osmotic dehydration experiments were performed. The average weight of the apples was 233.5 ± 17.7 g, and the soluble solids content was 13.4 ± 0.3 g · 100 g^{-1}. Apples were cut in cylinders (8-mm diameter) with a manual cork borer and cut to a length of 40 mm using a manual cutter designed for this purpose. Commercial sucrose (refined sugar, Eridania, Italy), L-ascorbic acid (Shandong Luwei Pharmaceutical Co., China) and calcium lactate (calcium-L-lactate 5-hydrate powder, PURACAL® PP Food, Corbion PURAC, Netherlands) were used in the experiments.

2.2. Osmotic dehydration

Apple cylinders were weighed (approximately 0.1 kg) in a mesh basket and immersed in the osmotic solution. Each basket corresponded to a single OD time: 0.5, 1, 2 and 4 h. The OD system consisted of a cylindrical glass vessel containing 4.5 kg of aqueous solution. The cylindrical baskets, coupled with an impeller of a mechanical stirrer, were continuously rotated. Two baskets were prepared for each process time. The syrup-to-fruit ratio was approximately 15:1 (w/w).

The OD was performed with four different aqueous solutions: 40% sucrose (Suc), 40% sucrose + 4% calcium lactate (Suc–CaLac), 40% sucrose + 2% ascorbic acid (Suc–AA) and 40% sucrose + 4% calcium lactate + 2% ascorbic acid (Suc–CaLac–AA). After the pre-established contact period, the samples were removed from the solution, rinsed with distilled water, blotted with absorbing paper, and weighed.

Immediately after the process, analyses of the total solids and soluble solids contents were performed for fresh and osmotically treated samples in triplicate. The proton transverse relaxation time (T_2) was also immediately measured for six replicates. Samples for calcium and ascorbic acid analyses were freeze-dried.

2.3. Analytical methods

The moisture content for 2 g of fresh and treated samples was determined gravimetrically, in triplicate, by drying at 70 °C until a constant weight was achieved. The soluble solids content was determined at 20 °C by measuring the refractive index with a digital refractometer (PR1, Atago, Japan). Water activity was measured in a water activity meter (AquaLab Series mod. CX-2, Decagon, USA).

2.3.1. Ascorbic acid

For ascorbic acid determination, an extraction was performed with 0.5 g of a freeze-dried sample added to 10 ml of meta phosphoric acid (62.5 mM) and sulfuric acid (5 mM) solution. The mixture was vortexed for 2 min and centrifuged at 10,000×g for 10 min at 4 °C. The supernatant was opportunely diluted and filtered through a 0.45 μm nylon filter. Ascorbic acid was determined

according to Odriozola-Serrano, Hernàndez-Jover, and Martìn-Belloso method (2007). The HPLC system (Jasco LC-1500, Carpi, MO, Italy) was equipped with a diode array UV/Vis detector. A reverse-phase C18 Kinetex (Phenomenex Inc., Torrance, CA, USA) stainless steel column (4.6 × 150 mm) was used as the stationary phase. Samples were introduced in the column through an autosampler (Jasco AS-2055 Plus). The mobile phase was a 0.01% solution of sulfuric acid adjusted to a pH of 2.6. The flow rate was fixed at 1.0 mL/min at room temperature. Data were processed by the software ChromNAV (ver. 1.16.02) from Jasco. The ascorbic acid content was quantified at 245 nm through a standard calibration curve.

2.3.2. Calcium

The calcium concentration was determined using a flame atomic absorption spectrophotometer (Model A Analyst 400, Perkin Elmer, Santa Clara, California, USA), using a lumina hollow cathode lamp (Perkin Elmer) based on the adapted methodology of AOAC – Association of Official Analytical Chemists. (1995). Approximately 6 g of fresh samples (without treatment) and 2 g of treated samples, i.e., freeze dried and previously ground, were weighed in a 50 ml glazed, porcelain crucible placed in a muffle furnace and heated up to 550 °C until complete ignition. Then, the porcelain crucibles were cooled in desiccators, where 20 ml of chloride acid (0.1 M) was added to the capsules with fresh samples and 30 ml was added to the treated samples. The ash was dissolved, and then, an aliquot of this solution was quantitatively taken and diluted 8 times (fresh samples) or 100 times (treated samples) with 0.1 M chloride acid. Standard calcium solutions between 2 and 20 ppm were used to determine a calibration curve of absorbance versus ppm of calcium.

2.4. Mass transfer of osmotic dehydration

Mass transfer during osmotic dehydration was evaluated on the basis of mass balances. The total mass variation in relation to the initial mass during osmotic dehydration was calculated from experimental data according to Eq. (1):

$$\Delta M = \frac{(m - m_0)}{m_0} \times 100 \quad (1)$$

where m = mass and 0 = initial time ($t = 0$).

Water loss (WL), calcium lactate gain (ΔCaLac), ascorbic acid gain (ΔAA) and sucrose gain (ΔSuc), all calculated in relation to initial mass, are shown in the following equations:

$$WL = \frac{(w_w \cdot m) - (w_{w_0} \cdot m_0)}{m_0} \times 100 \quad (2)$$

$$\Delta CaLac = \frac{w_{CaLac} \cdot m - w_{CaLac_0} \cdot m_0}{m_0} \times 100 \quad (3)$$

$$\Delta AA = \frac{w_{AA} \cdot m - w_{AA_0} \cdot m_0}{m_0} \times 100 \quad (4)$$

$$\Delta Suc = (\Delta M - \Delta W - \Delta CaLac - \Delta AA) \times 100 \quad (5)$$

where m = mass; w = mass fraction (w/w); w = water; CaLac = calcium lactate; AA = ascorbic acid; and 0 = initial time ($t = 0$).

In addition, the calcium gain (ΔCa) can be calculated by:

$$\Delta Ca = \frac{w_{Ca} \cdot m - w_{Ca_0} \cdot m_0}{m_0} \quad (6)$$

To evaluate the influence of the OD parameters on the efficiency of the water removal in relation to sugar impregnation of the apples, the efficiency was defined by the following equation:

$$\text{Efficiency} = \left| \frac{WL}{\Delta Suc} \right| \quad (7)$$

2.5. Microscopic analysis

Histological techniques with vital stains, which do not cause a short-term effect on the cell physiology, were used to evaluate the influence of the osmotic dehydration on cell viability using fluorescence intensity and neutral red accumulation for vacuole integrity in preserved vacuoles. Microscopic analysis was performed on osmotic solutions in the following concentrations: Suc (20%), Suc (30%), Suc (40%), Suc–CaLac (20–2%), Suc–CaLac (30–3%), Suc–CaLac (40–4%), Suc–AA (20–1%), Suc–AA (30–1.5%), Suc–AA (40–2%), Suc–CaLac–AA (20%, 2%, 1%), Suc–CaLac–AA (30%, 3%, 1.5%) and Suc–CaLac–AA (40%, 4%, 2%).

2.5.1. Fluorescein diacetate (FDA) staining

1 mm-thick apple slices were obtained using a sharp scalpel and then treated in the osmotic solutions mentioned above for 2 h. The cell viability test was performed using fluorescein diacetate (FDA, Sigma–Aldrich, USA, λ_{ex} = 495 nm, λ_{em} = 518 nm), as described by Tylewicz, Romani, Widell, and Gómez Galindo (2013) with some modifications. Apple slices were incubated for 30 min in a 10^{-4} M FDA in an isotonic sucrose solution (13%, w/w) in the darkness at room temperature. Fluorescein diacetate is known for its ability to passively penetrate protoplast and to be hydrolyzed by cytoplasmic esterases that produce the polar product fluorescein. This charged form is accumulated intracellularly in viable cells because it is unable to cross cellular membranes that remain intact (Saruyama et al., 2013). Viable cells could be easily identified by a bright fluorescence. Observations were performed under a fluorescent light in a Nikon upright microscope (Eclipse Ti-U, Nikon Co., Japan) equipped with a Nikon digital video camera (digital sight DS-Qi1Mc, Nikon Co., Japan) at a magnification of 20×.

2.5.2. Neutral red staining

Apple tissues were stained using a neutral red dye. Neutral red is a vital stain with a relatively low molecular weight and no electric charge that penetrates the vacuole of the intact protoplast of plant cells. In vacuoles, the neutral red is transformed to an ionic state because of the low pH inside the vacuoles; in this form, neutral red is incapable of penetrating the tonoplast, so the neutral red accumulates in the vacuole. Neutral red stain has been prepared in a concentration of 0.05% (Mauro, Tavares, & Menegalli, 2003; Panarese et al., 2012) in an isotonic sucrose solution at 13% (w/w). Slices (~0.5 mm) cut manually with a sharp scalpel were stained with neutral red for 20 min. Each stained slice was immersed in an osmotic solution for a minimum of 120 min. Slices were placed on a microscopic slide accompanied by a drop of solution and covered with the slide cover. The control slices were solely washed in the isotonic solution. Slides were immediately observed under a light microscope (Optech – Optical Technology, Germany) and recorded at a magnification of 10×. RGB images were acquired using a digital camera (Camedia C-4040-ZOOM, Tokyo, Japan) and stored in JPEG format.

Additionally, slides were recorded at a higher resolution in black and white using a Nikon upright microscope (Eclipse Ti-U, Nikon Co., Japan) without a fluorescent light at a magnification of 20×.

2.6. Time domain nuclear magnetic resonance (TD-NMR)

The proton transverse relaxation time (T_2) of the samples was measured for six replicas in a Bruker The Minispec spectrometer

(Bruker Corporation, Germany), operating at 20 MHz and 24 °C, using the Carr–Purcell–Meiboom–Gill (CPMG) pulse sequence. Fresh or osmotic dehydrated apple cylinders with an 8 mm initial diameter were cut (approximately 10-mm height, 250 mg) to not exceed the active region of the radio frequency coil and placed inside the 10-mm outer diameter NMR tubes. Each measurement comprised 16,000 echoes with a 90–180 interpulse spacing of 100 μs, with 32 scans and a recycle delay of 5 s. The specified instrumental parameters avoided heating the samples and allowed the measurement of the protons with a T_2 between 1 and 2000 ms.

The acquired CPMG curves were normalized by the sample weights and analyzed with the UPEN (uniform penalty inversion of multiexponential decay data) algorithm (Borgia, Brown, & Fantazzini, 1998) to give quasi-continuous distributions of relaxation time. The UPEN default fitting parameters were adjusted to obtain better resolved and more detailed peaks. The number of output relaxation times sampled logarithmically in the 1–2000-ms interval T_2 was set to 200, and the smoothing coefficient beta was increased to 2. However, the resulting T_2 distributions showed partially overlapped peaks. Three proton populations were found in each sample and were ascribed to cell compartment proton pools according to their T_2 and intensity values (Panarese et al., 2012): vacuole, cytoplasm-free space and cell wall. Free spaces are the spaces where the osmotic solution could interpenetrate, i.e., outside the protoplast boundaries.

To obtain quantitative information from the CMPG decay curves, sample signals were fitted using a discrete multi-exponential curve in Eq. (8):

$$S_{(\tau)} = \sum_{i=1}^{N} I_n \exp\left(\frac{-t}{T_{2,n}}\right) + E_{(\tau)} \quad (8)$$

where N is the number of the found protons populations (based on UPEN results, it was set to 3); and I and T_2 are the intensity value and average relaxation time, respectively, of the n proton pool.

The fitting was performed using the "Nonlinear Least Squared" function based on the Gauss–Newton algorithm and implemented in the "R" software (R Foundation for Statistical Computing, Austria), while the I and T_2 starting values were chosen based on the UPEN results.

2.7. Statistical analysis

The significance of the effects of the different osmotic solutions on water loss, sucrose gain, efficiency, transverse relaxation times (T_2) and intensity was evaluated by analysis of variance (ANOVA) and comparison of means using the Duncan test at a 5% probability level. The data were expressed as the mean ± standard deviation.

3. Results and discussion

3.1. Mass transfer: water loss and solid gain

Water loss (Eq. (2)) and sucrose gain (Eq. (5)) during osmotic dehydration of apples treated in different osmotic solutions are shown in Table 1. Samples treated in the sucrose solution show the smallest water loss and high sucrose uptake compared to the other treatments. When AA is added to the sucrose solution, the water loss increases but the sucrose gain also increases, especially during the first 30 min. A consequence of this relationship between the water loss and sugar gain is both the Suc and Suc–AA treatments have a lower process efficiency (Table 1) compared to the Suc–CaLac and Suc–CaLac–AA treatments.

As for the water chemical potential of these solutions, the water activity measured was 0.962 in the sucrose solution (40%), 0.953 in the Suc–CaLac (40–4%), 0.954 in the Suc–AA (40–2%) and 0.944 in the Suc–CaLac–AA (40–4–2%). Consequently, the highest water loss is expected from the Suc–CaLac–AA solution followed by the Suc–CaLac and Suc–AA solutions. Indeed, both the Suc–CaLac and Suc–CaLac–AA solutions promoted greater water loss and did not have significant differences between them. However, when comparing the sucrose gain values between these two treatments, differences were found at 30 and 240 min of the process, as seen in Table 1, which were reflected in the efficiency of these processes. CaLac in solution enhances the efficiency because it is able to promote high water loss and restricts sucrose impregnation, which has been verified by other authors (Mavroudis et al., 2012; Silva et al., 2014a). However, the inhibition in sugar gain is sometimes accompanied by water loss reduction and, hence, a good efficiency is not reached, as verified by Silva et al. (2014a) who exposed pineapple tissue to high concentrations (sucrose 50% solution with 4% CaLac) for 2 h. Barrera et al. (2009) observed that for apples, osmotic dehydration assisted by vacuum impregnation favors solid gain but also reduces water removal. Restriction of solute transport has been attributed to calcium pectate formation, which decreases the cell wall porosity and limits the transport of larger molecules. However, a decrease in the water loss could also be explained by changes in the cellular membranes because calcium can affect the water channel activity (Maurel, 2007). Nevertheless, the significance of the inhibition of plant aquaporins by calcium is complex and has not been clarified, as noted by Maurel (2007), who compared the water permeability of the *Arabidopsis* plasma membrane (Gerbeau et al., 2002) and *Beta vulgaris* roots (Alleva et al., 2006). A low sensitivity to Ca^{2+} was detected in the *Arabidopsis* plasma membrane, but a higher sensitivity was detected in the *B. vulgaris* roots. In the present work, inhibition of Ca^{2+} on water loss was not evident.

In contrast, effect of the addition of AA seems to increase the impregnation of solutes, which is the opposite effect of those promoted by calcium. This was verified by Silva et al. (2014b) and attributed to wall porosity increasing because of acidification (Zemke-White et al., 2000).

During the first 60 min of the Suc–CaLac–AA treatment, the efficiency was high probably because the calcium affected the restriction of the sucrose gain in a similar way to the behavior observed for the Suc–CaLac treatment (Table 1). Then, the efficiency decreased, which suggests that after 1 h of the process, the AA exerted an opposite influence on the sucrose transport. Silva et al. (2014b) also observed that AA positively influenced sucrose and calcium gain in pineapples treated in solutions composed of sucrose, calcium lactate and ascorbic acid. These results suggest that synergetic effects should not be ignored. Genevois, Flores, and De Escalada Pla (2014) fortified pumpkin with vitamin C and iron through a dry infusion process by sprinkling powdered sucrose on the vegetable to form a solution with the lost water from the food. The authors concluded that the addition of Fe or AA to the liquid solution increases the incorporation of sucrose into the pumpkin tissue, but the presence of both additives simultaneously produces an antagonistic effect that diminishes the solid gain.

Good impregnation of Ca and AA contents were observed during the treatments in the Suc–CaLac, Suc–AA and Suc–CaLac–AA solutions. The last solution slightly enhanced the AA and Ca impregnation; the AA content increased after 2 h of process while the Ca content increased after 4 h (Table 2). AA was not detected in the fresh samples. Indeed, very low ascorbic acid content has been previously found in the Pink Lady apples (2.3–3.0 mg/100 g, Castro et al., 2008).

In conclusion, according to mass transport evaluation, the OD efficiency was improved by CaLac, while AA presence exerted an opposite effect; when both additives were present simultaneously,

Table 1
Mean and standard deviation of water loss, sucrose gain and efficiency.

Osmotic solution	30 min	60 min	120 min	240 min
Water loss				
Suc	−9.36^{a} ± 0.50	−13.00*	−15.94^{a} ± 0.85	−24.66^{a} ± 0.13
Suc–CaLac	−12.49^{b} ± 0.86	−14.96^{a} ± 1.00	−22.30^{b} ± 0.68	−28.96^{b} ± 0.63
Suc–AA	−10.45^{a} ± 0.04	−13.61^{a} ± 0.86	−18.99^{ab} ± 0.19	−26.18^{a} ± 1.25
Suc–CaLac–AA	−12.87^{b} ± 0.52	−16.04^{a} ± 1.48	−20.58^{b} ± 2.21	−28.42^{b} ± 0.02
Sucrose gain				
Suc	2.28^{ab} ± 0.12	4.11*	5.51^{a} ± 0.26	6.70^{a} ± 0.05
Suc–CaLac	2.19^{a} ± 0.20	3.39^{a} ± 0.27	4.86^{a} ± 0.22	5.69^{b} ± 0.23
Suc–AA	3.18^{c} ± 0.01	4.11^{a} ± 0.23	4.93^{a} ± 0.06	6.75^{a} ± 0.45
Suc–CaLac–AA	2.61^{b} ± 0.12	3.20^{a} ± 0.41	4.76^{a} ± 0.69	7.41^{a} ± 0.01
Efficiency				
Suc	4.11^{ab} ± 0.43	3.90*	2.90^{a} ± 0.29	3.68^{a} ± 0.05
Suc–CaLac	5.75^{c} ± 0.93	4.44^{a} ± 0.65	4.60^{a} ± 0.35	5.10^{b} ± 0.32
Suc–AA	3.29^{a} ± 0.02	3.32^{a} ± 0.39	3.85^{a} ± 0.09	3.89^{a} ± 0.44
Suc–CaLac–AA	4.94^{bc} ± 0.43	5.08^{a} ± 1.11	4.41^{a} ± 1.10	3.98^{a} ± 0.01

The same letter on the same column means no significant difference by the Duncan test ($p < 0.05$).
* Replica not determined.

Table 2
Mean and standard deviation of calcium and ascorbic acid contents at different osmotic dehydration times and corresponding fresh apple (mg/100 g).

Osmotic solution	0 min (fresh)	30 min	60 min	120 min	240 min
Calcium content					
Suc–CaLac	2.78^{a} ± 0.03	79.80^{b} ± 0.55	110.70^{c} ± 1.88	142.44^{d} ± 0.21	163.45^{e} ± 5.35
Suc–CaLac–AA	2.78^{a} ± 0.03	81.05^{b} ± 4.00	108.57^{c} ± 2.18	140.01^{d} ± 12.75	195.20^{f} ± 8.30
Ascorbic acid content					
Suc–AA	Nd	429.02^{a} ± 13.82	608.88^{b} ± 13.47	733.32^{c} ± 54.61	1012.45^{e} ± 2.87
Suc–CaLac–AA	Nd	393.09^{a} ± 10.13	576.85^{b} ± 8.20	779.50^{d} ± 15.87	1076.53^{f} ± 33.50

The same letter on the same column for each component means no significant difference by the Duncan test ($p < 0.05$);
Nd: not detectable.

AA counterbalanced an initial increase of efficiency caused by calcium, as the OD proceeded. High levels of Ca and AA contents were reached in all treatments and the impregnation of both components was slightly enhanced when they were together in the solution.

3.2. Microscopic analysis

3.2.1. Microphotographs of tissues stained with fluorescein diacetate

Fig. 1 presents slides of apple tissue before and after 2 h of osmotic dehydration in different solutions followed by staining with FDA. For the 20%, 30% and 40% Suc solutions (Fig. 1b.1–b.3), all slides show cell viability with an intensity that was comparable to the fresh tissues (Fig. 1a). Tissues treated in the CaLac–Suc solution presented a higher intensity for the 20% Suc–2% CaLac (Fig. 1c.1) solution. However, as the concentrations of both components increased, the viability decreased, which suggests that the solution with 40% Suc + 4% CaLac (Fig. 1c.3) affected the viability of the cells. A low fluorescence intensity was detected in tissues treated with the Suc–AA treatments in the Suc 20%, AA 1% concentrations (Fig. 1d.1) and no viability at higher concentrations was found (Fig. 1d.2 and d.3). For treatments in the Suc–CaLac–AA solutions, the apple cells did not show any viability (Fig. 1e.1–e.3). If the protoplasts did not retain the FDA, this means disruption of the plasma membrane (cell lysis) or loss of membrane semipermeability (Halperin & Koster, 2006; Koster et al., 2003). The type of membrane injury could be verified by the number of intact protoplasts without ability to retain FDA. However, apples have a poor cytosol content, which makes it difficult to distinguish the protoplasts and vacuoles using light microscopy.

Cellular injury can be caused by low water activity, but all solutions used in these experiments had a relatively high a_w (in a range of 0.944–0.986). Another cause for cellular damage could be the low pH of the osmotic solutions with AA (Zemke-White et al., 2000). For instance, Suc–AA solutions have a pH close to 2.4 and Suc–CaLac–AA solutions near 4.0. Furthermore, it has been demonstrated that AA can cause severe damage in the cellular structure (Qian et al., 2014). Hence, the AA presence in high concentrations certainly affects the cellular membrane structure of plant tissues, but the mechanisms are still not clearly delineated.

3.2.2. Microphotographs of tissues stained with neutral red

Fig. 2 presents slides of apple tissue stained with neutral red, followed by 2 h of osmotic dehydration in different solutions. Fig. 2a shows the control with no osmotic treatment that appeared completely stained. Fig. 2b.1–b.3 represent tissues treated in Suc solutions and show a broad presence of preserved vacuoles and red-stained tissue, probably because neutral red can also provide some contrast to cytoplasm (Carpita et al., 1979). Plasmolysis can be identified by the arrows.

These results agree with cell viability verified by FDA experiments with Suc solution, since, if plasma membranes remain preserved, intact vacuoles must be found.

In Fig. 2c.1–c.3, with tissues treated in Suc–CaLac solutions, vacuoles are well defined. However, the color is not spread out like it was in cells exposed to Suc solutions alone, which suggests that the cytoplasm did not retain the color despite some protoplast viability remaining even in the 30% Suc + 3% CaLac solution (Fig. 1c.2). The possibility that some plasma membranes or tonoplasts have been disrupted is based on the high calcium concentration, which can damage membranes (Wang, Xie, & Long, 2014).

Interestingly, during osmotic dehydration of thin slices previously stained with neutral red, sucrose solutions remained without color but Suc–CaLac solutions changed to red with similar tonality

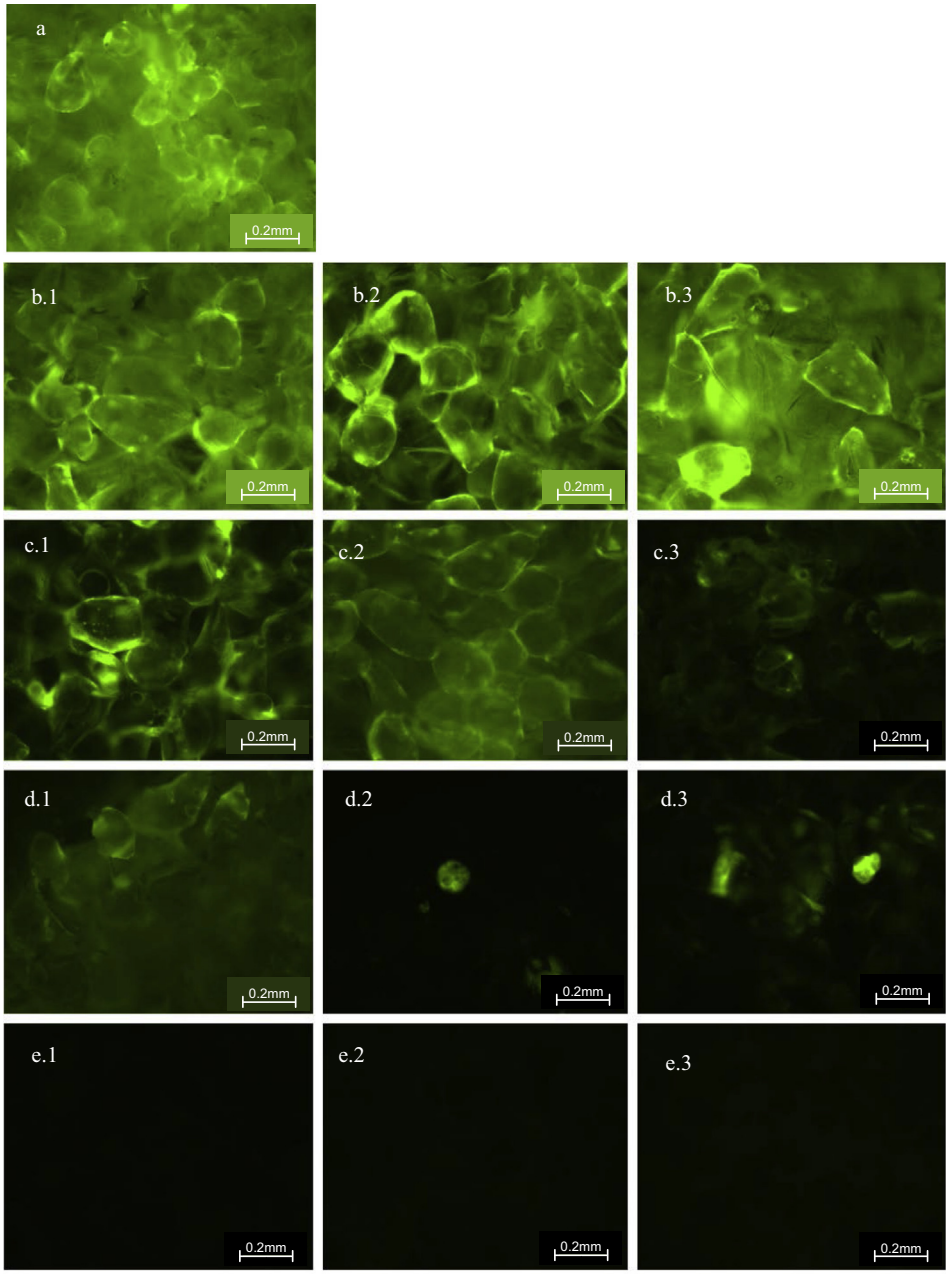

Fig. 1. Slides of parenchyma apple tissue stained with FDA after immersion in osmotic solutions for 120 min: (a) control; (b–e) osmotically dehydrated in osmotic solutions; (b.1) 20% Suc; (b.2) 30% Suc; (b.3) 40% Suc; (c.1) 20% Suc + 2% CaLac; (c.2) 30% Suc + 3% CaLac; (c.3) 40% Suc + 4% CaLac; (d.1) 20% Suc + 1% AA; (d.2) 30% Suc + 1.5% AA; (d.3) 40% Suc + 2% AA; (e.1) 20% Suc + 2% CaLac + 1% AA; (e.2) 30% Suc + 3% CaLac + 1.5% AA; (e.3) 40% Suc + 4% CaLac + 2% AA.

of the neutral red aqueous solution, Suc–AA solutions changed to pink and Suc–CaLac–AA solution changed to intense pink (registers are not shown). This confirms the loss of plasma and/or vacuole membrane permeability, thereby permitting neutral red to leave the tissue.

Effects of the pH of the Suc–CaLac solutions did not seem plausible because the pH of the solutions is nearly neutral. Conversely, tissues treated in the Suc–AA solutions had a complete absence of color, as shown in Fig. 2d.1–d.3. Very low protoplast viability and no stained vacuoles suggest that high AA concentrations and/or very low pH affect the membrane integrity and permeability. Nevertheless, it was a surprise to be able to distinguish some vacuoles without dye (see arrows in Fig. 2d.2 and d.3), which were more visible in images captured at high resolution (Appendix A).

Whether the vacuoles contours are still visible, the membranes exist, but impermeability to a charged form of neutral red must have been lost and the stain left the vacuoles because red contrast was not observed. Moreover, it is known that the loss of plasma membrane semipermeability does not necessary mean cell lyses even though it concerns plasma membranes (Halperin & Koster, 2006), but suggests that tonoplast selectivity must have been modified without complete disruption of the vacuoles.

Finally, treatments in Suc–CaLac–AA solutions showed unexpected results. Although it is possible to visualize vacuoles in Fig. 2e.1–e.3, the cell viability was completely lost in cells that underwent this treatment (Fig. 1e.1–e.3). Because the CaLac addition elevated the pH in comparison to the AA solutions, from 2.4 (Suc–AA) to 4 (Suc–CaLac–AA), it is possible that the tonoplast

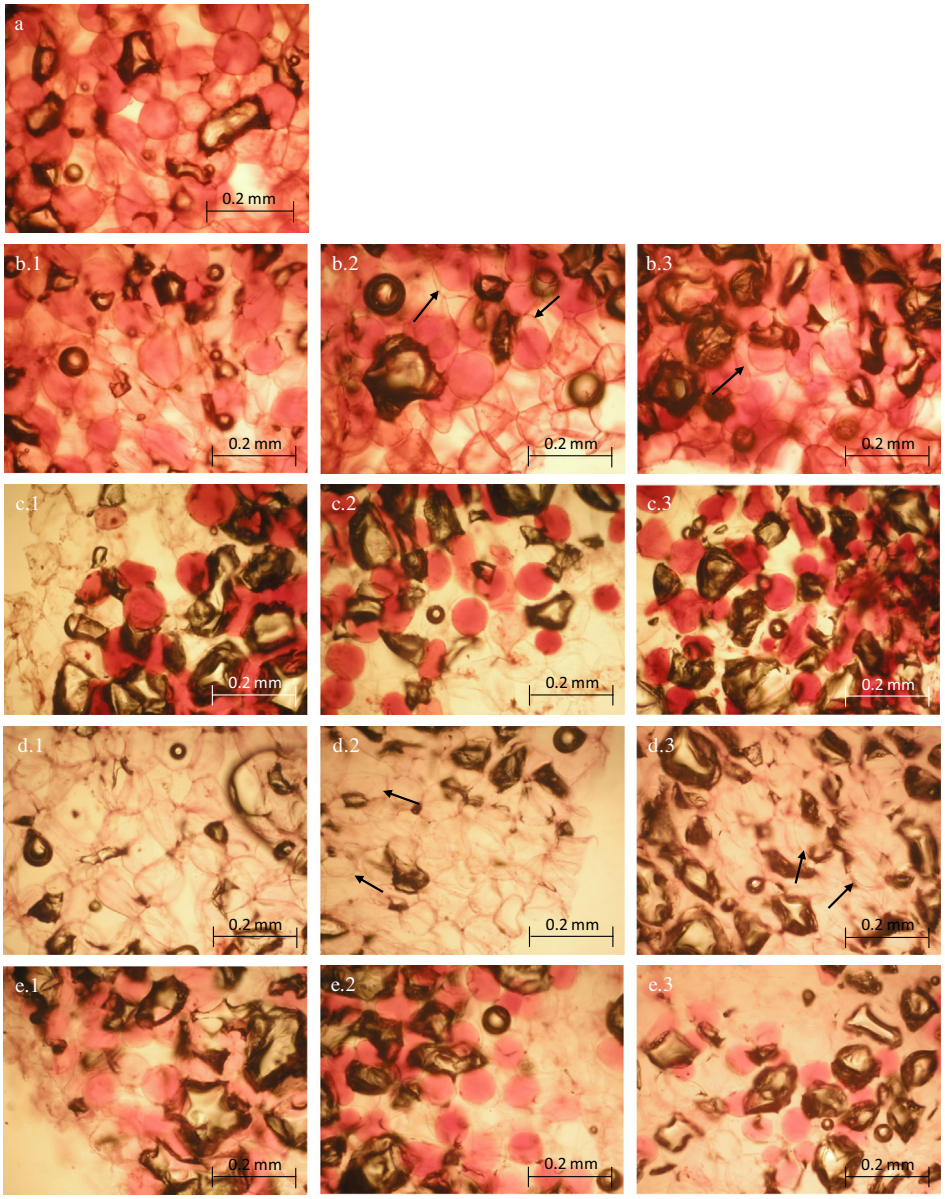

Fig. 2. Slides of apple tissue stained with neutral-red before immersion in osmotic solutions for 120 min: (a) control; (b–e) osmotically dehydrated in osmotic solutions; (b.1) 20% Suc; (b.2) 30% Suc; (b.3) 40% Suc; (c.1) 20% Suc + 2% CaLac; (c.2) 30% Suc + 3% CaLac; (c.3) 40% Suc + 4% CaLac; (d.1) 20% Suc + 1% AA; (d.2) 30% Suc + 1.5% AA; (d.3) 40% Suc + 2% AA; (e.1) 20% Suc + 2% CaLac + 1% AA; (e.2) 30% Suc + 3% CaLac + 1.5% AA; (e.3) 40% Suc + 4% CaLac + 2% AA.

semi permeability was better preserved, so the neutral red remained in some vacuoles. Conversely, plasmalemma was probably damaged due to the low pH and high CaLac and AA concentrations because no viability was detected.

These results show that plasmalemma was more sensitive to Suc–CaLac–AA solutions than tonoplast. AA caused red color absence in the vacuoles but they were visualized in images captured at high resolution, which led to the conclusion that tonoplasts maintained the vacuole content but its permeability was changed. The same inference could not be made for plasmalemma because the low cytoplasm content does not permit one to distinguish this phase.

3.3. Time domain nuclear magnetic resonance (TD-NMR): water mobility

Osmotic dehydration promotes important changes in cellular structure that can affect tissue selectivity and modify water mobility and its distribution through different parts of the cellular tissue.

Water mobility is related to the availability of water and, in this osmo-cellular system, could be modified by concentration of solids or by changes related to sites for hydrogen bonds because of macromolecule structure alteration.

T_2 and relative intensity results are shown in Table 3 and Fig. 3, respectively. Three protons populations were found in each sample at approximately 10, 200 and 1200 ms and were ascribed to cell compartment proton pools based on their T_2 and intensity values: cell wall, cytoplasm-free space and vacuole (Panarese et al., 2012). The free space comprises the plasmolysis space, which forms between the cell wall and plasmalemma, intra- and inter-cellular spaces and interstices in the cell walls (Mauro et al., 2003).

The total signal of raw apples was considered as a reference and set at 100. The intensities of cell wall, cytoplasm-free space and vacuole signals thus corresponded to 2.8 ± 0.4, 20.5 ± 2.3 and 76.7 ± 2.5, respectively. Results related to the water distribution showed a release of water from vacuoles to the cytoplasm-free spaces (Cyt/FS), so that the vacuoles shrank while the Cyt/FS water pools swelled. A more pronounced effect was observed for the

Table 3
Mean and standard deviation of the transverse relaxation time (T_2).

	T_2 (ms)			
	30 min	60 min	120 min	240 min
Vacuole				
Raw (fresh)	$1215.29^{a} \pm 39.78$	$1215.29^{a} \pm 39.78$	$1215.29^{a} \pm 39.78$	$1215.29^{a} \pm 39.78$
Suc	$1134.43^{b} \pm 43.64$	$1115.06^{b} \pm 61.10$	$1091.32^{b} \pm 19.86$	$995.99^{b} \pm 15.66$
Suc–CaLac	$1203.05^{a} \pm 27.62$	$1206.24^{a} \pm 59.40$	$1124.74^{b} \pm 28.35$	$1075.15^{c} \pm 43.15$
Suc–AA	$1147.25^{bc} \pm 24.42$	$1098.85^{b} \pm 24.42$	$1086.37^{b} \pm 19.14$	$1052.85^{c} \pm 44.34$
Suc–CaLac–AA	$1183.82^{ac} \pm 52.40$	$1138.28^{b} \pm 59.85$	$1090.47^{b} \pm 38.97$	$1003.12^{b} \pm 84.20$
Cytoplasm/free space				
Raw (fresh)	$209.19^{a} \pm 23.13$	$209.19^{ab} \pm 23.13$	$209.19^{ab} \pm 23.13$	$209.19^{a} \pm 23.13$
Suc	$211.71^{a} \pm 13.89$	$196.42^{a} \pm 19.73$	$188.18^{a} \pm 15.90$	$193.85^{a} \pm 11.72$
Suc–CaLac	$206.43^{a} \pm 15.90$	$231.98^{b} \pm 21.08$	$229.91^{b} \pm 13.60$	$212.12^{a} \pm 17.92$
Suc–AA	$211.86^{a} \pm 16.19$	$210.36^{ab} \pm 22.63$	$209.23^{ab} \pm 6.96$	$197.26^{a} \pm 12.32$
Suc–CaLac–AA	$210.26^{a} \pm 12.16$	$212.01^{ab} \pm 15.43$	$208.54^{ab} \pm 17.32$	$203.61^{a} \pm 15.69$
Cell wall				
Raw (fresh)	$9.81^{a} \pm 2.42$	$9.81^{a} \pm 2.42$	$9.81^{a} \pm 2.42$	$9.81^{a} \pm 2.42$
Suc	$8.93^{a} \pm 2.41$	$12.91^{b} \pm 4.10$	$10.47^{a} \pm 1.53$	$12.98^{abc} \pm 3.44$
Suc–CaLac	$9.68^{a} \pm 5.00$	$10.90^{ab} \pm 3.09$	$9.81^{a} \pm 6.40$	$15.22^{c} \pm 6.50$
Suc–AA	$8.90^{a} \pm 0.98$	$8.95^{a} \pm 0.85$	$11.05^{a} \pm 2.22$	$10.76^{abc} \pm 3.08$
Suc–CaLac–AA	$11.57^{a} \pm 2.41$	$11.15^{ab} \pm 1.69$	$15.12^{b} \pm 1.81$	$13.52^{bc} \pm 3.22$

The same letter on the same column means no significant difference by the Duncan test ($p < 0.05$).

osmotic treatment with the lowest a_w solution, Sac–CaLac–AA (0.944), than by the Suc–AA (0.954) and Suc–CaLac (0.953) treatments both with similar a_w solution and, finally, by the Suc treatment with the highest a_w solution (0.962) (Fig. 3).

Regarding T_2, while focusing on specific time points, most differences between treatments were insignificant. On the other hand, when T_2 was observed during the redistribution of water proton compartments, trends similar to those observed for signal intensities were registered. In this respect, some aspects should be emphasized. In the treated tissues, the transverse relaxation times T_2 assigned to cytoplasm and free spaces were, in general, very similar to those of raw apples (Table 3). During the first two hours of process in the Suc–CaLac solution, T_2 assigned to vacuoles was greater than those measured in other treatments and close to the raw value. If the water losses are the greatest for this condition (Fig. 1), it is not clear why vacuoles have the highest water mobility once concentration of the vacuole solute content would be expected. A likely explanation is that channels selectivity of the plasma and vacuole membranes for several original cell substances would be different for each osmotic treatment (Maurel, 2007; Peiter et al., 2005; Tapken et al., 2013). In addition, osmotic solutions as well as contact time can affect membrane integrity. Thus, the vacuoles and cytoplasm solute composition and consequent water interactions in these compartments could be different between treatments.

The fact that calcium can traverse both tonoplast and plasmalemma membranes is not ignored. According to Peiter et al. (2005), several classes of Ca^{2+} recently have been identified in plant cells even though not all of the ion channels that underlie these currents have been identified. These authors showed that the TPC1 ('two-pore channel 1') protein, a non-selective channel for Ca^{2+}, encodes a class of Ca^{2+}-dependent Ca^{2+}-release channel known as the slow vacuolar (SV) channel, and they demonstrated that the TPC1 protein is relatively abundant in plant vacuoles. In turn, the plasma membrane cation channels in plant cells have been related to AtGLRs (*A. thaliana* glutamate receptors), proteins that are members of an amino acid receptors family (Tapken et al., 2013). The authors showed that they function as ligand-gated and non-selective cation channels permeable to Ca^{2+}. Consequently, compositional changes involving calcium could influence but not explain the higher water mobility because molecules with low molecular weight have a high capacity to drop water activity.

Still for Suc–CaLac treatments, T_2 assigned to cytoplasm and free spaces increased in relation to the raw material, though not significantly (Table 3). This could mean once again slower compositional changes and modifications of water interactions because calcium limits sucrose entry into the Cyt/FS, as observed by the efficiency obtained from the Suc–CaLac treatment (Table 1). Then, it would be expected that this compartment would have a greater proportion of solutes from the original cell than sucrose arising from the osmotic solution compared to other treatments and, consequently, weaker water interactions than with sucrose during early osmosis. Of course, as osmotic dehydration proceeds, the water chemical potential in each compartment tends to equal those of the osmotic solution.

For cell walls, water mobility practically did not change. However, regarding intensity, the Suc–CaLac treatment promoted a significant reduction in the water amount associated with the wall biopolymers. Roy et al. (1994), investigating changes in the distribution of the anionic binding sites in the cell walls of apples, concluded that calcium could reduce fruit softening by strengthening the cell wall and limiting cell separation through a greater degree of cross-links with pectic acid polymers. An important observation of these authors is that these calcium bindings can restrict access of hydrolytic enzymes or the resulting increase in pH due to Ca could inhibit activity of the wall loosening enzymes that possess acidic pH optima. Nevertheless, T_2 times for the cell wall did not present a pattern, so it would be necessary for more registers because there were great variations between cells (Table 3).

In conclusion, according to TD-NMR results, the Suc treatment seemed to have a lower influence on the cellular compartmentation and functionality, so that a higher vacuole water population and lower cytoplasm-extracellular spaces were observed in comparison with the other treatments. The Suc–CaLac and Suc–AA treatments resulted in similar water populations of vacuoles and cytoplasm. This highlights the presence of the vacuole compartmentation in tissues treated with Suc–AA (Appendix A), although it was not visualized by neutral red staining (Fig. 2d.1–d.3).

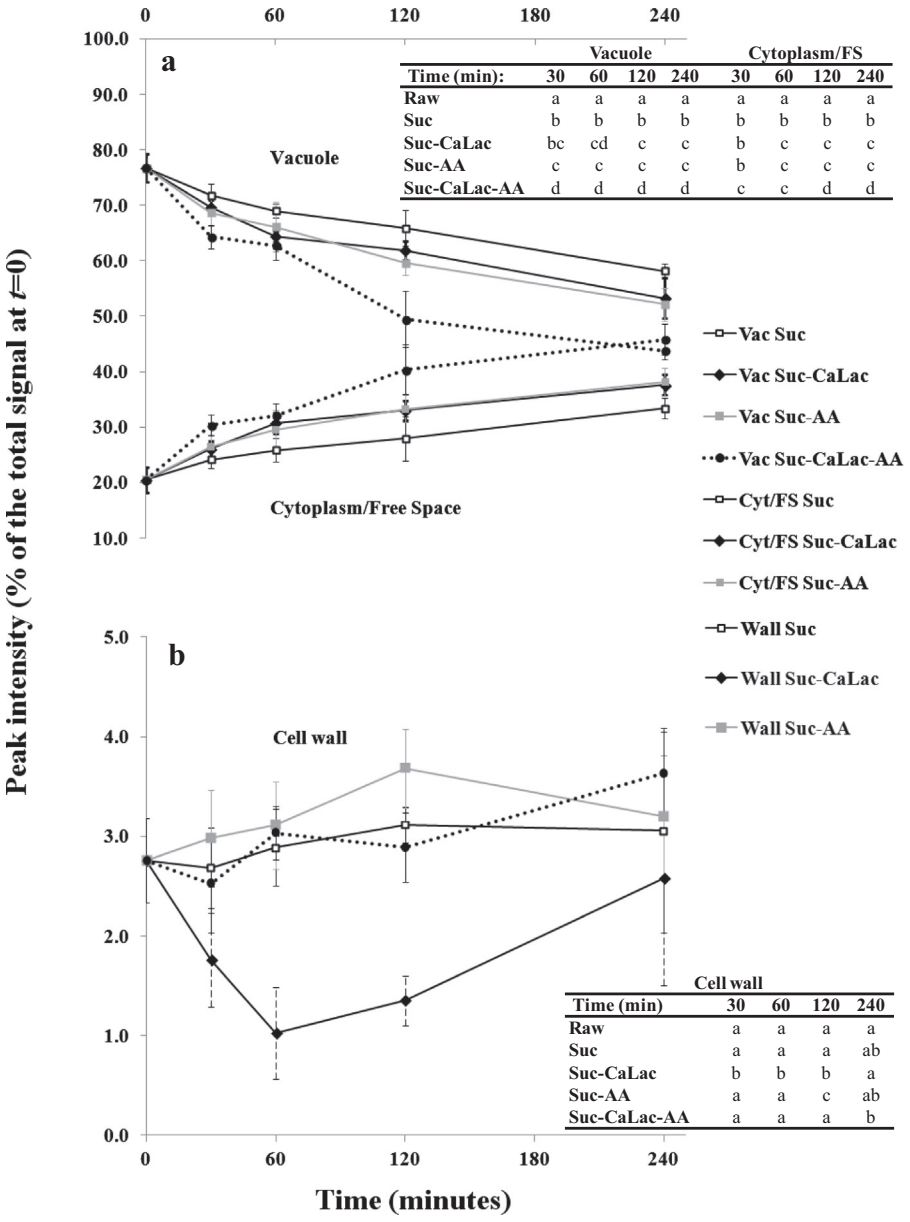

Time (min):	Vacuole 30	60	120	240	Cytoplasm/FS 30	60	120	240
Raw	a	a	a	a	a	a	a	a
Suc	b	b	b	b	b	b	b	b
Suc-CaLac	bc	cd	c	c	b	c	c	c
Suc-AA	c	c	c	c	b	c	c	c
Suc-CaLac-AA	d	d	d	d	c	c	d	d

Time (min)	Cell wall 30	60	120	240
Raw	a	a	a	a
Suc	a	a	a	ab
Suc-CaLac	b	b	b	a
Suc-AA	a	a	c	ab
Suc-CaLac-AA	a	a	a	b

Fig. 3. Peak intensity of the proton pools in different cellular compartments as a function of the osmotic dehydration time, in different osmotic solutions. All the intensities were scaled so that the total signal from fresh samples ($t = 0$) equals 100. (a) Vacuole and cytoplasm plus free space; (b) cell wall. The same letter on the same column in the auxiliary tables means no significant difference by the Duncan test ($p < 0.05$).

4. Conclusions

Sucrose treatments preserved the viability and slightly affected the apple cell structure during OD, as shown by a fluorescence intensity which was comparable to fresh tissue, by a broad presence of red-stained vacuoles and by moderate changes in the water distribution within the cells, according to TD-NMR.

CaLac in the sucrose solution contributed to extended cell viability, and TD-NMR allowed detection of its influence on the cell wall as the proton intensity reduced during the first two hours of the process. In contrast, proton pools related to cell walls expanded in all other treatments. CaLac also enhanced the OD efficiency, which is associated with cell wall pore reduction due to calcium pectate formation.

Only adding AA into the sucrose solution visibly affected the cell membrane permeability by revealing the loss of viability of protoplasts and capacity of retaining vital stain in vacuoles and, simultaneously, the presence of vacuole compartmentation, which was detected by TD-NMR and also by images captured in a high resolution.

AA together with calcium strongly affect the tissue functionality, showing no viability but still some stain retention by vacuoles, and a remarkable water redistribution by vacuole shrinkage and Cyt/FS swelling verified by TD-NMR. Plasmalemma was more sensitive to Suc–CaLac–AA solutions than tonoplast. The presence of AA reduced the process efficiency and enhanced Ca impregnation in the four process hours, which were related to increase the cell wall porosity and change the membrane permeability.

Acknowledgments

The authors acknowledge the financial support of the Italian Ministry for Education, Universities and Research (FIRB, Project RBFR100CEJ: innovative approach for the study of fresh-cut fruit:

qualitative, metabolic and functional aspects). Research work supported by POR-FESR 2007–2013 Emilia-Romagna Region.

Appendix A. Supplementary data

Supplementary data associated with this article can be found, in the online version, at http://dx.doi.org/10.1016/j.foodchem.2015.04.096.

References

Anino, S. V., Salvatori, D. M., & Alzamora, S. M. (2006). Changes in calcium level and mechanical properties of apple tissue due to impregnation with calcium salts. *Food Research International, 39*, 154–164.

Alleva, K., Niemietz, C. M., Sutka, M., Maurel, C., Parisi, M., Tyerman, S. D., et al. (2006). Plasma membrane of *Beta vulgaris* storage root shows high water channel activity regulated by cytoplasmic pH and a dual range of calcium concentrations. *Journal of Experimental Botany, 57*, 609–621.

Alzamora, S. M., Cerrutti, P., Guerrero, S., & López-Malo, A. (1995). Minimally processes fruits by combined methods. In G. V. Barbosa-Cánovas & J. Welti-Chanes (Eds.), *Food preservation by moisture control: Fundamentals and applications* (pp. 463–492). Lancaster: Technomics Publishing.

AOAC – Association of Official Analytical Chemists. (1995). *Official methods of analysis of the association of official analytical chemists* (16th ed., Vol. 1, p. 4). Arlington: Association of Official Analytical Chemists A.O.A.C., chapter 3 (method 985.01).

Barrera, C., Betoret, N., Corell, P., & Fito, P. (2009). Effect of osmotic dehydration on the stabilization of calcium-fortified apple slices (var. Granny Smith): Influence of operating variables on process kinetics and compositional changes. *Journal of Food Engineering, 92*(4), 416–424.

Barrera, C., Betoret, N., & Fito, P. (2004). Ca^{2+} and Fe^{2+} influence on the osmotic dehydration kinetics of apple slices (var. Granny Smith). *Journal of Food Engineering, 65*(1), 9–14.

Borgia, G. C., Brown, R. J. S., & Fantazzini, P. (1998). Uniform-penalty inversion of multiexponential decay data. *Journal of Magnetic Resonance, 132*(1), 65–77.

Carpita, N., Sabularse, D., Montezinos, D., & Delmer, D. P. (1979). Determination of the pore size of cell walls of living plant cells. *Science, 205*, 1144–1147.

Castro, E., Barrett, D. M., Jobling, J., & Mitcham, E. J. (2008). Biochemical factors associated with a CO_2-induced flesh browning disorder of Pink Lady apples. *Postharvest Biology and Technology, 48*(2), 182–191.

Cornillon, P. (2000). Characterization of osmotic dehydrated apple by NMR and DSC. *LWT – Food Science and Technology, 33*(4), 261–267.

Garcia Loredo, A. B., Guerrero, S. N., Gomez, P. L., & Alzamora, S. M. (2013). Relationships between rheological properties, texture and structure of apple (Granny Smith var.) affected by blanching and/or osmotic dehydration. *Food and Bioprocess Technology, 6*(2), 475–488.

Genevois, C., Flores, S., & De Escalada Pla, M. (2014). Effect of iron and ascorbic acid addition on dry infusion process and final color of pumpkin tissue. *LWT – Food Science and Technology, 58*(2), 563–570.

Gerbeau, P., Amodeo, G., Henzler, T., Santoni, V., Ripoche, P., & Maurel, C. (2002). The water permeability of Arabidopsis plasma membrane is regulated by divalent cations and pH. *Plant Journal, 30*(1), 71–81.

Halperin, S. J., & Koster, K. L. (2006). Sugar effects on membrane damage during desiccation of pea embryo protoplasts. *Journal of Experimental Botany, 57*(10), 2303–2311.

Hills, B. P., & Duce, S. L. (1990). The influence of chemical and diffusive exchange on water proton transverse relaxation in plant tissues. *Magnetic Resonance Imaging, 8*(3), 321–331.

Hills, B. P., & Remigereau, B. (1997). NMR studies of changes in subcellular water compartmentation in parenchyma apple tissue during drying and freezing. *International Journal of Food Science and Technology, 32*, 51–61.

Koster, K. L., Reisdorph, N., & Ramsay, J. L. (2003). Changing desiccation tolerance of pea embryo protoplasts during germination. *Journal of Experimental Botany, 54*(387), 1607–1614.

Maurel, C. (2007). Plant aquaporins: Novel functions and regulation properties. *FEBS Letters, 581*(12), 2227–2236.

Mauro, M. A., Tavares, D. Q., & Menegalli, F. C. (2003). Behavior of plant tissue in osmotic solution. *Journal of Food Engineering, 56*, 1–15.

Mavroudis, N. E., Gidley, M. J., & Sjöholm, I. (2012). Osmotic processing: Effects of osmotic medium composition on the kinetics and texture of apple tissue. *Food Research International, 48*(2), 839–847.

Nieto, A. B., Vicente, S., Hodara, K., Castro, M. A., & Alzamora, S. M. (2013). Osmotic dehydration of apple: Influence of sugar and water activity on tissue structure, rheological properties and water mobility. *Journal of Food Engineering, 119*(1), 104–114.

Odriozola-Serrano, I., Hernàndez-Jover, T., & Martìn-Belloso, O. (2007). Comparative evaluation of UV-HPLC methods and reducing agents to determine vitamin C in fruits. *Food Chemistry, 105*, 1151–1158.

Panarese, V., Laghi, L., Pisi, A., Tylewicz, U., Dalla Rosa, M., & Rocculi, P. (2012). Effect of osmotic dehydration on *Actinidia deliciosa* kiwifruit: A combined NMR and ultrastructural study. *Food Chemistry, 132*(4), 1706–1712.

Peiter, E., Maathuis, F. J. M., Mills, L. N., Knight, H., Pelloux, J., Hetherington, A. M., et al. (2005). The vacuolar Ca^{2+}-activated channel TPC1 regulates germination and stomatal movement. *Nature, 434*(7031), 404–408.

Qian, H. F., Peng, X. F., Han, X., Ren, J., Zhan, K. Y., & Zhu, M. (2014). The stress factor, exogenous ascorbic acid, affects plant growth and the antioxidant system in *Arabidopsis thaliana*. *Russian Journal of Plant Physiology, 61*(4), 467–475.

Rocculi, P., Panarese, V., Tylewicz, U., Santagapita, P., Cocci, E., Gómez Galindo, F., et al. (2012). The potential role of isothermal calorimetry in studies of the stability of fresh-cut fruits. *LWT – Food Science and Technology, 49*(2), 320–323.

Roy, S., Conway, W. S., Watada, A. E., Sams, C. E., Pooley, C. D., & Wergin, W. P. (1994). Distribution of the anionic sites in the cell wall of apple fruit after calcium treatment – Quantitation and visualization by a cationic colloidal gold probe. *Protoplasma, 178*(3–4), 156–167.

Saruyama, N., Sakakura, Y., Asano, T., Nishiuchi, T., Sasamoto, H., & Kodama, H. (2013). Quantification of metabolic activity of cultured plant cells by vital staining with fluorescein diacetate. *Analytical Biochemistry, 441*(1), 58–62.

Sereno, A. M., Moreira, R., & Martinez, E. (2001). Mass transfer coefficients during osmotic dehydration of apple in single and combined aqueous solutions of sugar and salt. *Journal of Food Engineering, 47*(1), 43–49.

Silva, K. S., Fernandes, M. A., & Mauro, M. A. (2014a). Effect of calcium on the osmotic dehydration kinetics and quality of pineapple. *Journal of Food Engineering, 134*, 37–44.

Silva, K. S., Fernandes, M. A., & Mauro, M. A. (2014b). Osmotic dehydration of pineapple with impregnation of sucrose, calcium, and ascorbic acid. *Food and Bioprocess Technology, 7*, 385–397.

Tapken, D., Anschütz, U., Liu, L. H., Huelsken, T., Seebohm, G., & Becker, D., et al. (2013). A plant homolog of animal glutamate receptors is an ion channel gated by multiple hydrophobic amino acids. *Science Signaling, 2*, 279, ra47.

Thebud, R., & Santarius, K. A. (1982). Effects of high-temperature stress on various biomembranes of leaf cells in situ and in vitro. *Plant Physiology, 70*, 200–205.

Tyerman, S. D., Niemietz, C. M., & Bramley, H. (2002). Plant aquaporins: Multifunctional water and solute channels with expanding roles. *Plant, Cell and Environment, 25*, 173–194.

Tylewicz, U., Romani, S., Widell, S., & Gómez Galindo, F. (2013). Induction of vesicle formation by exposing apple tissue to vacuum impregnation. *Food and Bioprocess Technology, 6*(4), 1099–1104.

Tylewicz, U., Panarese, V., Laghi, L., Rocculi, P., Nowacka, M., Placucci, G., et al. (2011). NMR and DSC water study during osmotic dehydration of *Actinidia deliciosa* and *Actinidia chinensis* kiwifruit. *Food Biophysics, 6*(2), 327–333.

Vicente, S., Nieto, A. B., Hodara, K., Castro, M. A., & Alzamora, S. M. (2012). Changes in structure, rheology, and water mobility of apple tissue induced by osmotic dehydration with glucose or trehalose. *Food and Bioprocess Technology, 5*(8), 3075–3089.

Wang, Y., Xie, X., & Long, L. E. (2014). The effect of postharvest calcium application in hydro-cooling water on tissue calcium content, biochemical changes, and quality attributes of sweet cherry fruit. *Food Chemistry, 160*, 22–30.

Weig, A., Deswarte, C., & Chrispeels, M. J. (1997). The major intrinsic protein family of Arabidopsis has 23 members that form three distinct groups with functional aquaporins in each group. *Plant Physiology, 114*, 1347–1357.

Zemke-White, W. L., Clements, K. D., & Harris, P. J. (2000). Acid lysis of macroalgae by marine herbivorous fishes: Effects of acid pH on cell wall porosity. *Journal of Experimental Marine Biology and Ecology, 245*, 57–68.

Paper IV

Dellarosa, **N.**, Ragni, L., Laghi, L., Tylewicz, U., Rocculi, P., & Dalla Rosa, M. (2016)

Time domain nuclear magnetic resonance to monitor mass transfer mechanisms in apple tissue promoted by osmotic dehydration combined with pulsed electric fields

Innovative Food Science & Emerging Technologies, 37(*C*), 345-351

Innovative Food Science and Emerging Technologies 37 (2016) 345–351

Contents lists available at ScienceDirect

Innovative Food Science and Emerging Technologies

journal homepage: www.elsevier.com/locate/ifset

Time domain nuclear magnetic resonance to monitor mass transfer mechanisms in apple tissue promoted by osmotic dehydration combined with pulsed electric fields

Nicolò Dellarosa [a,*], Luigi Ragni [a,b], Luca Laghi [a,b], Urszula Tylewicz [a], Pietro Rocculi [a,b], Marco Dalla Rosa [a,b]

[a] Department of Agricultural and Food Sciences, University of Bologna, Cesena, Italy
[b] Interdepartmental Centre for Agri-Food Industrial Research, University of Bologna, Cesena, Italy

ARTICLE INFO

Article history:
Received 16 October 2015
Received in revised form 4 January 2016
Accepted 9 January 2016
Available online 26 January 2016

Keywords:
PEF
Osmotic dehydration
Mass transfer
TD-NMR
Water distribution
Water self diffusion

ABSTRACT

Pulsed electric field (PEF) technology is gaining momentum as a pre-treatment to enhance mass transfer of vegetable tissues obtained by further processing. In this study PEF pre-treatment increased osmotic dehydration (OD) effectiveness, in terms of water loss and solid gain in apples, as a function of electric field strength and number of pulses. Mass transfer was particularly high when average electric fields of 250 and 400 V cm^{-1} were applied. Time domain nuclear magnetic resonance (TD-NMR), with the use of a contrast agent, clarified structural changes that drive mass transfer. Treatments at 100 V cm^{-1} redistributed water between vacuole, cytoplasm and extracellular space, while at 250 and 400 V cm^{-1} the membrane breakages caused the loss of cellular compartmentalization. Two non-destructive and fast acquirable parameters, the longest measured relaxation time (T_2) and water self diffusion coefficient (D_w), allowed the separate and accurate observation of PEF treatment and osmotic dehydration effects.

Industrial relevance: The developed non-destructive method, here described, allows the measure of the effects of PEF treatment on apple tissue which can be exploited to have reliable control of the process within minutes. Since mass transfer parameters depend on subcellular water redistribution, the present work provides a tool to boost the development and optimization of agri-food processes on fresh vegetable tissues.

© 2016 Elsevier Ltd. All rights reserved.

1. Introduction

Pulsed electric field (PEF) is an innovative non-thermal technology which delivers short pulses to food products, placed between two electrodes, generating electric fields, which usually span from 0.1 to 5 kV cm^{-1}. When coupled to extraction techniques, its application leads to an enhancement of mass transfer phenomena, which can be exploited to increase extraction yields from vegetable tissues (Donsì, Ferrari, & Pataro, 2010). In addition, its effectiveness has been demonstrated by combining PEF together with osmotic dehydration (Ade-Omowaye, Angersbach, Taiwo, & Knorr, 2001; Amami, Vorobiev, & Kechaou, 2006; Wiktor, Śledź, Nowacka, Chudoba, & Witrowa-Rajchert, 2014), air drying (Ade-Omowaye, Rastogi, Angersbach, & Knorr, 2003; Wiktor et al., 2013), compression (Bazhal, Lebovka, & Vorobiev, 2001) and thermal treatments (Lebovka, Praporscic, Ghnimi, & Vorobiev, 2005; Parniakov, Lebovka, Bals, & Vorobiev, 2015).

The application of PEF on vegetable tissue acts on the membrane permeability, inducing electroporation of cells (Teissie, Eynard, Gabriel, & Rols, 1999). The mechanism of electroporation includes different steps: polarization of membranes, creation of pores, expansion of pore radii and resealing of pores (Donsì et al., 2010; Vorobiev & Lebovka, 2008). In addition to the type of fruit and vegetable tissue, the extent of electroporation, especially the resealing of pores, which can last from seconds to hours, depends on the applied electric field strength, duration, number and shape of pulses, and interval between pulses. It is of practical importance that the application of electric fields lower than 1 kV cm^{-1}, and a total treatment time in the order of milliseconds, do not significantly contribute to a temperature increase, which would alter membrane permeability caused by heat related damages (Lebovka, Bazhal, & Vorobiev, 2002) and the quality of the obtained products.

In mass transfer applications, PEF effects on vegetable tissues are generally evaluated by the extraction yields, or by the release of some target compounds (Soliva-Fortuny, Balasa, Knorr, & Martín-Belloso, 2009). The measurement of the apparent diffusion coefficient, often compared to untreated and totally destroyed samples, is another index of macroscopic changes. This method has the drawback of being indirect and invasive, leading to inconsistent results due to possible modification of the structure of the tissue (Vorobiev, Jemai, Bouzrara, Lebovka, & Bazhal, 2005). Alternatively, changes of color and texture are also controlled as a side effect of PEF treatment, being even desirable, for instance, when material softening is the objective of the study (Lebovka,

* Corresponding author.
E-mail address: nicolo.dellarosa@unibo.it (N. Dellarosa).

http://dx.doi.org/10.1016/j.ifset.2016.01.009
1466-8564/© 2016 Elsevier Ltd. All rights reserved.

Praporscic, & Vorobiev, 2004). Direct effects on membrane permeabilization can be qualitatively observed by staining of plant tissues followed by microscope visualization (Fincan & Dejmek, 2002). However, the most commonly applied method to measure cell disintegration is based on changes in electrophysical properties, i.e. the impedance, that gives information on the damage degree of a sample when compared to both an untreated and a totally destroyed sample (Angersbach, Heinz, & Knorr, 1999; Lebovka et al., 2002).

Time domain nuclear magnetic resonance (TD-NMR) is a fast, non-destructive analytical technique that allows to evaluate spatial features in vegetable cellular compartments by the indirect measurement of water distribution inside and outside cells. Recently, the measurement of transverse relaxation time (T_2) curves has been successfully applied to study the subcellular water redistribution upon osmotic dehydration, its combination with ultrasound in kiwifruit (Nowacka, Tylewicz, Laghi, Dalla Rosa, & Witrowa-Rajchert, 2014; Tylewicz et al., 2011) and the addition of calcium and ascorbic salts to the osmotic solution in apple tissue (Mauro et al., 2015). Furthermore, through the evaluation of the water self diffusion coefficient, an overview of water possibility to explore the surrounding space can be achieved. Santagapita et al. (2013) found that water loss and solid gain, during the osmotic treatment of kiwifruit, were in good agreement with the reduction of the water self diffusion coefficient.

The present work evaluated the effect of PEF on apple tissue as preliminary treatment to osmotic dehydration, at three different electric field strengths (100, 250 and 400 V cm^{-1}) and total number of pulses (20 and 60 train series). Besides the control of the mass transfer parameters water loss and solid gain, a subcellular level observation was applied by means of TD-NMR to understand, in-depth, the PEF-induced mechanisms that affect mass balances. Differently from previous works, the transverse relaxation time (T_2) of the osmotic solution was selectively dropped by the addition of a contrast agent. This eased the discrimination of three characteristic cellular compartments, namely vacuole, cytoplasm and extracellular space, respectively delimited by plasma membrane and tonoplast. Moreover, once the membrane permeability was altered due to electroporation, the contrast agent was a key element to observe the external solution diffusing through the inner compartments of apples. In addition, the average water self diffusion coefficient (D_w) of water contained in apple tissue was evaluated as a non-destructive control tool for the osmotic dehydration process.

2. Material and methods

2.1. Material

Apples (*Malus domestica*) of the Cripps Pink variety, also known by the brand name Pink Lady®, were purchased at a local market and stored at 2 ± 1 °C for no longer than a month, within which experiments were run. Average moisture and soluble solid contents were, respectively, 83.5 ± 0.5 g and 14.0 ± 0.5 g per 100 g of fresh product (g_{fw}). The apples were cut with a manual cork borer and cutter to obtain cylinders of 8 mm diameter and a length of 10 mm.

2.2. Pulsed electric field (PEF) treatment

Pulsed electric field (PEF) treatments were applied to apple cylinders using an in-house developed pulse generator equipment based on MOSFET technology and on capacitors as energy tank. The PEF generator provides monopolar pulses of near-rectangular shape at different voltages, adjustable repetition time between pulses and variable total treatment duration which lead to a variable number of delivered pulses. Treatments were run at 20 °C in a 30 × 20 × 20 mm (length × width × height) chamber equipped with two stainless steel electrodes (active contact surface = 20 × 20 mm^2) with a distance between them fixed at 30 mm. For each treatment 12 apple cylinders (approximately 5 g) were inserted into the chamber with the two circle sides parallel to the electrodes (Fig. 1). The chamber was filled up with tap water, with an electrical conductivity of 328 ± 4 μS cm^{-1} at 25 °C, with product-to-water ratio around 1:1 (v/v).Table 1 shows the experimented pulse series and the average applied electric field strengths in the chamber of trials conducted at fixed pulse width (100 ± 2 μS) and repetition time (10.0 ± 0.1 ms) with a voltage of 300 V, 750 V, and 1200 V to the electrodes. The current and voltage values were registered by using a digital oscilloscope (PicoScope 2204a, Pico Technology, UK) connected to a personal computer.

2.3. Osmotic dehydration (OD) and mass transfer control

Immediately after PEF application, the treated apple cylinders were removed from the PEF treatment solution and placed into 7 different beakers containing a continuously stirred 30% (w/w) sucrose osmotic solution, in a product-to-solution ratio of approximately 1:20 (w/w), to avoid changes in the concentration of the solution during the treatment. The rotational speed was experimentally determined to assure negligible resistance to mass transfer. Besides, control samples were prepared by directly placing the apple cylinders into the osmotic solution without PEF pre-treatment. Iron (III) chloride (Sigma-Aldrich — Steinheim, Germany) was employed as a contrast agent for NMR analysis and added to the osmotic solution to obtain a final concentration of 0.01 M. Samples were collected 0 (fresh control), 15, 30, 60 and 120 min after the immersion, blotted with absorbing paper, weighted and analyzed. The moisture content of 3 apple cylinders (weighing approximately 1.5 g) of fresh and treated samples was determined gravimetrically by drying at 70 °C until a constant weight was achieved, as recommended for fruit products by AOAC International (2002). In parallel, the same experimental plan (Table 1) was run by replacing the osmotic treatment with an isotonic solution, to gain insight of mass transfer phenomena caused by PEF only, without an external osmotic driven force.

Mass transfer was evaluated by calculating the mass balances, in terms of mass variation, water loss and solid gain. The total mass variation (ΔM) in relation to the initial mass during osmotic dehydration was calculated from experimental data according to Eq. (1):

$$\Delta M = \frac{(m - m_0)}{m_0} \quad (1)$$

where m = mass and m_0 = mass at initial time (t = 0).

Water loss (ΔM_w) and solid gain (ΔM_s) were calculated in relation to the initial mass according to Eqs. (2) and (3), respectively:

$$\Delta M_w = \frac{(w \cdot m - w_0 \cdot m_0)}{m_0} \quad (2)$$

$$\Delta M_s = \Delta M - \Delta M_w \quad (3)$$

where w = water content and w_0 = water content at initial time (t = 0).

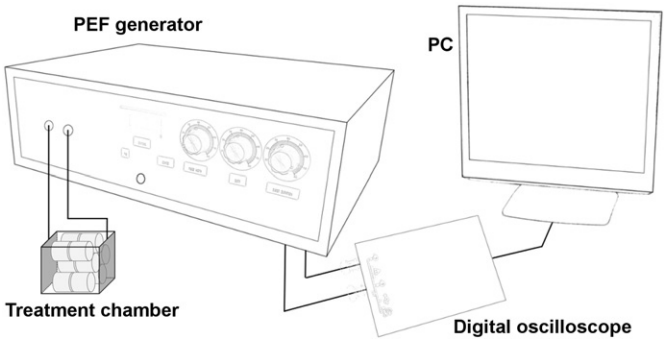

Fig. 1. Layout of the experimental setup.

Table 1
Experimental plan: sample codes and process parameters.

Sample code	Electric field ($V\ cm^{-1}$)	Number of pulses (n)	Applied energy to apple ($J\ kg^{-1}$)
NoPEF	0	0	0
20p100	100	20	8 ± 1
20p250	250	20	55 ± 1
20p400	400	20	135 ± 4
60p100	100	60	23 ± 1
60p250	250	60	164 ± 3
60p400	400	60	382 ± 36

Note: applied energy values are means, expressed as J per kg of fresh product, ± standard deviations ($n = 3$). Electric field is given as the average value for the treatment chamber with electrodes spaced 3 cm.

2.4. Time domain nuclear magnetic resonance (TD-NMR)

2.4.1. Transverse relaxation time curve measurement

Proton transverse relaxation time (T_2) decay was measured for each sample immersed in both the isotonic and osmotic solutions by applying the CPMG pulse sequence (Meiboom & Gill, 1958) using a Bruker 'The Minispec' spectrometer (Bruker Corporation, Germany) operating at 20 MHz. Apple cylinders were collected from the solutions, placed into 10-mm diameter NMR tubes and directly analyzed. Each measurement comprised 6000 echoes, with an interpulse spacing of 0.3 ms and a recycle delay of 10 s which allowed the measurement of proton decays included between 1 and 3000 ms and avoided sample overheat. Each acquisition was performed over 8 scans giving rise to a total time of analysis around 90 s.

The registered spectra were normalized to unitary area and analyzed by UpenWin software (Borgia, Brown, & Fantazzini, 1998) to give quasi-continuous distributions of relaxation time. The number of output relaxation times, sampled logarithmically in the 1–3000 ms range, was set to 100. To obtain quantitative information from the T_2-weighted decay curves, signals were fitted using a discrete multi-exponential curve. The fitting was run using the 'Levenberg–Marquardt nonlinear least-squares' algorithm implemented in 'R' software (R Foundation for Statistical Computing, Austria), according to Eq. (4):

$$S_{(t)} = \sum_{i=1}^{N} I_n \exp\left(\frac{-t}{T_{2,i}}\right) + E_{(t)} \quad (4)$$

where N = number of proton populations, which was set at 3 (vacuole, cytoplasm and extracellular space) according to UPEN results, I = signal intensity, T_2 = average relaxation time of each proton population (n) and E = residual error.

2.4.2. Water self-diffusion coefficient measurement

Water self-diffusion coefficient (D_w) was measured by means of pulsed magnetic field gradient spin echo (PGSE) sequence (Stejskal & Tanner, 1965). The sequence implemented in the Bruker 'The Minispec' spectrometer software allowed to apply a magnetic field gradient spanning from 0.04 to 2.00 T m^{-1} which was calibrated by using pure water with a known D_w value of $2.3 10^{-9}$ $m^2\ s^{-1}$ at 25 °C (Holz, Heil, & Sacco, 2000). To allow a comparison between the samples treated using different applied energies, the water inside the apple tissue was considered as characterized by a single self diffusion coefficient (D_w) according to Eq. (5) (Santagapita et al., 2013):

$$\ln \frac{A_G}{A_{G0}} = -\gamma^2 D_w \delta^2 \left(\Delta - \frac{1}{3}\delta\right) G^2 \quad (5)$$

where A_G = amplitude of PGSE with the applied gradient (G = 1 T m^{-1}), A_{G0} = amplitude of PGSE without the gradient, γ = proton gyromagnetic ratio, δ = gradient length set at 0.5 ms, and Δ = time between the gradients fixed at 7.5 ms.

2.5. Statistical analysis

To evaluate whether PEF pre-treatment significantly enhanced mass transfer during osmotic treatment, the analysis of variance (ANOVA) and Tukey multiple comparisons were applied, by accepting the significance level of 95% ($p < 0.05$). All the experiments were conducted in triplicate and the results were expressed as mean ± standard deviation of replications.

3. Results and discussion

3.1. Mass transfer

Immediately after PEF application, the treated apple cylinders appeared similar to the raw material. No loss of material was noticed, although the samples treated at 250 and 400 V cm^{-1} seemed to partially lose the original hardness of the apple tissue. Nevertheless, the pulsed electric fields applied as a pre-treatment for osmotic dehydration overall enhanced the mass transfer between apple tissue and the osmotic solution. Fig. 2 shows, indeed, water loss and solid gain of the samples treated at different voltages with trains of 60 pulses in comparison with control untreated samples. The numeric scores and statistical analysis for each treatment are shown in Table 2.

The measured initial water content of untreated apples (0.835 ± 0.005 g g_{fw}^{-1}) decreased by a minimum of 3.2 ± 0.1% (after 15 min) to a maximum of 15.8 ± 0.4% (after 120 min). During the first 15 min from the beginning of the osmotic treatment, water loss significantly increased when either the highest field strength (400 V cm^{-1}) or the combination medium field strength (250 V cm^{-1}) and 60 pulses were applied. As an example, the treatment with 400 V cm^{-1} 20 pulses led to a water loss of 4.6 ± 0.6%, while 60 pulses boosted this value to 6.7 ± 0.1%. Taking into account the whole osmotic process, both voltage and the number of pulses positively influenced the water loss. Indeed, at the end of the experimental trial (120 min), the untreated apple samples reached the water loss of 15.8 ± 0.4% while 20 pulses at 250 and 400 V cm^{-1} resulted in higher values, spanning from 20.1% to 20.2% and 60 pulses at the same field strengths led to the highest water

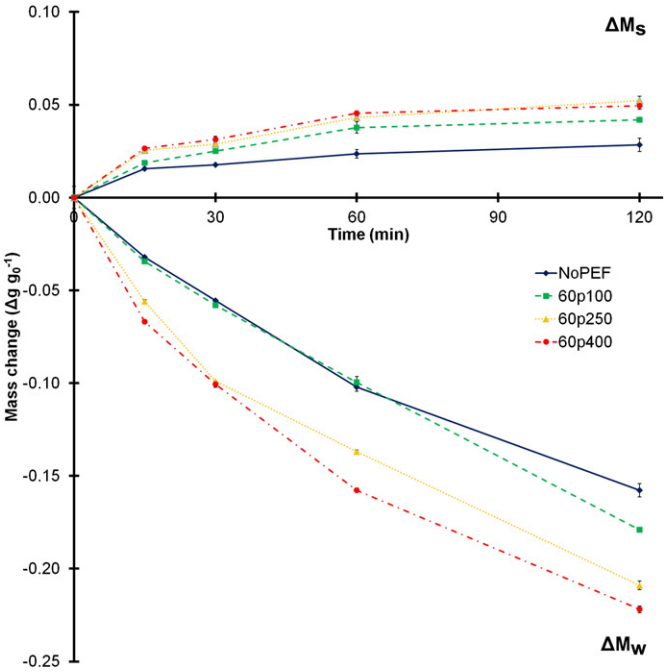

Fig. 2. Mass changes in terms of water loss (ΔM_w) and solid gain (ΔM_s) of PEF pre-treated samples with 60 pulses at different voltages throughout 120 min. Results are expressed as means ± standard deviation.

Table 2
Effect of pulsed electric fields combined with osmotic treatment on water loss and solid gain.

Osmotic treatment	15 min	30 min	60 min	120 min
Water loss				
NoPEF	$-0.032^{ab} \pm 0.001$	$-0.055^{b} \pm 0.001$	$-0.102^{b} \pm 0.002$	$-0.158^{b} \pm 0.004$
20p100	$-0.022^{a} \pm 0.003$	$-0.037^{a} \pm 0.004$	$-0.084^{a} \pm 0.002$	$-0.144^{a} \pm 0.002$
20p250	$-0.030^{ab} \pm 0.004$	$-0.081^{c} \pm 0.002$	$-0.129^{c} \pm 0.003$	$-0.201^{d} \pm 0.005$
20p400	$-0.046^{cd} \pm 0.006$	$-0.093^{d} \pm 0.001$	$-0.146^{d} \pm 0.002$	$-0.200^{d} \pm 0.001$
60p100	$-0.034^{bc} \pm 0.001$	$-0.058^{b} \pm 0.001$	$-0.099^{b} \pm 0.003$	$-0.179^{c} \pm 0.001$
60p250	$-0.056^{de} \pm 0.001$	$-0.099^{d} \pm 0.001$	$-0.137^{c} \pm 0.001$	$-0.209^{d} \pm 0.002$
60p400	$-0.067^{e} \pm 0.001$	$-0.101^{d} \pm 0.002$	$-0.158^{e} \pm 0.001$	$-0.222^{e} \pm 0.002$
Solid gain				
NoPEF	$0.016^{a} \pm 0.001$	$0.018^{c} \pm 0.001$	$0.024^{b} \pm 0.002$	$0.028^{d} \pm 0.004$
20p100	$0.023^{a} \pm 0.003$	$0.036^{a} \pm 0.004$	$0.039^{a} \pm 0.002$	$0.041^{c} \pm 0.002$
20p250	$0.022^{a} \pm 0.004$	$0.029^{ab} \pm 0.002$	$0.043^{a} \pm 0.003$	$0.051^{abc} \pm 0.005$
20p400	$0.024^{a} \pm 0.006$	$0.031^{ab} \pm 0.001$	$0.037^{a} \pm 0.002$	$0.054^{a} \pm 0.001$
60p100	$0.019^{a} \pm 0.001$	$0.025^{bc} \pm 0.001$	$0.038^{a} \pm 0.003$	$0.042^{bc} \pm 0.000$
60p250	$0.025^{a} \pm 0.001$	$0.029^{ab} \pm 0.001$	$0.043^{a} \pm 0.001$	$0.052^{ab} \pm 0.002$
60p400	$0.026^{a} \pm 0.001$	$0.031^{ab} \pm 0.002$	$0.045^{a} \pm 0.001$	$0.049^{abc} \pm 0.002$

Results are means expressed as Δg per $g_0(\text{time} = 0) \pm$ standard deviations and different letters show significant differences ($p < 0.05$) between treatments for each sampling time.

removal, around 20.9%–22.2%. This shows, in agreement with previous works (Amami et al., 2006; Parniakov et al., 2015; Wiktor et al., 2014), that the initial electroporation effect caused by PEF lasted for several minutes after application (Ade-Omowaye, Talens, Angersbach, & Knorr, 2003).

Similarly to water loss, solid gain showed an increased rate when PEF was applied. In detail, while the control samples gained 2.8 ± 0.4% of solid content in 2 h treatment, each PEF pre-treated sample reached a 4%–5% gain. Interestingly, the samples treated at the lowest field (100 V cm^{-1}) showed a similar behavior to the samples treated at higher fields, especially when a 60 pulse train was chosen. Indeed, the application of 60 pulses increased both solid gain and water loss after 120 min (Fig. 2 and Table 2) when compared to control even though the water removal was lower than the sample which underwent to 250 and 400 V cm^{-1} treatments. In the same way, some authors found that 100 V cm^{-1} were also able to improve mass transfer, in terms of juice extraction yields during the compression of apple tissue (Bazhal et al., 2001) and diffusion coefficient measured in apple discs (Jemai & Vorobiev, 2002). Although some studies on apple tissue highlighted that the number of pulses does not affect the mass transfer (Taiwo, Angersbach, & Knorr, 2003; Wiktor et al., 2014), the present study showed that the number of pulses had a significant effect. This difference can be probably ascribed to the different electric field strengths which were applied in the present work, lower than the other studies.

3.2. Water distribution and self diffusion

To gain insight into the mechanisms which drive mass transfer phenomena, TD-NMR was employed by registering T_2-weighted curves. Since the T_2 of protons depends on chemical exchange among water, solutes and biopolymers (Hills & Remigereau, 1997; Santagapita et al., 2013), this allowed the separate observation on raw apple tissue of extracellular space, cell wall, cytoplasm and vacuole, together with their modifications upon technological treatments (Mauro et al., 2015). In raw material, water was found to be distributed as follows: 77.5 ± 1.7% in vacuole (T_2 1391 ± 45 ms), 18.5 ± 1.5% (T_2 282 ± 25 ms) in cytoplasm/extracellular space and 4.0 ± 0.4% (T_2 17 ± 3 ms) was ascribed to the structural water of cell wall.

A preliminary study on osmotic dehydration showed that the T_2 of osmotic solution entering the extracellular space was similar to the one of the cytoplasm. In order to observe the two compartments separately this prompted us to lower the T_2 of the osmotic solution by means of iron (III) chloride, which therefore acted as a contrast agent. A concentration of 0.01 M was chosen in order to equal the T_2 of the cell wall, typically non-sensitive to technological treatments (Nowacka et al., 2014; Santagapita et al., 2013). Higher iron (III) chloride concentrations were discarded because they were leading to T_2 values lower than the instrument limits (Van Duynhoven, Voda, Witek, & Van As, 2010).

The continuous line in Fig. 3a shows the T_2-weigthed signal distribution of untreated apple tissue upon 120 min of dipping in isotonic solution. Besides the peak ascribable to the extracellular space solution, set to 12 ms with the addition of the contrast agent, vacuole and cytoplasm signals, centered around 200 and 1200 ms as in the raw apples, demonstrated that the contrast agent itself was not able to passively diffuse through the native intact plasma membranes. The osmotic dehydration without any PEF pre-treatment (continuous line in Fig. 3b) led to a partial water removal from the inner cellular compartments toward the external space so that, after 120 min, the T_2 of the extracellular space was slightly increased, resulting in a peak around 50 ms. This was due to the partial dilution promoted by the shrinkage of the inner compartments, which have a higher T_2, leading to a higher mean value of the extracellular population. As expected, the relative area of the vacuole peak, i.e. its water content, also showed a marked reduction after osmotic treatment.

The non-continuous lines of Fig. 3a allow to appreciate the water redistribution caused only by the application of the external electric field, in absence of any osmotic driven force, while Fig. 3b shows the joint contribution of PEF and OD treatments on water redistribution. Taking into account PEF treatments alone, the application of medium and high voltages (250 and 400 V cm^{-1}) led the extracellular space, cytoplasm and vacuole signals to collapse into a single broad proton population. This highlighted that the membranes were electrically damaged with the consequent loss of any compartmentalization. After PEF treatment at 100 V cm^{-1}, conversely, the structure was still apparent. Nevertheless, the vacuole/extracellular ratio was lower than the NoPEF sample as a consequence of the reduction of the vacuole population shown in Fig. 3a and b. This behavior suggested that electroporation took place but its effect was probably reversible. Fine tuning of the applied voltage allowed finding the no-reversibility threshold at around 150 V cm^{-1} with 60 train pulses (data not shown).

Table 3 offers a complete view of water distribution among cell compartments in case of osmotic dehydration, with and without a 100 V cm^{-1} PEF pre-treatment. Electrical pre-treatment using 60 pulses led to significantly higher vacuole shrinkage than control throughout the entire osmotic process, increasing the relative water content of both cytoplasm and extracellular spaces. This water rearrangement caused a vacuole T_2 decrease that can be qualitatively visualized from Fig. 3b, which was far less pronounced than what expected in case of contrast agent entrance. The two joint pieces of information strongly suggest that the treatment at 100 V cm^{-1} did not induce the permeabilization of the plasma membrane, but led to damages to tonoplast,

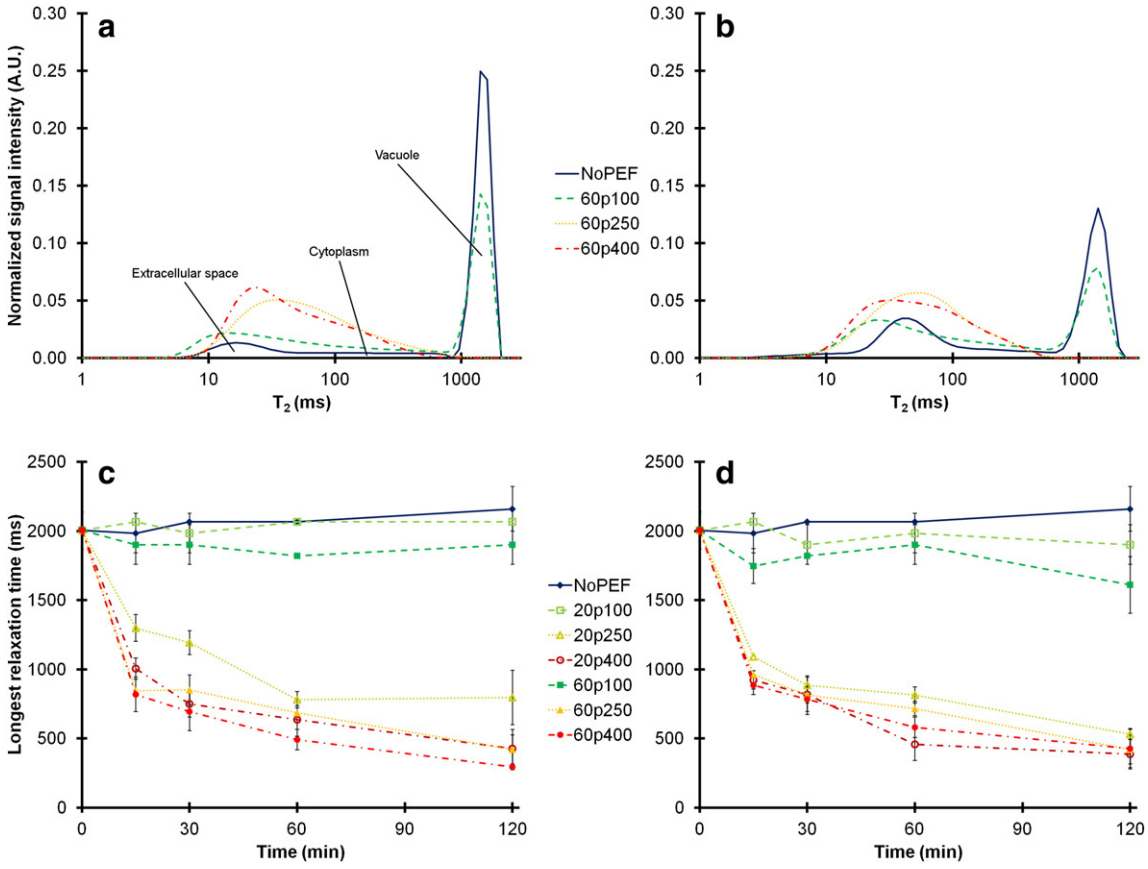

Fig. 3. T_2-weighted signal distribution, normalized to unitary area, of PEF pre-treated samples with 60 pulses at different voltages after 120 min in isotonic (a) and hypertonic (b) solutions. Longest relaxation time expressed as means ± standard deviation of samples after 120 min in isotonic (c) and hypertonic (d) solutions.

which surrounds vacuole, probably because it is more sensitive to electric fields. This water migration from the internal cellular compartments can explain the increase of mass transfer phenomena which were noticed both in the present work and in previous studies which applied moderate electric fields (Sensoy & Sastry, 2004; Vorobiev et al., 2005).

From an industrial point of view, it is important to highlight that after each of the tested treatments water distribution among cell compartments showed that PEF effects were time-dependent. This is in agreement with previous studies based on a macroscopic evaluation of mass transfer (Ade-Omowaye, Talens, et al., 2003; Angersbach, Heinz, & Knorr, 2002). This suggests that time after treatment can be a fundamental factor to be considered in order to optimize PEF application in a combined multi step manufacturing process.

Table 3
Water redistribution in sample treated at 100 V cm^{-1}.

	15 min	30 min	60 min	120 min
Extracellular space				
NoPEF	$0.066^{b} \pm 0.009$	$0.062^{a} \pm 0.003$	$0.082^{c} \pm 0.010$	$0.117^{b} \pm 0.007$
20p100	$0.097^{a} \pm 0.010$	$0.097^{a} \pm 0.010$	$0.132^{b} \pm 0.008$	$0.250^{a} \pm 0.022$
60p100	$0.102^{a} \pm 0.015$	$0.107^{a} \pm 0.005$	$0.172^{a} \pm 0.015$	$0.250^{a} \pm 0.009$
Cytoplasm				
NoPEF	$0.231^{b} \pm 0.018$	$0.248^{a} \pm 0.028$	$0.300^{a} \pm 0.039$	$0.307^{b} \pm 0.046$
20p100	$0.274^{ab} \pm 0.041$	$0.337^{a} \pm 0.041$	$0.353^{a} \pm 0.039$	$0.329^{ab} \pm 0.027$
60p100	$0.338^{a} \pm 0.048$	$0.373^{a} \pm 0.073$	$0.424^{a} \pm 0.068$	$0.493^{a} \pm 0.107$
Vacuole				
NoPEF	$0.703^{a} \pm 0.016$	$0.690^{a} \pm 0.031$	$0.619^{a} \pm 0.030$	$0.576^{a} \pm 0.046$
20p100	$0.629^{ab} \pm 0.031$	$0.565^{ab} \pm 0.050$	$0.515^{ab} \pm 0.047$	$0.422^{ab} \pm 0.048$
60p100	$0.560^{b} \pm 0.060$	$0.521^{b} \pm 0.072$	$0.404^{b} \pm 0.053$	$0.257^{b} \pm 0.107$

The intensity was scaled to have unitary values for each treatment and observation time. Results are means ± standard deviations and different letters show significant differences ($p < 0.05$) between treatments.

The present investigation showed that the three compartment model, which is typically applied to describe raw apple tissue relaxation curves (Mauro et al., 2015), can be effectively used to model the NMR signals of apple treated at 100 V cm^{-1} but it is, unfortunately, inadequate when a voltage above the irreversible electroporation threshold is applied. Efforts were therefore made to find a characteristic of T_2 curves which could be universally applied to estimate the electric cell damage. In this respect, the longest relaxation time, which can be directly obtained from the UpenWin software output, was found to be tailored to the goal. In the present experimental conditions, this T_2 could be ascribed to the water protons located in the middle of the vacuole, because it is characterized by the weakest interaction with biopolymers (Hills & Duce, 1990) and is unaffected by the contrast agent until plasma and tonoplast membrane breakage (Panarese et al., 2012).

Fig. 3c and d shows the longest relaxation time of the samples immersed in isotonic and hypertonic solutions, respectively. No differences were noticed in NoPEF samples throughout the entire process, showing that this value was independent from the immersion time in an isotonic solution or from the vacuole shrinkage which usually occurs when apple tissue is immersed into an osmotic solution (Mauro et al., 2015). The longest relaxation time of the samples treated at 250 and 400 V cm^{-1} in both isotonic and hypertonic solutions showed a high decrease of relaxation time which passed from the initial value around 2000 ms to around 1000 ms during the first 15 min after PEF treatments and reached values around 500 ms after 120 min. This parameter was therefore not only sensitive to the applied electric field strength, but also able to clearly discriminate reversible from irreversible effects. Furthermore, it is worth to notice that those results closely followed mass

transfer scores. For instance, 60 pulses at 400 V cm^{-1} led to the highest water removal, 20 pulses at 250 cm^{-1} to the lowest difference in mass transfer compared to control while 20 pulses at 400 V cm^{-1} and 60 pulses at 250 V cm^{-1} showed intermediate values which were similar between them.

In addition to water distribution analysis, water self diffusion coefficient (D_w) was evaluated by means of pulsed magnetic field gradient spin echo sequence. This parameter gives an overview of the ability of water molecules, contained inside apple tissue, to explore the surrounding space. In order to compare raw material and the samples treated at different electric field strengths, a single diffusion coefficient was calculated in both compartmentalized and non-compartmentalized samples. In the former case, this represents an average value of the diffusion coefficients in the different environments while in the latter case one population was found so that only a single coefficient model was applicable. This approximation granted the use of one universal coefficient for any of the studied cases, as suggested by Santagapita et al. (2013). When using isotonic solution no differences were found as a consequence of any PEF treatment, even when observed along 120 min. In case of osmotic solution, D_w showed once more behavior independent from PEF application, but a remarkable proportionality to the osmotic dehydration. Indeed, Fig. 4 shows the linear relationship between D_w and water content of apple tissues ($R^2 = 0.92$), either electrically pretreated or not, demonstrating the universal applicability of D_w for water loss estimation in case of osmotic treatments. These results are in agreement with a previous study where water self-diffusion coefficient was described as a useful non-destructive tool to monitor osmotic processes applied to kiwifruit (Santagapita et al., 2013).

4. Conclusions

In the present work osmotic dehydration found in PEF is an effective aid in removing water from apple tissue and increasing solute concentration, due to the alteration of the membrane permeability. A description of subcellular modifications which occurred upon the use of electric fields was achieved for the first time by TD-NMR. This highlighted a continuum of consequences of PEF treatments on tissue subcellular structure, from water redistribution to membrane disruption. The measurement of T_2-weighted relaxation curves and water self diffusion coefficients provided a fast and potentially non-destructive method to control PEF and osmotic processes, respectively. In particular, water redistribution through apple cellular compartments, vacuole, cytoplasm and extracellular space was found to be highly dependent on the electric field strength and number of pulses. Mass transfer data was in good agreement with the findings from TD-NMR, promoting the use of the developed method when, as in the case of pulsed electric fields, the process target is the alteration of subcellular compartmentalization. Finally, it is worth mentioning that PEF treatment produced time-dependence effects on apple tissue, suggesting that the optimization of industrial applications should take into account the time elapsed from the application of pulsed electric fields.

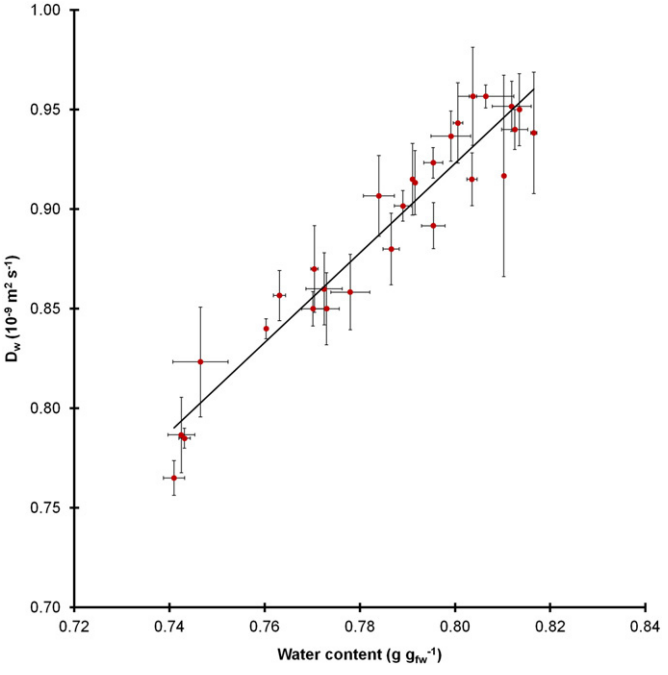

Fig. 4. Average ± standard deviation of water self diffusion coefficient versus water content.

References

Ade-Omowaye, B., Rastogi, N., Angersbach, A., & Knorr, D. (2003). Combined effects of pulsed electric field pre-treatment and partial osmotic dehydration on air drying behaviour of red bell pepper. *Journal of Food Engineering, 60*(1), 89–98.

Ade-Omowaye, B., Talens, P., Angersbach, A., & Knorr, D. (2003). Kinetics of osmotic dehydration of red bell peppers as influenced by pulsed electric field pretreatment. *Food Research International, 36*(5), 475–483.

Ade-Omowaye, B., Angersbach, A., Taiwo, K., & Knorr, D. (2001). Use of pulsed electric field pre-treatment to improve dehydration characteristics of plant based foods. *Trends in Food Science & Technology, 12*(8), 285–295.

Amami, E., Vorobiev, E., & Kechaou, N. (2006). Modelling of mass transfer during osmotic dehydration of apple tissue pre-treated by pulsed electric field. *LWT- Food Science and Technology, 39*(9), 1014–1021.

Angersbach, A., Heinz, V., & Knorr, D. (1999). Electrophysiological model of intact and processed plant tissues: Cell disintegration criteria. *Biotechnology Progress, 15*(4), 753–762.

Angersbach, A., Heinz, V., & Knorr, D. (2002). Evaluation of process-induced dimensional changes in the membrane structure of biological cells using impedance measurement. *Biotechnology Progress, 18*(3), 597–603.

AOAC International (2002). *Official methods of analysis (OMA) of AOAC International* (17th ed.) [USA. Method number: 920.15. Available at. http://www.eoma.aoac.org/].

Bazhal, M., Lebovka, N., & Vorobiev, E. (2001). Pulsed electric field treatment of apple tissue during compression for juice extraction. *Journal of Food Engineering, 50*(3), 129–139.

Borgia, G., Brown, R., & Fantazzini, P. (1998). Uniform-penalty inversion of multiexponential decay data. *Journal of Magnetic Resonance, 132*(1), 65–77.

Donsì, F., Ferrari, G., & Pataro, G. (2010). Applications of pulsed electric field treatments for the enhancement of mass transfer from vegetable tissue. *Food Engineering Reviews, 2*(2), 109–130.

Fincan, M., & Dejmek, P. (2002). In situ visualization of the effect of a pulsed electric field on plant tissue. *Journal of Food Engineering, 55*(3), 223–230.

Hills, B., & Duce, S. (1990). The influence of chemical and diffusive exchange on water proton transverse relaxation in plant tissues. *Magnetic Resonance Imaging, 8*(3), 321–331.

Hills, B., & Remigereau, B. (1997). NMR studies of changes in subcellular water compartmentation in parenchyma apple tissue during drying and freezing. *International Journal of Food Science and Technology, 32*(1), 51–61.

Holz, M., Heil, S., & Sacco, A. (2000). Temperature-dependent self-diffusion coefficients of water and six selected molecular liquids for calibration in accurate 1H NMR PFG measurements. *Physical Chemistry Chemical Physics, 2*(20), 4740–4742.

Jemai, A., & Vorobiev, E. (2002). Effect of moderate electric field pulses on the diffusion coefficient of soluble substances from apple slices. *International Journal of Food Science and Technology, 37*(1), 73–86.

Lebovka, N. I., Praporscic, I., & Vorobiev, E. (2004). Effect of moderate thermal and pulsed electric field treatments on textural properties of carrots, potatoes and apples. *Innovative Food Science & Emerging Technologies, 5*(1), 9–16.

Lebovka, N., Bazhal, M., & Vorobiev, E. (2002). Estimation of characteristic damage time of food materials in pulsed-electric fields. *Journal of Food Engineering, 54*(4), 337–346.

Lebovka, N., Praporscic, I., Ghnimi, S., & Vorobiev, E. (2005). Temperature enhanced electroporation under the pulsed electric field treatment of food tissue. *Journal of Food Engineering, 69*(2), 177–184.

Mauro, M., Dellarosa, N., Tylewicz, U., Tappi, S., Laghi, L., Rocculi, P., & Dalla Rosa, M. (2015). Calcium and ascorbic acid affect cellular structure and water mobility in apple tissue during osmotic dehydration in sucrose solutions. *Food Chemistry, 195*, 19–28.

Meiboom, S., & Gill, D. (1958). Modified spin-echo method for measuring nuclear relaxation times. *Review of Scientific Instruments, 29*(8), 688–691.

Nowacka, M., Tylewicz, U., Laghi, L., Dalla Rosa, M., & Witrowa-Rajchert, D. (2014). Effect of ultrasound treatment on the water state in kiwifruit during osmotic dehydration. *Food Chemistry, 144*, 18–25.

Panarese, V., Laghi, L., Pisi, A., Tylewicz, U., Dalla Rosa, M., & Rocculi, P. (2012). Effect of osmotic dehydration on *Actinidia deliciosa* kiwifruit: A combined NMR and ultrastructural study. *Food Chemistry, 132*(4), 1706–1712.

Parniakov, O., Lebovka, N., Bals, O., & Vorobiev, E. (2015). Effect of electric field and osmotic pre-treatments on quality of apples after freezing–thawing. *Innovative Food Science & Emerging Technologies, 29*, 23–30.

Santagapita, P., Laghi, L., Panarese, V., Tylewicz, U., Rocculi, P., & Dalla Rosa, M. (2013). Modification of transverse NMR relaxation times and water diffusion coefficients of kiwifruit pericarp tissue subjected to osmotic dehydration. *Food and Bioprocess Technology*, *6*(6), 1434–1443.

Sensoy, I., & Sastry, S. (2004). Extraction using moderate electric fields. *Journal of Food Science*, *69*(1), FEP7–FEP13.

Soliva-Fortuny, R., Balasa, A., Knorr, D., & Martín-Belloso, O. (2009). Effects of pulsed electric fields on bioactive compounds in foods: A review. *Trends in Food Science & Technology*, *20*(11), 544–556.

Stejskal, E., & Tanner, J. (1965). Spin diffusion measurements: Spin echoes in the presence of a time-dependent field gradient. *The Journal of Chemical Physics*, *42*(1), 288–292.

Taiwo, K. A., Angersbach, A., & Knorr, D. (2003). Effects of pulsed electric field on quality factors and mass transfer during osmotic dehydration of apples. *Journal of Food Process Engineering*, *26*(1), 31–48.

Teissie, J., Eynard, N., Gabriel, B., & Rols, M. (1999). Electropermeabilization of cell membranes. *Advanced Drug Delivery Reviews*, *35*(1), 3–19.

Tylewicz, U., Panarese, V., Laghi, L., Rocculi, P., Nowacka, M., Placucci, G., & Dalla Rosa, M. (2011). NMR and DSC water study during osmotic dehydration of *Actinidia deliciosa* and *Actinidia chinensis* kiwifruit. *Food Biophysics*, *6*(2), 327–333.

Van Duynhoven, J., Voda, A., Witek, M., & Van As, H. (2010). Time-domain NMR applied to food products. *Annual Reports on NMR Spectroscopy*, *69*, 145–197.

Vorobiev, E., & Lebovka, N. (2008). Pulsed-electric-fields-induced effects in plant tissues: Fundamental aspects and perspectives of applications. *Electrotechnologies for extraction from food plants and biomaterials* (pp. 39–81). Springer.

Vorobiev, E., Jemai, A. B., Bouzrara, H., Lebovka, N., & Bazhal, M. (2005). Pulsed electric field assisted extraction of juice from food plants. *Novel food processing technologies* (pp. 105–130).

Wiktor, A., Iwaniuk, M., Śledź, M., Nowacka, M., Chudoba, T., & Witrowa-Rajchert, D. (2013). Drying kinetics of apple tissue treated by pulsed electric field. *Drying Technology*, *31*(1), 112–119.

Wiktor, A., Śledź, M., Nowacka, M., Chudoba, T., & Witrowa-Rajchert, D. (2014). Pulsed electric field pretreatment for osmotic dehydration of apple tissue: Experimental and mathematical modeling studies. *Drying Technology*, *32*(4), 408–417.

Paper V

Dellarosa, **N.**, Tappi, S., Ragni, L., Laghi, L., Rocculi, P., & Dalla Rosa, M. (2016)

Metabolic response of fresh-cut apples induced by pulsed electric fields

Innovative Food Science & Emerging Technologies, *38*, 356-364

Innovative Food Science and Emerging Technologies 38 (2016) 356–364

Contents lists available at ScienceDirect

Innovative Food Science and Emerging Technologies

journal homepage: www.elsevier.com/locate/ifset

Metabolic response of fresh-cut apples induced by pulsed electric fields

Nicolò Dellarosa [a,*], Silvia Tappi [a], Luigi Ragni [a,b], Luca Laghi [a,b], Pietro Rocculi [a,b], Marco Dalla Rosa [a,b]

[a] Department of Agricultural and Food Sciences, University of Bologna, Cesena, Italy
[b] Interdepartmental Centre for Agri-Food Industrial Research, University of Bologna, Cesena, Italy

ARTICLE INFO

Article history:
Received 4 March 2016
Received in revised form 13 June 2016
Accepted 24 June 2016
Available online 27 June 2016

Keywords:
PEF
Apple tissue
Isothermal calorimetry
Respiration rate
HR-NMR
Metabolomics

ABSTRACT

Pulsed electric field (PEF) treatments can induce metabolic stress responses in plant tissue as a function of the applied conditions. This study highlighted the metabolic effects of reversible and irreversible electroporation in fresh-cut apple tissue, by adjusting the electric field strength to 100, 250 and 400 V/cm (100 μs pulse width, 60 pulses, 100 Hz). Metabolic heat, O_2 and CO_2 gas analysis, along with metabolomics, were employed to jointly evaluate the PEF-induced effects after 24 h at 10 °C. Marked metabolic changes were registered when the threshold of irreversible electroporation was exceeded, at 250 and 400 V/cm. With such treatments, a drop of metabolic heat and respiration rate was observed, as a probable consequence of the loss of the cell viability, anaerobic respiration pathways were noticeably lowered, while γ-aminobutyric acid metabolism was activated. Conversely, minimal modifications of the metabolism heat and metabolites concentrations were noticed when 100 V/cm was applied.

Industrial relevance: Metabolic response of fresh-cut fruit and vegetables as function of the manufacturing process is a fundamental aspect directly related to the quality of the final products. Pulsed electric fields (PEF), as well as other innovative technologies, can induce undesired effects on tissue metabolism that might limit the industrial application. Furthermore, the analytical methods used in the present work provide useful tools for the optimization of the PEF treatment conditions for fresh-cut manufacturers.

© 2016 Elsevier Ltd. All rights reserved.

1. Introduction

Pulsed electric field (PEF) technology is a non-thermal process, which has recently stimulated an increasing interest in the food field. The application of high electric fields between two electrodes can be exploited for different goals, for instance to enhance mass transfer phenomena (Donsì, Ferrari, & Pataro, 2010; Puértolas, Luengo, Álvarez, & Raso, 2012; Taiwo, Angersbach, & Knorr, 2002) or to inactivate microorganisms (González-Arenzana, Portu, López, López, Santamaría, Garde-Cerdán, & López-Alfaro, 2015; Timmermans, Groot, Nederhoff, van Boekel, Matser, & Mastwijk, 2014). The mechanism of action includes the creation of pores due to the application of electric fields high enough to induce a potential difference of approximately 0.2 V across the cell membrane (Teissie, Eynard, Gabriel, & Rols, 1999). In a second step, pores can expand, aggregate and, once the external electric field is removed, even reseal (Vorobiev & Lebovka, 2009). The extent of the process, also known as electroporation, strongly depends on the applied process parameters, such as electric field strength, number and shape of pulses, their width and frequency. Indeed, different goals and industrial applications can be achieved by adjusting the treatment conditions (Barba, Parniakov, Pereira, Wiktor, Grimi, Boussetta, Saraiva, Raso, Martin-Belloso, & Witrowa-Rajchert, 2015).

The effect of PEF in plant tissues has been studied by several techniques according to the desired objective: examples are the release of valuable compounds (Carbonell-Capella, Buniowska, Esteve, & Frígola, 2015; Luengo, Álvarez, & Raso, 2013), extraction yield (Bazhal, Lebovka, & Vorobiev, 2001), changes in colour and texture (Lebovka, Praporscic, & Vorobiev, 2004; Wiktor, Schulz, Voigt, Witrowa-Rajchert, & Knorr, 2015). Moreover, methods have been developed to indirectly evaluate the extent of electroporation based on electrical impedance (Angersbach, Heinz, & Knorr, 2002; Ivorra, 2010; Lebovka, Bazhal, & Vorobiev, 2002), microscopy (Fincan & Dejmek, 2002) and time domain nuclear magnetic resonance (TD-NMR) (Dellarosa, Ragni, Laghi, Tylewicz, Rocculi, & Dalla Rosa, 2016).

Pulsed electric fields, by acting at the level of membranes, can also deeply affect cell activities. As a consequence, metabolic stress responses of cells can be induced and lead to undesired effects on the

Abbreviations: GA, glutamic acid; GABA, γ-aminobutyric acid; HMDB, human metabolome database; HR-NMR, high resolution nuclear magnetic resonance; LD, linear discriminant; LDA, linear discriminant analysis; MOSFET, metal-oxide-semiconductor field-effect transistor; PC, principal component; PCA, principal component analysis; PEF, pulsed electric fields; R_A, resistance of apple sample; R_{WA}, resistance (in series) of water between the apple samples and the electrodes; R_{WP}, resistance (in parallel) of water which is parallel to the apple cylinders; RQ, respiration quotient; sPLSDA, sparse partial least squares discriminant analysis; TD-NMR, time domain nuclear magnetic resonance; VIP, variable importance in projection.

* Corresponding author.
E-mail address: nicolo.dellarosa@unibo.it (N. Dellarosa).

http://dx.doi.org/10.1016/j.ifset.2016.06.016
1466-8564/© 2016 Elsevier Ltd. All rights reserved.

quality of the final products. This might limit the application of PEF in fresh-cut products. Generally, fresh-cut fruit and vegetables undergo minimal processing, such as peeling, cutting or pre-treatment with different solutions (Mauro, Dellarosa, Tylewicz, Tappi, Laghi, Rocculi, & Dalla Rosa, 2016; Santagapita, Laghi, Panarese, Tylewicz, Rocculi, & Dalla Rosa, 2013) which, nevertheless, provokes metabolic responses (Rocculi, Panarese, Tylewicz, Santagapita, Cocci, Gómez Galindo, Romani, & Dalla Rosa, 2012). In this contest, the application of PEF, on one side can ease the mass exchange between the outer solution and the tissue, on the other side can trigger further stress responses. To the best of our knowledge, few works have been focused on the metabolic aspects induced by PEF in postharvest fruit and vegetable products (Galindo, Dejmek, Lundgren, Rasmusson, Vicente, & Moritz, 2009; Galindo, Wadsö, Vicente, & Dejmek, 2008).

Fresh-cut products are metabolic active tissues, that can therefore produce heat as a function of both normal cell activities, involving tens of metabolic pathways, and further technological processes applied. Thermal power and heat can be continuously monitored by isothermal calorimetry and this gives rise to gross values of the cell metabolisms where many metabolic pathways account for the overall thermal development (Galindo, Rocculi, Wadsö, & Sjöholm, 2005; Wadsö & Galindo, 2009). Of greater importance, when the sample conditions are standardized, a direct evaluation of the effects of the technologies can be carried out (Panarese, Laghi, Pisi, Tylewicz, Dalla Rosa, & Rocculi, 2012; Tappi, Berardinelli, Ragni, Dalla Rosa, Guarnieri, & Rocculi, 2014). Moreover, the measurement of the heat is often coupled with the analysis of the consumed O_2 and produced CO_2, which allow clarifying whether other non-aerobic metabolisms are activated (Cortellino, Gobbi, Bianchi, & Rizzolo, 2015).

A trait that all the above-mentioned methods have in common is their ability to easily estimate the gross stress response, with reduced possibilities to investigate how the different technological treatments fine-tune the physiology of the samples cells. In this respect, metabolomics, the comprehensive analysis of the soluble low weight metabolites by means of high-throughput techniques like mass spectrometry (MS) of high resolution nuclear magnetic resonance (HR-NMR), is considered the election approach (Fiehn, 2002; Laghi, Picone, & Capozzi, 2014). This has been successfully applied for food quality control, health and nutritional purposes, fingerprinting, including traceability and authenticity, and, recently, to assess and backwardly adjust technological processes (Trimigno, Marincola, Dellarosa, Picone, & Laghi, 2015). To the purpose, specific multivariate analytical tools need to be developed and tailored to discriminate the effects of the applied technologies on precursors, intermediates and products of different metabolic pathways (Laghi, Picone, & Capozzi, 2014).

The objective of the present work was to assess the metabolic response of fresh-cut apples upon pulsed electric field treatments, so as to obtain a deeper understanding of such promising technological treatment and outline instruments allowing its tuning. Three different levels of electric field strength, 100, 250 and 400 V/cm with fixed pulse width (100 μs), number of pulses ($n = 60$) and frequency (100 Hz) were studied, because they are known to produce both reversible and irreversible electroporation effects on cell membranes in apple tissue (Dellarosa, Ragni, Laghi, Tylewicz, Rocculi, & Dalla Rosa, 2016). A comprehensive evaluation by means of a multianalytical approach based on calorimetry, gas analysis and metabolomics was chosen to complementarily describe gross alteration on metabolic activities and specific fine changes in metabolites composition. High resolution ^{1}H nuclear magnetic resonance (HR-NMR) was employed for the analysis of the metabolic profiling, together with a novel non-targeted statistical tool based on sparse partial least square discriminant analysis (sPLSDA) and linear discriminant analysis (LDA). The investigation was conducted 24 h after PEF treatment, so to give to the fruit's tissue time to put in place strategies to defend themselves from possible damages.

2. Material and methods

2.1. Raw material

Apples (*Malus domestica*, cv Cripps Pink) were purchased at a local market and stored at 2 ± 1 °C for three weeks, during which all the experiments were conducted. Before experiments, apples were kept at room temperature for 2 h. Raw material had an average moisture content of 83.5 ± 0.5 g and was at commercial maturity, characterized by soluble solid content of 13.5 ± 0.5 g and titrable acidity of 0.36 ± 0.02 g of malic acid per 100 g of fresh product (corresponding to an average ripening index of 37.5). Cylindrical samples (8 mm diameter and 20 mm length with an average weight of 1 g) were obtained from apple parenchyma by cutting with a manual cork borer and a scalpel. Eight cylinders from each fruit were obtained and used for the experiments.

2.2. Pulsed electric field (PEF) treatments and monitoring

PEF treatments were applied to apple samples using an in-house developed pulse generator equipment based on capacitors as energy tank and controlled by a STW9N150 MOSFET (metal-oxide-semiconductor field-effect transistor) (STMicroelectronics, Geneve, Swiss). Briefly, 60 monopolar pulses of near-rectangular shape, fixed pulse width of 100 ± 2 μs and repetition time of 10.0 ± 0.1 ms (100 Hz) were chosen, according to the experimental conditions used by Dellarosa, Ragni, Laghi, Tylewicz, Rocculi, and Dalla Rosa (2016). PEF treatments were conducted at 20 °C in a 30 × 20 × 20 mm (length × width × height) chamber equipped with two stainless steel electrodes with an active contact surface of 20 × 20 mm^2. For each trial, six apple cylinders were arranged with the two circle sides parallel to the electrodes and the chamber was filled up with tap water (conductivity at 25 °C of 328 ± 1 μS cm^{-1}) with a final product-to-water ratio around 1:1 (v/v) (Fig. 1). Applied current and voltage values were measured at the electrodes by a digital oscilloscope (PicoScope 2204a, Pico Technology, UK) connected to the equipment and a personal computer.

Four samples groups, including control, were obtained by treating apple cylinders with a voltage of 300 V, 750 V and 1200 V to the electrodes (pulse width = 100 μs, number of pulses = 60, frequency = 100 Hz). These conditions led to the nominal electric field strength of 100, 250 and 400 V/cm in the chamber and the energy input of 19, 151 and 424 J/kg of sample, respectively. However, the presence of tap water between the samples and the electrodes (two different materials with different resistivity between the electrodes) gave rise to inhomogeneous distributions of the electric fields within the chamber. Taking into account the known resistivity (3.05 kΩ × cm) of the tap water and the geometries of the cylindrical samples within the chamber, the specific voltage values applied to the apple tissue could be calculated according to the Ohm's law. Fig. 1 shows the chamber arrangement and the equivalent electrical circuit used for the calculation, where tap water acts as resistor both in series and in parallel. Consequentially, treatments at the nominal field strength of 100, 250 and 400 V/cm gave rise to values of 115, 245 and 275 V/cm^3 of sample in the chamber. As commonly accepted throughout the literature, in the present work the treatments and the sample names were referred to the nominal electric field strength. Furthermore, the same approach based on equivalent circuits and the Ohm's law was employed to calculate possible changes of the electric resistivity of apple samples during the pulsation. To this respect, current and voltage values of the first and the last pulse of the 60-pulses train series (frequency = 100 Hz, pulse width = 100 μs) were monitored at each applied electric field.

2.3. Metabolic heat

Three fresh cylindrical samples (about 3 g) were placed in 20 mL glass ampoule and sealed with a teflon coated rubber seal and an

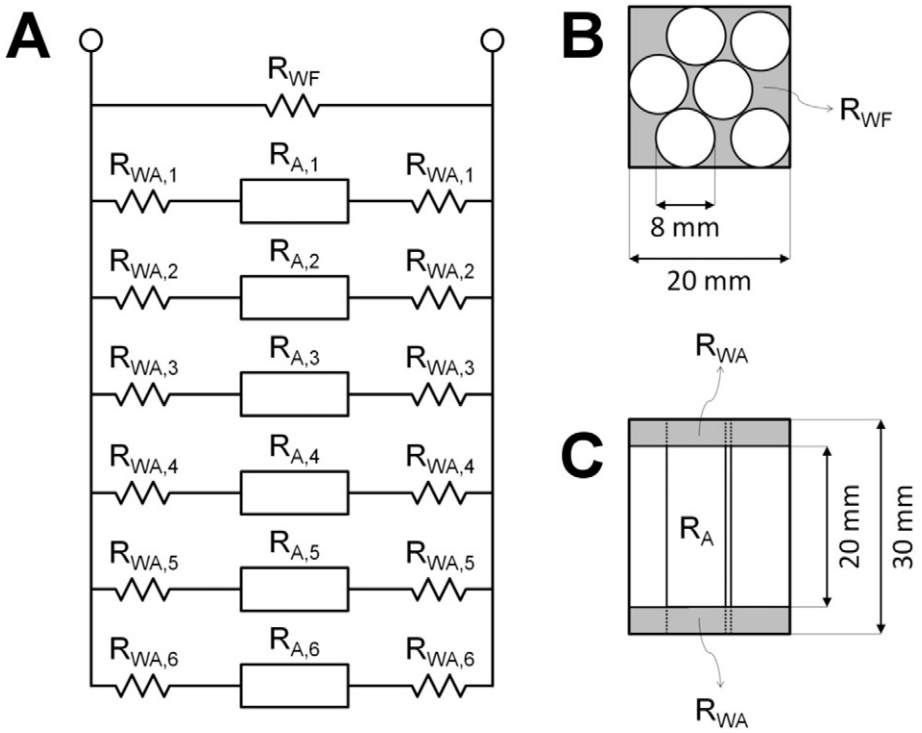

Fig. 1. Equivalent circuit (A), side-view (B) and top-view (C) of the arrangement of the six cylindrical samples in the treatments chamber. R_{WF} and R_{WA} are the resistance of tap water in parallel and in series, respectively, while R_A is the resistance of the apple cylinders.

aluminium crimp cap. For each sample, two replicates for three independent PEF treatments were analysed. A TAM air isothermal calorimeter (TA Instruments, New Castel, USA), with a sensitivity (precision) of ± 10 μW was used to measure the heat production. This instrument contained eight twin calorimeters in which each sample was coupled with its own reference (Wadsö & Galindo, 2009). As reference material we choose an amount of water calculated, according to Panarese, Laghi, Pisi, Tylewicz, Dalla Rosa, and Rocculi (2012), so as to match the heat capacity of each sample. The analysis was carried out at 10 °C and required 24 h, with the baseline recorded before and after each measurement. Specific thermal powers (mW g^{-1}) were calculated according to Galindo, Wadsö, Vicente, and Dejmek (2008).

2.4. Respiration rate

The concentration of O_2 and CO_2 (%) was measured in the ampoule headspaces by a gas analyser (MFA III S/L gas analyser, Witt-Gasetechnik, Witten, Germany) at the end of the calorimetric measurements and on other twin ampoules with samples treated at the same conditions, stored in the dark for the same period of time (24 h) at the same temperature (10 °C), for a total of 18 repetitions per sample. Respiration rate was calculated as mg of consumed O_2 (RRO_2) and produced CO_2 ($RRCO_2$) $kg^{-1}\ h^{-1}$ according to the following equations (Panarese, Laghi, Pisi, Tylewicz, Dalla Rosa, & Rocculi, 2012; Tappi, Berardinelli, Ragni, Dalla Rosa, Guarnieri, & Rocculi, 2014):

$$RRO_2 = \frac{mm_{O_2} \cdot V_{head} \cdot \frac{(20.8 - \%O_{2,head})}{100} \cdot 101.325}{t \cdot m \cdot R \cdot 283} \quad (1)$$

$$RRCO_2 = \frac{mm_{CO_2} \cdot V_{head} \cdot \frac{\%CO_{2,head}}{100} \cdot 101.325}{t \cdot m \cdot R \cdot 283} \quad (2)$$

where mmO_2 and $mmCO_2$ refer to gas molar mass (g mol^{-1}), V_{head} represents the ampoule headspace volume (dm^3), % $O_{2,head}$ and % $CO_{2,head}$ refer to gas percentages in the ampoule headspace at time t (h); m is the sample mass (kg); R is the gas constant (8.314472 dm^3 kPa K^{-1} mol^{-1}), P is the pressure (101.325 kPa) and T is the absolute temperature (283 K).

2.5. NMR-based metabolomics

2.5.1. High resolution ^1H nuclear magnetic resonance (HR-NMR)

Apple cylinders were collected after 24 h at the same experimental conditions applied for metabolic heat and respiration rate analysis (stored in the dark at 10 °C). For each experimental condition, cylinders were squeezed three by three (about 3 g) until an aliquot of 1 mL was obtained, for a total of 36 repetitions per experimental condition. Samples were then centrifuged at 21,380 × *g* and 4 °C for 20 min in an Eppendorf tube. An aliquot of 700 μL of the supernatant was collected and added to 70 μL of 10 mM TSP (3-TrimethylSilyl-Propanoic-2,2,3,3-d4 acid sodium salt) in deuterium oxide, with the addition of sodium azide at the final concentration of 0.04% to prevent microbial activities. Samples were frozen at −20 °C until analysis, when they were thawed and successively centrifuged at 21,380 × *g* and 4 °C for 20 min to further remove impurities. Finally, the supernatants were placed in a 5-mm internal diameter NMR tube for metabolomic analysis.

^1H spectra were recorded at 298 K with an Avance III spectrometer (Bruker, Italy) operating at a frequency of 600.13 MHz. Residual water signal was suppressed using the NOESY sequence. Each acquisition included 32 K data points over 7796 Hz spectral width and 128 scans while the 90° pulse time was calculated for each acquisition. Spectra were pre-processed using TOP SPIN 3.0 software (Bruker, Italy), by alignment toward TSP signal (set to 0 ppm) and line broadening of 0.3. The principle of reciprocity (Hoult, 2011) was used to normalize each spectrum, so that quantitative results could be obtained. Using citric acid as external standard, high linearity ($R^2 = 0.9997$) was found in the range of 0.01–800 mM. A total of 144 NMR spectra, homogeneously distributed among the four investigated treatments, were acquired and exported for further data analysis.

2.5.2. Data pre-processing and analysis

HR-NMR spectra were subjected to baseline correction, carried out in R statistical software (R Foundation for Statistical Computing, Vienna, Austria), as reported by De Filippis, Pellegrini, Vannini, Jeffery, La Storia, Laghi, Serrazanetti, Di Cagno, Ferrocino, and Lazzi (2015). Signals of the spectra were manually integrated resulting in 38 protons peaks belonging to alcohols, amino acids, organic acids, sugars and other secondary metabolites. Their identification was performed using Chemomx (Chenomx inc, Edmonton, Canada) software, available in literature (Belton, Delgadillo, Gil, Roma, Casuscelli, Colquhoun, Dennis, & Spraul, 1997; Capitani, Mannina, Proietti, Sobolev, Tomassini, Miccheli, Di Cocco, Capuani, De Salvador, & Delfini, 2012; Monakhova, Schütz, Schäfer, Spraul, Kuballa, Hahn, & Lachenmeier, 2014; Tomita, Nemoto, Matsuo, Shoji, Tanaka, Nakagawa, Ono, Kikuchi, Ohnishi-Kameyama, & Sekiyama, 2015; Vandendriessche, Schäfer, Verlinden, Humpfer, Hertog, & Nicolaï, 2013) and human metabolome database (HMDB) (Wishart, Jewison, Guo, Wilson, Knox, Liu, Djoumbou, Mandal, Aziat, & Dong, 2012) and Madison (Cui, Lewis, Hegeman, Anderson, Li, Schulte, Westler, Eghbalnia, Sussman, & Markley, 2008) public databases. The obtained 144 (samples) × 38 (metabolites) matrix was scaled to unit variance and centred before undergoing to multivariate statistical analysis.

To gain insight into metabolic changes which occurred upon PEF treatments, two chemometric approaches, the principal component analysis (PCA) and sparse partial least square discriminant analysis (sPLSDA) followed by linear discriminant analysis (LDA), were employed. Both are non-targeted, that is leave to the clustering of the samples the goal of sorting the molecules based on their discrimination power (Laghi, Picone, & Capozzi, 2014). The R packages 'mixOmics' and 'MASS' were used for both approaches (Lê Cao, Boitard, & Besse, 2011).

PCA is a multivariate technique that rigidly rotates the original axis, here represented by the concentration of 38 molecules, to show the samples from the point of view accounting for the highest variance. Being unsupervised, that is blind to the expected results, this technique is ideally tailored to obtain a first insight to the similarities of the observed samples. sPLSDA and LDA techniques, being supervised, have been demonstrated to be more powerful in highlighting the fine differences among the studied groups, which, in the present work, consist of different PEF treatments (Laghi, Picone, & Capozzi, 2014). Among other supervised techniques, the approach based on sPLSDA-LDA was chosen because it is an embedded chemometric method that allows us to both find correlation between predictors and response classes, while simultaneously sorting and selecting the relevant variables (Mehmood, Liland, Snipen, & Sæbø, 2012). This powerful tool was used to evaluate the changes in the metabolic profiles as a consequence of the different technological treatments and, at the same time, to focus the discussion on the few metabolites significantly affected by PEF.

The analytical process included the splitting of the 144 samples spectra into a training set, represented by the 70% of the samples, used to generate the mathematical models, and a test, represented by the remaining samples, employed to test the performance of the models. The training set was used to build the sPLSDA model, validated through the M-fold validation step (M = 10) which also optimized the selection of latent variables and metabolites, as a function of the error rate. A thousand models were iteratively trained and tested by randomly dividing training and test sets to enhance the robustness of the analysis. Finally, the class prediction errors over the repetitions were expresses, scaled to the unit, as incorrect assignments in the confusion matrix. In parallel, the metabolites arisen from the multivariate analysis were considered as important whether their mean VIP (variable importance in projection) value was higher than one and their frequency in the models was higher than 70% (Chong & Jun, 2005). For any multivariate technique applied, scoreplots and loadingplots were generated. The former represents the samples in the new space, thus allowing a visual impression of their similarities and clustering; the latter evidences the molecule contributing most to the spreading of the samples in the new space, thus visually allowing their qualitative scoring.

2.6. Statistical analysis

Significant differences between control and PEF-treated samples were evaluated by the analysis of variance (ANOVA), Student's *t*-test and Tukey's multiple comparisons at the significance level of 95% ($p < 0.05$) implemented in R statistical software (R Foundation for Statistical Computing, Vienna, Austria). All the experiments were repeated at least six times and results were expressed as mean ± standard standard deviation of replications.

3. Results and discussion

3.1. Changes in electrical resistivity

The effect of electroporation on apple tissue was primarily observed by means of the resistance changes of the material during the electric treatments. The electrical resistivity of apple tissue was found to be a function of the electric field strength and significantly varied all through the PEF treatments. Indeed, Fig. 2 shows the resistivity at the beginning and at the end of the treatments, respectively, calculated taking into account the first (left bar) and the last pulse (right bar) of the 60-pulse trains, for each field strength. The resistivity of the tissue linearly decreased from about 4900 Ω × cm to around 2900 and 1300 Ω cm when the electric field strength was increased from 100 V/cm to 250 and 400 V/cm, respectively, upon the application of the first pulse of the train series (60 pulses of 100 μs width, 100 Hz). Nevertheless, solely the samples treated at 250 and 400 V/cm highlighted a significant decrease of the resistivity when the first pulse was compared to the last one of the series. These changes suggested that the two highest electric field strength levels irreversibly altered the structure of the tissue. The lack of differences at 100 V/cm might be due to the lack of sensitivity of the resistivity measurement or to the presence of reversible effects on membranes. A previous work (Dellarosa, Ragni, Laghi, Tylewicz, Rocculi, & Dalla Rosa, 2016) at the same treatment conditions, monitored the water migration between cell compartments by time domain nuclear magnetic resonance and clearly indicated that the effect of PEF

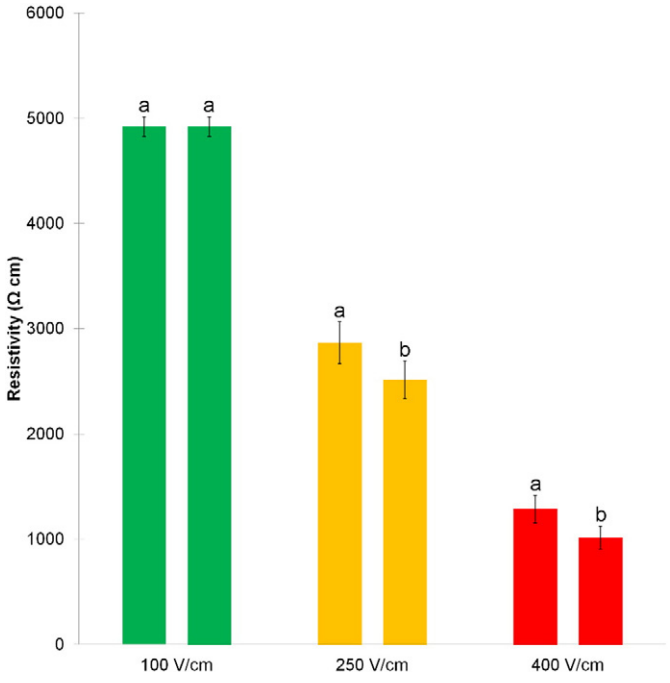

Fig. 2. Resistivity of the apple samples calculated using equivalent circuits on the first (left bar) and the last (right bar) pulse of the 60 pulses (100 μs pulse width, frequency of 100 Hz) train series for each electric field strength. Values are means ± standard deviations ($n = 16$) and differences between means with the same letter are not significant at $p < 0.05$.

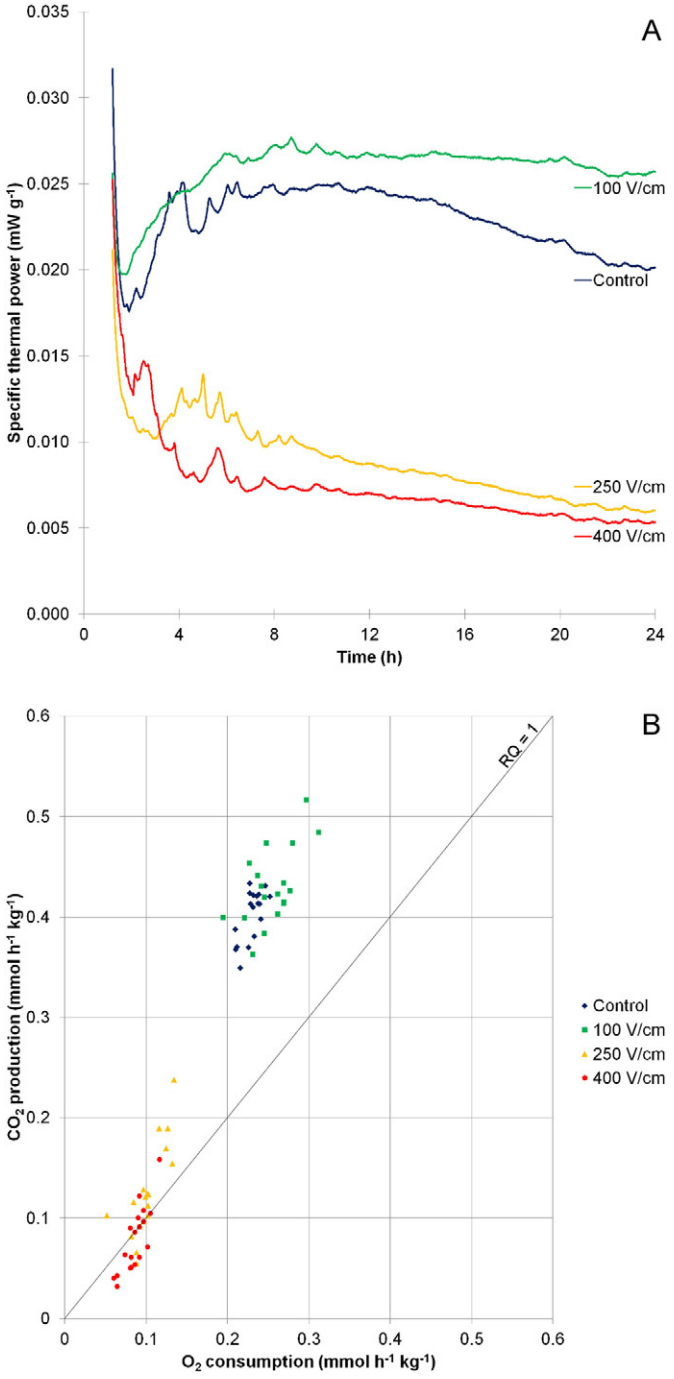

Fig. 3. Specific thermal power of apple samples during 24 h of analysis at 10 °C (A), each thermogram is an average of six replicates. CO_2 production ($RRCO_2$) vs. O_2 consumption (RRO_2) during 24 h at 10 °C (B); RQ = respiration quotient.

was significant even at 100 V/cm. This allowed us to safely attribute the effects obtained at 100 V/cm to the reversibility of the damages at the level of the cell membranes.

The irreversible loss of plasma membrane selectivity at average electric field strength higher than 150 V/cm caused the leakage of the cellular solutions toward the extracellular spaces which probably contributed to the decrease of the resistivity during the pulsation (Angersbach, Heinz, & Knorr, 2000; Vorobiev & Lebovka, 2009). Similarly, Galindo, Dejmek, Lundgren, Rasmusson, Vicente, and Moritz (2009) found in potato tissue that, although different field strength levels led to the electroporation of the cells, only samples irreversibly damaged showed a change in resistivity.

3.2. Heat production and respiration rate: gross metabolic response of the tissue

Fresh apple tissue is a metabolic active tissue which produces heat and CO_2 while consuming O_2 as a consequence of the respiration activities. In the absence of microbial growth on the sample, the metabolic heat production of fresh-cut fruit is mainly due to the sum of the normal respiration activity and of the wounding response (Rocculi, Panarese, Tylewicz, Santagapita, Cocci, Gómez Galindo, Romani, & Dalla Rosa, 2012; Wadsö & Galindo, 2009; Wadsö, Gomez, Sjöholm, & Rocculi, 2004) upon cutting and further treatments, for instance pulsed electric fields (Galindo, Dejmek, Lundgren, Rasmusson, Vicente, & Moritz, 2009). The average thermograms acquired by means of isothermal calorimetry of PEF-treated samples at different field strength are shown in Fig. 3a. At fixed pulse width (100 μs), number ($n = 60$) and frequency (100 Hz), a clear difference between samples treated at 250 and 400 V/cm was noticed when compared to both 100 V/cm and control samples. The lowest field strength seemed to induce a stress response in the tissue possibly ascribable to both the recovery activity due to the reversible alteration of plasma membrane (Vorobiev & Lebovka, 2009) and the subcellular changes, in particular, the water and solutes migration from vacuole toward cytoplasm and extracellular space (Dellarosa, Ragni, Laghi, Tylewicz, Rocculi, & Dalla Rosa, 2016).

The average metabolic heat production was calculated by integrating the metabolic heat profiles. The first 4 h of analysis was excluded in order to prevent the influence of the initial disturbance due to sample loading and conditioning, hence values reported in Table 1 refer to 20 h at 10 °C. It is worth observing that significant differences were only found when irreversible electroporation took place. At 250 and 400 V/cm the metabolic heat dropped 2.5–3.5 times in comparison to the control as a consequence of the likely loss of the cell viability due to the irreversible membrane poration. In this direction, pulsed electric fields led to a similar effect on metabolic heat to that previously observed as a consequence of different non-thermal treatments on fresh vegetable tissue. Indeed, Tappi, Berardinelli, Ragni, Dalla Rosa, Guarnieri, and Rocculi (2014) found a significant decrease of metabolic heat when fresh-cut apples were treated by cold gas plasma and a direct correlation of the effect with the treatment intensity. Nevertheless, in contrast to atmospheric gas plasma, PEF is known to produce more homogeneously distributed effects through the material (Parniakov, Lebovka, Bals, & Vorobiev, 2015), thus, not only limited to the surface, explaining the higher inhibition of heat. Similarly, other studies regarding different fresh-cut vegetable subjected to more traditional treatments such as blanching (Gómez, Toledo, Wadsö, Gekas, & Sjöholm, 2004) and osmotic dehydration (Panarese, Laghi, Pisi, Tylewicz, Dalla Rosa, & Rocculi, 2012) showed a partial reduction of

Table 1
Means values of the metabolic heat and respiration rates during 24 h at 10 °C.

	Metabolic heat (J/kg h^{-1})	RRO_2 (mg kg^{-1} h^{-1})	$RRCO_2$ (mg kg^{-1} h^{-1})
Control	82.79 ± 14.69[a]	7.39 ± 0.39[a]	16.93 ± 3.60[a]
100 V/cm	94.46 ± 22.35[a]	8.15 ± 0.88[a]	18.83 ± 1.65[a]
250 V/cm	30.22 ± 6.73[b]	3.17 ± 0.70[b]	5.77 ± 2.25[b]
400 V/cm	23.78 ± 5.21[b]	2.76 ± 0.45[b]	3.27 ± 1.59[c]

RRO_2: O_2 respiration rate (O_2 consumption). $RRCO_2$: CO_2 respiration rate (CO_2 production). Values are means ± standard deviations ($n = 6$ for metabolic heat, $n = 18$ for O_2 and CO_2 respiration rates) and differences between means with the same letter are not significant at $p < 0.05$.

Table 2
Metabolites in NMR profiles observed in the samples under investigation.

Alcohols	Amino acids	Organic acids	Sugars	Others
Butanol	Alanine	Acetic acid	Fructose	Acetaldehyde
Ethanol	Asparagine	Chlorogenic acid	Maltose	Acetoin
Isopropanol	Aspartic acid	Citramalic acid	Sucrose	Epicatechin
Methanol	Glutamic acid	Formic acid	Trehalose	myo-Inositol
Propanol	Isoleucine	Lactic acid	Xylose	Trigonelline
	Leucine	Malic acid	α-Galactose	
	Phenylalanine	Pyruvic acid	β-Galactose	
	Valine	Quinic acid	α-Glucose	
		Succinic acid	β-Glucose	
		Tartaric acid		
		γ-Aminobutyric acid		

metabolic activity proportionally to the treatment parameters. Conversely to other treatments, the main effect of PEF on cell processes, at the present treatment conditions, is only ascribable to the alteration of the membrane permeability and functionality while the direct enzyme inactivation is negligible. Indeed, according to several authors finding, a significant decrease of enzymes activities only occurred when an electric field strength higher than 5 kV/cm was applied (Giner, Gimeno, Barbosa-Cánovas, & Martín, 2001; Zhong, Wu, Wang, Chen, Liao, Hu, & Zhang, 2007).

Besides, the respiration rate was measured using a static method after 24 h at the same experimental conditions applied for the isothermal calorimetry measurements. Table 1 shows the results, including the statistical analysis. Accordingly, a marked decrease of both O_2 consumption and CO_2 production was observed upon PEF treatments at 250 and 400 V/cm. This confirmed the severe loss of viability of apple tissue caused by the irreversible electroporation. A significant difference was also noticed in the $RRCO_2$ between the two highest field strength levels, leading to the conclusion that the metabolic response was affected by the field strength even over the threshold of the irreversible electroporation.

The aerobic cell respiration of fresh fruit produces 455 kJ/mol of O_2 consumed, hence results obtained by calo-respirometric could be compared (Wadsö & Galindo, 2009). However, because for metabolic heat production the first 4 h of analysis was excluded, in order to obtain comparable data, the O_2 consumed during that interval was measured in a parallel experiment and RRO_2 data adjusted consequentially. Results showed that the first 4 h accounted for the 27.0 ± 0.8% of the total O_2 confirming the non-linear consumption throughout 24 h highlighted in previous works (Tappi, Berardinelli, Ragni, Dalla Rosa, Guarnieri, & Rocculi, 2014; Tappi, Gozzi, Vannini, Berardinelli, Romani, Ragni, & Rocculi, 2016; Torrieri, Cavella, & Masi, 2009). Metabolic heat and RRO_2 were found linearly correlated (R^2 = 0.9994), nevertheless, O_2 consumption calculated from metabolic heat was found to be lower, in all the samples, with a bias spanning from 0.50 to 0.75 mg kg^{-1} h^{-1}. The achieved difference was attributed to the wounding response as consequence of both cutting (Wadsö, Gomez, Sjöholm, & Rocculi, 2004) and PEF treatments (Galindo, Wadsö, Vicente, & Dejmek, 2008).

Taking into account the respiration quotient (RQ), i.e. the ratio between $RRCO_2$ and RRO_2 expressed in mmol kg^{-1} h^{-1} (Fig. 3b), control and treated samples at 100 V/cm were the highest, with similar scores around 1.7. Several authors pointed out that the anaerobic processes were prompted by either low oxygen or high carbon dioxide conditions, respectively lower than 2–5% and higher than 4–5% (Cortellino, Gobbi, Bianchi, & Rizzolo, 2015; Iversen, Wilhelmsen, & Criddle, 1989; Yearsley, Banks, Ganesh, & Cleland, 1996). Even though the recorded O_2 values around 18% and the highest CO_2 level around 4% stood below the anaerobic threshold reported in literature, the high respiration quotients suggested that metabolic pathways different from the aerobic respiration were triggered. In order to clarify the metabolic response of fresh-cut apples upon PEF treatments, samples were collected and analysed by means of an NMR-based metabolomic approach.

3.3. Metabolomics: specific metabolic response of the tissue

The metabolic profiles of the four samples groups, acquired by HR-NMR analysis, gave rise to the quantification of 38 molecules (Table 2), identified by comparing the chemical shift and fine structure of their signals with literature and databases. A multivariate non-targeted approach was chosen to investigate the differences in the metabolic profiles upon the application of PEF at different electric field strength levels. Initially the PCA unsupervised method was applied to highlight the main sources of variation among the quantified metabolites. The first and second PCA axes, displayed in Fig. 4a, explained only the 25.65 and 15.47% of the variance, respectively. A separation of two main clusters was observable, corresponding to the samples treated above and below the threshold of irreversible electroporation. However, to boost the discrimination among the 4 classes a supervised chemometric tool based on sPLSDA-LDA was used. The two steps data process was tailored to both enhance the separation of the different treatments and, simultaneously, reduce the complexity of the model, by selecting and sorting the metabolites by importance. Firstly, the iterative sPLSDA step analysis resulted in parsimonious selection of 8 metabolites, which showed average VIP values higher than 1 in more than 70% out of one thousand repetitions. Secondly, a LDA model was built, based on the selected metabolites, so that an improved discrimination of the four classes was achieved. Fig. 4b–c illustrates score and loading plots while Table 3 shows the confusion matrix arisen from the chemometric analysis. The first projection of LDA (LD1) accounted

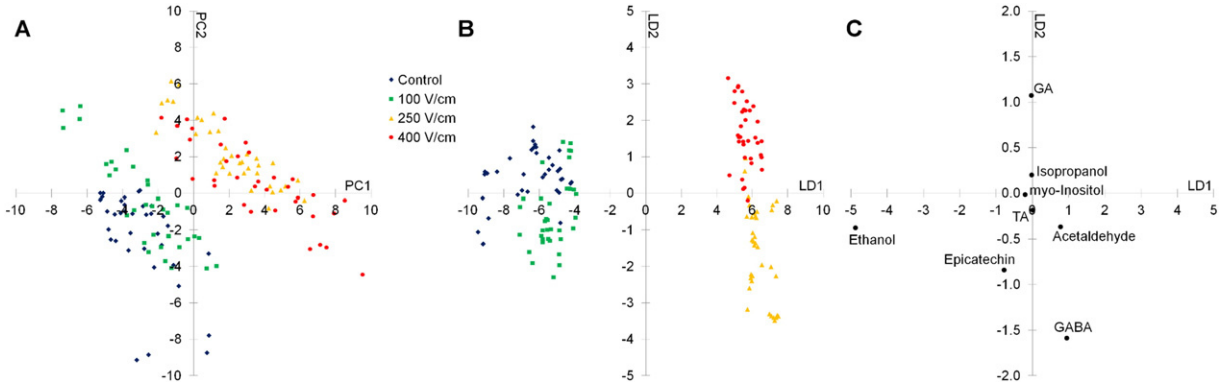

Fig. 4. PCA scores of the first two components (A), sPLSDA-LDA scores (B) and loadings (C) of the first two latent variables; GA = Glutamic acid, GABA = γ-Aminobutyric acid. Further details are reported in Material and methods section.

Table 3
Confusion matrix of 4-class LDA.

	Control	100 V/cm	250 V/cm	400 V/cm
Control	0.231	0.006	0.000	0.000
100 V/cm	0.019	0.244	0.000	0.000
250 V/cm	0.000	0.000	0.231	0.006
400 V/cm	0.000	0.000	0.019	0.244

for the 93.37% of the variance and clearly discriminated samples permanently electroporated from the others which, in agreement with PCA results, gave rise to the highest differences in the metabolic profiles. The second (LD2) and third (LD3) projections of LDA helped observing the fine-tuning of the modifications of the profiles between 250 and 400 V/cm and control-100 V/cm, respectively. In addition, the confusion matrix of Table 3 describes the correct assignment of the 95% of the cases. Interestingly, the remaining 5% of the samples were incorrectly assigned by the model only between control-100 V/cm and 250–400 V/cm.

Being intrinsically quantitative and high reproducible, HR-NMR analysis allowed the accurate estimation of the concentrations of the 8 metabolites resulting from sPLSDA analysis as characterized by the highest discriminative power among the studied groups of samples (Fig. 5). Interestingly, among these molecules, the concentrations of ethanol, acetaldehyde and isopropanol appeared as significantly affected by the application of the different electric fields, confirming that anaerobic fermentative metabolisms took place (Cortellino, Gobbi, Bianchi, & Rizzolo, 2015). Both ethanol and isopropanol contents were lowered by the PEF treatments, especially when the threshold of the irreversible electroporation was exceeded. The high alcohol levels detected could be a consequence of the microbial metabolism (Barth, Hankinson, Zhuang, & Breidt, 2009), but the reduction observed at the highest adopted PEF treatment confirmed their endogenous generation, as a consequence of apple tissue metabolism. Actually, according to Heinz, Alvarez, Angersbach, and Knorr (2001), the threshold value for the onset of microbial inactivation is about 5 kV/cm, thus extremely higher than the one applied in the present study. In this direction, according to the calorimetric and respiration results, the loss of the cell viability was the most probable cause.

Moreover, the concentration of acetaldehyde was different between samples treated at 250 V/cm and those subjected to 400 V/cm. However, it is worth mentioning that acetaldehyde has been reported to be produced in small amount, in particular, during the first day of storage after the cutting of the fresh tissue and remains constant afterwards (Soliva-Fortuny, Ricart-Coll, & Martín-Belloso, 2005). Due to the high volatility of this metabolite it was usually found in the headspace (Cortellino, Gobbi, Bianchi, & Rizzolo, 2015) and this can explained the high variability and the low concentration observed on the collected data, in the present work, by the analysis of the metabolome.

Beside anaerobic respiration, epicatechin showed a similar trend to the one evidenced for the two alcohols. In fact, PEF treatment above the irreversibility threshold lowered the amount of epicatechin without a linear correlation with the applied electric field. In addition, tartaric acid was diminished by the application of PEF at every condition. Both the metabolites could be affected by the oxidative stress due to the generation of reactive oxygen species (ROS) induced immediately after the formation of pores (Teissie, Eynard, Gabriel, & Rols, 1999). Indeed, epicatechin, as well as other phenolic compounds of plant tissues, is a source of active antioxidants which are easily oxidized by the technological processes (Berregi, Santos, del Campo, & Miranda, 2003). On the other hand, the pathway that leads to the biosynthesis of tartaric acid involves the degradation of ascorbic acid to threonic acid and, subsequently, to tartaric acid (Saito, Morita & Kasai, 1984). Similarly to the present work, this pathway was also subjected to PEF-specific response in potato tissue as observed by Galindo, Dejmek, Lundgren, Rasmusson, Vicente, and Moritz (2009).

Another metabolic pathway, previously described in potato tissue, is the one which involves the alteration of the Krebs cycle. Galindo, Dejmek, Lundgren, Rasmusson, Vicente, and Moritz (2009) stated that glutamic acid was affected by the application of PEF, within few hours after treatment, in a similar way to the wounding response. In the present work, two metabolites, i.e. glutamic acid and γ-aminobutyric acid (GABA), showed an accordant behaviour. Shelp, Bozzo, Trobacher, Zarei, Deyman and Brikis (2012) demonstrated that the production of γ-aminobutyric acid in plant tissue, including apples, was the results of the abiotic stress. In addition, the alteration of the Krebs cycle might also account for the lower heat and CO_2 productions.

To the best of our knowledge, hitherto the PEF-induced stress of vegetable tissues has been mainly described as short-term response. Indeed, previous works demonstrated that the generation of reactive oxygen species (ROS) occurs within seconds after the application of electric fields (Teissie, Eynard, Gabriel, & Rols, 1999; Ye, Huang, Chen, & Zhong, 2004). However, the effect of electroporation on plant tissue can last for hours or days due to the recovery processes, for instance the resealing of pores (Teissié, Escoffre, Rols, & Golzio, 2008; Vorobiev & Lebovka, 2009). In the present work, mainly long

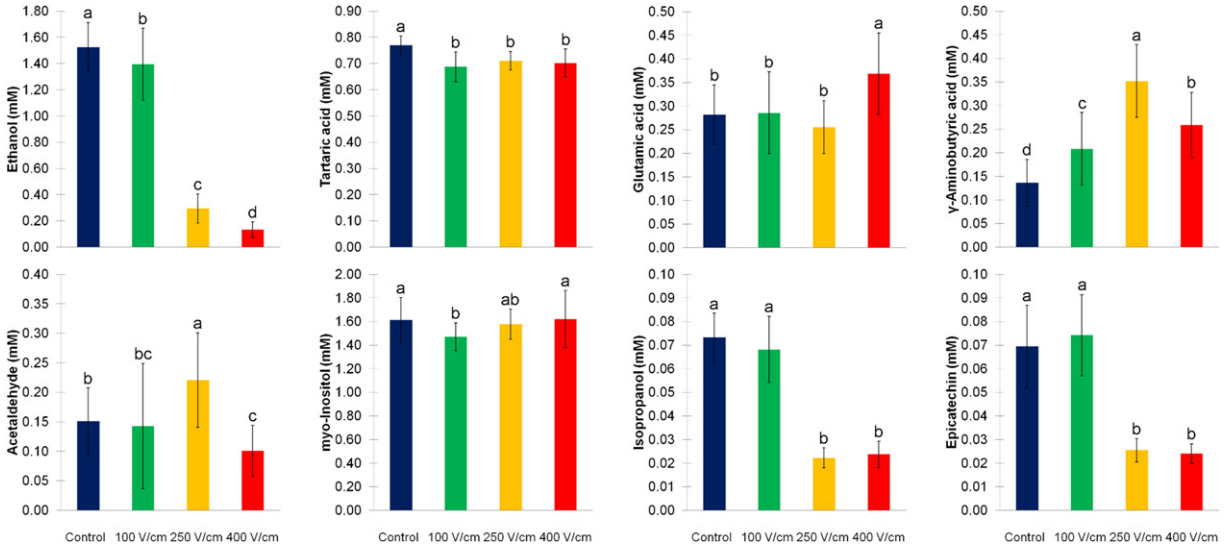

Fig. 5. Concentrations of the important metabolites as arisen from metabolomic analysis. Values are means ± standard deviations ($n = 36$) and differences between means with the same letter are not significant at $p < 0.05$.

term effects could be highlighted in agreement with Galindo, Dejmek, Lundgren, Rasmusson, Vicente, and Moritz (2009). The combination of data acquired by a multianalytical approach allowed us to clarify the PEF-induced stress responses and to hypothesize which metabolic pathways were triggered in accordance with the applied electric field.

4. Conclusions

The metabolic stress response induced by pulsed electric fields was strongly related to the electric field strength. The accurate control of the process parameters appears therefore fundamental for the feasible application of PEF in fresh-cut products, since irreversible damages of the membranes lead to a severe loss of the cell viability, with likely undesirable effects on the shelf life. Conversely, by applying electric field treatments below the threshold of irreversibility, merely slight effects on metabolic profiles of fresh-cut apple tissue were noticed, promoting the employment of PEF at those conditions.

The multianalytical approach based on calorimetry, gas analysis and NMR-based metabolomics led us to clarify important metabolic aspects of apples. Indeed, different PEF-induced metabolic pathways were revealed by analysing tens of metabolites simultaneously through a non-targeted approach. The measurement of heat production and gas analysis clustered the samples according to the reversibility or the irreversibility of the treatments, encouraging the use of this method for the assessment of PEF treatments in the fresh-cut sector. Nonetheless, only the combination of complementary techniques based on different physical principles resulted in a clear and comprehensive picture of the effects of pulsed electric fields on the metabolic response.

Acknowledgements

The authors acknowledge the financial support of the Italian Ministry for Education, Universities and Research (FIRB, Project RBFR100CEJ: *Innovative approach for the study of fresh-cut fruit: qualitative, metabolic and functional aspects*).

References

Angersbach, A., Heinz, V., & Knorr, D. (2000). Effects of pulsed electric fields on cell membranes in real food systems. *Innovative Food Science & Emerging Technologies*, *1*(2), 135–149.

Angersbach, A., Heinz, V., & Knorr, D. (2002). Evaluation of process-induced dimensional changes in the membrane structure of biological cells using impedance measurement. *Biotechnology Progress*, *18*(3), 597–603.

Barba, F. J., Parniakov, O., Pereira, S. A., Wiktor, A., Grimi, N., Boussetta, N., ... Witrowa-Rajchert, D. (2015). Current applications and new opportunities for the use of pulsed electric fields in food science and industry. *Food Research International*, *77*, 773–798.

Barth, M., Hankinson, T. R., Zhuang, H., & Breidt, F. (2009). Microbiological spoilage of fruits and vegetables. *Compendium of the microbiological spoilage of foods and beverages* (pp. 135–183). New York: Springer.

Bazhal, M., Lebovka, N., & Vorobiev, E. (2001). Pulsed electric field treatment of apple tissue during compression for juice extraction. *Journal of Food Engineering*, *50*(3), 129–139.

Belton, P., Delgadillo, I., Gil, A., Roma, P., Casuscelli, F., Colquhoun, I., ... Spraul, M. (1997). High-field proton NMR studies of apple juices. *Magnetic Resonance in Chemistry*, *35*(13), S52–S60.

Berregi, I., Santos, J. I., del Campo, G., & Miranda, J. I. (2003). Quantitative determination of (−)-epicatechin in cider apple juices by 1H NMR. *Talanta*, *61*(2), 139–145.

Capitani, D., Mannina, L., Proietti, N., Sobolev, A. P., Tomassini, A., Miccheli, A., ... Delfini, M. (2012). Metabolic profiling and outer pericarp water state in Zespri, Cl. GI, and Hayward kiwifruits. *Journal of Agricultural and Food Chemistry*, *61*(8), 1727–1740.

Carbonell-Capella, J. M., Buniowska, M., Esteve, M. J., & Frígola, A. (2015). Effect of *Stevia rebaudiana* addition on bioaccessibility of bioactive compounds and antioxidant activity of beverages based on exotic fruits mixed with oat following simulated human digestion. *Food Chemistry*, *184*, 122–130.

Chong, I. -G., & Jun, C. -H. (2005). Performance of some variable selection methods when multicollinearity is present. *Chemometrics and Intelligent Laboratory Systems*, *78*(1), 103–112.

Cortellino, G., Gobbi, S., Bianchi, G., & Rizzolo, A. (2015). Modified atmosphere packaging for shelf life extension of fresh-cut apples. *Trends in Food Science & Technology*, *46*(2), 320–330.

Cui, Q., Lewis, I. A., Hegeman, A. D., Anderson, M. E., Li, J., Schulte, C. F., ... Markley, J. L. (2008). Metabolite identification via the madison metabolomics consortium database. *Nature Biotechnology*, *26*(2), 162–164.

De Filippis, F., Pellegrini, N., Vannini, L., Jeffery, I. B., La Storia, A., Laghi, L., ... Lazzi, C. (2015). High-level adherence to a Mediterranean diet beneficially impacts the gut microbiota and associated metabolome. *Gut* (gutjnl-2015-309957).

Dellarosa, N., Ragni, L., Laghi, L., Tylewicz, U., Rocculi, P., & Dalla Rosa, M. (2016). Time domain nuclear magnetic resonance to monitor mass transfer mechanisms in apple tissue promoted by osmotic dehydration combined with pulsed electric fields. *Innovative Food Science & Emerging Technologies*, *37*(Part C), 345–351.

Donsì, F., Ferrari, G., & Pataro, G. (2010). Applications of pulsed electric field treatments for the enhancement of mass transfer from vegetable tissue. *Food Engineering Reviews*, *2*(2), 109–130.

Fiehn, O. (2002). Metabolomics—the link between genotypes and phenotypes. *Plant Molecular Biology*, *48*(1–2), 155–171.

Fincan, M., & Dejmek, P. (2002). In situ visualization of the effect of a pulsed electric field on plant tissue. *Journal of Food Engineering*, *55*(3), 223–230.

Galindo, F. G., Dejmek, P., Lundgren, K., Rasmusson, A. G., Vicente, A., & Moritz, T. (2009). Metabolomic evaluation of pulsed electric field-induced stress on potato tissue. *Planta*, *230*(3), 469–479.

Galindo, F. G., Rocculi, P., Wadsö, L., & Sjöholm, I. (2005). The potential of isothermal calorimetry in monitoring and predicting quality changes during processing and storage of minimally processed fruits and vegetables. *Trends in Food Science & Technology*, *16*(8), 325–331.

Galindo, F. G., Wadsö, L., Vicente, A., & Dejmek, P. (2008). Exploring metabolic responses of potato tissue induced by electric pulses. *Food Biophysics*, *3*(4), 352–360.

Giner, J., Gimeno, V., Barbosa-Cánovas, G., & Martín, O. (2001). Effects of pulsed electric field processing on apple and pear polyphenoloxidases. *Food Science and Technology International*, *7*(4), 339–345.

Gómez, F., Toledo, R. T., Wadsö, L., Gekas, V., & Sjöholm, I. (2004). Isothermal calorimetry approach to evaluate tissue damage in carrot slices upon thermal processing. *Journal of Food Engineering*, *65*(2), 165–173.

González-Arenzana, L., Portu, J., López, R., López, N., Santamaría, P., Garde-Cerdán, T., & López-Alfaro, I. (2015). Inactivation of wine-associated microbiota by continuous pulsed electric field treatments. *Innovative Food Science & Emerging Technologies*, *29*, 187–192.

Heinz, V., Alvarez, I., Angersbach, A., & Knorr, D. (2001). Preservation of liquid foods by high intensity pulsed electric fields—Basic concepts for process design. *Trends in Food Science & Technology*, *12*(3), 103–111.

Hoult, D. (2011). The principle of reciprocity. *Journal of Magnetic Resonance*, *213*(2), 344–346.

Iversen, E., Wilhelmsen, E., & Criddle, R. (1989). Calorimetric examination of cut fresh pineapple metabolism. *Journal of Food Science*, *54*(5), 1246–1249.

Ivorra, A. (2010). Tissue electroporation as a bioelectric phenomenon: Basic concepts. *Irreversible electroporation* (pp. 23–61). Springer.

Laghi, L., Picone, G., & Capozzi, F. (2014). Nuclear magnetic resonance for foodomics beyond food analysis. *TrAC Trends in Analytical Chemistry*, *59*, 93–102.

Lê Cao, K. -A., Boitard, S., & Besse, P. (2011). Sparse PLS discriminant analysis: Biologically relevant feature selection and graphical displays for multiclass problems. *BMC Bioinformatics*, *12*(1), 1.

Lebovka, N., Bazhal, M., & Vorobiev, E. (2002). Estimation of characteristic damage time of food materials in pulsed-electric fields. *Journal of Food Engineering*, *54*(4), 337–346.

Lebovka, N., Praporscic, I., & Vorobiev, E. (2004). Effect of moderate thermal and pulsed electric field treatments on textural properties of carrots, potatoes and apples. *Innovative Food Science & Emerging Technologies*, *5*(1), 9–16.

Luengo, E., Álvarez, I., & Raso, J. (2013). Improving the pressing extraction of polyphenols of orange peel by pulsed electric fields. *Innovative Food Science & Emerging Technologies*, *17*, 79–84.

Mauro, M. A., Dellarosa, N., Tylewicz, U., Tappi, S., Laghi, L., Rocculi, P., & Dalla Rosa, M. (2016). Calcium and ascorbic acid affect cellular structure and water mobility in apple tissue during osmotic dehydration in sucrose solutions. *Food Chemistry*, *195*, 19–28.

Mehmood, T., Liland, K. H., Snipen, L., & Sæbø, S. (2012). A review of variable selection methods in partial least squares regression. *Chemometrics and Intelligent Laboratory Systems*, *118*, 62–69.

Monakhova, Y. B., Schütz, B., Schäfer, H., Spraul, M., Kuballa, T., Hahn, H., & Lachenmeier, D. W. (2014). Validation studies for multicomponent quantitative NMR analysis: The example of apple fruit juice. *Accreditation and Quality Assurance*, *19*(1), 17–29.

Panarese, V., Laghi, L., Pisi, A., Tylewicz, U., Dalla Rosa, M., & Rocculi, P. (2012). Effect of osmotic dehydration on *Actinidia deliciosa* kiwifruit: A combined NMR and ultrastructural study. *Food Chemistry*, *132*(4), 1706–1712.

Parniakov, O., Lebovka, N., Bals, O., & Vorobiev, E. (2015). Effect of electric field and osmotic pre-treatments on quality of apples after freezing–thawing. *Innovative Food Science & Emerging Technologies*, *29*, 23–30.

Puértolas, E., Luengo, E., Álvarez, I., & Raso, J. (2012). Improving mass transfer to soften tissues by pulsed electric fields: Fundamentals and applications. *Annual Review of Food Science and Technology*, *3*, 263–282.

Rocculi, P., Panarese, V., Tylewicz, U., Santagapita, P., Cocci, E., Gómez Galindo, F., ... Dalla Rosa, M. (2012). The potential role of isothermal calorimetry in studies of the stability of fresh-cut fruits. *LWT- Food Science and Technology*, *49*(2), 320–323.

Saito, K., Morita, S. -i., & Kasai, Z. (1984). Synthesis of L (+) tartaric acid from 5-keto-D-gluconic acid in pelargonium. *Plant and Cell Physiology*, *25*(7), 1223–1232.

Santagapita, P., Laghi, L., Panarese, V., Tylewicz, U., Rocculi, P., & Dalla Rosa, M. (2013). Modification of transverse NMR relaxation times and water diffusion coefficients of kiwifruit pericarp tissue subjected to osmotic dehydration. *Food and Bioprocess Technology*, *6*(6), 1434–1443.

Shelp, B. J., Bozzo, G. G., Trobacher, C. P., Zarei, A., Deyman, K. L., & Brikis, C. J. (2012). Hypothesis/review: Contribution of putrescine to 4-aminobutyrate (GABA) production in response to abiotic stress. *Plant Science*, *193*, 130–135.

Soliva-Fortuny, R. C., Ricart-Coll, M., & Martín-Belloso, O. (2005). Sensory quality and internal atmosphere of fresh-cut golden delicious apples. *International Journal of Food Science and Technology*, *40*(4), 369–375.

Taiwo, K., Angersbach, A., & Knorr, D. (2002). Influence of high intensity electric field pulses and osmotic dehydration on the rehydration characteristics of apple slices at different temperatures. *Journal of Food Engineering*, *52*(2), 185–192.

Tappi, S., Berardinelli, A., Ragni, L., Dalla Rosa, M., Guarnieri, A., & Rocculi, P. (2014). Atmospheric gas plasma treatment of fresh-cut apples. *Innovative Food Science & Emerging Technologies*, *21*, 114–122.

Tappi, S., Gozzi, G., Vannini, L., Berardinelli, A., Romani, S., Ragni, L., & Rocculi, P. (2016). Cold plasma treatment for fresh-cut melon stabilization. *Innovative Food Science & Emerging Technologies*, *33*, 225–233.

Teissié, J., Escoffre, J., Rols, M., & Golzio, M. (2008). Time dependence of electric field effects on cell membranes. A review for a critical selection of pulse duration for therapeutical applications. *Radiology and Oncology*, *42*(4), 196–206.

Teissie, J., Eynard, N., Gabriel, B., & Rols, M. (1999). Electropermeabilization of cell membranes. *Advanced Drug Delivery Reviews*, *35*(1), 3–19.

Timmermans, R., Groot, M. N., Nederhoff, A., van Boekel, M., Matser, A., & Mastwijk, H. (2014). Pulsed electric field processing of different fruit juices: Impact of pH and temperature on inactivation of spoilage and pathogenic micro-organisms. *International Journal of Food Microbiology*, *173*, 105–111.

Tomita, S., Nemoto, T., Matsuo, Y., Shoji, T., Tanaka, F., Nakagawa, H., ... Sekiyama, Y. (2015). A NMR-based, non-targeted multistep metabolic profiling revealed L-rhamnitol as a metabolite that characterised apples from different geographic origins. *Food Chemistry*, *174*, 163–172.

Torrieri, E., Cavella, S., & Masi, P. (2009). Modelling the respiration rate of fresh-cut Annurca apples to develop modified atmosphere packaging. *International Journal of Food Science and Technology*, *44*(5), 890–899.

Trimigno, A., Marincola, F. C., Dellarosa, N., Picone, G., & Laghi, L. (2015). Definition of food quality by NMR-based foodomics. *Current Opinion in Food Science*, *4*, 99–104.

Vandendriessche, T., Schäfer, H., Verlinden, B. E., Humpfer, E., Hertog, M. L., & Nicolaï, B. M. (2013). High-throughput NMR based metabolic profiling of Braeburn apple in relation to internal browning. *Postharvest Biology and Technology*, *80*, 18–24.

Vorobiev, E., & Lebovka, N. (2009). Pulsed-electric-fields-induced effects in plant tissues: Fundamental aspects and perspectives of applications. *Electrotechnologies for extraction from food plants and biomaterials* (pp. 39–81). New York: Springer.

Wadsö, L., & Galindo, F. G. (2009). Isothermal calorimetry for biological applications in food science and technology. *Food Control*, *20*(10), 956–961.

Wadsö, L., Gomez, F., Sjöholm, I., & Rocculi, P. (2004). Effect of tissue wounding on the results from calorimetric measurements of vegetable respiration. *Thermochimica Acta*, *422*(1), 89–93.

Wiktor, A., Schulz, M., Voigt, E., Witrowa-Rajchert, D., & Knorr, D. (2015). The effect of pulsed electric field treatment on immersion freezing, thawing and selected properties of apple tissue. *Journal of Food Engineering*, *146*, 8–16.

Wishart, D. S., Jewison, T., Guo, A. C., Wilson, M., Knox, C., Liu, Y., ... Dong, E. (2012). HMDB 3.0—The human metabolome database in 2013. *Nucleic Acids Research* (gks1065).

Ye, H., Huang, L. L., Chen, S. D., & Zhong, J. J. (2004). Pulsed electric field stimulates plant secondary metabolism in suspension cultures of Taxus chinensis. *Biotechnology and Bioengineering*, *88*(6), 788–795.

Yearsley, C. W., Banks, N. H., Ganesh, S., & Cleland, D. J. (1996). Determination of lower oxygen limits for apple fruit. *Postharvest Biology and Technology*, *8*(2), 95–109.

Zhong, K., Wu, J., Wang, Z., Chen, F., Liao, X., Hu, X., & Zhang, Z. (2007). Inactivation kinetics and secondary structural change of PEF-treated POD and PPO. *Food Chemistry*, *100*(1), 115–123.

Paper VI

Betoret, E., Mannozzi, C., **Dellarosa**, **N.**, Laghi, L., Rocculi, P., & Dalla Rosa, M. (2017)

Metabolomic studies after high pressure homogenization processed low pulp mandarin juice with trehalose addition. Functional and technological properties

Journal of Food Engineering, 200, 22-28

Journal of Food Engineering 200 (2017) 22–28

Contents lists available at ScienceDirect

Journal of Food Engineering

journal homepage: www.elsevier.com/locate/jfoodeng

Metabolomic studies after high pressure homogenization processed low pulp mandarin juice with trehalose addition. Functional and technological properties

E. Betoret [a, *], C. Mannozzi [a], N. Dellarosa [a], L. Laghi [a, b], P. Rocculi [a, b], M. Dalla Rosa [a, b]

[a] Department of Agricultural and Food Sciences, University of Bologna, Cesena, Italy
[b] Interdepartmental Centre for Agri-Food Industrial Research, University of Bologna, Cesena, Italy

ARTICLE INFO

Article history:
Received 30 September 2016
Received in revised form
15 December 2016
Accepted 16 December 2016
Available online 18 December 2016

Keywords:
High pressures homogenization
Trehalose
Vitamin C
Flavonoids
NMR

ABSTRACT

This work aimed to determine the effect of homogenization pressures (HPH) and addition of trehalose on the functional and technological properties of low pulp mandarin juice (LPJ). A set of experiments was designed, combining a non-targeted metabolomic ^{1}H NMR based approach together with suspended pulp and transmittance, hesperidin, vitamin C and antioxidant activity analysis. Suspended pulp increased with HPH and trehalose addition. Flavonoid hesperidin initially decreased with HPH but trehalose addition resulted in less flavonoid degradation during storage, increasing the effect with the HPH. Vitamin C was not affected by trehalose and pressure treatment but more Vitamin C degradation was observed in trehalose samples during storage. Antiradical activity improvement by trehalose was conditioned by homogenization pressures and specific bioactive compounds. ^{1}H NMR based approach highlighted the HPH effect on the microbiological aspects of low pulp mandarin juice by the identification of key molecules responsible of the microorganism profile evolution during storage.

© 2016 Elsevier Ltd. All rights reserved.

1. Introduction

High pressure homogenization (HPH) process is a non-thermal technology applied in the food industry, mainly used to disrupt pathogens and spoilage microorganisms, inactivate enzymes and improve the nutritional and technological quality of food products. HPH has been demonstrated, in comparison with other technologies such as thermal treatments, to be less destructive of food compounds when related to sensory and nutritional properties. HPH can be used in the citrus industry for increasing the yield of citrus juices (Lortkipanidze et al., 1972) and for improving quality factors such as viscosity (Crandall and Davis, 1991; Patrignani et al., 2009), shelf-life (Maresca et al., 2011) and colour (Lee and Coates, 2004). The application of HPH to mandarin juices has been demonstrated to increase the stability of suspension and therefore improve the availability of bioactive compounds with antioxidant activity (Betoret et al., 2012). However, the degradation of those compounds during processing and storage is important. Previous studies have demonstrated that management of processing technologies can have influence on the functional properties of the final products obtained (Betoret et al., 2015; Barba et al., 2015a; Barba et al., 2012, 2015b; Zinoviadou et al., 2015). The addition of ingredients able to interact with food matrix can have a significant influence on bioactive compounds activity, degradation or release. Trehalose is a disaccharide able to maintain and preserve a wide group of biologically active molecules. This effect is due to the establishment of interactions that can contribute to the formation of a barrier able to maintain the integrity of the cellular structures and to prevent the decay during processing operations and/or storage (Colaço and Roser, 1994).

Juices are complex mixtures of macro- and micro- components. In most cases, the process treatment can modulate the entire molecular profile of the juices, beyond the few molecules at the center of attention, with possible unexpected consequences on the overall quality and acceptance. This is particularly important when the studied treatment is known to influence simultaneously several quality aspects, such as microbial spoilage, enzymatic activity or bioactivity. When possible unknown consequences of a treatment are looked for, a non-targeted screening exploration, analysing tens of compounds simultaneously, is highly desirable. In this respect, proton nuclear magnetic resonance (^{1}H NMR) spectroscopy has

* Corresponding author.
E-mail address: maria.betoretvalls@unibo.it (E. Betoret).

http://dx.doi.org/10.1016/j.jfoodeng.2016.12.011
0260-8774/© 2016 Elsevier Ltd. All rights reserved.

recently gained interest in food and nutritional sectors, due to its ability to give intrinsically quantitative information about the metabolic profile of foodstuff. Being non-destructive and highly reproducible over a wide range of metabolites concentration, ^{1}H NMR is able to analyze hundreds of compounds simultaneously within minutes and with minimal sample preparation (Laghi et al., 2014).

The aim of this work is to study the effect of high pressure homogenization (20 and 100 MPa) and trehalose (10 and 30%) addition, on technological and functional properties of Ortanique citrus fruit low pulp juices (LPJ). With the goal of obtaining a combination of information both on aspects of known interest and on the overall molecular profile of juices, a set of experiments was designed, combining a non-targeted metabolomic investigation based ^{1}H NMR together with suspended pulp and transmittance, hesperidin, vitamin C and antioxidant activity analysis.

2. Material and methods

2.1. Sample preparation and processing

Ortanique fruit, a hybrid of tangerine and sweet orange (*Citrus sinensis* x *Citrus reticulata*) was provided by Rural S. Vicent Ferrer cooperative located in Benaguacil (Valencia), Spain. The preparation of the juices was carried out according to the patent WO/2007/042593 titled "Method of obtaining refrigerated pasteurized citrus juices" (Izquierdo et al., 2007). The fruits were washed by immersing them in tap water, drained, and squeezed in an extractor ("GAM" MOD.SPA 1400 rpm, Cesena, Italy). Raw juice was centrifuged at 3645 g during 5 min at 4 °C (Beckman Coulter AvantiTM J-25, Milan, Italy), homogenized with a Panda Plus pilot homogenizer (Niro Soavi, Parma, Italy) 20 and 100 MPa and no homogenized, pasteurized at 63 °C for 15 s (Roboqbo, Bologna, Italy), collected in sterile jars, and quickly frozen at −18 °C until analyzed. In juice samples with trehalose, an amount of 10 and 30% (w/w) was added before homogenization.

2.2. Physicochemical characterization

Total soluble solids were measured as Brix with a digital refractometer (Pal-1; Atago Co., Ltd., Tokyo, Japan). Total titratable acidity was assessed by titration with 0.1 N NaOH and expressed as the percentage of citric acid. pH was measured with a potentiometer (micropH Crison GLP21). The values provided are the average of three replicates.

2.3. Suspended pulp and transmittance

Suspended pulp was evaluated reading the separated pulp (%) by centrifugation at 3500g during 10 min at 27 °C (FMC FoodTech, 2005). The supernatant was collected and evaluated its transmittance at 650 nm in spectrophotometer (Shimadzu UV-1601). The values provided are the average of six replicates.

2.4. Flavonoid hesperidin

The content of the main flavonoid hesperidin was determined using HPLC LC-1500 (Jasco, Carpi, MO, Italy) with a diode array detector (DAD) and filled with a C18 reversed-phase column (150 × 4.60 mm, Phenomenex Kinetex® 5U C18 100°) following the method described in Betoret et al., 2009. The juice samples were measured after 0, 3 and 10 days of storage. The values provided are the average of three replicates.

2.5. Vitamin C

Vitamin C content was measured by HPLC LC-1500 (Jasco, Carpi, MO, Italy) equipped with thermostat autosampler and diode array detector (DAD).

Fresh juice samples were centrifuged at 15,000 g (4 °C, 5 min) and aliquots (1 mL) of supernatant were filtered with nylon filter 0.45 μm and then 10 μL were injected into the HPLC C18 reverse phase column (150 × 4.60 mm, Phenomenex Kinetex® 5U C18 100°). System conditions were established according to Odriozola-Serrano et al. (2007).

The juice samples were measured after 0, 3 and 10 days of storage. The values provided are the average of three replicates.

2.6. Antiradical activity

The antiradical activity was determined by ABTS and DPPH tests. The ABTS test was based on the method proposed by Polydera et al. (2005). A volume of 15.3 μL juice was added to ABTS solution. The absorbance was measured with a spectrophotometer Beckman Coulter DU 730 Life Science model every 30 s for a total time of 30 min. The results were expressed as TEAC (Trolox Equivalent Antiradical Capacity). The values provided are the average of twelve replicates. The DPPH test was based on the method proposed by Brand-Williams et al. (1995). A volume of 30 μL of juice was added to DPPH solution. The absorbance was measured with a spectrophotometer (Beckman Coulter model DU 730 Life Science) at 515 nm every 2 min for a total time of 70 min. The results were expressed as $mmol \cdot L^{-1}$ equivalents of ascorbic acid. The values provided are the average of twelve replicates.

2.7. Untargeted metabolomics approach

Samples were prepared for analysis, and ^{1}H NMR spectra were registered and processed, according to Dellarosa et al., 2016. Spectra were manually integrated giving rise to 89 protons signals in the typical regions of sugars, amino acids, organic acids, alcohols, polyphenols and nucleotides. At least five replicates were analyzed for each sample group. The obtained 102 × 89 (samples × signals) matrix, scaled and centred, underwent signals assignments and multivariate analysis.

NMR signals assignment was performed by comparison with works performed on similar food matrices at comparable pH (Capitani et al., 2012; de Oliveira et al., 2014; Le Gall et al., 2001; Spraul et al., 2009), assignment through Chenomx software (Chenomx, Alberta, CA) and comparison with HMDB and Madison public databases. In case of unresolved ambiguity, suitable 2D experiments were performed.

To study the changes occurring during the storage period and upon the tested treatments, sparse Partial Least Square Regression (sPLSR) (Lê Cao et al., 2008) and its discriminant analysis counterpart (sPLSDA) (Lê Cao et al., 2011), were performed, as implemented in mixOmics package in R statistical software (R Foundation for Statistical Computing, Vienna, Austria). Train and test sets accounted for 70% and 30% of the samples respectively. The sPLSR and sPLSDA models were trained by 10-fold validation based on minimal root mean square error (RMSEP) and error rate, respectively. The maximum parsimony of the models was looked for by building and testing 1000 models, and by retaining only the molecules with average VIP value (Variable Importance in Projection) (Eriksson et al., 2001) above one and accepted by sparsity algorithm more than 500 times. The key metabolites arisen from the sPLS models were employed for linear regression and linear discriminant analysis (Ripley, 1996), in order to describe changes during storage and upon HPH treatments. This approach led to

models where single coefficients were needed to correlate metabolite concentration with each response. Such choice combined user-friendliness to high accuracy and precision.

2.8. Statistical analysis

In order to evaluate whether the average values were significantly different a multi factorial ANOVA and Tukey's multiple comparisons, with 95% confidence level, were performed in R statistical software (R Foundation for Statistical Computing, Austria). All the experiments were repeated at least three times and results were expressed as mean ± standard deviation of replications.

3. Results and discussion

3.1. Physicochemical characterization of LPJ and evaluation of suspended pulp and cloudiness

Fresh LPJ samples were characterized by measuring the soluble solids content (13.40 ± 0.02 $g_{soluble\ solids}/g_{liquid\ phase}$), acidity (2.35 ± 0.02 $mg_{citric\ acid}/100g_{juice}$), maturity index (5.7 ± 0.3) and pH (2.83 ± 0.06).

Suspended pulp and supernatant transmittance at 3500 g of all samples homogenized at 20 and 100 MPa and no homogenized with trehalose addition in proportion 0, 10 and 30 (%) (w/w) were determined. The results are shown in Table 1. An analysis of variance showed, with a confidence level of 95%, than both variables pressure homogenization and trehalose addition, as well as their interaction, have a significant effect on suspended pulp and transmittance.

Homogenization is a unit operation that involves pressure application to liquids to fragment the solid particles and oil droplets into smaller particles. Orange cloud particles ranges in size from 400 to 5000 nm are more stable than those smaller than 2000 nm (Buslig and Carter, 1974). As expected, there is a tendency to decrease the suspended pulp with homogenization pressures applied (Table 1). The homogenization pressures decrease the particle size of the LPJ cloud making the juice suspension more stable. In the same way, low values of suspended pulp result in low levels of transmittance and high levels of cloudiness.

In the industrial juices processing, trehalose addition varies between 0.4% of final product to 50% of sugar replacement. It has been used traditionally in order to improve the aromatic profile, colour, reduce sweetness and stabilize pH in processed juices (Richards and Dexter, 2011). On an equal level of pressure applied, the addition of trehalose results in a decrease of separated pulp and transmittance values (Table 1). LPJ cloud is formed by different particles types such as cellular organelles and membranes, oil droplets, flavonoids and cell wall fragments such as pectin, cellulose and hemicellulose (Baker and Cameron, 1999). Trehalose is a disaccharide able to interact with various compounds, forming a glassy amorphous matrix around the tertiary structure of the proteins and phospholipids exerting a protective effect on various technological processes (Colaço and Roser, 1994; Crowe et al., 1990; Rudolph and Crowe, 1985). Trehalose could interact with LPJ cloud compounds stabilizing the suspension and maintaining the juice cloudiness. These interactions could be promoted by homogenization pressures as a result of smaller particle size after treatment.

3.2. Functional compounds determination

The main mandarin juice flavonoid hesperidin was determined by HPLC in LPJ samples homogenized at 20 and 100 MPa and no homogenized with trehalose addition in a proportion 0, 10 and 30% (w/w) after 0, 3 and 10 storage days. The results obtained are shown in Table 2.

In general terms, with a 95% confidence level, both homogenization pressures and trehalose addition have a significant effect on hesperidin content during storage. The application of homogenization pressures results in a flavonoid content decrease that it is bigger when higher pressures are applied. These results are different to those obtained by Betoret et al., 2012 in which the application of 20 MPa pressures resulted in maintaining and even increased flavonoids content.

The biosynthesis of flavonoid depends on genetic, environmental factors (Bae et al., 2014) and shows different peaks during fruits development which generally are owed to the formation of protective compounds in early stages on the one side, and the formation of optical signals at the end of fruit ripening on the other side (Griesser et al., 2008; Halbwirth et al., 2006). Flavonoid content decreases with more advanced ripening stages explaining the differences observed in the flavonoid content determined in Betoret et al., 2012. Maturity index together with the forces and temperature stresses created in the homogenization valve as well as the low pulp juice content could lead a degradation of flavonoid during homogenization in this case.

In Table 2, it is possible to see a tendency to increase flavonoid content on third storage day, being bigger in those samples homogenized at 100 MPa with trehalose content. This effect could be related to a physical effect on previous flavonoid extraction procedure. At 100 MPa greater particle size reduction could result on bigger interaction capacity between particles, more stable LPJ cloud and therefore difficult flavonoid extraction. On third storage day, the interaction between particles could have been weakened facilitating flavonoid extraction. Food matrix has an important influence on bioactive compounds, the structure changes caused by processing or by storage, in those cases in which degradation of bioactive compounds has not been occurred yet, can facilitate the extraction of bioactive compounds (Betoret et al., 2015).

To evaluate the effect of storage together with homogenization

Table 1
Suspended pulp and turbidity determination. Separated pulp at 3500 g and transmittance of the supernatant. Values expressed as mean ± standard deviation. The values provided are the average of six replicates.

Homogenization pressure (MPa)	Trehalose (%)	Separated pulp (%)	Transmittance (%)
0	0	9.03 ± 0.02^{a}	22.3 ± 0.8^{a}
0	10	5.30 ± 0.05^{d}	19.2 ± 2.6^{b}
0	30	2.00 ± 0.05^{f}	14.8 ± 1.6^{c}
20	0	8.50 ± 0.02^{b}	7.5 ± 1.5^{e}
20	10	5.110 ± 0.012^{e}	7.3 ± 2.2^{e}
20	30	1.00 ± 0.03^{g}	4.7 ± 3.3^{f}
100	0	7.10 ± 0.02^{c}	8.3 ± 0.9^{d}
100	10	5.22 ± 0.03^{e}	8.20 ± 1.02^{d}
100	30	1.000 ± 0.012^{g}	4.3 ± 1.6^{f}

* Values with different superscript letters in a column are significantly different ($p \leq 0.05$).

Table 2
Hesperidin content (mg/L) in LPJ samples during 0, 3 and 10 days of storage and percentage of degradation calculated from 10 to 0 days of storage. Values expressed as mean ± standard deviation. The values provided are the average of three replicates.

Homogenization pressure (MPa)	Trehalose (%)	0 days	3 days	10 days	Degradation (%)
0	0	138.1 ± 0.8^{a}	132.2 ± 0.4^{a}	51.51 ± 17.07^{e}	62.7 ± 12.6
0	10	133.5 ± 3.9^{b}	143.4 ± 1.6^{a}	74.7 ± 0.5^{bc}	18.2 ± 2.9
0	30	145.7 ± 3.2^{a}	145.8 ± 3.7^{a}	76.7 ± 3.8^{bc}	1.5 ± 4.4
20	0	88.8 ± 0.4^{d}	83.6 ± 1.9^{be}	72.7 ± 2.2^{c}	44 ± 2
20	10	97.2 ± 0.6^{d}	83.4 ± 2.9^{bf}	84.1 ± 2.2^{ab}	13.5 ± 2.8
20	30	106.3 ± 9.6^{c}	93.4 ± 1.7^{bc}	94.7 ± 3.8^{a}	4.1 ± 4.6
100	0	69.1 ± 1.9^{f}	79.3 ± 18.5^{cdef}	68.01 ± 1.13^{d}	47.3 ± 3.7
100	10	72.1 ± 0.3^{ef}	85.8 ± 0.2^{bd}	69.1 ± 2.9^{d}	10.7 ± 4.5
100	30	79.430 ± 3.108^{e}	99.0 ± 7.7^{b}	74.9 ± 1.2^{bc}	5.66 ± 2.13

* Values with different superscript letters in a column are significantly different ($p \leq 0.05$).

pressures and trehalose addition, the degradation percentage was calculated. The obtained results are shown in Table 2. Generally, an increase in homogenization pressures results in a decrease of bioactive compounds degradation during storage. Trehalose addition also results in less flavonoid degradation, increasing the effect with the homogenization pressures. This effect could be related with cloudiness stability and trehalose capacity interacting and forming complexes with bioactive compounds. Smaller particles are able to interact better with LPJ cloud and thus are less available for degradative reactions.

Vitamin C content was determined by HPLC in LPJ samples homogenized at 20 and 100 MPa and no homogenized with trehalose addition in a proportion 0, 10 and 30% (w/w) after 0, 3 and 10 storage days. Vitamin C is an important bioactive compound very well known for its beneficial effects but characterized by its easy degradation and low stability. In all analyzed samples, during all storage time, vitamin C content was in range 110–140 mg/L (Table 3). The statistical analysis showed, with a 95% confidence level, that both variables pressure and trehalose have a significant effect of vitamin C content and this effect depends on storage time. On day 0, homogenization pressures together with trehalose addition interaction have a significant effect on vitamin C content. On days 3 and 10, the analysis of variance indicates that both variables as well as their interaction have a significant effect on the content of vitamin C.

It is possible to observe the same tendency behaviour in all analyzed samples, with non-homogenized and 20 MPa trehalose samples slightly higher vitamin C content and 100 MPa trehalose samples slightly lower content than non trehalose samples. As in the case of flavonoid, it is possible to observe a tendency to increase vitamin C content until the third day of storage. Physical effect network created by trehalose and homogenization pressures can decrease until the third day of storage in which is possible to observe the maximum quantity of Vitamin C. As previously said, food matrix has an important influence on bioactive compounds, the structure changes caused by processing or by storage time, in those cases in which degradation of bioactive compounds has not been occurred yet, can facilitate the extraction of bioactive compounds (Betoret et al., 2015). Higher degradation on vitamin C content has been observed in all samples after 10 days of storage. Table 3 shows the degradation percentage of vitamin C during storage. As it is possible to see, addition of trehalose seems to increase vitamin C degradation in 2–4%.

The protective effect of trehalose on bioactive compounds seems to depend specifically on each compound to be protected. Literature lacks specific studies on the effect of adding sucrose substitutes on the content of polyphenols in fruit products. There are some reports describing the effect of adding sucrose, maltose, fructose and trehalose on bioactive compounds degradation during storage (Kopjar et al., 2009, 2012). Kopjar et al., 2008 reported a positive effect on anthocyanins protection with trehalose having the most positive effect of all investigated sugars. In contrast to most other disaccharides, trehalose has no direct internal hydrogen bonds. All four internal bonds are indirectly connected via the two water molecules, which form part of the native dihydrated structure. This arrangement gives the molecule an unusual flexibility around the disaccharide bond, which may allow it to fit more closely with the irregular surface of macromolecules than other, more rigid disaccharides, in which the rings are directly hydrogen bonded to each other (Colaço and Roser, 1994). According to Bordat et al. (2004), trehalose has effect on “destructuring” the network of water and on slowing down its dynamics. This property could play a key role in the understanding of the microscopic mechanisms of bioprotection.

3.3. Antiradical determination

The ABTS and DPPH tests were performed on distilled water containing trehalose 10 and 30% (w/w) and on homogenized LPJ with and without trehalose addition. The results obtained are

Table 3
Vitamin C content (mg/L) in LPJ samples during 0, 3 and 10 days of storage and percentage of degradation calculated from 10 to 0 days of storage. Values expressed as mean ± standard deviation. The values provided are the average of three replicates.

Homogenization pressure (MPa)	Trehalose (%)	0	3	10	Degradation (%)
0	0	129.2 ± 0.7^{b}	135.63 ± 2.09^{c}	119.3 ± 1.4^{b}	7.7 ± 0.6
0	10	134.1 ± 1.4^{a}	139.3 ± 1.6^{ab}	119.6 ± 1.4^{b}	8.2 ± 0.4
0	30	133.4 ± 1.4^{a}	137.0 ± 1.6^{bc}	123.1 ± 1.4^{a}	8.44 ± 1.06
20	0	128.7 ± 0.4^{b}	135.66 ± 0.15^{c}	118.1 ± 0.5^{b}	10.8 ± 1.3
20	10	133.9 ± 1.4^{a}	141.5 ± 0.7^{a}	118.4 ± 0.8^{b}	11.5 ± 1.2
20	30	131.56 ± 3.03^{ab}	141.59 ± 3.02^{a}	122.1 ± 2.3^{a}	10.7 ± 1.4
100	0	128.6 ± 1.6^{b}	134.9 ± 0.3^{c}	117.7 ± 0.7^{b}	7.7 ± 1.5
100	10	122.6 ± 2.6^{c}	131.8 ± 0.6^{d}	109.4 ± 0.7^{d}	7.2 ± 0.9
100	30	125.4 ± 1.9^{c}	131.5 ± 0.6^{d}	112.2 ± 1.7^{c}	10.4 ± 0.2

* Values with different superscript letters in a column are significantly different ($p \leq 0.05$).

shown in Table 4.

Two analytical methods were used to determine the total antiradical activity of LPJ, since both have some limitations (Shui and Peng, 2004; Prior et al., 2005). DPPH method seems to be more sensitive to the flavanones while ABTS method seems to be more sensitive to the radical scavengers such as vitamin C (Del Caro et al., 2004). Indeed, these two methods represent a useful tool to evaluate the antiradical scavenging activity of different fruits (Gil et al., 2000; Shui and Peng, 2004).

The analysis of variance indicated, with a probability of 95%, that the homogenization pressures, the trehalose addition as well as their interaction have a significant effect on the activity antiradical determined through both ABTS and DPPH methods.

In the ABTS method, considering the samples without trehalose, the increase in the homogenization pressure causes a slight increase in the antiradical activity. This increment is bigger in samples no homogenized and homogenized at 20 MPa that from no homogenized and homogenized at 100 MPa without significant differences between the two levels of pressure applied. In not homogenized samples, trehalose addition supposes an increasing in antiradical activity that it is maintained without significant differences between 10 and 30%. However, for homogenized samples, the antiradical activity increases in the case of samples with 10% of trehalose and decreases for 30% trehalose samples. Samples with trehalose addition have less quantity of LPJ thus a lower antiradical activity expected. As shown in the water solutions, trehalose alone appears to not have antiradical activity. Nevertheless, it is possible that trehalose could have an interaction effect with LPJ cloud as observed in above turbidity measures and this could have an effect on those bioactive compounds that are more sensitive to ABTS method.

In DPPH method, the application of homogenization pressures increases the antiradical activity more from no homogenized samples to homogenized at 20 MPa than from no homogenized samples to homogenized at 100 MPa but the differences observed are not significant. Nevertheless, in not homogenized samples the addition of trehalose results in a minor antiradical activity. It seems that the decreasing particle size by homogenization operation affects trehalose interaction capacity with LPJ cloud and this has an influence on those compounds more sensitive to DPPH method.

Kopjar et al. (2009, 2012) showed the addition of trehalose and sucrose might improve the antiradical activity of fruits products. In our obtained results, antiradical activity improvement by trehalose is conditioned by homogenization pressures and specific bioactive compounds. Antiradical activity results correspond with those obtained for suspended pulp and functional compounds determinations.

3.4. Evolution of molecular profile with storage and HPH treatment

^{1}H NMR was employed as an unbiased screening tool for HPH treatments by following a non-targeted approach (Trimigno et al., 2015). Due to the reduced mobility of the solutes caused by the high viscosity, NMR analysis gave rise, in samples added with trehalose, to signals excessively broad and superimposed. The desired untargeted approach by ^{1}H NMR was therefore limited to the study of the effects of HPH treatments and storage.

When considering the storage time, VIP and sparsity criteria highlighted in sPLSR models 4 signals with the highest variation along time, at 8.27, 2.55, 0.79 and 0.81 ppm respectively, that were assigned, through literature comparison, database and 2D-NMR experiments, to formic acid, glutamic acid and two phenolic moieties respectively. The consequent dramatic reduction of the information complexity allowed outlining the correlation between storage time and molecular profile based on a linear model, based on the evidenced 4 molecules only (Fig. 1a). Such model was characterized by an uncertainty to 0.7 days, with a coefficient of determination (R2) as high as 0.96.

When considering HPH treatment, there were no biological reasons suggesting a linear relationship between molecular profile and treatment pressures, so that a 3 classes discriminant analysis was setup, by means of sPLSDA algorithm. Among the 89 signals, only four were selected by VIP and sparsity criterion, glucose, gallic acid, alanine and, again, glutamic acid. The 4 molecules were employed to substitute sPLSDA model with its linear counterpart (Fig. 1b), resulting in an error rate lower than 1%. Interestingly the two dimensions of the linear model ended up representing separately the peculiarities of 100 MPa and of 20 MPa treatments, on LD1 and LD2 respectively.

The molecules showing the greatest variations along storage time and upon high-pressure treatments, highlighted by multivariate analysis, were employed to explore the interactions between the two factors analyzed, a possible key point in order to finely tailor the juice technological treatments. Fig. 1c shows their concentrations at the beginning and the end of the storage period, organized per HPH treatment. Formic acid concentration in samples at day 0 did not show any correlation with HPH, thus highlighting that this treatment had no direct effect on its solubilization. Formic acid concentration, nevertheless, systematically increased with storage time and such increase was now proportional to the applied pressure levels.

Contrary to formic acid, concentrations of glutamic acid and glucose were proportional to the applied pressures at day 0, suggesting a direct effect of HPH on their solubilization. Once more, dissimilarly from formic acid, glutamic acid and glucose, together with alanine, decreased proportionally to storage time in untreated

Table 4
Antiradical activity of low pulp juice samples by ABTS and DPPH methods. Results expressed as TEAC and mmol·L^{-1} ascorbic acid respectively. Values expressed as mean ± standard deviation. The values provided are the average of three replicates.

Sample	Homogenization pressure (MPa)	Trehalose (%)	ABTS	DPPH
Water	0	10	0.0 ± 0.0	0.0 ± 0.0
Water	0	30	0.040 ± 0.012	0.0 ± 0.0
Low pulp juice	0	0	0.70 ± 0.06^{d}	1.6 ± 0.2^{bd}
Low pulp juice	0	10	0.99 ± 0.08^{a}	0.91 ± 0.12^{f}
Low pulp juice	0	30	0.92 ± 0.08^{b}	0.80 ± 0.06^{f}
Low pulp juice	20	0	0.88 ± 0.12^{b}	1.7 ± 0.2^{a}
Low pulp juice	20	10	0.94 ± 0.02^{ab}	1.69 ± 0.02^{ab}
Low pulp juice	20	30	0.59 ± 0.04^{e}	1.57 ± 0.08^{acd}
Low pulp juice	100	0	0.81 ± 0.02^{c}	1.59 ± 0.12^{bc}
Low pulp juice	100	10	0.87 ± 0.02^{bc}	1.42 ± 0.04^{cde}
Low pulp juice	100	30	0.70 ± 0.07^{d}	1.3 ± 0.2^{e}

* Values with different superscript letters in a column are significantly different ($p \leq 0.05$).

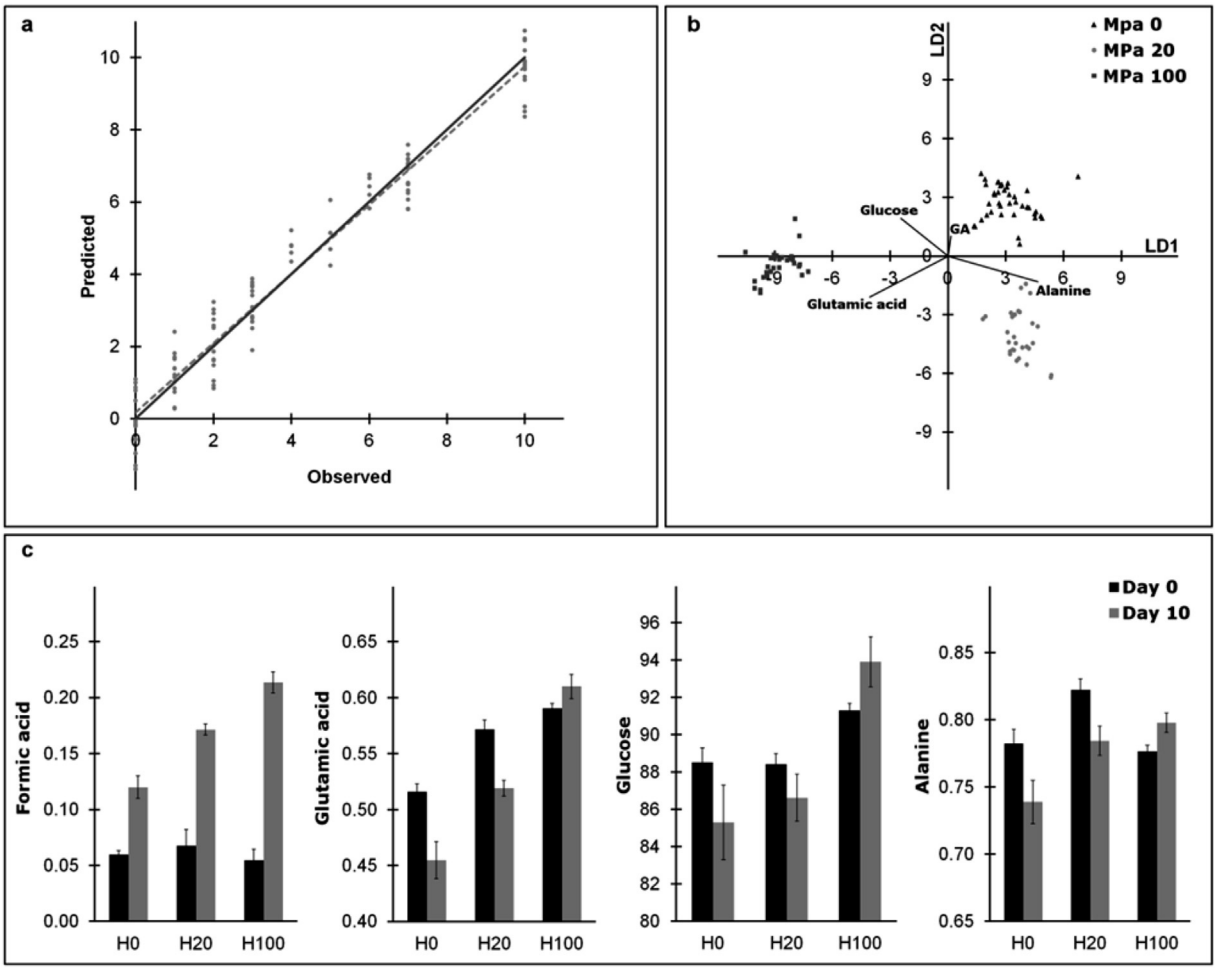

Fig. 1. **(a)** Storage time (days) predicting ability of a linear model based on the concentration of formic acid, glutamic acid and the two phenolic moieties, selected by sPLSR model. **(b)** Consequences of high pressure homogenization treatments (0 MPa (H0); 20 MPa (H20); 100 MPa (H100) on the concentration of glucose, glutamic acid, alanine and gallic acid (GA), highlighted by representing the samples treated at 0 (triangles), 20 (circles) and 100 (squares) MPa on the first (LD1) and second (LD2) direction of a linear discriminant model. **(c)** Concentrations (mM), at the beginning (Day 0) and at the end (Day 10) of the storage period, expressed as mean ± standard deviation, of the metabolites mostly influenced by storage time and high pressure homogenization treatment.

samples and HPH samples at 20 MPa, but increased in HPH samples at 100 MPa.

The overall observation of these trends suggests that HPH solubilization ability and different microbial activities had a joint effect on the concentration of these molecules. The systematic increase of formic acid with storage, proportional to the pressure levels even when 100 MPa were selected, suggests that this molecule was probably the result of microbial activity and that microbes responsible for its production were not significantly hampered by pressure treatments. In this context it is worth underlining that Patrignani et al. (2009) found that a treatment with HPH at 100 MPa inactivates yeasts. Moreover, Maresca et al. (2011) showed that a single-pass treatment at 100 MPa led to a significant reduction of yeasts, with no effects on bacteria. Bacteria can be therefore suggested as the main responsible for formic acid production in the observed juices. Glutamic acid and glucose trends show that the concentration of these molecules was reduced by microbes, which growth was hampered by 100 MPa HPH treatments. Following Patrignani and Maresca findings, yeast can therefore be suggested as the main responsible for their concentration changes. Finally, a contribution to the reduced anabolic activity at 100 MPa may be exerted also by formic acid, with known antimicrobial proprieties (Berregi et al., 2007).

4. Conclusions

HPH and trehalose addition have a significant effect on functional and technological properties of low pulp mandarin juice. HPH affects the juice cloud structure influencing trehalose interactions. The protecting effect of trehalose during storage it is affected by HPH and it is compound specific. ^{1}H NMR based approach highlighted the HPH effect on the microbiological aspects of low pulp mandarin juice by the identification of key molecules responsible of the microorganism profile evolution during storage.

Acknowledgements

This research was supported by a Marie Curie Intra European Fellowship (626643) within the 7th European Community Framework Programme.

References

Bae, H., Jayaprakasha, G.K., Crosby, K., Yoo, K.S., Leskovar, D.I., Jifon, J., Patil, B.S., 2014. Ascorbic acid, capsaicinoid, and flavonoid aglycone concentrations as a function of fruit maturity stage in greenhouse-grown peppers. J. Food Compos. Anal. 33, 195–202.

Baker, R.A., Cameron, R.G., 1999. Clouds of citrus juices and juice drinks. Food

Technol. 53, 64–69.
Barba, F.J., Esteve, M.J., Frígola, A., 2012. High pressure treatment effect on physicochemical and nutritional properties of fluid foods during storage: a review. Compr. Rev. Food Sci. Food Saf. 11 (3), 307–322.
Barba, F.J., Pereira, S.A., Wiktor, A., Grimi, N., Boussetta, N., Saraiva, J.A., Raso, J., Martin-Belloso, O., Witrowa-Rajchert, D., Lebovka, N., Vorobiev, E., 2015b. Current applications and new opportunities for the use of pulsed electric fields in food science and industry. Food Res. Int. 77, 773–798.
Barba, F.J., Terefe, N.S., Buckow, R., Knorr, D., Orlien, V., 2015a. New opportunities and perspectives of high pressure treatment to improve health and safety attributes of foods. A review. Food Res. Int. 77 (4), 725–742.
Berregi, I., del Campo, G., Caracena, R., Miranda, J.I., 2007. Quantitative determination of formic acid in apple juices by 1H-NMR spectrometry. Talanta 72 (3), 1049–1053.
Betoret, E., Betoret, N., Carbonell, J.V., Fito, P., 2009. Effects of pressure homogenization on particle size and the functional properties of citrus juices. J. Food Eng. 92 (1), 18–23.
Betoret, E., Betoret, N., Rocculi, P., Dalla Rosa, M., 2015. Strategies to improve food functionality: structure-property relationships on high pressures homogenization, vacuum impregnation and drying technologies. Trends Food Sci. Technol. 46 (1), 1–12.
Betoret, E., Betoret, N., Santandreu, E., Fito, P., 2012. Homogenization pressures applied to citrus juice manufacturing. Functional properties and application. J. Food Eng. 111 (1), 28–33.
Bordat, P., Lerbret, A., Demaret, J.-P., Affouard, F., Descamps, M., 2004. Comparative study of trehalose, sucrose and maltose in water solutions by molecular modelling. Europhys. Lett. 65, 41–47.
Brand-Williams, W., Cuvelier, M.E., Berset, C., 1995. Use of a free radical method to evaluate antioxidant activity. Lebensm. Wiss. Technol. 28, 25–30.
Buslig, B.S., Carter, R.D., 1974. Particle size distribution in orange juices. Proc. Fla. State Hortic. Soc. 87, 302–305.
Capitani, D., Mannina, L., Proietti, N., Sobolev, A.P., Tomassini, A., Miccheli, A., Delfini, M., 2012. Metabolic profiling and outer pericarp water state in Zespri, CI. GI, and Hayward kiwifruits. J. Agric. food Chem. 61 (8), 1727–1740.
Colaço, C.A.L.S., Roser, B., 1994. Trehalose, a multifunctional additive for food preservation. In: Mathlouthi, M. (Ed.), Food Packaging and Preservation, pp. 123–140.
Crandall, P.G., Davis, K.C., 1991. Viscosity reduction and reformation of structure in orange concentrate as affected by homogenization within commercial taste evaporators. J. Food Sci. 56, 1360–1364.
Crowe, J.H., Carpenter, J.F., Crowe, L.M., Anchordoguy, T.J., 1990. Are freezing and dehydration similar stress vectors? A comparison of modes of interaction of stabilizing solutes with biomolecules. Cryobiology 27, 219–231.
de Oliveira, C.R., Carneiro, R.L., Ferreira, A.G., 2014. Tracking the degradation of fresh orange juice and discrimination of orange varieties: an example of NMR in coordination with chemometrics analyses. Food Chem. 164, 446–453.
Del Caro, A., Piga, A., Vacca, V., Aggabio, M., 2004. Changes of flavonoids, vitamin C and antioxidant capacity in minimally processed citrus segments and juices during storage. Food Chem. 84, 99–105.
Dellarosa, N., Tappi, S., Ragni, L., Laghi, L., Rocculi, P., Dalla Rosa, M., 2016. Metabolic response of fresh-cut apples induced by pulsed electric fields. Innov. Food Sci. Emerg. Technol. 38, 356–364.
Eriksson, L., Johansson, E., Kettaneh-Wold, N., Wold, S., 2001. Multi-and Megavariate Data Analysis: Principles and Applications. Umetrics Academy.
FoodTech, F.M.C., 2005. Laboratory Manual. Procedures for Analysis of Citrus Products, Fourth ed., pp. 49–50 Manual No. 054R10020.000.
Gil, M.I., Tomás-Barberán, F.A., Hess-Pierce, B., Holcroft, D.M., Kader, A.A., 2000. Antioxidant activity of pomegranate juice and its relationship with phenolic composition and processing. J. Agric. Food Chem. 48, 4581–4589.
Griesser, M.T., Hoffmann, M.L., Bellido, C., Rosati, B., Fink, R., Kurtzer, A., Aharoni, J., Muñoz-Blanco, W., 2008. Redirection of flavonoid biosynthesis through the down-regulation of an anthocyanidin glucosyltransferase in ripening strawberry fruit. Plant Physiol. 146, 1528–1539.
Halbwirth, H., Puhl, I., Haas, U., Jezik, K., Treutter, D., Stich, K., 2006. Two-phase flavonoid formation in developing strawberry (Fragariaananassa) fruit. J. Agric. Food Chem. 54, 1479–1485.
Izquierdo, L., Carbonell, J.V., Navarro, J.L., & Sendra, J.M. (2007). Method of Obtaining Refrigerated Pasteurized Citrus Juices. Patent WO/2007/042593. Consejo Superior de Investigaciones Científicas, Spain.
Kopjar, M., Jakšic, K., Pilizota, V., 2012. Influence of sugar and chlorogenic acid addition on anthocyanin content, antioxidant activity and color of blackberry juice during storage. J. Food Process. Preserv. 36, 545–552.
Kopjar, M., Piližota, V., Hribar, J., Simcic, M., Zlatic, E., Tiban, N.N., 2008. Influence of trehalose addition and storage conditions on the quality of strawberry cream fillings. J. Food Eng. 87, 341–350.
Kopjar, M., Tiban, N.N., Piližota, V., Babic, J., 2009. Stability of anthocyanins, phenols and free radical scavenging activity through sugar addition during frozen storage of blackberries. J. Food Process. Preserv. 33, 1–11.
Laghi, L., Picone, G., Capozzi, F., 2014. Nuclear magnetic resonance for foodomics beyond food analysis. Trends Anal. Chem. 59, 93–102.
Lê Cao, K.A., Boitard, S., Besse, P., 2011. Sparse PLS discriminant analysis: biologically relevant feature selection and graphical displays for multiclass problems. BMC Bioinform. 12 (1), 253.
Lê Cao, K.A., Rossouw, D., Robert-Granié, C., Besse, P., 2008. A sparse PLS for variable selection when integrating omics data. Stat. Appl. Genet. Mol. Biol. 7 (1).
Le Gall, G., Puaud, M., Colquhoun, I.J., 2001. Discrimination between orange juice and pulp wash by 1H nuclear magnetic resonance spectroscopy: identification of marker compounds. J. Agric. Food Chem. 49, 580–588.
Lee, H.S., & Coates, G.A. (2004). Pigment extraction system and method. US patent US20040258809–A1.
Lortkipanidze, R.K., Anikeichik, N.M., Yakobashvili, R.A., Bolkovadze, M.K., 1972. Homogenizer in citrus juice production line. Konservn. i Ovoshchesushil'naya Promyshlennost 7, 9–10.
Maresca, P., Donsì, F., Ferrari, G., 2011. Application of a multi-pass high-pressure homogenization treatment for the pasteurization of fruit juices. J. Food Eng. 104, 364–372.
Odriozola-Serrano, I., Hernàndez-Jove, T., Martìn-Belloso, O., 2007. Comparative evaluation of UV-HPLC methods and reducing agents to determine vitamin C in fruits. Food Chem. 105, 1151–1158.
Patrignani, F., Vannini, L., Kamdem, S.L.S., Lanciotti, R., Guerzoni, M.E., 2009. Effect of high pressure homogenization on Saccharomyces cerevisiae inactivation and physico-chemical features in apricot and carrot juices. Int. J. Food Microbiol. 136 (1), 26–31.
Polydera, A.C., Stoforos, N.G., Taoukis, P.S., 2005. Effect of high hydrostatic pressure treatment on post processing antioxidant activity of fresh Navel orange juice. Food Chem. 91, 495–503.
Prior, R.L., Wu, X., Schaich, K., 2005. Standarized methods for the determination of antioxidant capacity and phennolics in foods and dietary supplements. J. Agric. Food Chem. 53, 4290–4302.
Richards, A.B., Dexter, L.B., 2011. Trehalose. In: Alternative Sweeteners, Quarta Edizione. CRC Press, Lyn O'Brien-Nabors, pp. 439–470.
Ripley, B.D., 1996. Pattern Recognition and Neural Networks. Cambridge University Press.
Rudolph, A.S., Crowe, J.H., 1985. Membrane stabilization during freezing: the role of two natural cryo- protectants, trehalose and proline. Cryobiology 22, 367–377.
Shui, G., Peng, L.L., 2004. An improved method for the analysis of major antioxidants of Hibiscus esculentus Linn. J. Chromatogr. A 1048, 17–24.
Spraul, M., Schütz, B., Rinke, P., Koswig, S., Humpfer, E., Schäfer, H., Mörtter, M., Fang, F., Marx, U.C., Minoja, A., 2009. NMR-based multi parametric quality control of fruit juices: SGF profiling. Nutrients 1, 148–155.
Trimigno, A., Marincola, F.C., Dellarosa, N., Picone, G., Laghi, L., 2015. Definition of food quality by NMR-based foodomics. Curr. Opin. Food Sci. 4, 99–104.
Zinoviadou, K.G., Galanakis, C.M., Brnčić, M., Grimi, N., Boussetta, N., Mota, M.J., Saraiva, J.A., Patras, A., Tiwari, B., Barba, F.J., 2015. Fruit juice sonication: implications on food safety and physicochemical and nutritional properties. Food Res. Int. 77, 743–752.

Paper VII

Tappi, S., Mauro, M. A., Tylewicz, U., **Dellarosa**, **N.**, & Dalla Rosa, M., & Rocculi, P. (2017)

Effects of calcium lactate and ascorbic acid on osmotic dehydration kinetics and metabolic profile of apples

Food and Bioproducts Processing, 103, 1-9

Contents lists available at ScienceDirect

Food and Bioproducts Processing

journal homepage: www.elsevier.com/locate/fbp

Effects of calcium lactate and ascorbic acid on osmotic dehydration kinetics and metabolic profile of apples

Silvia Tappi[a,*], Maria A. Mauro[b], Urszula Tylewicz[a], Nicolò Dellarosa[a], Marco Dalla Rosa[a,c], Pietro Rocculi[a,c]

[a] Department of Agricultural and Food Sciences, University of Bologna, Cesena, Italy
[b] Department of Food Engineering and Technology, São Paulo State University (UNESP), São José do Rio Preto, Brazil
[c] Interdepartmental Centre for Agri-Food Industrial Research, University of Bologna, Cesena, Italy

ARTICLE INFO

Article history:
Received 14 July 2016
Received in revised form 4 January 2017
Accepted 26 January 2017
Available online 16 February 2017

Keywords:
Minimally processed apples
Sucrose
Mass transfer
Solutes impregnation
Endogenous metabolic activity
Respiration rate

ABSTRACT

The influence of the addition of calcium lactate (CaLac) and ascorbic acid (AA) to sucrose (Suc) osmotic solutions on osmotic dehydration kinetics and endogenous metabolic heat production of apple tissue was evaluated. Our research goal was to characterize mass transfer and endogenous metabolic phenomena of the tissue to obtain minimally processed apples. The presence of CaLac and AA in solution affected the mass transfer of water and solutes, which was attributed to the changes in the cellular structure and thus to spaces available for solute transport. The metabolic heat production in samples treated in sucrose solutions was slightly lower than in untreated samples, and it was further reduced with CaLac addition. However, samples impregnated with AA exhibited a higher heat production due to a metabolic response of the tissue to AA treatment. When combined with CaLac, the heat production decreased to a level lower than untreated samples, except for those that were treated for 120 and 240 min (higher impregnation), achieving the highest heat production values. These results confirm previous findings, suggesting that AA solution can promote a stress response on specific fresh-cut vegetable tissues, as well as an increase of their endogenous metabolic activity, as confirmed by the higher O_2 consumption observed with the head space gas determination.

© 2017 Institution of Chemical Engineers. Published by Elsevier B.V. All rights reserved.

1. Introduction

Osmotic dehydration (OD) of plant foods is a concentration process in which water is removed from the plant tissue to a hypertonic solution and solutes flow from the solution into the food. The water removal from fresh plant tissues is usually greater than the solute gain because of the semi-permeability of the cell membranes (Ahmed et al., 2016). OD depends on the tissue structure, which changes according to the environment and structure itself. Consequently, the complexity of structures and properties of plant tissues are challenging factors for optimizing processes and designing equipment (Fernandez et al., 2004).

In addition to the advantages of lowering the water content, the OD modifies the food composition. As a result, impregnation of desirable solutes can improve the nutritional and sensorial characteristics (Akbarian et al., 2014; Silva et al., 2014b; Barrera et al., 2004). OD is becoming popular as a technique for obtaining minimally processed fruits, improving their quality and stability, and most recently, this method has been combined with other innovative techniques, such as pulsed high electric field, high hydrostatic pressure, ultrasound, centrifugal force, vacuum and gamma and irradiation, which can enhance its efficiency and improve the quality of the final products (Ahmed et al., 2016).

* Corresponding author.
E-mail address: silvia.tappi2@unibo.it (S. Tappi).
http://dx.doi.org/10.1016/j.fbp.2017.01.010
0960-3085/© 2017 Institution of Chemical Engineers. Published by Elsevier B.V. All rights reserved.

The type of solute used in the osmotic solution is a fundamental issue, because beyond affecting the dehydration kinetics and process cost, it impacts the organoleptic and nutritional properties of the final product. Sucrose (Suc) is considered by many authors to be the optimal osmotic agent because it is associated with a higher efficiency than glucose (Saputra 2001), reducing enzymatic browning and aroma losses (Cortellino et al., 2011; Qi et al., 1998; Lenart, 1996).

OD with calcium in solution has been used to increase the firmness of plant tissue and enhance the process efficiency, restricting the sugar gains and increasing the water losses (Ferrari et al., 2010; Mavroudis et al., 2012; Pereira et al., 2006). Calcium can reinforce cell walls by cross linking pectic polymers and is thus able to reduce damage from dehydration (Pereira et al., 2006). At the same time, when the concentration increases or as the treatment proceeds, damage to cell membranes may occur, as reported by Anino et al. (2006). Moreover, calcium has been used in osmotic solutions as a method for obtaining nutritionally fortified products that can increase consumer intake (Silva et al., 2014b; Barrera et al., 2004).

The addition of ascorbic acid (AA) to the osmotic solution has been used to reduce enzymatic browning (Robbers et al., 1997; Lenart, 1996) and compensate for the loss of ascorbic acid in fruits during dehydration (Guiamba et al., 2016; Ramallo and Mascheroni, 2010).

Various solutes can be added to the osmotic medium to obtain minimally processed products that can be stored at refrigerated temperatures. Nevertheless, it is important to consider that in addition to affecting the compositional and nutritional profile, they can affect the tissue metabolism, which can have consequences on the final product stability and shelf-life. Various authors have observed a reduction in the respiration rate of osmotically dehydrated mangoes, strawberries, pineapples and kiwifruit (Castelló et al., 2010; Moraga et al., 2009; Torres et al., 2008). Nevertheless, after a few days of storage, the respiratory quotient is generally observed to increase, as a result of the development of fermentative routes, which is an optional metabolic pathway triggered by osmotic stress.

Salvatori and Alzamora (2000) found that a 25% w/w sucrose solution can cause vesciculation and rupture of cell membranes in apple tissue. According to Mavroudis et al. (2004), few layers of cells on the surface are expected to die upon osmotic treatment, while plasmolysis and shrinkage occur in the remaining tissue. In a previous study, the authors found that 40% w/w sucrose treatment generally preserved the viability of apple cells, which only slightly affected the cell structure observed by fluorescence microscopy and the water distribution within the cells, as observed by time domain nuclear magnetic resonance (TD-NMR) (Mauro et al., 2016).

For different fruit species types, calcium can decrease the metabolic activity of tissue as well as the respiration rate (Castelló et al., 2010; Lester, 1996; Luna-Guzmán et al., 1999), which potentially enhances the product stability during storage, especially considering that a lower respiration rate may lead to a longer shelf life. In addition, Ca^{2+} can affect the membrane and cell wall structure and functioning (Maurel, 2007; Peiter et al., 2005).

On the other hand, the presence of AA can cause serious injury to the cellular structure, as has been previously reported by Mauro et al. (2016), who observed a loss in the capacity to retain FDA colorant due to cell membrane damage following exposure to OD in a sucrose-ascorbic acid solution. As the AA concentration increased from 0 up to 2%, a loss of vitality was detected.

Rocculi et al. (2005) found a higher metabolic activity in potato tissue upon dipping treatments with citric and ascorbic acid, suggesting that AA solution can promote a stress response in specific fresh-cut vegetable tissues, as well as an acceleration of their endogenous metabolic activity, which was confirmed by a higher O_2 consumption according to head space gas determination. Limbo and Piergiovanni (2007) detected an increase in the respiration rate of sliced potatoes that were subjected to dipping treatment with 2.5% AA. However, when the AA concentration was 5%, the respiration rate decreased.

Isothermal calorimetry has been recognized as a useful tool for assessing metabolic responses of various plant tissues to wounding stress (Wadsö et al., 2004), dipping treatment (Rocculi et al., 2005), thermal treatments (Gómez et al., 2004) and OD (Panarese et al., 2012).

Generally, when a tissue is wounded, certain signal paths are triggered, and the plant starts a number of protective processes that increase the produced metabolic heat (Wadsö et al., 2004). As reported by Gómez et al. (2004), after wounding, the energy released by the cellular tissue corresponds to the sum of that from the 'basic' cell metabolic activity and of that originating from wounding stress that is produced by the cells near the cut surface. Some of the processes that occur after wounding are aimed at membrane restoration and strengthening of cell walls by cells close to the site of injury (Rolle and Chism, 1987). A progressive reduction in the metabolic heat production during OD in kiwifruit slices was observed by Panarese et al. (2012) using isothermal calorimetry. The authors suggested that the decrease was due to a reduction in the cell viability that was induced by osmotic stress. Finally, the metabolic response of fruit tissues to OD was found to depend on the botanical origin, exerted osmotic pressure (Ferrando and Spiess, 2001; Mavroudis et al., 2004) and physiological state because loss of membrane integrity upon ripening that increases the permeability then makes the tissue more sensitive to osmotic stress (Panarese et al., 2012).

This study evaluated the effects of the addition of calcium lactate (CaLac) and ascorbic acid on sucrose osmotic solutions, mass transfer kinetics and raw endogenous metabolic response (respiration and heat production) of the tissue. The obtained information can be very useful for investigating the potential stability of minimally processed apples.

2. Materials and methods

2.1. *Raw materials*

Apples (*Malus domestica* Borkh; 30 kg) of the Cripps Pink variety, popularly known by the brand name Pink Lady (de Castro et al., 2008), were bought at the local market and stored at $5 \pm 1\,^{\circ}C$ for 2 weeks, during which the experimental research was performed. Apples were characterized by an average weight of 234 ± 18 g and soluble solid content of 13.4 ± 0.3 g/100 g. From the central part of the mesocarp fruit, cylindrical samples (8-mm diameter, 40-mm length) were cut with a manual cork borer and a manual cutter designed for the purpose. For osmotic treatments, commercial sucrose (refined sugar, Eridania Italia Spa, Italy), L-ascorbic acid (Shandong Luwei Pharmaceutical Co., China) and calcium lactate (calcium-L-lactate 5-hydrate powder, PURACAL® PP Food, Corbion PURAC, Netherlands) were used.

2.2. *Osmotic dehydration*

OD was performed at $25\,^{\circ}C$ using four different osmotic solutions (w/w): 40% sucrose (Suc), 40% sucrose + 4% calcium lactate (Suc-CaLac), 40% sucrose + 2% ascorbic acid (Suc-AA) and 40% sucrose + 4% calcium lactate + 2% ascorbic acid (Suc-CaLac-AA).

Approximately 100 g of apple cylinders were weighed for each treatment time (0.5, 1, 2 and 4 h) and placed in mesh baskets that were immersed in 4.5 kg of aqueous osmotic solution with a syrup-to-fruit ratio of approximately 15:1 (w/w) to avoid changes in the concentration of the solution during the treatment. Through an impeller of a mechanical stirrer, the cylindrical baskets were continuously rotated. The rotational speed (0.2 g) was experimentally determined to assure negligible external resistance to mass transfer. Two baskets were prepared for each process time.

After each treatment time, samples were removed from the solution, rinsed with distilled water, blotted with absorbing paper, and weighed. Subsequently, cylinders were placed in glass sealed ampoules to measure the endogenous metabolic heat production with isothermal calorimetry over 16 h, which

was followed by the determination of the O_2 and CO_2 levels on ampoule headspaces.

Total and soluble solid contents were determined in triplicate immediately after treatment. Samples for calcium and ascorbic acid analyses were freeze-dried.

2.3. Analytical methods

The moisture content of fresh and osmotically dehydrated samples was gravimetrically determined, in triplicate, by drying cylindrical apple samples at 70 °C until a constant weight was reached. Soluble solid content was determined at 20 °C by measuring the refractive index with a digital refractometer (PR1, Atago, Japan) that was calibrated with distilled water.

2.3.1. Ascorbic acid

Ascorbic acid was determined by HPLC analysis according to the method described by Odriozola-Serrano et al. (2007). Briefly, approximately 0.5 g of freeze-dried sample was added to 10 ml of meta-phosphoric acid (62.5 mM) and sulfuric acid (5 mM) solution, which was vortexed for 2 min and centrifuged at 10,000 × *g* for 10 min at 4 °C. The supernatant was directly used for the fresh sample and diluted tenfold for the impregnated samples; it was then filtered through a 0.45 μm nylon filter. The HPLC system LC-1500 (Jasco, Carpi, MO, Italy) was equipped with a diode array UV/Vis detector. A reverse-phase C18 Kinetex (Phenomenex Inc., Torrance, CA, USA) stainless steel column (4.6 mm × 150 mm) was used as the stationary phase. A Jasco AS-2055 Plus autosampler was used to introduce samples into the column. The mobile phase was a 0.01% solution of sulfuric acid that was adjusted to a pH of 2.6. The flow rate was fixed at 1.0 ml/min at room temperature. Data were processed with ChromNAV software (ver. 1.16.02) from Jasco. The ascorbic acid content was quantified at 245 nm through a standard calibration curve that was set up using an ascorbic acid solution between 0.5 to 30 ppm. The determination was performed in triplicate.

2.3.2. Calcium

The calcium concentration was determined using a flame atomic absorption spectrophotometer (Model A Analyst 400, Perkin Elmer, Santa Clara, California, USA) with a lumina hollow cathode lamp (Perkin Elmer) based on the adapted methodology of AOAC (2002). Briefly, approximately 6 g of freeze-dried, untreated samples and 2 g of freeze-dried treated samples, were weighed in a 50 ml glazed, porcelain crucible; placed in a muffle furnace and heated up to 550 °C until complete ignition. After cooling in desiccators, the ash was dissolved in 20 ml (fresh samples) or 30 ml (treated samples) of HCl (0.1 M); then, the solutions were appropriately diluted with 0.1 M HCl. A calibration curve of the absorbance versus ppm of calcium was established using standard calcium solutions between 2 to 20 ppm. The initial sample level and subsequent dilution permits to obtain solutions with a concentration that was suitable to the standard solutions used for establishing a calibration curve of absorbance versus ppm of calcium (2–20 ppm). The determination was performed in triplicate.

2.3.3. Metabolic heat production

Two fresh cylindrical samples (8-mm diameter, 40-mm length) and three osmotically dehydrated samples were placed in 20 ml glass ampoules and sealed with a teflon coated rubber seal and an aluminium crimp cap. Three replicates for each sample were performed. The rate of heat production was continuously measured in a TAM air isothermal calorimeter (Thermometric AB, Järfälla, Sweden) with a sensitivity (precision) of ±10 μW (Wadsö and Gómez Galindo, 2009). This instrument contains eight twin calorimeters in which each sample is inserted with its own reference, and the measured signal is the difference between the sample and reference signals. The reference has to be a material that does not produce any heat, but it is characterized by thermal properties that are similar to the sample. For this, water was chosen as the reference material and its quantity in each reference ampoule (m_w^0) was previously determined based on the average composition of the samples and on the heat capacities (J g^{-1} K^{-1}) of water (C_w) and total solids (C_{TS}), as in the following equation:

$$m_w^0 = \frac{C_{TS} \cdot m_{TS} + C_w \cdot m_w}{C_w} \quad (1)$$

where m_{TS} is the dry matter content (g) and m_w is the water content of the fruit sample (g), and the average heat capacity of the total solids of the apple samples was assumed to be 1 J g^{-1} K^{-1}. The analysis was performed at 10 °C for 16 h. The first 4 h of analysis were discarded because of the instability of the signal due to the loading and conditioning of samples.

2.3.4. Respiration rate

Immediately after the ampoules were discharged from the calorimeters, the O_2 and CO_2 percentages were measured in the ampoule headspaces by a check point gas analyser O_2/CO_2 mod. MFA III S/L (Witt-Gasetechnik, Witten, Germany). The apparatus has a paramagnetic sensor for O_2 and a mini-IR spectrophotometer for CO_2 detection. The instrument was calibrated with O_2 and CO_2 air percentages.

The respiration rate was calculated as mol of consumed O_2 (RR_{O_2}) or produced CO_2 (RR_{CO_2}) h^{-1} g^{-1} according to the following equations:

$$RR_{O_2} = \frac{V_{head} \cdot \frac{(20.8 - \%O_{2,head})}{100} \cdot P}{t \cdot m \cdot R \cdot T} \quad (2)$$

$$RR_{CO_2} = \frac{V_{head} \cdot \frac{\%CO_{2,head}}{100} \cdot P}{t \cdot m \cdot R \cdot T} \quad (3)$$

where V_{head} represents the ampoule headspace volume (dm^3), $\%O_{2,head}$ and $\%CO_{2,head}$ refer to molar gases percentages in the ampoule headspace at time *t* (h), *m* is the sample mass (g); R is the gas constant (8.314472 dm^3 kPa K^{-1} mol^{-1}), P is the pressure (101.325 kPa) and *T* is the absolute temperature (283.15 K).

2.4. Osmotic dehydration kinetics

Mass transfer of water, sucrose, calcium and ascorbic acid during the osmotic process was modelled according to the model proposed by Peleg (1988) to describe moisture sorption curves and was further used by Palou et al. (1994) to model OD, as follows:

$$\Delta w_k = w_{k,t} - w_{k,0} = -\frac{t}{k_1 + k_2 t} \quad (4)$$

where w_k is the mass fraction (g g^{-1} total mass) of the following *k* species: water (w_w), sucrose (w_{Suc}), calcium ($w_{Ca^{2+}}$) or ascorbic acid (w_{AA}) at time 0 ($w_{k,0}$) and time t ($w_{k,t}$). The constants of Peleg's model are k_1 [s (g g^{-1} total mass)$^{-1}$] and k_2 [1 (g g^{-1} total mass)$^{-1}$]. This kinetic model permits, by calculating the inverse of the two constants, to obtain the initial ($t = 0$) rate

of mass transfer ($1/k_1$) and the mass fraction at equilibrium ($t \to \infty$) conditions $\left(w_{k,eq} = w_{k,0} \pm 1/k_2\right)$ (Sacchetti et al., 2001).

2.5. Statistical analysis and fitting

The significance of the treatments was statistically evaluated by analysis of variance (ANOVA) and comparison of means using the Tukey's post-hoc test that was applied at a 5% level of significance.

The Peleg's model was fitted to the experimental data using the Levenberg–Marquardt algorithm for the least-square estimation of the non-linear parameters (Marquardt, 1963). The fitting efficiency was evaluated by the coefficient of determination (R^2) and the relative root mean square error (*RRMSE*); the latter was evaluated according to Eq. (5):

$$RRMSE(\%) = \sqrt{\frac{1}{N}\sum_{n=1}^{N}\left(\frac{y_{obs} - y_{calc}}{y_{calc}}\right)^2} \cdot 100 \quad (5)$$

where y_{obs} represents the observed value, y_{calc} the calculated value and N the number of observations.

3. Results and discussion

3.1. Osmotic dehydration kinetics

The Peleg's equation (Eq. (4)) was used to model the kinetics of water loss and solute uptake during OD. Constants of the Peleg's equation (k_1 and k_2) and their inverse and equilibrium concentrations are reported in Table 1. The predictive capability of the Peleg's model can be observed in Fig. 1, which compares the observed and calculated values of the mass fraction, which is expressed as a function of the process time, for water (a), sucrose (b), calcium (c) and ascorbic acid (d).

In general, the model showed a good fit with the experimental data, as high R^2 values and low *RRMSE* were found (Table 1), confirming its suitability for describing mass transfer phenomena in OD, as reported by Palou et al. (1994). The same model was also successfully applied by other researchers, such as Sacchetti et al. (2001).

Regarding Table 1, it can be observed that the initial rate of dehydration was increased by the presence of Ca^{2+} and AA in the osmotic solution, as higher $1/k_1$ values were found for Suc-CaLac, Suc-AA and Suc-CaLac-AA treatments compared to the one with only sucrose in the solution. As reported in Fig. 1a, the presence of calcium in both Suc-CaLac and Suc-CaLac-AA solutions promoted a higher reduction in the water content than the treatments without Ca^{2+}. Contrary to Ca^{2+}, the presence of AA in the sucrose solution (Suc-AA treatment) caused only a slight depletion in the water content. In addition, the equilibrium water contents, calculated on the basis of the parameter k_2, were more affected by Ca^{2+}, showing lower values than the other treatments (Table 1). It should be noted that when the osmotic solution contained both Ca^{2+} and AA solutes, the equilibrium water content was reduced to the lowest value (0.6428 g g^{-1}, Table 1), which corresponds to the lowest water activity of all solutions. The water activities were 0.962 ± 0.002 for Suc, 0.953 ± 0.001 for Suc-CaLac, 0.954 ± 0.001 for Suc-AA and 0.944 ± 0.004 for Suc-CaLac-AA osmotic solutions. Conversely, despite the differences between the initial rates of water transfer found for the Suc and Suc-AA treatments (Table 1) as well as between the water activities of these two solutions, their equilibrium water levels were quite sim-

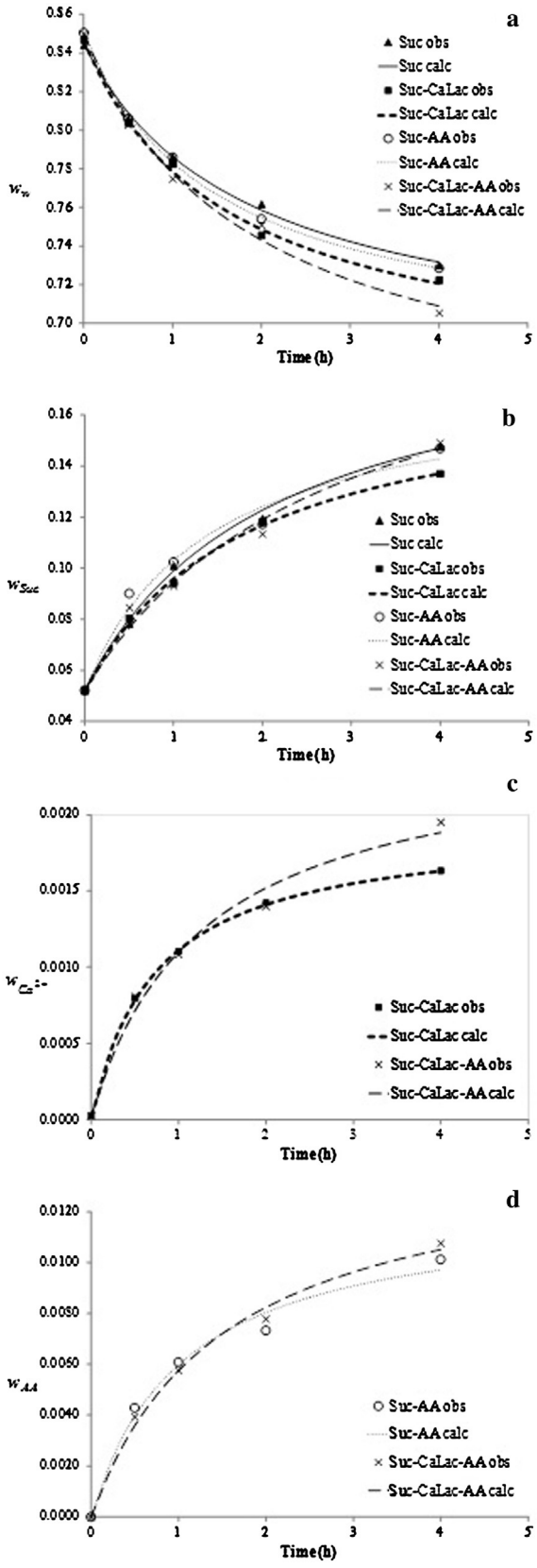

Fig. 1 – Comparison between the observed (obs) and calculated (calc) mass fraction of water (a), sucrose (b), calcium (c) and ascorbic acid (d) according to Peleg's model (Eq. (4)), in g g^{-1} total mass, for the different treatments.

Table 1 – Kinetic model of water, sucrose, calcium and ascorbic acid transfer in each osmotic solution according to Peleg's model (Eq. (4)) and equilibrium content (g g^{-1} total mass).

Solution	k_1 (s)	SD	p-Level	$1/k_1 \times 10^3$ (s^{-1})	k_2 (g total mass g^{-1})	SD	p-Level	$1/k_2 \times 10^3$ (g total mass $g^{-1})^{-1}$	R^2	RRMSE (%)	$w_{k,eq}$ (g g^{-1} total mass)
					Water						
Suc	11.18	0.78	<0.001	89.45	6.10	0.33	<0.001	163.90	0.997	3.8	0.6802
Suc-CaLac	9.12	0.64	<0.001	109.70	5.68	0.28	<0.001	176.09	0.997	3.1	0.6708
Suc-AA	8.93	0.46	<0.001	112.00	5.98	0.21	<0.001	167.26	0.998	3.1	0.6832
Suc-CaLac-AA	9.10	1.07	<0.01	109.92	4.83	0.45	<0.01	206.88	0.992	5.3	0.6428
					Sucrose						
Suc	14.51	1.32	<0.01	68.92	6.92	0.54	<0.001	144.54	0.998	3.8	0.1967
Suc-CaLac	14.59	1.53	<0.001	68.53	8.08	0.64	<0.001	123.79	0.998	3.2	0.1759
Suc-AA	11.49	2.18	0.01	87.05	8.13	1.01	<0.01	123.03	0.980	8.60	0.1752
Suc-CaLac-AA	17.36	3.17	0.01	57.62	6.25	1.19	0.01	160.02	0.979	12.0	0.2122
					Calcium						
Suc-CaLac	392.99	7.40	<0.001	2.54	523.45	4.31	<0.001	1.91	1.000	0.7	0.0019
Suc-CaLac-AA	524.34	83.76	<0.01	1.91	408.00	40.04	<0.01	2.45	0.986	7.0	0.0025
					Ascorbic acid						
Suc-AA	85.44	14.08	<0.01	11.70	81.48	7.24	<0.01	12.27	0.986	5.9	0.0123
Suc-CaLac-AA	104.72	10.56	<0.01	9.55	68.83	4.76	<0.001	15.53	0.994	4.8	0.0145

ilar. These discrepancies are related to the presence of AA, which can affect the cellular structure and thus influence the water and solutes transfer, as well as the equilibrium contents, as further discussed below. Effects promoted by Ca^{2+} and AA, however, can be better observed when also assessing the sucrose transfer.

The initial rates of sucrose mass transfer ($1/k_1$) found in all treatments were lower than the ones calculated for water (Table 1). This behaviour is expected in plant tissue because the cell wall porosity and selective permeability of the cellular membranes reduce the transport of larger molecules, such as sucrose, through the cell tissue. While the cell membranes remain intact, intracellular spaces occupied by protoplasts and vacuoles are unavailable to sucrose transport. Conversely, water can diffuse throughout the cell walls and membranes and occupy all liquid phases of the plant cell (Mauro and Menegalli, 2003). The addition of Ca^{2+} and AA had a variable and unexpected influence on sucrose transport. When only Ca^{2+} was added, the treatment promoted an increase in the initial rate of the water transfer, but did not cause any change in the initial rateof the sucrose transfer, in comparison with the Suc treatment (Table 1). Moreover, it can be seen that the Suc-CaLac treatment led to the lowest sucrose content after four hours of processing (Fig. 1b).

Conversely, the highest value of $1/k_1$ corresponded to the Suc-AA treatment. However, the addition of AA affected the behaviour of the sucrose content with time in both Suc-AA and Suc-CaLac-AA treatments, which sharply increased after 2 h of processing, as shown in Fig. 1b. Moreover, because of this change in the trend of these curves, the fitting efficiency worsened, as confirmed by the highest *RRMSE* values in Table 1, 8.6% for Suc-AA and 12% for Suc-CaLac-AA. The worst fittings were related to the presence of AA that would have caused damage to the structure of cell walls and cellular membranes, changing transport during OD. The effects of AA on the microstructure of apple tissue and water distribution within the different cellular compartments changed the cell membranes permeability, as reported in a previous study (Mauro et al., 2016). In fact, AA can affect cellular tissue in different ways. Several studies have evaluated the role of AA in plant tissues that undergo stress; however, little is known regarding the mechanisms that explain its effects when plant tissues are not exposed to stress, as reported by Qian et al. (2014), who observed severe damage in the cellular structure of *Arabidopsis thaliana* seedlings that were exposed to exogenous AA. Additionally, an increase in the cell wall porosity is also expected because of the medium acidification (Zemke-White et al., 2000).

In addition, discrepancies were more visible in the Suc-CaLac-AA treatment, which presented the lowest initial rate $1/k_1$ and the highest equilibrium value of 0.2122 g g^{-1} (Table 1). The poor fittings related to the presence of AA in osmotic solutions added some uncertainty to the equilibrium content calculated for the Suc-AA and Suc-CaLac-AA treatments.

During OD, damages in the tissue promoted by the solution components and/or by the dehydration could release enzymes and cause depolymerisation, solubilisation and demethylation of pectins. Pectin, an important component of the primary cell wall, is mainly formed by homogalacturonan blocks. In the presence of divalent cations, such as Ca^{2+} and, depending on the degree of methylesterification and the distribution of the methyl-substituent groups, homogalacturonan can dimerise, reinforcing the cell adhesion and controlling the wall porosity (Bonnin and Lahaye, 2013). The calcium effect on firmness has been observed in various fruit tissues that undergo OD in the presence of calcium salts, and it has been attributed to reduction in the cell wall porosity and to the formation of calcium pectate (Mavroudis et al., 2012; Pereira et al., 2006; Silva et al., 2014a,b). Consequently, Ca^{2+} limited sucrose impregnation because of these interactions with pectin.

Good impregnation levels of both Ca^{2+} and AA were obtained, as shown in Fig. 1c and d. The Ca^{2+} contents in both Suc-AA and Suc-CaLac-AA were very close until two hours of processing; afterwards, the impregnation quickly increased in those samples treated in Suc-CaLac-AA solution (Fig. 1c). Regarding the AA levels in Fig. 1d, a similar behaviour was observed, where, after two hours of processing, the AA impregnation tended to increase in both,= Suc-AA and Suc-CaLac-AA. The equilibrium concentrations of both Ca^{2+} and AA were also higher when samples were treated in Suc-CaLac-AA solution (Table 1). However, when Ca^{2+} was combined with AA, only after 2 h of OD was an increase in solute impregnation noticed, which is probably observed because the damage caused by AA surpassed the restraining effects of the cell structure impregnated with Ca^{2+} to the solute transport.

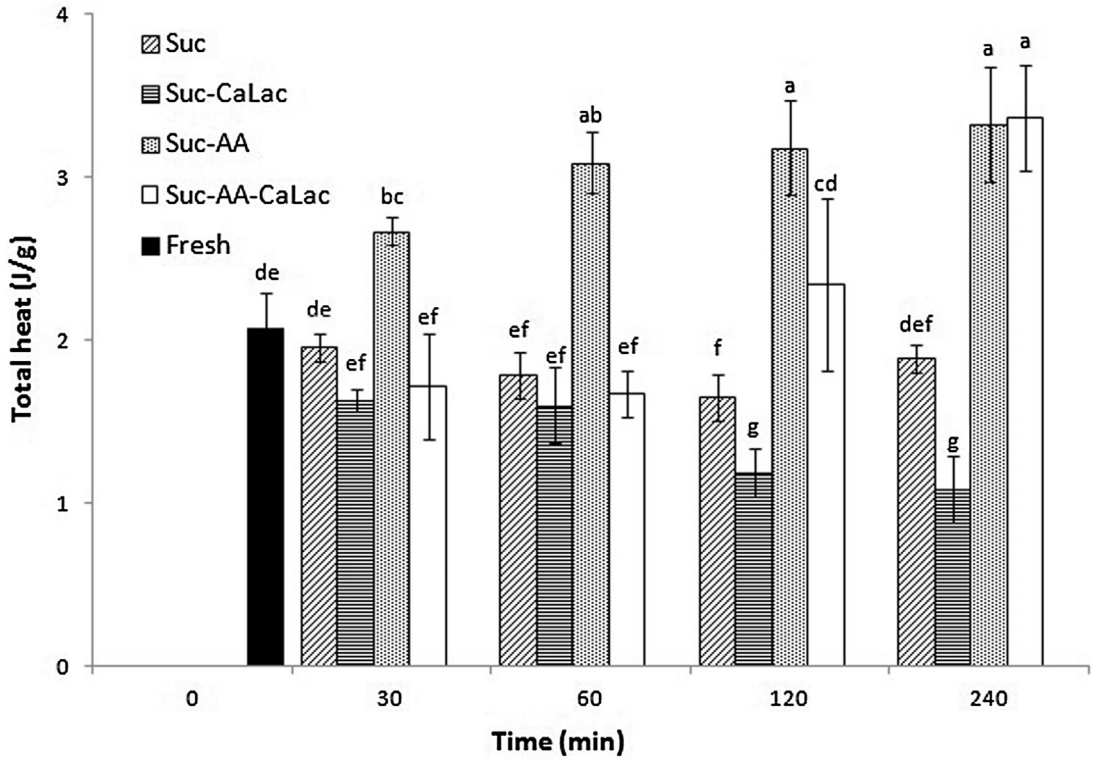

Fig. 2 – Total heat production (J/g) of fresh and osmotically dehydrated samples during 16 h at 10 °C. Different letters indicate significant differences by the Tukey test at $p < 0.05$.

3.2. *Metabolic profiles*

The results of the total metabolic heat produced during 16 h at 10 °C, measured through isothermal calorimetry after osmotic treatments, were performed for 0, 30, 60, 120 and 240 min and are given in Fig. 2. Provided that the concentration of O_2 and CO_2 can also give useful information about tissue metabolism, after calorimetric analysis, the composition of the headspace of the vials was evaluated. The measured respiration rates (RRO_2 and $RRCO_2$) are presented in Fig. 3.

As a consequence of Suc treatment, there was a slightly decreasing trend in metabolic heat production (Fig. 2), which was proportional to treatment time until two hours of processing, as well as a lower respiration rate compared to the fresh samples, both in terms of the CO_2 produced and O_2 consumed (Fig. 3). A partial loss of cell viability could be expected after OD treatment, even if the osmotic solution concentration was very low (Panarese et al., 2012). In a previous experiment (Mauro et al., 2016), cell viability was found to be preserved in apple tissue subjected to OD treatment with 40% sucrose solution, as observed by an FDA staining technique that allows for determination of the plasma membrane integrity. Conversely, neutral red staining revealed the incidence of plasmolysis that could help explain the decrease in the metabolic heat produced by the tissue. Salvatori and Alzamora (2000) found that a 25% w/w sucrose solution can cause vesciculation and rupture of the cell membranes in apple tissue. According to Mavroudis et al. (2004), only few layers of cells on the surface are expected to die upon osmotic treatment, while plasmolysis and shrinkage occur in the remaining tissue.

The presence of calcium in the osmotic solution caused a further decrease in the metabolic heat production. This result is in accordance with previous literature reports (Castelló et al., 2010; Luna-Guzmán et al., 1999), and it confirms the ability of calcium to slow down tissue metabolic activity and thus to enhance the stability of minimally processed fruit.

In various fruits, both whole and cut, an effect of calcium on respiration has been observed together with a reduction of ethylene production and general slowing of ripening and senescence (Lester, 1996; Saftner et al., 1999).

In particular, different explanations have been put forward for the reduction of the respiration rate: a protective osmotic effect due to the high salt concentration (Ferguson, 1984); an indirect effect on substrate transport from the alteration of the membrane permeability (Bangerth et al., 1972); the formation of a transient barrier between fruit and atmosphere that hinders gas exchange (Saftner et al., 1999); inhibition of plant aquaporins that regulate membrane permeability, causing an increase in the cytoplasmic ATP concentration that remains available for other biochemical routes (Kinoshita et al., 1995); and delay of senescence-related changes (Lester, 1996). At the same time, an excess of calcium has been related to a hastening of senescence because of damages to the plasma membrane structure and functionality.

Nevertheless, the effect of calcium on respiration has not been fully clarified to date. In the present experiment, the respiration rate values were similar to those of samples that were only dehydrated with sucrose, and they were only slightly lower after 30 and 240 min, indicating that the reduction of heat produced could be related more to other biochemical phenomena than to the reduction of respiratory activity.

Conversely, the presence of AA in the osmotic solution promoted a drastic increase in the metabolic heat production as the treatment time increased up until 50% compared to the fresh sample. This increase can probably be attributed to the physiological stress caused on the tissue, as already observed for sliced potatoes (Limbo and Piergiovanni, 2007; Rocculi et al., 2005). The damage to cellular structures, which is promoted by osmotic AA solution, can mainly be caused

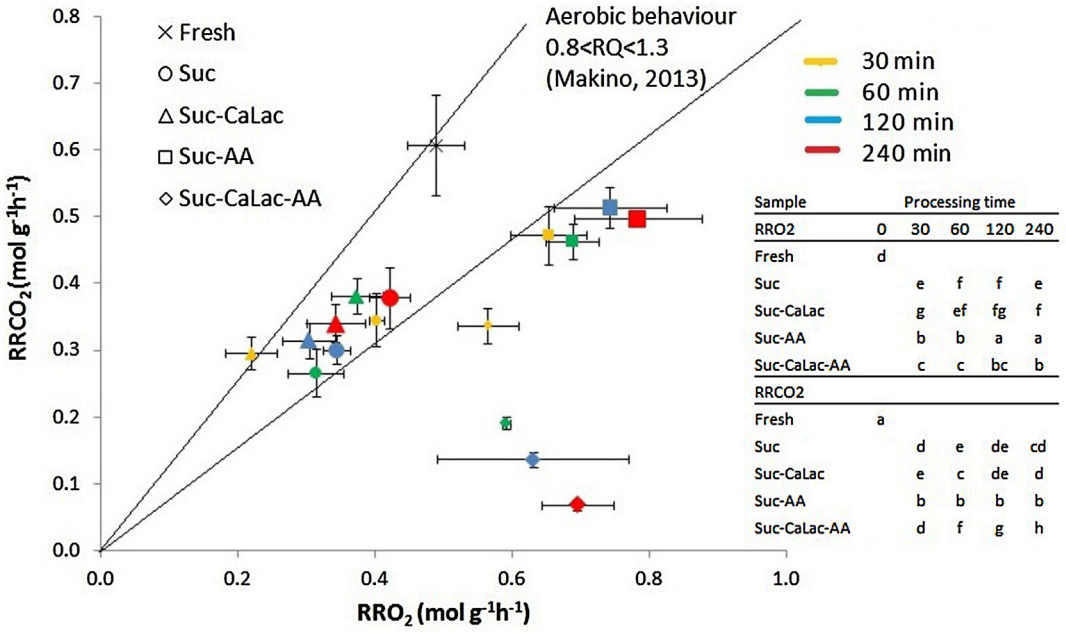

Sample	Processing time				
RRO2	0	30	60	120	240
Fresh	d				
Suc		e	f	f	e
Suc-CaLac		g	ef	fg	f
Suc-AA		b	b	a	a
Suc-CaLac-AA		c	c	bc	b
RRCO2					
Fresh	a				
Suc		d	e	de	cd
Suc-CaLac		e	c	de	d
Suc-AA		b	b	b	b
Suc-CaLac-AA		d	f	g	h

Fig. 3 – Respiration rates, expressed as the oxygen consumed (RRO_2) and carbon dioxide produced ($RRCO_2$), for treatment times of 30 min (yellow), 60 min (green), 120 min (blue) and 240 min (red). Error bars indicate standard deviation. Different letters in the auxiliary tables indicate significant differences according to the Tukey test at $p < 0.05$. (For interpretation of the references to color in this figure legend, the reader is referred to the web version of this article.)

by its lower pH. At low pH, plasma membrane ATPases in the tissue increase active H+ pumping to address the excess of H+ uptake, increasing the demand for respiratory energy. An ulterior pH decrease can also cause a decline in the respiration rates.

The combination of AA with Ca initially promoted a decrease in the heat production to a level that was lower than untreated samples; however, after 2 h of OD, the metabolism sharply rose. This behaviour suggests that, during the first part of the treatment, calcium acted as stabilizer and reduced the metabolic activity of the tissue; however, as the treatment proceeded, a progressive damage to cellular structures occurred, which was probably related to the AA intake.

Conversely, for samples dehydrated in the presence of AA, both alone or in combination with CaLac, there was a noticeable change in the respiratory pathway, particularly in terms of the increased oxygen consumption compared with Suc and Suc-Ca samples (Fig. 3). The highest standard deviations were observed for RRO_2 measurements in some AA samples. Although high variability was found in the respiration rates, reflecting the large natural variability of the raw and the treated material, useful indications were obtained. CO_2 production was constant for all treatment times in AA samples, and there was a reduction of approximately 20% compared to the fresh tissue. The production was higher compared to in Suc and Suc-CaLac samples. Conversely, a noticeable $RRCO_2$ decrease was verified in the Suc-CaLac-AA condition, which was proportional to the treatment time.

The respiratory quotient (RQ), calculated as the ratio $RRO_2/RRCO_2$, is an indicator of the respiration pathway adopted by tissues. The complete oxidation of glucose through the aerobic pathway produces an equal CO_2 level compared to the O_2 consumed; as a result, the respiratory quotient is 1. Variations in the RQ may depend on a different substrate used for respiration, such as malate or long chain fatty acids, although an increase in RQ generally indicates the onset of fermentative routes (Taiz and Zeiger, 1998). However, according to Makino (2013), an RQ in the range of 0.7–1.3 could be considered an indicator of aerobic respiration. Approximately following this indication, it was possible to identify the samples that were characterized by aerobic metabolism in Fig. 3 that shows values of RRO_2 and $RRCO_2$ of samples at different OD times. In our experiment, fresh samples had an RQ value of 1.24, while in Suc and Suc-CaLac, RQ values were lower and closer to 1, showing negligible anaerobic metabolism.

Anaerobic metabolism can be prompted by either low oxygen or high carbon dioxide concentrations in the environment that are, respectively, lower than 2%–5% and higher than 4%–5% (Cortellino et al., 2015; Iversen et al., 1989). Although these values were never exceeded, in some samples, and in particular in the fresh ones, the CO_2 content was very close to this limit after 20 h, which may have caused the development of some fermentative pathways, leading to an imbalance between CO_2 production and O_2 consumption in the tissue. This, in turn, increased the RQ. As a result, only samples treated with Suc-AA and Suc-CaLac-AA solutions seemed to have a non-aerobic response to the treatment.

As a consequence of OD, an increase in the RQ was observed by Torres et al. (2008) and by Castelló et al. (2010) on mango and strawberry tissues. Anaerobic metabolism is often found in plant tissue as a physiological response to stress conditions, such as dehydration, and as an optional metabolic pathway (Torres et al., 2008). While oxygen diffusion through the tissue decreases because of structural alteration in the cells as treatment proceeds, an increase of CO_2 production has generally been observed by these authors. The oxygen consumed was attributed to the effort of some enzymatic systems to react to the stress caused by osmotic treatment (Lewicki et al., 2001). Conversely, Moraga et al. (2009) did not find changes from the presence of calcium lactate in the RQ of osmo-dehydrated grapefruit, although the respiration rate generally decreased.

In samples that were dehydrated in the presence of AA, a lower RQ was calculated and was found to decrease slightly by increasing the treatment time between 0.72 and 0.64 (data not

shown). The combination of sucrose and ascorbic acid caused cellular damage to the tissue, and the effect on the plasmalemma and tonoplast was different and unclear, but there was a strong influence on tissue functionality (Mauro et al., 2016). When both AA and CaLac were used, the RQ decreased sharply, from 0.59 to 0.09, as dehydration proceeded. This decrease is mainly due to the higher oxygen consumption observed compared to CO_2 production.

It is important to note that the variation of the gas composition in the sample headspace could be from both the respiratory metabolism of the tissue and the presence of other enzymatic reactions. According to Igual et al. (2008), this O_2 consumption can be considered as the "apparent" respiration rate. Because molecular oxygen can be used as substrate by many enzymes in plant tissue, it can contribute to the "apparent" respiration rate if measured in terms of oxygen consumption and not in terms CO_2 production (Taiz and Zeiger, 1998). Concerning this particular issue, the effect of sugar, calcium and ascorbic acid on the complexity of fresh tissue enzymatic activity must be considered.

4. Conclusions

The investigated osmotic dehydration treatments showed different effects on the product in terms of both mass transfer phenomena during processing and metabolic activity of the apple tissue. The presence of calcium lactate (CaLac) and ascorbic acid (AA) affected the water and solute transport, which was attributed to changes in the cellular structure. Significant impregnation of solutes promoted by AA was related to severe damage caused to the cell structure, increasing spaces viable for solute transport. Ca^{2+} contributed to the improvement of dehydration and to limit the sucrose impregnation; however, in combination with AA, its capacity to restrain solute transport was diminished after 2 h of OD, which was probably because of the excessive AA gain.

Metabolic heat production in samples treated in sucrose solutions was slightly lower than in untreated samples, and it was further reduced with calcium lactate (CaLac) addition. However, samples impregnated with ascorbic acid (AA) showed higher heat production because there was a metabolic response of the apple tissue to AA treatment. When combined with Ca^{2+}, heat production decreased sharply to a level that was lower than untreated samples, except for those treated for 240 min (higher solid gain), which showed the highest heat production values. These results confirm previous findings, suggesting that AA solution can promote a stress response on specific fresh-cut vegetable tissues and an increase of their endogenous metabolic activity, which was further confirmed by a higher O_2 consumption that was observed by head space gas determination.

To clarify the effect on enzymatic activity in apples that were osmotically dehydrated in sucrose, calcium and ascorbic acid osmotic solutions and the real influence of these phenomena on respiration pathways, further studies are warranted that can couple the calo-respirometric approach with metabolomic analytical techniques.

Acknowledgments

The authors acknowledge the financial support of the Italian Ministry for Education, Universities and Research (FIRB, Project RBFR100CEJ: Innovative approach for the study of fresh-cut fruit: qualitative, metabolic and functional aspects).

References

Ahmed, I., Qazi, I.M., Jamal, S., 2016. Developments in osmotic dehydration technique for the preservation of fruits and vegetables. Innov. Food Sci. Emerg. Technol. 34, 29–43.

Akbarian, M., Ghasemkhani, N., Moayedi, F., 2014. Osmotic dehydration of fruits in food industrial: a review. Int. J. Biosci. 4 (1), 42–57.

Anino, S.V., Salvatori, D.M., Alzamora, S.M., 2006. Changes in calcium level and mechanical properties of apple tissue due to impregnation with calcium salts. Food Res. Int. 39 (2), 154–164.

AOAC International, 2002. Official methods of analysis (OMA) of AOAC International, 17th ed, USA. Method number: 920.15. Available at http://www.eoma.aoac.org/.

Bangerth, F., Dilley, D.R., Dewey, D.H., 1972. Effect of postharvest calcium treatments on internal breakdown and respiration of apple fruits. J. Am. Soc. Hortic. Sci.

Barrera, C., Betoret, N., Fito, P., 2004. Ca^{2+} and Fe^{2+} influence on the osmotic dehydration kinetics of apple slices (var. Granny Smith). J. Food Eng. 65 (1), 9–14.

Bonnin, E., Lahaye, M., 2013. Contribution of cell wall-modifying enzymes to the texture of fleshy fruits. The example of apple. J. Serb. Chem. Soc. 78 (3), 417–427.

Castelló, M.L., Fito, P.J., Chiralt, A., 2010. Changes in respiration rate and physical properties of strawberries due to osmotic dehydration and storage. J. Food Eng. 97 (1), 64–71.

Cortellino, G., Gobbi, S., Bianchi, G., Rizzolo, A., 2015. Modified atmosphere packaging for shelf life extension of fresh-cut apples. Trends Food Sci. Technol. 46 (2, Part B), 320–330.

Cortellino, G., Pani, P., Torreggiani, D., 2011. Crispy air-dried pineapple rings: optimization of processing parameters. Procedia Food Sci. 1, 1324–1330.

de Castro, E., Barrett, D.M., Jobling, J., Mitcham, E.J., 2008. Biochemical factors associated with a CO_2-induced flesh browning disorder of Pink Lady apples. Postharvest Biol. Technol. 48 (2), 182–191.

Ferguson, I.B., 1984. Calcium in plant senescence and fruit ripening. Plant Cell Environ. 7 (6), 477–489.

Fernandez, C.M.O., Mazzanti, G., LeMaguer, M., 2004. Development of methods to classify mass transfer behaviour of plant tissues during osmotic dehydration. Food Bioprod. Process. 82 (1), 49–53.

Ferrando, M., Spiess, W.E.L., 2001. Cellular response of plant tissue during the osmotic treatment with sucrose, maltose, and trehalose solutions. J. Food Eng. 49 (2), 115–127.

Ferrari, C.C., Carmello-Guerreiro, S.M., Bolini, H.M.A., Hubinger, M.D., 2010. Structural changes, mechanical properties and sensory preference of osmodehydrated melon pieces with sucrose and calcium lactate solutions. Int. J. Food Prop. 13 (1), 112–130.

Gómez, F., Toledo, R.T., Wadsö, L., Gekas, V., Sjöholm, I., 2004. Isothermal calorimetry approach to evaluate tissue damage in carrot slices upon thermal processing. J. Food Eng. 65 (2), 165–173.

Guiamba, I., Ahrné, L., Khan, M.A., Svanberg, U., 2016. Retention of β-carotene and vitamin C in dried mango osmotically pretreated with osmotic solutions containing calcium or ascorbic acid. Food Bioprod. Process. 98, 320–326.

Igual, M., Castelló, M.L., Ortolá, M.D., Andrés, A., 2008. Influence of vacuum impregnation on respiration rate, mechanical and optical properties of cut persimmon. J. Food Eng. 86 (3), 315–323.

Iversen, E., Wilhelmsen, E., Criddle, R., 1989. Calorimetric examination of cut fresh pineapple metabolism. J. Food Sci. 54 (5), 1246–1249.

Kinoshita, T., Nishimura, M., Shimazaki, K.I., 1995. Cytosolic concentration of Ca^{2+} regulates the plasma membrane H^+-ATPase in guard cells of fava bean. Plant Cell 7 (8), 1333–1342.

Lenart, A., 1996. Osmo-convective drying of fruits and vegetables: technology and application. Dry. Technol. 14 (2), 391–413.

Lester, G., 1996. Calcium alters senescence rate of postharvest muskmelon fruit disks. Postharvest Biol. Technol. 7 (1), 91–96.
Lewicki, P.P., Gondek, E., Witrowa-Rajchert, D., Nowak, D., 2001. Effect of drying on respiration of apple slices. J. Food Eng. 49 (4), 333–337.
Limbo, S., Piergiovanni, L., 2007. Minimally processed potatoes: Part 2. Effects of high oxygen partial pressures in combination with ascorbic and citric acid on loss of some quality traits. Postharvest Biol. Technol. 43 (2), 221–229.
Luna-Guzmán, I., Cantwell, M., Barrett, D.M., 1999. Fresh-cut cantaloupe: effects of $CaCl_2$ dips and heat treatments on firmness and metabolic activity. Postharvest Biol. Technol. 17 (3), 201–213.
Makino, Y., 2013. Oxygen consumption by fruits and vegetables. Food Sci. Technol. Res. 19 (4), 523–529.
Marquardt, D.W., 1963. An algorithm for least-squares estimation of nonlinear parameters. J. Soc. Ind. Appl. Math. 11 (2), 431–441.
Maurel, C., 2007. Plant aquaporins: novel functions and regulation properties. FEBS Lett. 581 (12), 2227–2236.
Mauro, M.A., Dellarosa, N., Tylewicz, U., Tappi, S., Laghi, L., Rocculi, P., Rosa, M.D., 2016. Calcium and ascorbic acid affect cellular structure and water mobility in apple tissue during osmotic dehydration in sucrose solutions. Food Chem. 195, 19–28.
Mauro, M.A., Menegalli, F.C., 2003. Evaluation of water and sucrose diffusion coefficients in potato tissue during osmotic concentration. J. Food Eng. 57 (4), 367–374.
Mavroudis, N.E., Dejmek, P., Sjöholm, I., 2004. Osmotic-treatment-induced cell death and osmotic processing kinetics of apples with characterised raw material properties. J. Food Eng. 63 (1), 47–56.
Mavroudis, N.E., Gidley, M.J., Sjöholm, I., 2012. Osmotic processing: effects of osmotic medium composition on the kinetics and texture of apple tissue. Food Res. Int. 48 (2), 839–847.
Moraga, M.J., Moraga, G., Fito, P.J., Martínez-Navarrete, N., 2009. Effect of vacuum impregnation with calcium lactate on the osmotic dehydration kinetics and quality of osmodehydrated grapefruit. J. Food Eng. 90 (3), 372–379.
Odriozola-Serrano, I., Hernández-Jover, T., Martín-Belloso, O., 2007. Comparative evaluation of UV-HPLC methods and reducing agents to determine vitamin C in fruits. Food Chem. 105 (3), 1151–1158.
Palou, E., Lopez-Malo, A., Argaiz, A., Welti, J., 1994. The use of Peleg's equation to model osmotic concentration of papaya. Dry. Technol. 12 (4), 965–978.
Panarese, V., Tylewicz, U., Santagapita, P., Rocculi, P., Dalla Rosa, M., 2012. Isothermal and differential scanning calorimetries to evaluate structural and metabolic alterations of osmo-dehydrated kiwifruit as a function of ripening stage. Innov. Food Sci. Emerg. Technol. 15, 66–71.
Peiter, E., Maathuis, F.J.M., Mills, L.N., Knight, H., Pelloux, J., Hetherington, A.M., et al., 2005. The vacuolar Ca^{2+}-activated channel TPC1 regulates germination and stomatal movement. Nature 434 (7031), 404–408.
Peleg, M., 1988. An empirical model for the description of moisture sorption curves. J. Food Sci. 53 (4), 1216–1217.
Pereira, L., Ferrari, C., Mastrantonio, S., Rodrigues, A., Hubinger, M., 2006. Kinetic aspects, texture, and color evaluation of some tropical fruits during osmotic dehydration. Dry. Technol. 24 (4), 475–484.
Qi, H., LeMaguer, M., Sharma, S.K., 1998. Design and selection of processing conditions of a pilot scale contactor for continuous osmotic dehydration of carrots. J. Food Process Eng. 21 (1), 75–88.
Qian, H.F., Peng, X.F., Han, X., Ren, J., Zhan, K.Y., Zhu, M., 2014. The stress factor, exogenous ascorbic acid, affects plant growth and the antioxidant system in *Arabidopsis thaliana*. Russ. J. Plant Physiol. 61 (4), 467–475.
Ramallo, L.A., Mascheroni, R.H., 2010. Dehydrofreezing of pineapple. J. Food Eng. 99 (3), 269–275.
Robbers, M., Singh, R., Cunha, L.M., 1997. Osmotic-convective dehydrofreezing process for drying kiwifruit. J. Food Sci. 62 (5), 1039–1042.
Rocculi, P., Romani, S., Dalla Rosa, M., Wadsö, L., Gómez, F., Sjöholm, M., 2005. Influence of pre-treatments on metabolism and wounding response of fresh cut potatoes evaluated with isothermal calorimetry. Int. Postharvest Symp. 682, 1833–1838.
Rolle, R.S., Chism, G.W., 1987. Physiological consequences of minimally processed fruits and vegetables. J. Food Qual. 10 (3), 157–177.
Sacchetti, G., Gianotti, A., Dalla Rosa, M., 2001. Sucrose–salt combined effects on mass transfer kinetics and product acceptability. Study on apple osmotic treatments. J. Food Eng. 49 (2), 163–173.
Saftner, R.A., Conway, W.S., Sams, C.E., 1999. Postharvest calcium infiltration alone and combined with surface coating treatments influence volatile levels, respiration, ethylene production, and internal atmospheres of 'Golden Delicious' apples. J. Am. Soc. Hortic. Sci. 124 (5), 553–558.
Salvatori, D., Alzamora, S.M., 2000. Structural changes and mass transfer during glucose infusion of apples as affected by blanching and process variables. Dry. Technol. 18 (1–2), 361–382.
Saputra, D., 2001. Osmotic dehydration of pineapple. Dry. Technol. 19 (2), 415–425.
Silva, K.S., Fernandes, M.A., Mauro, M.A., 2014a. Effect of calcium on the osmotic dehydration kinetics and quality of pineapple. J. Food Eng. 134, 37–44.
Silva, K.S., Fernandes, M.A., Mauro, M.A., 2014b. Osmotic dehydration of pineapple with impregnation of sucrose, calcium, and ascorbic acid. Food Bioprocess Technol. 7 (2), 385–397.
Taiz, L., Zeiger, E., 1998. Plant Physiology, 2nd ed. Sinauer, Sunderland, Massachussets, pp. 111–143.
Torres, J.D., Castelló, M.L., Escriche, I., Chiralt, A., 2008. Quality characteristics, respiration rates, and microbial stability of osmotically treated mango tissue (*Mangifera indica* L.) with or without calcium lactate. Food Sci. Technol. Int. 14 (4), 355–365.
Wadsö, L., Gomez, F., Sjöholm, I., Rocculi, P., 2004. Effect of tissue wounding on the results from calorimetric measurements of vegetable respiration. Thermochim. Acta 422 (1–2), 89–93.
Wadsö, L., Gómez Galindo, F., 2009. Isothermal calorimetry for biological applications in food science and technology. Food Control 20 (10), 956–961.
Zemke-White, W.L., Clements, K.D., Harris, P.J., 2000. Acid lysis of macroalgae by marine herbivorous fishes: effects of acid pH on cell wall porosity. J. Exp. Mar. Biol. Ecol. 245 (1), 57–68.

Paper VIII

Dellarosa, **N.**, Frontuto, D., Laghi, L., Dalla Rosa, M., & Lyng, J. G. (2017)

The impact of pulsed electric fields and ultrasound on water distribution and loss in mushrooms stalks

Food Chemistry, In press

Food Chemistry xxx (2017) xxx–xxx

Contents lists available at ScienceDirect

Food Chemistry

journal homepage: www.elsevier.com/locate/foodchem

The impact of pulsed electric fields and ultrasound on water distribution and loss in mushrooms stalks

Nicolò Dellarosa [a,*], Daniele Frontuto [b], Luca Laghi [a,c], Marco Dalla Rosa [a,c], James G. Lyng [b]

[a] Department of Agricultural and Food Sciences, University of Bologna, Cesena, Italy
[b] School of Agriculture and Food Science, University College Dublin, Dublin 4, Ireland
[c] Interdepartmental Centre for Agri-Food Industrial Research, University of Bologna, Cesena, Italy

ARTICLE INFO

Article history:
Received 4 December 2016
Received in revised form 18 January 2017
Accepted 19 January 2017
Available online xxxx

Keywords:
Mushroom by-products
Pulsed electric fields
Ultrasound
Microstructure
Disintegration index
Time domain nuclear magnetic resonance

ABSTRACT

Pulsed electric fields (PEF) and ultrasound (US) are promising innovative technologies with the potential to increase mass transfer when combined with further processes which in turn can provide potential benefits in the recovery of valuable compounds from food by-products. To provide evidence of the mechanism of mass transfer enhancement, the present study assessed the impact of PEF and US treatments, applied individually and in combination, at low and high temperatures, on the tissue microstructure of mushroom stalks. Different indices such as quantitative water redistribution, water loss and qualitative release of compounds were evaluated. The combination of these physical methods demonstrated that PEF redistributed a greater proportion of intracellular water into extracellular spaces than US. However, the application of high temperature treatments alone showed an even greater proportion of intracellular water migration compared to PEF. When PEF was combined with US at low temperatures the difference was not significant.

© 2017 Elsevier Ltd. All rights reserved.

1. Introduction

Recent research on innovative technologies such as pulsed electric fields (PEF) and ultrasound (US) have shown great potential for applications in a number of areas within the food industry. As an example, they have been studied as an alternative to traditional thermal treatments for microbial inactivation (Raso & Barbosa-Cánovas, 2003) or for the enhancement of mass transfer in various processes (Donsì, Ferrari, & Pataro, 2010). Pulsed electric fields treatments create pores at the level of biological membranes which can be transient and reseal or pores can be permanent leading to irreversible cell disruption. The extent to which transient/permanent pores occur is a function of the treated matrix and the applied PEF protocol (Vorobiev & Lebovka, 2009). Overall these phenomena are generally recognized as electroporation. Recent research, used electroporation in its irreversible form for the valorisation of food by-products and waste with a view to reducing the waste disposal problems (Barba et al., 2015). Generally, electric field strengths between 0.5 and 3 kV and short pulses (pulse width of 1–100 μs) at the frequency of 1–100 Hz have been successful for irreversible electroporation of plant tissues (Vorobiev & Lebovka, 2009). Similarly, the application of ultrasound leads to an increase in mass transfer phenomena by physically affecting the treated tissue. US induces the formation of gas bubbles which collapse generating high energy shock waves and intense shear forces, a phenomena known as the cavitation effect (Patist & Bates, 2008). As a consequence, extraction and purification processes of food by-products assisted by high intensity ultrasound, commonly 100–400 W applied at 20–100 kHz, resulted in high recoveries of valuable compounds from several plant materials (Roselló-Soto, Galanakis et al., 2015).

These innovative technologies were tested for the recovery of different components from mushroom by-products (Cheung, Siu, Liu, & Wu, 2012; Cheung, Siu, & Wu, 2013; Parniakov, Lebovka, Van Hecke, & Vorobiev, 2014; Xue & Farid, 2015), being rich in several high value compounds, namely proteins, chitins, glucans and other polysaccharides from cell wall, polyphenols and ergosterol (Roselló-Soto, Parniakov, et al., 2015). The potential simultaneous extraction of several compounds promotes the recovery of the by-products for different industrial sectors such as food, pharmaceutics and cosmetic. For example, cell walls of *Agaricus bisporus* are an important source of chitinous biopolymers, which can be used as antimicrobial agent or coating material in the food sector. It sustainable extraction from mushroom by-products can also reduce allergenic problems and inconveniences arisen from the use of harsh solvents that are needed for the extraction from the traditional sources like shrimp and crab shells (Wu, Zivanovic,

* Corresponding author.
E-mail address: nicolo.dellarosa@unibo.it (N. Dellarosa).

http://dx.doi.org/10.1016/j.foodchem.2017.01.105
0308-8146/© 2017 Elsevier Ltd. All rights reserved.

Please cite this article in press as: Dellarosa, N., et al. The impact of pulsed electric fields and ultrasound on water distribution and loss in mushrooms stalks. *Food Chemistry* (2017), http://dx.doi.org/10.1016/j.foodchem.2017.01.105

Draughon, & Sams, 2004). Moreover, taking advantage of their non-thermal mechanisms of action, PEF and US can affect the quality of the extracted material, preventing the damage of some thermolabile components which usually occurs with traditional methods when heat is provided to ease the extraction. In previous studies (Luo, Han, Zeng, Yu, & Kennedy, 2010; Pingret, Fabiano-Tixier, & Chemat, 2013), various food materials subjected to heat, US and PEF treatments were examined to find possible degradations of different chemical compounds. Non-thermal technologies, i.e. PEF and US, resulted in lower degradation of thermolabile vitamins and proteins when compared to heat processes. Conversely, polysaccharides, including those that compose the mushroom cell wall, were influenced by PEF and US processes that produced changes of their morphology and molecular weight. The induced modifications might result in a different water uptake of these biopolymers and in a different viscosity of the extracts.

Rapid methods are very valuable in screening the impact of innovative process technologies applied across a range of conditions. Appropriate methods include acoustic, texture and colour measurements (Lespinard, Bon, Cárcel, Benedito, & Mascheroni, 2015; Parniakov, Lebovka, Bals, & Vorobiev, 2015; Wiktor et al., 2016) but assessments can also be made using direct measures of cell metabolite release (Dellarosa, Tappi, et al., 2016; Luengo, Condón-Abanto, Condón, Álvarez, & Raso, 2014). In addition to the aforementioned methods, measuring the changes in electrical impedance, known as cell disintegration index, has been extensively investigated in recent years and it is the most commonly accepted quantitative index of the extent of electroporation (Angersbach, Heinz, & Knorr, 1999; Lebovka, Bazhal, & Vorobiev, 2002). Such indices provide an estimate of microstructural modifications in the inner compartments of plant tissues (Vorobiev & Lebovka, 2009) and have been recently adopted to compare the effect of different technologies on the food matrix (Barba, Brianceau, Turk, Boussetta, & Vorobiev, 2015; Barba, Galanakis, Esteve, Frigola, & Vorobiev, 2015). Another approach to assess microstructural effects of novel processes is based on the optical and electronic microscopy, but these results are qualitative (Faridnia, Burritt, Bremer, & Oey, 2015; Fincan & Dejmek, 2002; Nowacka, Tylewicz, Laghi, Dalla Rosa, & Witrowa-Rajchert, 2014) and can be vulnerable to the subjectivity of the analyst. Further quantitative methods focused on tissue microstructure and take into consideration water distribution through the food matrix. Indeed, water drip loss as a function of technological treatments also provides an index of the extent of cell damage which is generally accompanied with the release of intra-cellular water (Sun & Li, 2003). In addition, direct insights into water distribution and possible redistribution upon the application of different process technologies were recently obtained by means of time domain nuclear magnetic resonance (TD-NMR) (Dellarosa, Ragni, et al., 2016; McDonnell et al., 2013; Santagapita et al., 2013). The analysis of the transverse relaxation time (T_2) curves led to the non-destructive estimation of water distribution through the cell compartments, including the intra/extra-cellular water repartition.

The present study was focused on microstructural changes of mushrooms stalks, an abundant by-product of the mushroom industry. The main goal was to gain insight into fine modifications which affect the mechanisms of mass transfer, aiming at improving the extraction of valuable compounds. Different innovative technological treatments were tested, i.e. pulsed electric fields (PEF) and ultrasound (US), and compared to traditional water extraction processes. A novel multianalytical approach which combined several physical techniques, such as cell disintegration index, drip loss and water distribution by TD-NMR, was employed. Moreover, various combinations of different technologies were experimented to highlight possible synergistic or antagonistic effects of the different mechanisms of action. Results of the study provide useful tools for the evaluation of the feasible and efficient industrial application of the tested technologies.

2. Materials and methods

2.1. Mushroom stalks

Mushrooms (*Agaricus bisporus*) were purchased from a local market in Dublin (Ireland) and were analysed within 2 days of purchase. The stalks were manually separated from the caps and cut with a knife. In order to obtain a homogenous size distribution and standardize the surface-to-volume ratio, the cut stalks were sieved and pieces between 1.70 and 4.75 mm were selected for experimental trials.

2.2. Sample preparation

For all treatments 10 g of mushroom stalks were immersed in tap water (conductivity = 0.6 mS/cm) for 10 min at a standardized solid/liquid ratio of 1/10 and constant agitation by magnetic stirrer at 60 rpm. The temperature was controlled by an external water bath (DMS360, Fisher Scientific, UK) and monitored by a digital thermocouple (TC-08, Pico Technology, UK). Two different temperatures were used for the experiments to be representative of the room temperature (25 °C) and the ideal temperature for the extraction of valuable compounds in mushrooms (90 °C).The latter was also chosen because it is the lowest temperature value within the optimal range of temperatures reported in the literature (XuJie & Wei, 2008), so to minimize the cost of the process from an industrial angle. Each sample batch was weighed before and after treatments and water, possibly evaporated at 90 °C, was added again in order to restore the solid/liquid ratio. Control samples were obtained by only dipping mushroom stalks at both 25 °C (DIP) and 90 °C (H). Pulsed electric fields, as a pre-treatment, and/or ultrasound were tested, either alone or in combination, at both temperatures, resulting in the following sample groups: PEF, US, PEF + US, US + H, PEF + H, PEF + US + H.

2.2.1. Pulsed electric fields (PEF)

PEF was applied, as a pre-treatment either alone or in combination with other technologies, using a 5 kW PEF generator ELCRACK HVP 5 (DIL ELEA, Quakenbrück, Germany). The electric pulses of near-rectangular shape were delivered in a batch $4 \times 4 \times 4$ cm chamber with two 4×4 cm stainless steel parallel electrodes.

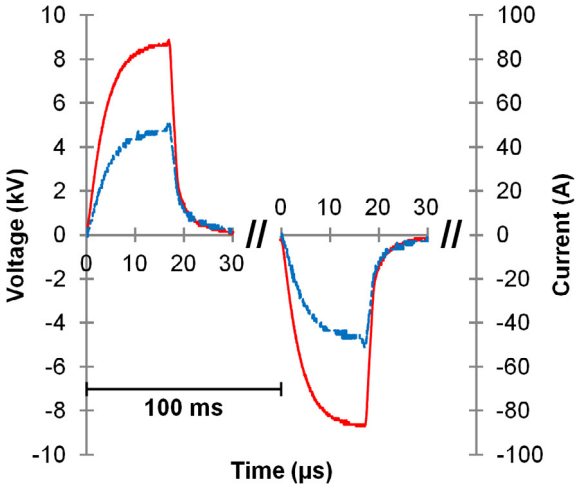

Fig. 1. An example of bipolar electric pulses used in the present investigation; solid and dashed lines are voltage and current, respectively.

Please cite this article in press as: Dellarosa, N., et al. The impact of pulsed electric fields and ultrasound on water distribution and loss in mushrooms stalks. *Food Chemistry* (2017), http://dx.doi.org/10.1016/j.foodchem.2017.01.105

Fig. 1. shows an example of two bipolar pulses used for the experiments. Each treatment, which included a series of 500 bipolar pulses of 17 μs width at 2.15 kV/cm (frequency = 10 Hz), was applied to 10 g of mushroom stalks and the chamber was filled up with approx. 50 mL of tap water (conductivity = 0.6 mS/cm). Immediately after treatment the stalks and the filling water were transferred into a beaker and the solid/liquid ratio was restored to 1/10. The voltage and current applied were monitored using a digital oscilloscope Picoscope 2205MSO (Pico Technology, UK). The specific energy provided per treatment on average was 344 kJ/kg.

2.2.2. Ultrasound (US)

Ultrasound treatment were carried out for 10 min in a jacketed beaker containing 10 g of mushroom stalks in water (solid/liquid ratio of 1/10) and a magnetic stirrer. US treatments were applied using a power sonicator UP 400S (Hielscher, Germany) which operates at 24 kHz and 400 W in continuous mode, equipped with a 22 mm diameter titanium probe. The power input was measured calorimetrically according to Raso, Manas, Pagan, and Sala (1999), resulting in an efficiency of the energy transformation equals to 28.4%. Therefore, the energy input of the US treatment was 6816 kJ/kg. The control of temperature was with external water at 10 °C flowing through the jacketed beaker and was monitored by a digital thermocouple (TC-08, Pico Technology, UK) in order to have profiles similar to those of the dipping experiments.

2.3. Analytical determinations

2.3.1. Disintegration index

The cell disintegration index (Z) was calculated according to Angersbach et al. (1999) by measuring the electrical impedance of the tissue at suitably 'low' and 'high' frequencies, namely 0.5 kHz and 20 MHz, respectively (Angersbach, Heinz, & Knorr, 2002). The Z value was calculated measuring the impedance of the material (i.e. mushroom stalks and tap water with a conductivity = 0.6 mS/cm) placed inside a 4 × 4 × 4 cm chamber. The measurement was taken before and after each treatment at 25 °C and Z index was calculated as follows (Eq. (1)):

$$Z = \frac{\left(\frac{\sigma_{b,high}}{\sigma_{a,high}}\right)(\sigma_{a,low} - \sigma_b, low)}{(\sigma_{b,high} - \sigma_{b,low})} \quad (1)$$

where σ is the measured electrical impedance (S/m), the subscripts b and a refer to the impedances before and after the treatment and 'low' and 'high' refer to 'low' and 'high' frequencies (0.5 kHz and 20 MHz).

The 'low' and 'high' frequencies signals were generated by a function generator DG 1022 (Rigol, Germany) which provides a 4 V peak to peak sinusoidal signal of 0.5 kHz and 20 MHz. The voltage drop after the wave passed through the sample was recorded by using an oscilloscope TDS 2012 (Tektronix, UK). To remove the parasitic capacitance of the system that becomes important at high frequencies a calibration curve, using known resistors spanning from 25 to 200 O, was prepared at the frequency of 20 MHz.

2.3.2. Drip loss

Approximately 1 g of treated mushroom stalks were weighted and inserted into a 23 mm centrifuge tube with false bottom. The lower part was filled with cotton wool and closed with filter paper (Whatman 3, Sigma-Aldrich). Samples were centrifuged at 2900g for 10 min using a Rotofix 32A centrifuge (Sartorius, Germany). Drip loss was calculated as the ratio between the weight loss after centrifugation and the initial weight of the samples.

2.3.3. Time domain nuclear magnetic resonance (TD-NMR)

Proton transverse relaxation time (T_2) curves were acquired using a CPMG pulse sequence implemented in an Oxford Maran Ultra (Oxford Instruments, UK) operating at 25 °C, 0.5 T and a proton resonance frequency of 23 MHz. Relaxation decays were obtained from mushrooms stalks before (control) and after treatments. Furthermore, the same samples were measured following centrifugation for water loss analysis. Samples for TD-NMR analysis, approximately 2g, were placed into a 18 mm internal diameter tubes and directly analysed. Each acquisition included 8192 echoes over 16 scans with an inter-pulse spacing of 0.3 ms and a recycle delay of 10 s. The signals, registered by the RINMR ver. 5.2.0.1 software (Oxford Instruments, UK), were exported and subjected to a quasi-continuous fitting by means of UPEN Software as described by Mauro et al. (2016). Following this, quantitative water distribution results were achieved by means of an in-house developed discrete fitting based on the 'Levenberg–Marquardt' algorithm implemented in an R statistical software (R Foundation for Statistical Computing, Austria) according to the following equation (Dellarosa, Ragni, et al., 2016):

$$S_{(t)} = \sum_{i=1}^{N} I_n \exp\left(\frac{-t}{T_{2,i}}\right) \quad (2)$$

where N = number of water populations (set at 3 according to UPEN results), I = signal intensity and T_2 = average relaxation time of each protons population (n).

In addition to the analysis of the mushroom stalks, TD-NMR was applied to the liquid media used for each process technology. For this purpose, an aliquot of 1 mL of the liquid media used for processing was immediately recovered after each treatment and analysed using the same acquisition protocol. To calculate the transverse relaxation time (T_2) of the solutions, Eq. (2) was used to fit the relaxation decays to a mono-exponential decay (N = 1).

2.3.4. UV–Vis spectroscopy

UV–Vis spectra of the recovered liquid media were registered using a spectrophotometer UVmini 1240 (Shimadzu, Japan). The water solutions remaining from each technological treatment were filtered with a filter paper (Whatman 1, Sigma-Aldrich) and then in succession, the UV and visible spectra were acquired in the regions between 220–360 nm and 400–800 nm, respectively. The former analysis required a 1/10 dilution of samples with distilled water to maintain absorbance values spanning from 0 to 1 in the UV region.

2.3.5. Statistics

In order to investigate whether the various treatments led to significantly different results, analysis of variance (ANOVA) followed by Tukey's multiple comparisons, as a post hoc test, were performed. Both were run at the significance level of 95% ($p < 0.05$) and carried out with R statistical software (R Foundation for Statistical Computing, Austria). All experiments were repeated three times and results were expressed as mean ± standard deviation of replications.

3. Results and discussion

Cell disintegration index (Z) was measured in order to gain an insight into changes of electrical impedance in mushroom stalks as a function of the internal microstructural modifications imposed by the technological treatments. This index ranges from 0, associated to a perfectly intact sample, to 1, indicating the cells total disintegration (Ivorra, 2010). Fig. 2. reports Z values for each of the technologies applied on their own. In this context, the DIP sample which contained stalks which were immersed in tap water with

Please cite this article in press as: Dellarosa, N., et al. The impact of pulsed electric fields and ultrasound on water distribution and loss in mushrooms stalks. *Food Chemistry* (2017), http://dx.doi.org/10.1016/j.foodchem.2017.01.105

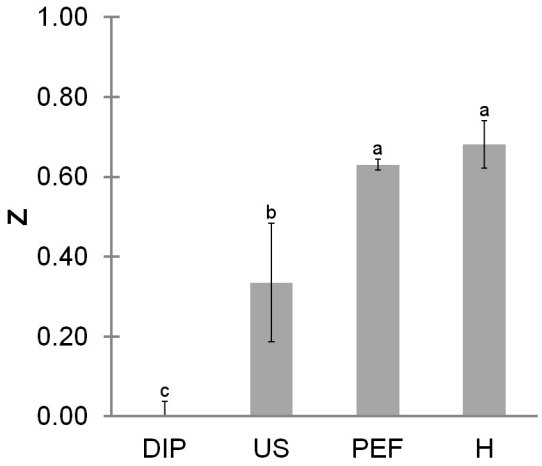

Fig. 2. Disintegration index (Z) based on electrical impedance. Results are means ± standard deviations of the replicates and different letters show significant differences ($p < 0.05$). Sample codes: DIP = dipping (25 °C); US = ultrasound; PEF = pulsed electric fields; H = high temperature treatments (90 °C).

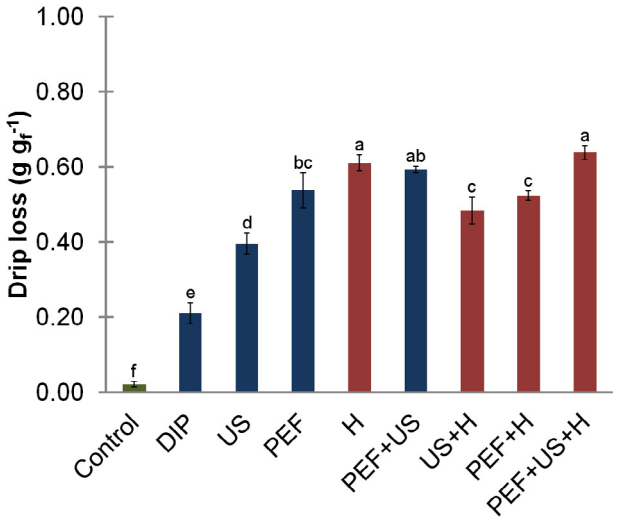

Fig. 3. Drip loss expressed as weight loss (g) per fresh weight (g_f). Results are means ± standard deviations of the replicates and different letters show significant differences ($p < 0.05$). Sample codes: DIP = dipping (25 °C); US = ultrasound; PEF = pulsed electric fields; H = high temperature treatments (90 °C).

known conductivity (0.6 mS/cm) with no further treatment, was set to 0 as reference. The application of US brought the disintegration index to 0.34 ± 0.15, a value far lower than 0.63 ± 0.02 and 0.68 ± 0.06 registered for PEF and H. Despite having a considerably higher energy input (i.e. US was 20 time higher than PEF in terms of energy), PEF induced a greater degree of disruption. This confirms previous findings in various foodstuffs where US always showed lower efficiency than PEF in terms of cell disintegration at the same energy input (Barba, Brianceau, et al., 2015; Barba, Galanakis, et al., 2015). In parallel, it is interesting to notice that all the combined treatments (i.e. PEF + US, US + H, PEF + H, PEF + US + H) (data not shown) did not exceed Z values of 0.7 with no significant differences when they were compared to PEF or H treatments applied individually. This finding might be ascribed to the high extent of cell disruption reached in the present conditions, which partially hid potential additive or synergistic effects.

According to the literature, the impact on cell disintegration index mainly reflects microstructural changes through the tissue (Lebovka et al., 2002). The changes induced by PEF, for instance, have been attributed to the breakage of the cell membranes, with the consequent redistribution of water which led to an increased conductivity (Lebovka, Bazhal, & Vorobiev, 2001). Likewise, regardless of the different mechanisms of action of the other applied technologies, it can be hypothesized that the application of external energy boosted water migration from the inner cell compartments toward the extracellular ones. To verify these effects, the drip loss of the mushroom tissue was also evaluated.

Drip loss of mushroom stalks which were exposed to the various processes are illustrated in Fig. 3. Mushroom stalks, used as a control, exhibited an average loss of around 2 ± 1% of their initial weight, which increased ten times when the stalks were immersed in water (DIP), probably due to a partial absorbance of the external water into the mushroom due to the porosity of the tissue. Significantly higher drip loss scores were achieved when US, PEF or high temperature (H) were employed, with mean values of 40 ± 3, 54 ± 5 and 61 ± 2%, respectively. This trend was in agreement with the cell disintegration index, confirming the differing efficiencies of the studied technologies in terms of their impact on the release of intracellular solutions. A synergistic effect, expected when differing technologies were combined, was not observed. On the contrary, an unexpected slight antagonistic behaviour on drip loss was noticed when high temperatures were used in combination with PEF and US. On one hand, microstructural changes promoted by these two technologies were probably partially hidden by high temperatures which in turn caused a high extent of cell disruption. On the other hand, temperature plays a big role on efficiency of US cavitation by affecting viscosity, vapor pressure and surface tension of the liquid media. This can result in a non-linear correlation between temperature and effects of cavitation (Patist & Bates, 2008) which might lead to the antagonistic effects observed in the present work. Moreover, both US and PEF can induce substantial modifications of structural compounds as previously reported in literature (Luo et al., 2010; Pingret et al., 2013). Both technologies generate hydroxyl radicals that have been demonstrated to degrade polysaccharides, including chitosan. Consequently, those works found a different morphology and a lower molecular weight of chitosan upon PEF and US treatments which could affect the water holding capacity of mushrooms stalks and explain the lower drip loss achieved in the present study.

To further characterize the microstructural changes leading to increased water migration and release, an investigation of water distribution and its redistribution upon treatments through the tissue compartments was performed by TD-NMR. In particular, indirect insight into compartment modifications could be gained as a result of the different interactions of water with solutes and biopolymers. Indeed, short transverse relaxation times (T_2 1–50 ms) was expected to reveal water pools interacting to rigid structures like cell wall, while long times (T_2 200–1500 ms) was expected to describe water pools located inside the cells that, in intact tissues, usually represent the highest quantitative contribution to the total signal (Dellarosa, Ragni, et al., 2016; Panarese et al., 2012). Nevertheless, in the region with the T_2 included between 50 and 200 ms, ascribable to extracellular water (Lagnika, Zhang, & Mothibe, 2013), significant changes caused by the treatments studied were expected.

Fig. 4 shows the water redistribution of mushroom stalks before and after drip loss induced by centrifugation, respectively. In agreement with drip loss results, spectra belonging to control samples did not reveal marked modifications upon centrifugation. On average, the distribution of the signal intensities of the three compartments were 66 ± 2%, 25 ± 2% and 11 ± 1% with respect of the total signal, for intracellular, extracellular and cell wall water, respectively.

Please cite this article in press as: Dellarosa, N., et al. The impact of pulsed electric fields and ultrasound on water distribution and loss in mushrooms stalks. *Food Chemistry* (2017), http://dx.doi.org/10.1016/j.foodchem.2017.01.105

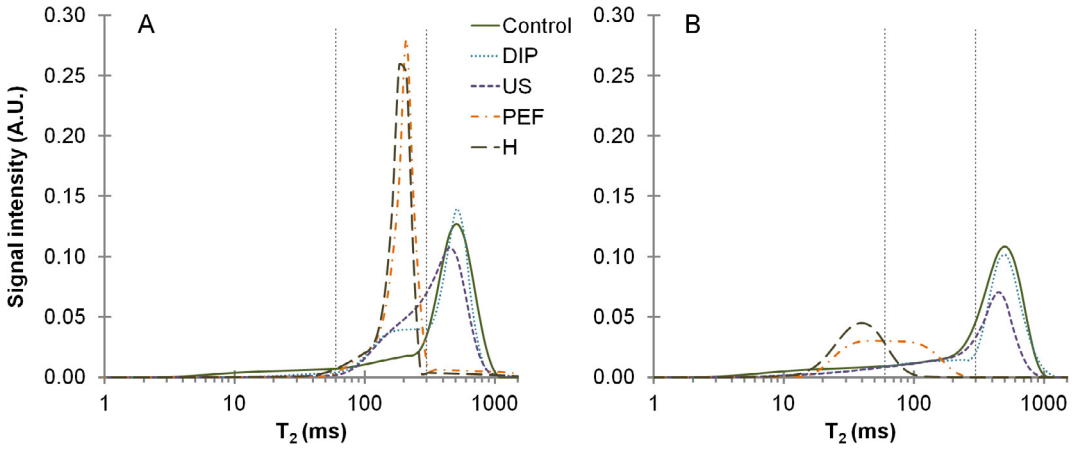

Fig. 4. TD-NMR signal distribution normalized to unitary area before drip loss (A). Residual signals scaled based on the residual amount of water after drip loss according to drip loss results (B). The vertical dashed lines delimit the signals belonging to the three water pools: cell wall (T_2 1–50 ms), extracellular (T_2 50–200 ms) and intracellular (T_2 200–1500 ms) populations. Sample codes: DIP = dipping (25 °C); US = ultrasound; PEF = pulsed electric fields; H = high temperature treatments (90 °C).

Conversely, both DIP and US enhanced the fraction of water protons relaxing between 50 and 200 ms (Fig. 4a), achieving values of 36 ± 2 and 46 ± 2% of the total signal, respectively. In the former case, the major contribution to that signal was solely ascribable to the diffusion of the external water solution through the stalks tissue, while, in the latter case, water was also partially removed from intracellular compartments (T_2 200–1500 ms) and redistributed toward extracellular spaces (T_2 50–200 ms). Interestingly, in both cases water that migrated toward the extracellular compartments was totally removed when an external force, i.e. centrifugation, was applied (Fig. 4b). Cavitation induced by ultrasound generates high shock waves and shear force with a known solubilising effect mainly on fixed cell structures like cell walls (Chemat, Tomao, & Virot, 2008). Water redistribution investigated in the present experiments showed that these microstructural alterations influenced also the intra/extra-cellular repartition. This suggests that technological treatments involving mass transfer, for instance extraction or dehydration, may benefit from the application of US due to both the solubilisation effect of the solid parts and the partial loss of compartmentalization resulting in consequent higher water diffusivity. Indeed, as qualitatively highlighted by Cheung et al. (2013), powerful ultrasound can provoke the modification of the internal channel porosity and fragmentation of the mushroom tissue, with a significant contribution to the extraction yields. In another work on osmotically dehydrated kiwifruit (Nowacka et al., 2014), results showed that micro-channels were created when ultrasound was applied during dipping and the moisture content of the fruit was slightly redistributed through the cell compartments. Even though the energy input was far lower than that applied in present work, US significantly contributed to the enhancement of mass transfer during dehydration.

In the present work, the highest redistribution values, which were in agreement with cell disintegration index and drip loss results, were registered for PEF and H treatments, which markedly affected the internal structure and water partition throughout the tissue (Fig. 4a). Water was noticeably redistributed, so that 82–85% of the total signal was now ascribable to the extracellular compartments, while cell wall and intracellular water pools accounted for 10 and 5%, respectively. No significant differences were found among samples treated with PEF, H and their combination. It is worth observing that the main peak of the extracellular water was sensibly reduced after centrifugation (Fig. 4b) leading to the conclusion that both H and PEF provoked a severe loss of compartmentalization of the mushroom tissue. However, the extent of disruption efficiency, resulting in different Z values abovementioned, was further noticed taking into consideration the distribution of residual amount of water after drip loss. On one side, high temperature treatments gave rise to a narrow peak, normally distributed, centred at T_2 = 40 ms, on the other, PEF resulted in a broad peak ascribable to a probable bimodal distribution (T_2 = 40 and T_2 = 100 ms), equally split between water which was tightly bound to the fixed structures of the tissue and extracellular water. The higher efficiency provided by high temperatures, however, may be counterbalanced by drawbacks in terms of negative heat induced impact on the quality of valuable compounds when extraction is the main goal. In this context, PEF applied in the present work at 25 °C can bring advantages because it prevents possible degradations due to the thermolability of the extracted mushroom components (Roselló-Soto, Parniakov, et al., 2015). Earlier work on other thermo-sensitive food matrixes demonstrated, that PEF used as upstream treatment increased the processes' efficiency in terms of intracellular water diffusivity, for example during osmotic dehydration of fresh-cut fruit (Dellarosa, Ragni, et al., 2016; Parniakov et al., 2015). In order to enhance the effectiveness of the treatments at low temperatures, PEF can be combined with US. Water distribution results together with Z and drip loss values of these combined techniques were not significantly different from high temperature treatments. Another possible benefit described by several authors is related to the selective extraction operated by PEF (Parniakov et al., 2014; Xue & Farid, 2015). Taking advantage of the targeted electroporation of the cell membranes, water extracts were characterized by a high content of intracellular components with a high colloidal stability.

Due to the microstructural changes induced by the various treatments, the liquid media employed for each treatment was analysed by means of TD-NMR and UV–Vis spectroscopy. The measurement of the transverse relaxation time (T_2) by TD-NMR was employed as a biopolymer extraction index. Protons from cell biopolymers lead to a fast chemical exchange with water protons which reduces the average T_2 (Santagapita et al., 2013). Results, illustrated in Table 1, show that the highest reduction of T_2, around 400 ms, was registered for every treatment at high temperature and for the combination of PEF with US. On the contrary, PEF and US, separately applied, did not modify T_2 significantly.

In parallel, UV/Vis spectra were evaluated taking into account the whole visible spectra and specific regions of UV spectra (Fig. 5). In particular, UV spectra, especially those belonging to US and H samples, showed an absorbance peak centred at 260 nm. That peak, which markedly increased when US and H were applied both alone and in combination (Table 1), was found in pre-

Please cite this article in press as: Dellarosa, N., et al. The impact of pulsed electric fields and ultrasound on water distribution and loss in mushrooms stalks. *Food Chemistry* (2017), http://dx.doi.org/10.1016/j.foodchem.2017.01.105

Table 1
Liquid media features: transverse relaxation time (T_2), absorbance at 260 nm (ABS_{260}), ratio between absorbance at 260 and 280 nm ($ABS_{260/280}$) and total absorbance of the visible spectra between 400 and 800 nm ($ABS_{400-800}$). Values show means ± standard deviations of the three replications. Different letters within the same column indicated significant differences ($p < 0.05$) for each parameter.

	T_2 (ms)	ABS_{260}	$ABS_{260/280}$	$ABS_{400-800}$
DIP	2860 ± 156 ab	0.187 ± 0.004 e	1.384 ± 0.066 de	22.787 ± 0.060 f
US	2724 ± 21 b	0.480 ± 0.008 bc	1.325 ± 0.064 ef	83.133 ± 4.298 b
PEF	2907 ± 100 a	0.267 ± 0.021 d	1.276 ± 0.035 f	68.080 ± 3.117 c
H	2454 ± 25 c	0.580 ± 0.038 a	2.013 ± 0.035 a	24.412 ± 2.979 f
PEF + US	2429 ± 24 c	0.508 ± 0.030 b	1.451 ± 0.027 d	98.645 ± 2.591 a
US + H	2450 ± 54 c	0.525 ± 0.009 b	1.800 ± 0.007 b	37.785 ± 1.891 d
PEF + H	2547 ± 24 c	0.435 ± 0.008 c	1.846 ± 0.023 b	31.464 ± 0.849 e
PEF + US + H	2485 ± 49 c	0.485 ± 0.013 b	1.661 ± 0.031 c	41.023 ± 3.164 d

Sample codes: DIP = dipping (25 °C); US = ultrasound; PEF = pulsed electric fields; H = high temperature treatments (90 °C).

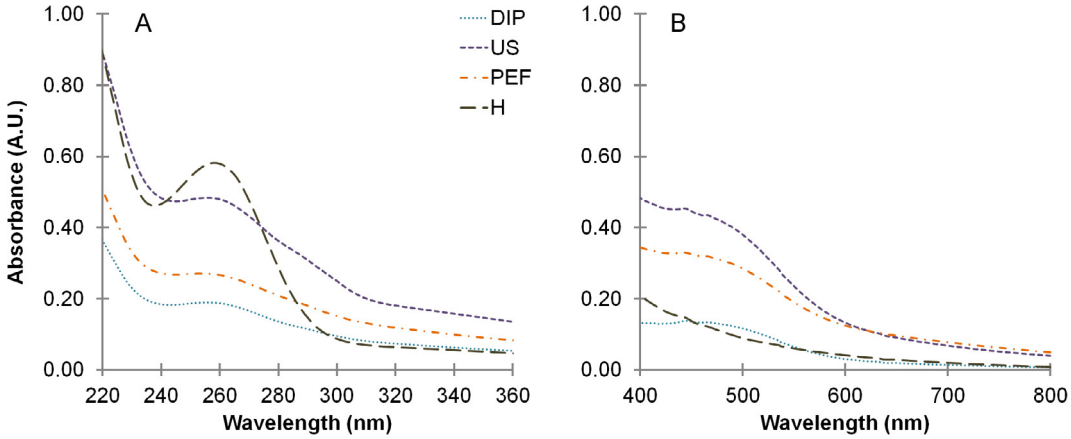

Fig. 5. UV (A) and visible (B) spectra of liquid media used for treatments. Samples were diluted 1/10 for UV analysis to fit the 0–1 absorbance range. Sample codes: DIP = dipping (25 °C); US = ultrasound; PEF = pulsed electric fields; H = high temperature treatments (90 °C).

vious work (Parniakov et al., 2014) to be correlated to the concentration of the extracted mushroom compounds in the liquid media. In fact, the results obtained in the present investigation showed a good negative correlation with transverse relaxation time ($r = -0.88$), suggesting that the absorbance at 260 nm can be a gross index of the release of biopolymers from the mushroom tissue. Beside the overall release of the mushroom compounds, PEF and US applications can also induce modifications of their chemical structure. As previously reported by Luo et al. (2010) the carbonyl and carboxyl groups of mushroom chitosan can be degraded by high voltages leading to different absorbances in specific regions of the UV spectra. Similarly, US treatments can also alter the physico-chemical morphology of polysaccharides (Pingret et al., 2013) which probably influenced the quality of the extract. Furthermore, as reported in literature (Glasel, 1995; Parniakov et al., 2014; Xue & Farid, 2015), the ratio between the absorbance at 260 and 280 nm illustrates the level of proteins/nucleotides that usually varies in the range between 1 for pure proteins and 2 for pure nucleotides extracts. Values around 1.3–1.4 were registered for DIP, US, PEF and their combination while higher values were reached when treatments were combined with high temperatures. Interestingly, while H treatment alone showed values around 2, indicating the selective extraction of pure nucleotides, when H was combined with either US or PEF that value significantly decreased probably due to the higher release of proteins. That ratio was further lowered when PEF was followed by US at high temperature, demonstrating an additive effect on the protein release. In addition to the UV, the overall visible spectra absorption were evaluated in the range of 400–800 nm. Although every treatment increased the total absorbance, the highest values were noticed for treatments at low temperature among which US (and its combination with PEF) played the major role. The different visible absorbances can be attributable to both the ability of US and PEF to extract pigments, abundant in the cell walls of mushrooms (Roselló-Soto, Parniakov, et al., 2015) and the thermolability of those mushroom compounds.

4. Conclusions

Microstructural changes in the mushroom stalks were evaluated by a combination of various physical methods that were able to describe fine modifications of the internal structure of the mushroom stalks. The cell disintegration index, drip loss upon centrifugation and water redistribution illustrated the migration of the intracellular solutions toward extracellular spaces. Pulsed electric fields and ultrasound differentially influenced the extent of loss of compartmentalization through the tissue which was quantitatively monitored by TD-NMR. In particular, results showed that the water pools included between 50 and 200 ms can be used as an efficiency index in food processes whenever further downstream treatments affecting water have to be applied to mushroom, for instance dehydration, extraction or purification processes. Moreover, a different selective release of the inner compounds was noticed upon ultrasound, pulsed electric field and heat treatments as a consequence of their different mechanism of action, even though no particular target compounds were analysed in the present work. This promotes the choice of a specific appropriate technology depending on the required target effect and their combination with other technologies which may enhance the effectiveness of the whole processes. Further investigations need to be carried out to evaluate in depth the quality of the valuable compounds which can be extracted from mushroom by-products

Please cite this article in press as: Dellarosa, N., et al. The impact of pulsed electric fields and ultrasound on water distribution and loss in mushrooms stalks. *Food Chemistry* (2017), http://dx.doi.org/10.1016/j.foodchem.2017.01.105

and estimate the potential use of these innovative technologies in terms of production cost.

Acknowledgements

The authors wish to acknowledge the financial support of Food Institutional Research Measure (FIRM) funded by the Irish Department of Agriculture, Food and the Marine (Project no. 11 F 050). Nicolò Dellarosa acknowledges also the Marco Polo Programme (University of Bologna) for the travel grant.

References

Angersbach, A., Heinz, V., & Knorr, D. (1999). Electrophysiological model of intact and processed plant tissues: cell disintegration criteria. *Biotechnology Progress, 15*(4), 753–762.

Angersbach, A., Heinz, V., & Knorr, D. (2002). Evaluation of process-induced dimensional changes in the membrane structure of biological cells using impedance measurement. *Biotechnology Progress, 18*(3), 597–603.

Barba, F. J., Brianceau, S., Turk, M., Boussetta, N., & Vorobiev, E. (2015a). Effect of alternative physical treatments (ultrasounds, pulsed electric fields, and high-voltage electrical discharges) on selective recovery of bio-compounds from fermented grape pomace. *Food and Bioprocess Technology, 8*(5), 1139–1148.

Barba, F. J., Galanakis, C. M., Esteve, M. J., Frigola, A., & Vorobiev, E. (2015b). Potential use of pulsed electric technologies and ultrasounds to improve the recovery of high-added value compounds from blackberries. *Journal of Food Engineering, 167*, 38–44.

Barba, F. J., Parniakov, O., Pereira, S. A., Wiktor, A., Grimi, N., Boussetta, N., ... Witrowa-Rajchert, D. (2015c). Current applications and new opportunities for the use of pulsed electric fields in food science and industry. *Food Research International, 77*, 773–798.

Chemat, F., Tomao, V., & Virot, M. (2008). Ultrasound-assisted extraction in food analysis. *Handbook of Food Analysis Instruments*, 85–103.

Cheung, Y.-C., Siu, K.-C., Liu, Y.-S., & Wu, J.-Y. (2012). Molecular properties and antioxidant activities of polysaccharide–protein complexes from selected mushrooms by ultrasound-assisted extraction. *Process Biochemistry, 47*(5), 892–895.

Cheung, Y.-C., Siu, K.-C., & Wu, J.-Y. (2013). Kinetic models for ultrasound-assisted extraction of water-soluble components and polysaccharides from medicinal fungi. *Food and Bioprocess Technology, 6*(10), 2659–2665.

Dellarosa, N., Ragni, L., Laghi, L., Tylewicz, U., Rocculi, P., & DallaRosa, M. (2016a). Time domain nuclear magnetic resonance to monitor mass transfer mechanisms in apple tissue promoted by osmotic dehydration combined with pulsed electric fields. *Innovative Food Science & Emerging Technologies, 37*(C), 345–351.

Dellarosa, N., Tappi, S., Ragni, L., Laghi, L., Rocculi, P., & Dalla Rosa, M. (2016b). Metabolic response of fresh-cut apples induced by pulsed electric fields. *Innovative Food Science & Emerging Technologies, 38*, 356–364.

Donsì, F., Ferrari, G., & Pataro, G. (2010). Applications of pulsed electric field treatments for the enhancement of mass transfer from vegetable tissue. *Food Engineering Reviews, 2*(2), 109–130.

Faridnia, F., Burritt, D. J., Bremer, P. J., & Oey, I. (2015). Innovative approach to determine the effect of pulsed electric fields on the microstructure of whole potato tubers: Use of cell viability, microscopic images and ionic leakage measurements. *Food Research International, 77*, 556–564.

Fincan, M., & Dejmek, P. (2002). In situ visualization of the effect of a pulsed electric field on plant tissue. *Journal of Food Engineering, 55*(3), 223–230.

Glasel, J. (1995). Validity of nucleic acid purities monitored by 260nm/280nm absorbance ratios. *BioTechniques, 18*(1), 62–63.

Ivorra, A. (2010). Tissue electroporation as a bioelectric phenomenon: Basic concepts. In *Irreversible electroporation*, (pp. 23–61): Springer.

Lagnika, C., Zhang, M., & Mothibe, K. J. (2013). Effects of ultrasound and high pressure argon on physico-chemical properties of white mushrooms (*Agaricus bisporus*) during postharvest storage. *Postharvest Biology and Technology, 82*, 87–94.

Lebovka, N., Bazhal, M., & Vorobiev, E. (2001). Pulsed electric field breakage of cellular tissues: visualisation of percolative properties. *Innovative Food Science & Emerging Technologies, 2*(2), 113–125.

Lebovka, N., Bazhal, M., & Vorobiev, E. (2002). Estimation of characteristic damage time of food materials in pulsed-electric fields. *Journal of Food Engineering, 54*(4), 337–346.

Lespinard, A. R., Bon, J., Cárcel, J. A., Benedito, J., & Mascheroni, R. H. (2015). Effect of ultrasonic-assisted blanching on size variation, heat transfer, and quality parameters of mushrooms. *Food and Bioprocess Technology, 8*(1), 41–53.

Luengo, E., Condón-Abanto, S., Condón, S., Álvarez, I., & Raso, J. (2014). Improving the extraction of carotenoids from tomato waste by application of ultrasound under pressure. *Separation and Purification Technology, 136*, 130–136.

Luo, W. B., Han, Z., Zeng, X. A., Yu, S. J., & Kennedy, J. F. (2010). Study on the degradation of chitosan by pulsed electric fields treatment. *Innovative Food Science & Emerging Technologies, 11*(4), 587–591.

Mauro, M. A., Dellarosa, N., Tylewicz, U., Tappi, S., Laghi, L., Rocculi, P., & Dalla Rosa, M. (2016). Calcium and ascorbic acid affect cellular structure and water mobility in apple tissue during osmotic dehydration in sucrose solutions. *Food Chemistry, 195*, 19–28.

McDonnell, C. K., Allen, P., Duggan, E., Arimi, J. M., Casey, E., Duane, G., & Lyng, J. G. (2013). The effect of salt and fibre direction on water dynamics, distribution and mobility in pork muscle: a low field NMR study. *Meat Science, 95*(1), 51–58.

Nowacka, M., Tylewicz, U., Laghi, L., Dalla Rosa, M., & Witrowa-Rajchert, D. (2014). Effect of ultrasound treatment on the water state in kiwifruit during osmotic dehydration. *Food Chemistry, 144*, 18–25.

Panarese, V., Laghi, L., Pisi, A., Tylewicz, U., Dalla Rosa, M., & Rocculi, P. (2012). Effect of osmotic dehydration on Actinidia deliciosa kiwifruit: A combined NMR and ultrastructural study. *Food Chemistry, 132*(4), 1706–1712.

Parniakov, O., Lebovka, N., Bals, O., & Vorobiev, E. (2015). Effect of electric field and osmotic pre-treatments on quality of apples after freezing–thawing. *Innovative Food Science & Emerging Technologies, 29*, 23–30.

Parniakov, O., Lebovka, N., Van Hecke, E., & Vorobiev, E. (2014). Pulsed electric field assisted pressure extraction and solvent extraction from mushroom (*Agaricus bisporus*). *Food and Bioprocess Technology, 7*(1), 174–183.

Patist, A., & Bates, D. (2008). Ultrasonic innovations in the food industry: From the laboratory to commercial production. *Innovative Food Science & Emerging Technologies, 9*(2), 147–154.

Pingret, D., Fabiano-Tixier, A. S., & Chemat, F. (2013). Degradation during application of ultrasound in food processing: A review. *Food Control, 31*(2), 593–606.

Raso, J., & Barbosa-Cánovas, G. V. (2003). Nonthermal preservation of foods using combined processing techniques. *Critical Reviews in Food Science and Nutrition, 43*(3), 265–285.

Raso, J., Manas, P., Pagan, R., & Sala, F. J. (1999). Influence of different factors on the output power transferred into medium by ultrasound. *Ultrasonics Sonochemistry, 5*(4), 157–162.

Roselló-Soto, E., Galanakis, C. M., Brnčić, M., Orlien, V., Trujillo, F. J., Mawson, R., ... Barba, F. J. (2015a). Clean recovery of antioxidant compounds from plant foods, by-products and algae assisted by ultrasounds processing. Modeling approaches to optimize processing conditions. *Trends in Food Science & Technology, 42*(2), 134–149.

Roselló-Soto, E., Parniakov, O., Deng, Q., Patras, A., Koubaa, M., Grimi, N., ... Lebovka, N. (2015b). Application of non-conventional extraction methods: toward a sustainable and green production of valuable compounds from mushrooms. *Food Engineering Reviews*, 1–21.

Santagapita, P., Laghi, L., Panarese, V., Tylewicz, U., Rocculi, P., & Dalla Rosa, M. (2013). Modification of transverse NMR relaxation times and water diffusion coefficients of kiwifruit pericarp tissue subjected to osmotic dehydration. *Food and Bioprocess Technology, 6*(6), 1434–1443.

Sun, D.-W., & Li, B. (2003). Microstructural change of potato tissues frozen by ultrasound-assisted immersion freezing. *Journal of Food Engineering, 57*(4), 337–345.

Vorobiev, E., & Lebovka, N. (2009). Pulsed-electric-fields-induced effects in plant tissues: fundamental aspects and perspectives of applications. In *Electrotechnologies for extraction from food plants and biomaterials*, (pp. 39–81): Springer.

Wiktor, A., Gondek, E., Jakubczyk, E., Nowacka, M., Dadan, M., Fijalkowska, A., & Witrowa-Rajchert, D. (2016). Acoustic emission as a tool to assess the changes induced by pulsed electric field in apple tissue. *Innovative Food Science & Emerging Technologies, 37*(C), 375–383.

Wu, T., Zivanovic, S., Draughon, F. A., & Sams, C. E. (2004). Chitin and chitosan value-added products from mushroom waste. *Journal of Agricultural and Food Chemistry, 52*(26), 7905–7910.

Xue, D., & Farid, M. M. (2015). Pulsed electric field extraction of valuable compounds from white button mushroom (*Agaricus bisporus*). *Innovative Food Science & Emerging Technologies, 29*, 178–186.

XuJie, H., & Wei, C. (2008). Optimization of extraction process of crude polysaccharides from wild edible BaChu mushroom by response surface methodology. *Carbohydrate Polymers, 72*(1), 67–74.

Please cite this article in press as: Dellarosa, N., et al. The impact of pulsed electric fields and ultrasound on water distribution and loss in mushrooms stalks. *Food Chemistry* (2017), http://dx.doi.org/10.1016/j.foodchem.2017.01.105

Paper IX

Tylewicz, U., Tappi, S., Mannozzi, C., Romani, S., **Dellarosa**, **N.**, Laghi, L., Ragni, L., Rocculi, P., & Dalla Rosa, M. (2017)

Effect of pulsed electric field (PEF) pre-treatment coupled with osmotic dehydration on physico-chemical characteristics of organic strawberries

Journal of Food Engineering, Under review

Effect of pulsed electric field (PEF) pre-treatment coupled with osmotic dehydration on physico-chemical characteristics of organic strawberries

Urszula Tylewicz[a], Silvia Tappi[a], Cinzia Mannozzi[a], Santina Romani[a,b], Nicolò Dellarosa[a], Luca Laghi[a,b], Luigi Ragni[a,b], Pietro Rocculi[a,b], Marco Dalla Rosa[a,b]

[a] *Department of Agricultural and Food Sciences, University of Bologna, Cesena, Italy*

[b] *Interdepartmental Centre for Agri-Food Industrial Research, University of Bologna, Cesena, Italy*

Corresponding author: Urszula Tylewicz (urszula.tylewicz@unibo.it)

Keywords: fruit quality; strawberries; organic; texture; colour; non-thermal treatment

ABSTRACT

The aim of this work was to evaluate the effect of pulsed electric field (PEF) pre-treatment on mass transfer phenomena, water distribution and some physico-chemical parameters of osmo-dehydrated organic strawberries. For PEF treatments 100 near-rectangular shaped pulses, with fixed pulse width of 100 µs and repetition time of 10 ms were used. Electric fields strength applied were 100, 200 and 400 V cm^{-1}. Afterwards, samples were subjected to OD treatments carried out in two different hypertonic solutions (40% w/w), one with sucrose and the other one with trehalose. The results shown that PEF treatment positively affected the mass transfer during OD even at the lowest electric field strength applied (100 V cm^{-1}), partially preserving the cell viability and maintaining at the same time the fresh-like characteristics of strawberries.

1. Introduction

Increased consumer demand for safety, health and environmental friendly food products make the organic production one of the fastest growing market segments over the last few years. Consumers expect the quality of organic fruits to be higher or at least comparable with the conventionally produced ones, protecting at the same time the nature and reducing the environmental pollution (Barański et al., 2014).

Berries, and in particular strawberries, are very attractive for consumers, because of their unique flavour, texture and red vivid colour, both in a fresh form and in a variety of food products and snacks. They are also highly appreciated by consumers due to their high amount of ascorbic acid and antioxidants (Velickova et al., 2013; Gamboa-Santos et al., 2014). However, strawberries are highly susceptible to mechanical injury and also highly perishable (Badawy et al., 2016; Kadivec et al., 2016); these characteristics could be even more pronounced in the organic fruit. Therefore, there is a need to improve the processing of these fruits in order to obtain semi-dried or intermediate moisture products with longer shelf-life. With regards to organic production practices, applied treatments and processes should be aimed at avoiding the chemical additives, while non-thermal processing is used with the aim of maintaining the nutritional and sensorial properties of food products.

Osmotic dehydration (OD) is one of the non-thermal processes used to obtain intermediate moisture products with improved stability over storage. This because, during OD a partial dewatering of plant tissue takes place, reducing both freezable water content and the water activity of the system (Tylewicz et al., 2011; Mauro et al., 2016). The application of OD process on strawberry tissue has been widely studied. Cheng et al. (2014) studied the effect of power ultrasound and pulsed vacuum treatments on the dehydration kinetics and the status of water during osmotic dehydration of strawberries, showing that the highest water loss (lower freezable water content) and the highest decrease in firmness occurred using ultrasound treatment, while the highest solid gain and the highest firmness values were achieved by pulsed vacuum treatment. Castelló et al. (2010) observed that OD treatment promoted the structural collapse, however, when calcium was added to the osmotic solution a beneficial effect on the maintenance of the sample texture was observed. Since OD treatment, especially when applied at room temperature, is a time-requiring process, other pre-treatments could be used before OD in order to increase the velocity of mass transfer kinetics.

Pulsed electric filed is a process which promotes the modification of the membrane permeability by application of high voltage short time pulses (Barba et al., 2015). The application of low electric field strength

creates pores in the biological membrane which affect the mass transfer in tissues. In fact, several studies of PEF-assisted OD have been carried out on different plant tissues such as apples (Dellarosa et al., 2016a; Dellarosa et al., 2016b; Amami et al., 2006), kiwifruits (Dermesonlouoglou et al., 2016; Traffano-Schiffo et al., 2016), carrots (Amami et al., 2007), potatoes (Fincan & Dejmek, 2003) etc. While the effect of PEF pre-treatment on enhancing the water loss of OD treated tissues seems to be clearly and well stated, its effect on the solid gain is ambiguous. In fact, some authors reported an increase in solid uptake, for example in mango pieces (Taiwo et al., 2002) and apples (Amani et al., 2006; Dellarosa et al., 2016a), while in PEF pre-treated kiwifruit samples the solutes uptake was lower compared to untreated ones (Traffano-Schiffo et al., 2016). The impact of high-intensity electric field pulses on the mass transfer and on some physical characteristics (leaching of cell constituents, colour and texture) of strawberry halves during osmotic dehydration (OD) has been studied (Taiwo et al., 2003). Higher water loss was obtained in samples treated with a high-intensity electric field before OD. Moreover, the application of PEF before OD minimized changes in product colour and allowed to retain product compactness.

To the best of our knowledge, this is the first work aimed to the evaluation of the effect of PEF+OD low temperature processes on the mass transfer phenomena and water redistribution of strawberry tissue. Moreover, the changes in some quality parameters of treated strawberries from organic production were evaluated.

2. Material and methods

2.1 Raw material handling

Organic strawberries (*Fragaria+ananassa)* var 'Alba' (10 ± 1 °Brix) were purchased from the local market in Cesena (Italy). The strawberries were stored at 4 ± 1 ºC and high relative humidity until use, for no longer than one week. Before processing, fruits were tempered at 25 ºC, washed, hand stemmed and cut into rectangular shape pieces of the dimension 5 x 10 x 20 mm (height x width x length).

2.2 Pulsed electric field (PEF) treatment

Two rectangular pieces (approximately 1.3 g) were placed into a rectangular treatment chamber equipped with two stainless steel electrodes (20 x 20 mm^2) with a gap between them of 30 mm and filled with 5 mL of a sodium chloride solution with the same conductivity as the strawberries (1.6 mS/cm). The PEF treatments were applied to the strawberry samples at 25 °C using an in-house developed pulse generator equipment based on MOSFET technology that delivers near-rectangular shape pulses. PEF pre-treatments were carried out by applying a train of 100 pulses at three different pulsed electric field (E) strength (100, 200 and 400 V cm^{-1}), a fixed pulse width of 100 µs and a repetition time of 10 ms (100 Hz). The procedure setting was chosen on bases of preliminary experiments.

2.3 Osmotic dehydration (OD) treatment

The OD treatment was carried out by immersing the strawberry samples in 40 % (w/w) hypertonic solutions. Two different solutions were prepared, one with sucrose and one with trehalose dissolved in distilled water. Calcium lactate (CaLac) at a concentration of 1 % (w/w) was added to both the solutions as a structuring agent. The treatment was performed at 25 ºC with continuous stirring maintaining a fruits:OD solution ratio of 1:4 (w/w) that allowed to avoid significant changes in the solution concentration during the whole treatment (data not shown). The samples were analyses at different treatment times: 0, 15, 30, 60 and 120 min. Both PEF and OD procedures were repeated twice for each solution. All obtained samples are summarised with related abbreviations as reported in table 1.

Table 1. Codification of analysed samples

Sample code	Electric field (V cm^{-1})	Type of solution
NoPEF_S	0	Sucrose
PEF_100_S	100	Sucrose
PEF_200_S	200	Sucrose
PEF_400_S	400	Sucrose
NoPEF_T	0	Trehalose
PEF_100_T	100	Trehalose
PEF_200_T	200	Trehalose
PEF_400_T	400	Trehalose

2.4. Analytical determinations

2.4.1 Mass transfer phenomena

Mass transfer phenomena during osmotic dehydration of strawberry samples was evaluated by calculating weight reduction (WR, kg kg^{-1}), water loss (WL, kg kg^{-1}) and solutes gain (SG, kg kg^{-1}) adopting the following equations:

$$WR = \frac{m_t - m_0}{m_0} \quad (1)$$

$$\mathrm{W}L = \frac{m_t x_{wt} - m_0 x_{w0}}{m_0} \quad (2)$$

$$SG = \frac{m_t x_{ST t} - m_0 x_{ST 0}}{m_0} \quad (3)$$

where:

m_0 - initial weight before osmotic treatment (kg)
m_t - weight after a time t (kg)
x_{w0}- initial water mass fraction (kg · kg^{-1})
x_{wt} - water mass fraction after a time t (kg · kg^{-1})
x_{ST0} - initial total solids (dry matter) mass fraction (kg · kg^{-1})
x_{STt} - total solids (dry matter) mass fraction after a time t (kg · kg^{-1})

Moisture content was determined gravimetrically by drying the samples at 70 °C until a constant weight was achieved (AOAC, 2002).

2.4.2 Water distribution by TD-NMR measurements

In order to measure the proton transverse relaxation time (T_2), strawberry cylinders of about 250 mg (h = 10 mm, d = 8 mm) were cut with a core borer. The samples were placed inside 10 mm outer diameter NMR tubes, in order to not exceed the active region of the radio frequency coil, and analyzed at 25 °C with the CPMG pulse sequence (Meiboom & Gill, 1958) using a 'The Minispec' spectrometer (Bruker Corporation, Germany) operating at 20 MHz. Each measurement comprised 4000 echoes over 16 scans, with an interpulse spacing of 0.3 ms and a recycle delay set at 10 s. The specified parameters, chosen to prevent sample and radio frequency coil overheat, allowed the observation of the protons with T_2 higher than a few milliseconds. According to the protocol set up by Panarese et al. (2012), the CPMG decays were analyzed with the UPEN software (Borgia et al., 1998), which inverts the CPMG signal using a quasi-continuous distribution of exponential curves, and through fittings to the sum of an increasing number of exponential curves. Furthermore, a multi exponential discrete fitting was successively applied to accurately determine T_2 and relative intensities of the water populations (Mauro et al., 2016). The experiment was conducted in triplicate at each treatment condition.

2.4.3 Cell viability test by Fluorescein diacetate (FDA) staining

The cell viability test was performed on 1 mm-thick strawberry slices, cut with a sharp scalpel, using fluorescein diacetate (FDA, Sigma-Aldrich, USA, λ_{ex} = 495 nm, λ_{em} = 518 nm), as described by Tylewicz et al. (2013) with some modifications. Strawberry slices were incubated for 5 min in a solution containing FDA (10^{-4} M) and sucrose in isotonic concentration (10 %, w/w) in the darkness at room temperature. The dye used in the experiment can passively penetrate the protoplast and then it is hydrolysed by cytoplasmic esterases, producing the polar product named fluorescein that only the viable cells are able to accumulate intracellularly, because it is unable to cross cellular membranes that remain intact (Mauro et al., 2016). Hence, viable cells could be easily identified by a bright fluorescence. Observations were performed under a fluorescent light in a Nikon upright microscope (Eclipse Ti-U, Nikon Co, Japan) equipped with a Nikon digital video camera (digital sight DS-Qi1Mc, Nikon Co, Japan) at a magnification of 4 ×.

2.4.4 Colour

The colour changes of fresh, PEF pre-treated and osmo-dehydrated samples were investigated using a spectro-photocolorimeter mod. Colorflex (Hunterlab, USA). The measurements were made using CIE *L*a*b** scale. The instrument was calibrated with a black and white tile (*L** 93.47, *a** 0.83, *b** 1.33) before the measurements. Moreover, the hue angle (h°) parameter was calculated using the following equation:

$$h° = tan^{-1}\frac{b^*}{a^*} \qquad (4)$$

where: a* (red–green) and b* (yellow–blue) are parameters of color measurement (Vega-Gálvez et al., 2012). The analysis was conducted in twelve repetitions for randomly selected strawberry samples for each PEF pre-treatment and osmotic dehydration condition.

2.4.5 Texture analysis

Firmness (N) was evaluated by performing a penetration test on strawberry rectangular pieces using a TA-HDi500 texture analyzer (Stable Micro Systems, Surrey, UK) equipped with a 5 N load cell. A stainless-steel probe of 2 mm diameter was used and rate and depth of penetration were of 1 mm/s and 95 %, respectively. The analysis was performed in twelve replicates.

2.5 Statistical analysis

Significance of the PEF treatment and OD effects was evaluated by one-way analysis of variance (ANOVA, 95% significance level) and comparison of means by Duncan test at a 5% probability level using the software STATISTICA 6.0 (Statsoft Inc., Tulsa, UK).

3. Results and discussion

3.1 Mass transfer phenomena

The kinetics of water loss and solid gain during OD are shown in Fig. 1 and Fig. 2 for sucrose and trehalose solutions, respectively. Fig. 1 shows also the effect of the different electric field strength applied on water loss and solid gain during osmotic dehydration of strawberries immersed in sucrose-based solution. Samples subjected to the PEF pre-treatment presented a significantly higher water loss compared to the untreated strawberry samples.

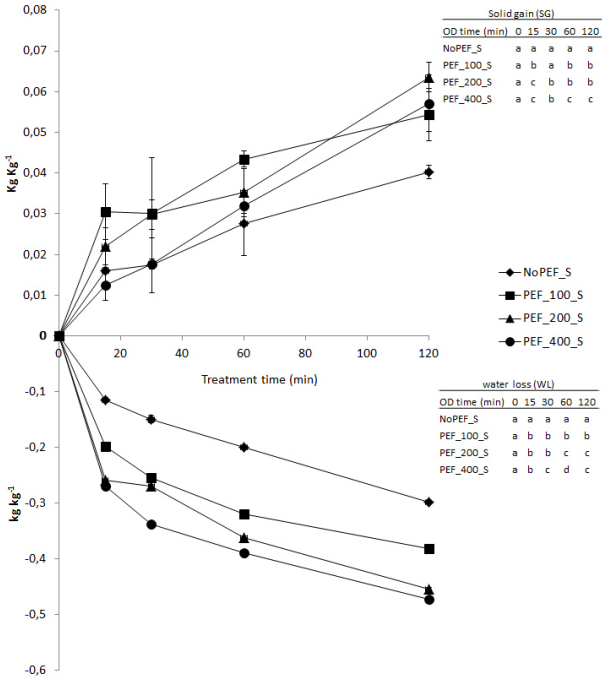

Fig. 1. Solid gain and water loss of untreated and PEF pre-treated strawberry samples, as a function of the osmotic dehydration time in sucrose-based solution. The same letter on the same column means no significant difference between the samples by the Duncan test ($p < 0.05$).

An improvement of water loss upon PEF pre-treatment has already been observed by Taiwo et al. (2003) on strawberries (1200 V cm^{-1}) and by Traffano-Schiffo et al. (2016) on kiwifruit (up to 400 V cm^{-1}). The acceleration of the kinetics of water and solids transfer is due to the effect of permeabilization of the cell membranes induced by the PEF treatment (Amani et al., 2006; Barba et al., 2015). In the present study, the application of the lowest electric field intensity (100 V cm^{-1}) resulted already sufficient to increase the water loss by 12 % after one hour of osmotic dehydration. This result is in contrast with those obtained by Dellarosa et al. (2016), who observed that the treatment with 100 V cm^{-1} did not have any effect on mass transfer of apple cylinders during the OD conducted for 60 min. This difference could probably be explained by the different microstructure of strawberries which resulted in a different sensitivity to the electric field strength. In addition, it needs to be mentioned that, due to both the different conductivity of samples/media and the higher number of delivered pulses, the energy input applied to the strawberry samples (123 J kg^{-1}) was much higher compared to the one delivered to the apples (8 J kg^{-1}). The initial mass transfer rate in PEF treated samples was faster compared to the untreated one, proportionally to the PEF intensity. Although at the end of the osmotic treatment the samples treated at 250 and 400 V cm^{-1} did not differ significantly, in agreement with Traffano-Schiffo et al. (2016). As reported by various authors (Ade-Omowaye et al., 2003; Angersbach et al., 2002; Dellarosa et al. 2016a), PEF effects can be considered time-dependent and the formation of pores and their growth in the membrane are not immediate but continue for several minutes after the treatment. This highlights the importance of taking into account the time elapsed from the application of pulsed electric fields before any other treatment in order to optimize PEF application in a combined multi step manufacturing process.

Similarly to water loss, solid gain was favoured by the application of PEF. After 120 min of OD, the solid gain was about 4 % in the strawberry untreated tissue, while PEF pre-treated sample reached a 5–6 % gain, in agreement with the results of Dellarosa et al. (2016a). The lower enhancement of solid gain compared to the water loss has already been observed by Ade-Omowaye et al., (2003), that attributed this result to the higher molecular size of solutes compared to water and to a selective membrane permeabilization that favour dewatering rather than solute diffusion through the tissue.

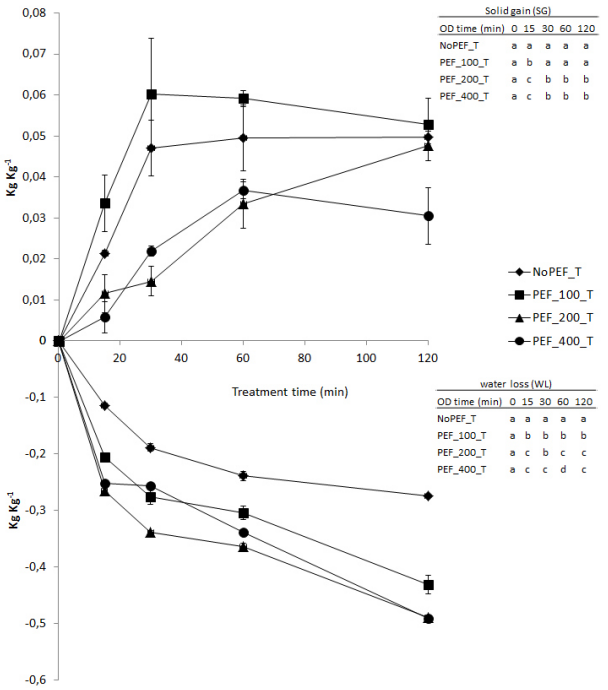

Fig. 2. Solid gain and water loss of untreated and PEF pre-treated strawberry samples, as a function of the osmotic dehydration time in trehalose-based solution. The same letter on the same column means no significant difference between the samples by the Duncan test ($p < 0.05$).

The SG and WL behaviours of strawberry samples dehydrated in the trehalose-based solution were similar (Fig.2). However, water loss in trehalose-based solution was characterized by a higher initial rate compared to the treatment in the sucrose solution but by a lower final dehydration level. At the end of the treatment, the samples treated at 200 and 400 V cm^{-1} reached the highest WL of about 50 %.

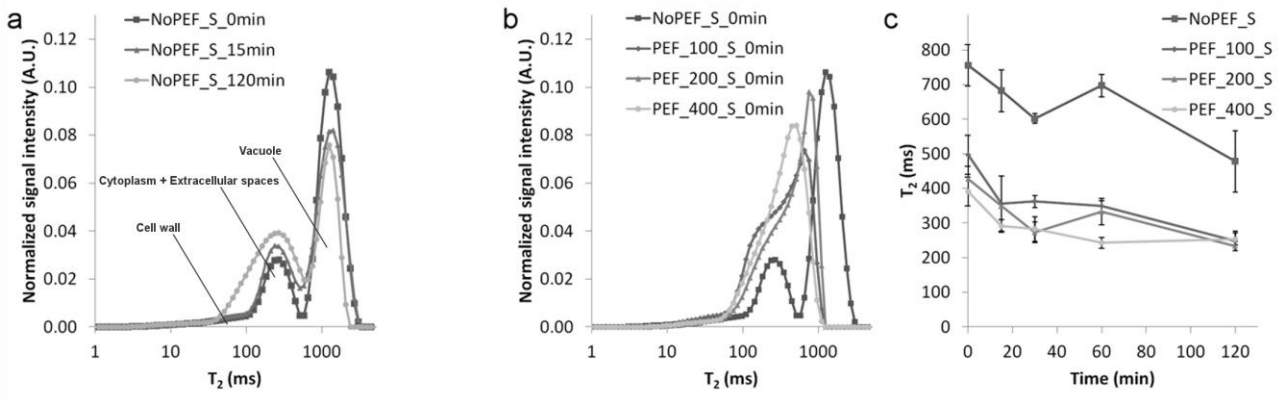

Fig. 3. T_2-weighted signal distribution, normalized to unitary area, of OD samples with sucrose (a) and sample immediately after PEF pre-treatments (b). Mean transverse relaxation time (T_2) values ± standard deviation PEF pre-treated and control strawberries.

Interesting results were observed for solid gain. Up to 120 min, only the treatment with the lowest electric field strength caused a higher solid gain compared to the untreated sample, while the treatment at 200 and 400 V cm^{-1} reduced the trehalose uptake due to a lower initial mass transfer rate. Generally thought, samples treated at 400 V cm^{-1} showed a noticeably lower solids impregnation. Trehalose is known to exert a protective effect on cell membranes during drying or freezing (Ferrando & Spiess, 2001; Atarés et al., 2008), thanks to its ability to form hydrogen bonds with the biomolecules that allows to stabilize cells and tissues preserving viability and structures (Vicente et al. 2012). In the present study, the combination of PEF with trehalose allowed to obtain a higher dewatering effect without increasing solute uptake or even reducing it. This could be considered a positive effect if you want to increase the stability of a perishable organic product while maintaining/considering its nutritional properties.

3.2 Water redistribution upon treatments

Osmotic dehydration itself, generally, promotes important changes in cellular structure of different plan tissues, that can affect the water mobility and its distribution through different parts of the cellular tissue (Tylewicz et al., 2011; Panarese et al., 2012; Mauro et al., 2016). TD-NMR permitted to separately observe two main water populations located in vacuoles and cytoplasm plus extracellular spaces of strawberry tissue that corresponded to the relaxation time (T_2) of 1139.82 ± 129.56 and 251.24 ± 23.51, respectively. During OD treatment, it was possible to observe the decrease of the signal intensity related to the water protons located in the vacuole throughout 120 min. As a consequence, the shrinkage of vacuole led to the increase of the intensity of the water protons belonging to the cytoplasm and extracellular space, as shown in the way of example for the sucrose treated samples in Fig. 3a.

Results are in agreement with those reported by Cheng et al. (2014), who studied the effect of water-osmotic solute exchange on the strawberry cell compartments (vacuole, cytoplasm plus intercellular space, and cell wall) subjected to the ultrasound and vacuum assisted OD treatment in sucrose solution. The authors also observed that, upon OD treatments, the relative space occupied by the vacuole decreased while the one occupied by the cytoplasm and intercellular space increased. In other fruit, such as kiwifruit (Tylewicz et al., 2011; Panarese et al., 2012) and apples (Mauro et al., 2016) similar behaviour on water distribution was observed, confirming the migration of water from the inner compartments toward the external ones.

Fig. 3b shows the effect on water distribution due to the application of PEF on the strawberry tissue before immersion in the hypertonic solution. The electroporation induced by the treatment led to a loss of compartmentalization that is highlighted by the merging of the two proton populations into a single one. This effect was more pronounced when applied E was increased from 100 to 400 V cm^{-1}. Dellarosa et al. (2016) studied the water distribution in apple tissue subjected to PEF treatments at similar voltages and determined a no-reversibility threshold at around 150 V cm^{-1} with 60 train pulses. In the present study, even the lower voltage applied (100 V cm^{-1}) seemed to promote a collapse of the cellular structures although less markedly compared to the higher voltages. As mentioned above, this discrepancy could be explained by the higher energy input applied in the present experiment and the different sensitivity of strawberry tissue to the field strength in comparison with apples.

Fig. 3c illustrates mean T_2 values of the water populations throughout 120 min of the osmotic treatment. As expected, this value decreased during OD due to the water removal and the different water-solutes-biopolymers interaction. Indeed, the water that is leaving the tissue during OD is characterized by high mobility,

hence with long T_2. Therefore, a marked decrease of T_2 values, from 755 ± 60 ms to 478 ± 89 ms, for untreated strawberries was observed. Interestingly, each applied electric field strength also showed values spanning in the range 390-500 ms, immediately after PEF treatment. Such results might not be attributed to the different water content, but to the dissimilar water-solutes-biopolymers induced by the loss of compartmentalization within the strawberry tissue. In addition, similarly to control trends, T_2 values continued to decline during the whole duration of the osmotic dehydration process, so when water was also removed. These results, in accordance with mass transfer data, demonstrated that OD efficiency could be highly influenced by PEF pre-treatments which eased the diffusion of inner water by markedly affecting the permeability of membranes. The samples dehydrated in trehalose-based solution (data not shown) followed a similar trend as the samples dehydrated in sucrose. Probably the marked effect of PEF contributed to hide the effect of different solutes used for dehydration.

3.3 Cell viability test by Fluorescein diacetate (FDA) staining

Fig. 4 presents images of strawberry tissue after the PEF treatment followed by staining with FDA in order to investigate the possible loss of cell viability. Indeed, the creation of pores in the cell membrane, through the phenomenon of electroporation, which is a function of temperature, intensity of the applied electric field, number of pulses, pulse shape, type of tissue etc. (Buckow et al., 2013), may lead to irreversible damages causing loss of cell viability.

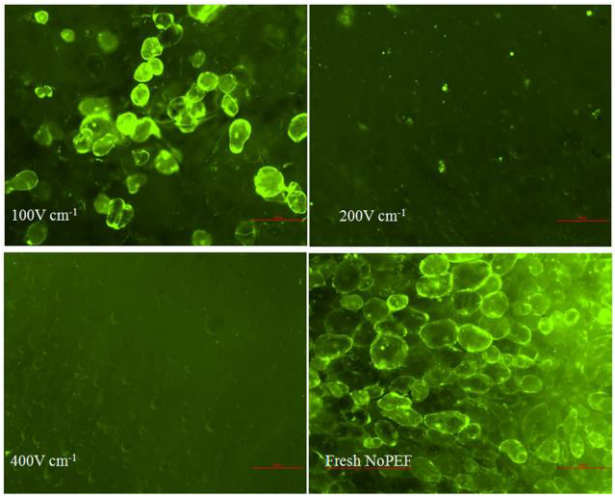

Fig. 4. Microscopy images of fresh strawberry tissue and after the PEF treatment followed by staining with FDA.

In order to determine the threshold of irreversible electroporation, Dellarosa et al. (2016 b) measured the metabolic heat production and the respiration rate of apple cylinders subjected to 100, 250 and 400 V cm^{-1}. The authors found that the medium and the high applied voltages promoted a drastic loss of cell viability that was attributed to the irreversible damages of the membranes. On the other hand, the tissue treated with 100 V cm^{-1} showed metabolic indexes comparable to the fresh tissue indicating that the electroporation was only reversible and did not cause loss of cell viability. In the present experiment, although cell viability was not completely lost, strawberry samples treated with an intensity of the electric field strength of 100 V cm^{-1}, showed residual cell viability, also if much lower than the fresh sample intensity, as shown in Fig. 4. The increase of the electric field strength induced a greater structural damage, as found in samples treated at 200 and 400 V cm^{-1} where there was a complete loss of cell viability. Consequently, cell viability was maintained even after 120 min of osmotic treatment of untreated samples (data not shown). The preservation of cell viability was observed also by Mauro et al. (2016) after 120 min in 40 % of sucrose solution. In the Mauro's study when 30% sucrose + 3 % of calcium lactate was used the cell viability was also preserved, while increasing quantity of calcium lactate up to 4% in 40% of sucrose compromised the cell viability. However, in the present study, only 1 % of calcium lactate was used, therefore this parameter was not affected by OD process, but just by PEF pre-treatment. Moreover, the PEF treated samples at 100 V cm^{-1} partially preserved their viability also after OD process (data not shown), while samples treated with higher E were not further investigated, due to the viability loss following PEF treatment. Therefore, with the aim of increasing the shelf-life of an organic product, characterized by quality parameters as close as possible to the fresh one, the lowest electric field strength applied in the tested range seems to be the suitable.

3.4 Colour

Table 2 shows the L* and hue angle (h°) values of untreated and PEF treated strawberry tissues subjected to osmotic dehydration for 120 min in both solutions. L* parameter of untreated samples did not change during the whole OD treatment. Similar results were obtained by Nuñez-Mancilla et al. (2013) who did not notice any variation of the L* parameter in strawberry samples subjected to the OD process, while this parameter was influenced significantly by the application of high hydrostatic pressure.

The luminosity of the samples resulted to be affected by the electric field intensity. In fact, this parameter increased significantly after the application of PEF at the intensity of 100 V cm^{-1}, while decreased due to the application of PEF at highest field intensity.

Table 2. Colour parameters (L* - Lightness, h° - hue angle) of untreated and PEF pre-treated strawberry samples, as a function of the osmotic dehydration time in both sucrose and trehalose solutions.

OD Time	0 min	15 min	30 min	60 min	120 min
			L*		
NoPEF_S	35 ± 4 ^{b}	32 ± 6 ^{b}	40 ± 6 ^{a}	38 ± 3 ^{bc}	37 ± 4 ^{de}
PEF_100_S	42 ± 4 ^{a}	38 ± 5 ^{ab}	38 ± 3 ^{ab}	42 ± 3 ^{a}	45 ± 5 ^{a}
PEF_200_S	35 ± 1 ^{b}	35 ± 2 ^{b}	34 ± 2 ^{bc}	39 ± 2 ^{ab}	42 ± 2 ^{ab}
PEF_400_S	26 ± 2 ^{c}	42 ± 2 ^{a}	34 ± 2 ^{bc}	35 ± 2 ^{cd}	41 ± 2 ^{abc}
NoPEF_T	35 ± 4 ^{b}	37 ± 6 ^{ab}	36 ± 5 ^{abc}	37 ± 5 ^{bc}	34 ± 5 ^{e}
PEF_100_T	41 ± 4 ^{a}	35 ± 6 ^{ab}	33 ± 2 ^{c}	35 ± 3 ^{cd}	35 ± 4 ^{ce}
PEF_200_T	28 ± 3 ^{c}	30 ± 1 ^{c}	34 ± 2 ^{bc}	33 ± 2 ^{d}	39 ± 3 ^{cd}
PEF_400_T	27 ± 2 ^{c}	37 ± 4 ^{ab}	33 ± 3 ^{c}	35 ± 3 ^{cd}	38 ± 2 ^{cde}
			h°		
NoPEF_S	40 ± 2 ^{a}	36 ± 4 ^{a}	36 ± 2 ^{a}	35 ± 1 ^{a}	35 ± 2 ^{a}
PEF_100_S	35 ± 2 ^{c}	29.9 ± 0.9 ^{b}	29 ± 2 ^{cd}	29 ± 2 ^{b}	29 ± 2 ^{c}
PEF_200_S	38 ± 2 ^{ab}	29 ± 1 ^{b}	31 ± 2 ^{bc}	28 ± 1 ^{b}	25 ± 3 ^{de}
PEF_400_S	35 ± 4 ^{bc}	24 ± 1 ^{c}	27 ± 3 ^{de}	24 ± 1 ^{c}	23 ± 2 ^{e}
NoPEF_T	40 ± 1 ^{a}	37 ± 2 ^{a}	38 ± 1 ^{a}	33 ± 1 ^{a}	32.1 ± 0.7 ^{b}
PEF_100_T	35 ± 2 ^{bc}	30 ± 2 ^{b}	24 ± 2 ^{e}	24 ± 5 ^{bc}	26 ± 2 ^{d}
PEF_200_T	34 ± 3 ^{d}	28 ± 1 ^{b}	27 ± 1 ^{d}	25.5 ± 0.8 ^{c}	23 ± 2 ^{e}
PEF_400_T	36 ± 2 ^{bc}	28 ± 2 ^{b}	32 ± 3 ^{b}	28 ± 1 ^{b}	24 ± 2 ^{e}

The same letter on the same column means no significant difference by the Duncan test ($p < 0.05$).

Also, Wiktor et al. (2015) observed that the colour measurement showed unchanged or lower L* value of PEF treated samples at E=1.85 kV cm^{-1} and E=3 or E=5 kV cm^{-1}, respectively, in comparison with the untreated apple tissue. The darkening of the PEF treated samples at 400 V cm^{-1} could be related to the higher release of enzymes such as peroxidase (POD) and polyphenol oxidase (PPO) and their substrates after the electroporation of the strawberry cells membrane. In fact, Chisani et al. (2007) observed that the browning of the strawberry fruit during the storage was related to both oxidase activities. However, after 120 min of OD treatment the PEF treated samples increased their L* values, which was significantly higher in comparison to untreated ones.

Since the colour of strawberries is the mixture of red and yellow, the hue angle (h°) was also calculated and its values are reported in table 2, respectively for strawberries treated in sucrose and trehalose solution. In general OD treatment promoted a decrease of this parameter. The application of PEF promoted a further decrease of hue angle in comparison with untreated samples, which was proportional to the electric field strength applied, at least in samples dehydrated in sucrose solution. Similar results were observed by Osorio et al. (2007). The reduction of h° colorimetric parameter could be due to both solubilisation of pigments in the osmotic solution and degradation of anthocyanin induced by PEF-treatment (Fathi et al., 2011; Odriozola-Serrano et al., 2008). In samples dehydrated in trehalose not significant differences were observed among PEF-treated samples, if not for the samples treated by 100 V cm^{-1} at 30 min after OD that showed a significantly lower h° value compared to the others. Wiktor et al. (2015) observed that the effect of PEF treatment strongly depends on the raw material properties and the treatment conditions. In fact, the authors noticed the different behaviour of carrot and apple tissue subjected to electric field strength at different intensities. In both cases browning of the tissue was observed, however in carrots it was more pronounced when the low voltage treatment was applied, while in apple with high voltage.

3.5 Texture

It is well known that OD induces plasmolysis, shrinkage of the vacuole compartment, changes in size and structure of the cell walls of outer pericarp and dissolution of the middle lamella, which could be translated in decreasing of the firmness of the plant tissue (Chiralt & Talens, 2005; Panarese et al. 2012). The changes of firmness of untreated and PEF treated strawberry tissue subjected to OD treatment up to 120 min in sucrose-based solution is shown in Fig. 5. OD of untreated samples promoted a decrease of strawberry firmness, already 15 min after the treatment, and increased slightly during the OD treatment. In the present experiment, PEF pre-treatment drastically reduced the hardness of strawberry samples; further, the PEF treated samples remained below the untreated ones during the whole OD process and the effect was proportional to the electric field strength applied. Also, Taiwo et al. (2003) observed the decrease in firmness of strawberries halves treated with PEF (1200 V cm^{-1}; 350 µs) and then osmo-dehydrated for 4 hours in binary (sucrose, NaCl) solution. The reduction of firmness of PEF treated samples could be due to the alteration of the membrane permeability due to the pores creation and the rupture of internal structure, which promotes the softening of the tissue (Fincan & Dejmek, 2002; Wiktor et al., 2016).

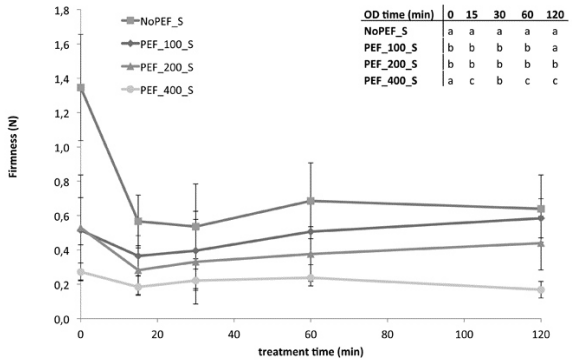

Fig. 5. Firmness (N) of untreated and PEF pre-treated strawberry samples, as a function of the osmotic dehydration time in sucrose-based solution. The same letter on the same column means no significant difference between the samples by the Duncan test ($p < 0.05$).

The slight increase of the texture observed after longer OD times could be probably due to the penetration of Ca^{2+} into the strawberry tissue. The structural role of calcium ions in the cell wall is due to their interaction with pectic acid polymers to form cross-bridges that reinforce the cell adhesion, thereby reducing cell separation, which is one of the major causes of plant tissue softening (Van Buggenhout et al., 2008; Mauro et al., 2016). This increase has not been observed in the samples treated at 400 V cm^{-1}, probably because the tissue was already completely disintegrated after the PEF treatment, and did not permit the incorporation of calcium ions in the cell walls.

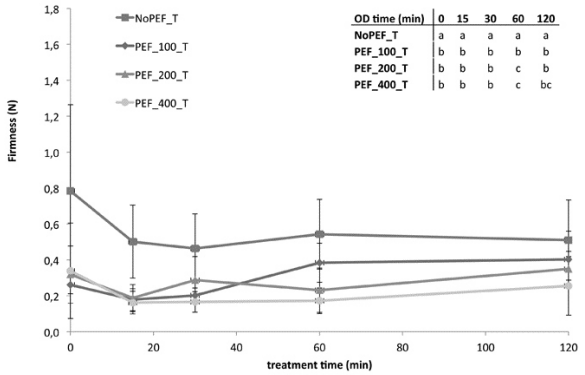

Fig. 6. Firmness (N) of untreated and PEF pre-treated strawberry samples, as a function of the osmotic dehydration time in trehalose-based solution. The same letter on the same column means no significant difference between the samples by the Duncan test ($p < 0.05$).

Similar results were observed in strawberries samples dehydrated in trehalose-based solution (Fig. 6). However, considering that the firmness of the material (0.8 ± 0.1 N) used for the experiment was almost half compared with the value relative to the raw material used in the experiment with sucrose (1.35 ± 0.2 N), the decrease of firmness following the OD process was less marked. In fact, the firmness of samples dehydrated in trehalose decreased only by 36 % in comparison to 57 % of decrease observed in sucrose dehydrated samples already 15 min after the treatment. This behaviour could probably be due to the protective effect of trehalose on the tissue structure, as reported by Phoon et al. (2008). The intensity of the applied electric field strength seems to be not so relevant in comparison to samples dehydrated with sucrose. Shayanfar et al. (2013) observed texture softening and loss of turgor in frozen/thawed potatoes after the PEF treatment. However, when $CaCl_2$ and trehalose were added to the liquid medium used in PEF treatment, the samples maintained their firmness when compared to solely PEF treated samples.

4. Conclusions

PEF treatment prior to osmotic dehydration was found to positively affect the mass transfer, in term of water loss from the strawberry tissue. The application of the lowest electric field intensity (100 V cm^{-1}) resulted already sufficient to increase the water loss by 12 % and 6%, after one hour of osmotic dehydration, respectively for strawberries dehydrated in sucrose and trehalose solution, partially preserving the cell viability and maintaining at the same time the fresh-like characteristics of fruits. Concerning the solid gain results, while the solid gain was favoured by the application of all the PEF intensities in samples dehydrated in sucrose solution, the treatment at 200 and 400 V cm^{-1} reduced the trehalose uptake due to a lower initial mass transfer rate. In most of the cases, the PEF effect on different strawberry characteristics investigated was proportional to the electric field strength applied.

TD-NMR results showed that the diffusion of inner water was eased by PEF application because of a marked effect on membranes permeability. Although similar effects on the investigated parameters were observed by using sucrose or trehalose solutions, the combination of PEF with trehalose allowed to obtain a higher dewatering effect without increasing solute uptake or even reducing it. Definitely, the application of the lower field intensity and the use of trehalose for the dehydration process, seem to be the optimal combination for obtaining a semi-dried strawberry product with quality characteristics similar to the fresh one, that is a fundamental requirement for an organic production.

REFERENCES

Ade-Omowaye, B., Talens, P., Angersbach, A., & Knorr, D. (2003). Kinetics of osmotic dehydration of red bell peppers as influenced by pulsed electric field

pretreatment. *Food Research International,* 36(5), 475–483.

Amami, E., Fersi, A., Vorobiev, E., & Kechaou, N. (2007). Osmotic dehydration of carrot tissue enhanced by pulsed electric field, salt and centrifugal force. *Journal of Food Engineering,* 83(4), 605-613.

Amami, E., Vorobiev, E., & Kechaou, N. (2006). Modelling of mass transfer during osmotic dehydration of apple tissue pre-treated by pulsed electric field. *LWT - Food Science and Technology,* 39, 1014–1021.

Angersbach, A., Heinz, V., & Knorr, D. (2002). Evaluation of process-induced dimensional changes in the membrane structure of biological cells using impedance measurement. *Biotechnology Progress,* 18(3), 597–603.

AOAC International (2002). Official methods of analysis (OMA) of AOAC International (17th ed.) [USA. Method number: 920.15].

Atarés, L., Chiralt, A., & González-Martínez, C. (2008). Effect of solute on osmotic dehydration and rehydration of vacuum impregnated apple cylinders (cv. Granny Smith). *Journal of Food Engineering,* 89(1), 49-56.

Badawy, M.E.I., Rabea, E.I., El-Nouby, M.A.M., Ismail, R.I.A., & Taktak, N.E.M. (2016). Strawberry Shelf Life, Composition, and Enzymes Activity in Response to Edible Chitosan Coatings. *International Journal of Fruit Science,* In press.

Barański, M., Średnicka-Tober, D., Volakakis, N., Seal, Ch., Sanderson, R., Stewart, G. B., Benbrook, Ch., Biavati, B., Markellou, E., Giotis, Ch., Gromadzka-Ostrowska, J., Rembiałkowska, E., Skwarło-Sońta K., Tahvonen, R., Janovská, D., Niggli, U., Nicot, P., & Leifert, C. (2014). Higher antioxidant and lower cadmium concentrations and lower incidence of pesticide residues in organically grown crops: a systematic literature review and meta-analyses. *British Journal of Nutrition,* 112, 794–811.

Barba, F.J., Parniakov, O., Pereira, S.A., Wiktor, A., Grimi, N., Boussetta, N., Saraiva, J., Raso, J., Martin-Belloso, O., Witrowa-Rajchert, D., Lebovka, N., & Vorobiev, E. (2015). Current applications and new opportunities for the use of pulsed electric fields in food science and industry. *Food Research International,* 77(4), 773–798.

Borgia, G.C., Brown, R.J.S., & Fantazzini, P. (1998). Uniform-penalty inversion of multiexponential decay data. *Journal of Magnetic Resonance,* 132(1), 65-77.

Buckow, R., Ng, S., & Toepfl, S. (2013). Pulsed electric field processing of orange juice: a review on microbial, enzymatic, nutritional, and sensory quality and stability. *Comprehensive Reviews in Food Science and Food Safety,* 12(5), 455-467.

Castelló, M.L., Fito, P.J., & Chiralt, A. (2010). Changes in respiration rate and physical properties of strawberries due to osmotic dehydration and storage. *Journal of Food Engineering,* 97(1), 64–71.

Cheng, X.F., Zhang, M., Adhikari, B., & Islam, M.N. (2014). Effect of Power Ultrasound and Pulsed Vacuum Treatments on the Dehydration Kinetics, Distribution, and Status of Water in Osmotically Dehydrated Strawberry: a Combined NMR and DSC Study. *Food and Bioprocess Technology, 7*(10), 2782-2792.

Chiralt A., & Talens P. (2005). Physical and chemical changes induced by osmotic dehydration in plant tissues. *Journal of Food Engineering*, 67(1-2), 167–177.

Chisari, M., Barbagallo, R. N., & Spagna, G. (2007). Characterization of Polyphenol Oxidase and Peroxidase and Influence on Browning of Cold Stored Strawberry. *J. Agric. Food Chem., 55, 3469−3476.*

Dellarosa, N., Ragni, L., Laghi, L., Tylewicz, U., Rocculi, P., & Dalla Rosa, M. (2016a). Time domain nuclear magnetic resonance to monitor mass transfer mechanisms in apple tissue promoted by osmotic dehydration combined with pulsed electric fields. *Innovative Food Science & Emerging Technologies,* 37, Part C, 345-351.

Dellarosa, N., Tappi, S., Ragni, L., Laghi, L., Rocculi, P., & Dalla Rosa, M. (2016b). Metabolic response of fresh-cut apples induced by pulsed electric fields. *Innovative Food Science and Technologies,* 38, 356-364.

Dermesonlouoglou, E., Zachariou, I., Andreou, V., & Taoukis, P.S. (2016). Effect of pulsed electric fields on mass transfer and quality of osmotically dehydrated kiwifruit. *Food and Bioproducts Processing,* 100, Part B, 535-544.

Fathi, M., Mohebbi, M., & Razavi, A.M.S. (2011). Application of image analysis and artificial neural network to predict mass transfer kinetics and color changes of osmotically dehydrated kiwifruit. *Food Bioprocess Technology,* 4(8), 1357–1366.

Ferrando, M., & Spiess, W.E.L. (2001). Cellular response of plant tissue during the osmotic treatment with sucrose, maltose, and trehalose solutions. *Journal of Food Engineering,* 49(2), 115-127.

Fincan, M., & Dejmek P. (2003). Effect of osmotic pretreatment and pulsed electric field on the viscoelastic properties of potato tissue. *Journal of Food Engineering,* 59(2–3), 169-175.

Gamboa-Santos, J., Montilla, A., Soria, A.C., Cárcel, J.A., García-Pérez, J.V., & Villamiel, M. (2014). Impact of power ultrasound on chemical and physicochemical quality indicators of strawberries dried by convection. *Food Chemistry,* 161, 40–46.

Kadivec, M., Tijskens, L.M.M., Kopjar, M., Simčič, M., & Požrl, T. (2016). Modelling the Colour of Strawberry Spread During Storage, Including Effects of Technical Variations. *Polish Journal of Food and Nutrition Sciences,* 66(4), 271–276.

Mauro, M.A, Dellarosa, N, Tylewicz, U., Tappi, S., Laghi, L, Rocculi, P. & Dalla Rosa, M. (2016). Calcium and ascorbic acid affect cellular structure and water mobility in apple tissue during osmotic dehydration in sucrose solutions. *Food Chemistry,* 195, 19-28.

Meiboom, S., & Gill, D. (1958). Modified spin-echo method for measuring nuclear relaxation times. *Review of Scientific Instruments, 29(8), 688–691.*

Nuñez-Mancilla, Y., Pérez-Won, M., Uribe, E., Vega-Gálvez, A. & Di Scala, K. (2013). Osmotic dehydration under high hydrostatic pressure: Effects on antioxidant activity, total phenolics compounds, vitamin C and colour of strawberry (Fragaria vesca). *LWT - Food Science and Technology 52, 151-156.*

Odriozola-Serrano, I., Soliva-Fortuny, R., & Martın-Belloso, O. (2008). Phenolic acids, flavonoids, vitamin C and antioxidant capacity of strawberry juices processed by high-intensity pulsed electric fields or heat treatments. *European Food Research and Technology,* 228, 239-248.

Osorio, C., Franco, M.S., Castano, M.P., Gonzalez-Miret, M.L., Heredia, J.F., & Morales, L.A (2007). Colour and flavor changes during osmotic dehydration of fruit. *Innovative Food Science and Emerging Technologies,* 8, 353-359.

Panarese, V., Laghi, L., Pisi, A., Tylewicz, U., Dalla Rosa, M., & Rocculi, P. (2012). Effect of osmotic dehydration on Actinidia deliciosa kiwifruit: A combined NMR and ultrastructural study. *Food Chemistry,* 132, 1706–1712.

Peleg, M. (1988). An empirical model for the description of moisture sorption curves. *Journal of Food Science,* 53, 1216–1217.

Phoon, P. Y., Galindo, F. G., Vicente, A., Dejmek, P. (2008). Pulsed electric field in combination with vacuum impregnation with trehalose improves the freezing tolerance of spinach leaves. *Journal of Food Engineering, 88(1), 144–148.*

Shayanfar, S., Chauhan, O. P., Toepfl, S., & Heinz, V. (2013). The interaction of pulsed electric fields and texturizing — antifreezing agents in quality retention of defrosted potato strips. *International Journal of Food Science & Technology,* 48(6), 1289–1295.

Taiwo, K.A., Eshtiaghi, M.N., Ade-Omowaye, B.I.O., & Knorr, D. (2003). Osmotic dehydration of strawberry halves: influence of osmotic agents and pretreatment methods on mass transfer and product characteristics. *International Journal of Food Science and Technology,* 38, 693–707.

Taiwo, K.A., Angersbach, A., & Knorr D. (2002). Influence of high intensity electric field pulses and osmotic dehydration on the rehydration characteristics of apple slices at different temperatures. *Journal of Food Engineering,* 52(2), 185-192.

Traffano-Schiffo, M.V., Tylewicz U., Castro-Giraldez, M., Fito P.J. , Ragni L., & Dalla Rosa M. (2016). Effect of pulsed electric fields pre-treatment on mass transport during the osmotic dehydration of organic kiwifruit. *Innovative Food Science & Emerging Technologies,* 38, Part A, 243–251.

Tylewicz, U., Panarese, V., Laghi, L., Rocculi, P., Nowacka, M., Placucci, G., & Dalla Rosa, M. (2011). NMR and DSC Water Study during Osmotic Dehydration of Actinidia deliciosa and A. chinensis kiwifruit. *Food Biophysics,* 6(2), 327-333.

Tylewicz, U., Romani, S., Widell, S., & Gómez Galindo, F. (2013). Induction of Vesicle Formation by Exposing Apple Tissue to Vacuum Impregnation. *Food and Bioprocess Technology,* 6(4), 1099-1104.

Van Buggenhout, S., Grauwet, T., Van Loey, A., & Hendrickx, M. (2008). Use of pectinmethylesterase and calcium in osmotic dehydration and osmodehydrofreezing of strawberries. *European Food Research and Technology,* 226, 1145–1154.

Vega-Gálvez, A., Ah-Hen, K., Chacana, M., Vergana, J., Martínez-Monzó, J., García-Segovia, P., Lemus-Mondaca, R., & Di Scala, K. (2012). Effect of temperature and air velocity on drying kinetics, antioxidant capacity, total phenolic content, colour, texture and microstructure of apple (var. Granny Smith) slices. *Food Chemistry,* 132(1), 51-59.

Velickova, E., Winkelhausen, E., Kuzmanova, S., Alves, V.D., & Moldão-Martins, M. (2013). Impact of chitosan-beeswax edible coatings on the quality of fresh strawberries (*Fragaria ananassa cv Camarosa*) under commercial storage conditions. *LWT - Food Science and Technology, 52*, 80-92.

Vicente, S., Nieto, A. B., Hodara, K., Castro, M. A., & Alzamora, S. M. (2012). Changes in structure, rheology, and water mobility of apple tissue induced by osmotic dehydration with glucose or trehalose. *Food and Bioprocess Technology,* 5(8), 3075-3089.

Wiktor, A., Gondek, E., Jakubczyk, E., Nowacka, M., Dadan, M., Fijalkowska, A., & Witrowa-Rajchert, D. (2016). Acoustic emission as a tool to assess the changes induced by pulsed electric field in apple tissue. *Innovative Food Science and Emerging Technologies*, 37, 375–383.

Wiktor, A., Sledz, M., Nowacka, M., Rybak, K., Chudoba, T., Lojkowski, W., & Witrowa-Rajchert, D. (2015). The impact of pulsed electric field treatment on selected bioactive compound content and color of plant tissue. *Innovative Food Science and Emerging Technologies,* 30, 69–78.

Paper X

Dellarosa, **N.**, Laghi, L., Ragni, L., Dalla Rosa, M., Alecci, M., Florio, T. M., & Galante, A. (2017)

Pulsed electric fields processing of apple tissue: spatial distribution of electroporation

Innovative Food Science & Emerging Technologies, Under review

Pulsed electric fields processing of apple tissue: spatial distribution of electroporation

Nicolò Dellarosa[a], Luca Laghi[a,b], Luigi Ragni[a,b], Marco Dalla Rosa[a,b], Marcello Alecci[c,d], Tiziana Marilena Florio[c,d], Angelo Galante[c,d]

[a] *Department of Agricultural and Food Sciences, University of Bologna, Cesena, Italy*

[b] *Interdepartmental Centre for Agri-Food Industrial Research, University of Bologna, Cesena, Italy*

[c] *Department of Life, Health and Environmental Sciences, University of L'Aquila, L'Aquila, Italy*

[d] *National Institute for Nuclear Physics, Gran Sasso National Laboratory, Assergi, Italy*

Corresponding author: Luca Laghi (l.laghi@unibo.it)

Keywords: PEF; Magnetic resonance imaging, Computer vision system; Vacuum impregnation; Electric field distribution

ABSTRACT

Food industry takes advantage of pulsed electric fields (PEF) technology to assist mass transfer processes, however, the optimal application depends on the effectiveness of the induced electroporation. The present work aimed at exploring the application of magnetic resonance imaging (MRI), aided with a contrast agent, combined with computer vision system (CVS) analysis to assess the spatial distribution of electroporation in apple tissue. PEF-treated apple samples were compared with dipping and vacuum impregnation to gain insight into mechanisms that lead to microstructural modifications. CVS results described the heterogeneously distributed enzymatic browning as a consequence of irreversible electroporation. Accordingly, the MRI analysis of transverse relaxation time through the apple tissue confirmed the inhomogeneous distribution and extent of the cell disruption while longitudinal relaxation time weighted images enabled monitoring the migration of the intracellular content.

Industrial relevance: The novel applications of pulsed electric fields require fast and reliable methods to detected and estimate the breakage of the membranes integrity in order to boost their industrial adoption and optimization. The present study provided analytical tools able to monitor the spatial distribution of electroporation in plant tissue within minutes and consequentially to speed up and improve the assessment of the impact of different PEF treatments.

1. Introduction

Pulsed electric field (PEF) technology is an innovative process with a growing interest in the food sector for many potential purposes, mainly related to the microbial inactivation and the enhancement of mass transfer. The application of high electric fields induces the breakage of plasma membranes, also known as electroporation, which can be exploited to increase the efficiency of several food processes, for instance juice extraction (Praporscic, Lebovka, Vorobiev, & Mietton-Peuchot, 2007), air and osmotic dehydration (Traffano-Schiffo et al., 2016; Wiktor et al., 2013) or extraction of valuable compounds (Luengo, Condón-Abanto, Condón, Álvarez, & Raso, 2014; Parniakov et al., 2015). In general, when the electric field exceeds a critical value, membranes break down and, whether the field strength is largely higher than such threshold, electroporation becomes irreversible (Donsì, Ferrari, & Pataro, 2010). In fact, the extent of electroporation is strongly affected by several treatment parameters, therefore their accurate control is fundamental for the correct implementation of PEF in food industry. Particularly, electric field strength, shape, duration, number and frequency of pulses have an effect on electroporation (Barba et al., 2015).

Screening methods based on several physical approaches have been proposed to directly estimate the extent of electroporation, especially in its irreversible form and consequentially to optimize the novel industrial PEF applications. Those procedures include the evaluation of the impedance (Lebovka, Bazhal, & Vorobiev, 2002), optical (Fincan & Dejmek, 2002), acoustic (Wiktor, Sledz, Nowacka, Rybak, & Witrowa-Rajchert, 2016) or magnetic (Dellarosa, Ragni, et al., 2016) properties of the plant material. Furthermore, the assessment of effects induced by electroporation, for instance changes of colour and texture (Lebovka, Praporscic, & Vorobiev, 2004), release of specific compounds (Luengo, Álvarez, & Raso, 2013) or metabolic consequences (Dellarosa, Tappi, et al., 2016), aims at indirectly evaluating the extent of electroporation by means of appreciable variations of relevant food features.

The abovementioned tools have demonstrated to be able to quantitatively detect the effects of electroporation in various matrices, but they are not capable to monitor its distribution through the treated tissue. Indeed, the assessment of the spatial distribution of the electric field strength is fundamental to assure the effectiveness of the process, especially when the enhancement of mass transfer is the main target of the PEF treatment. Generally, two approaches are considered and often combined to overcome this lack of knowledge. On one hand, the simulation of the process by means of finite element methods is particularly tailored to design the treatment chambers for liquids (Buckow, Schroeder, Berres, Baumann, & Knoerzer, 2010), on the other hand, the use of non-destructive techniques, such as magnetic resonance imaging (MRI), can provide indirect information to spatially characterized the electroporation through solid plant tissues. In the latter case, a recent innovative work in potato (Kranjc, Bajd, Serša, de Boevere, & Miklavčič, 2016) showed that magnetic resonance electrical impedance tomography technique can detect the electric field distribution during the application of the pulses while quantitative information on the induced membrane breakage could be obtained by observing the modification of the transverse relaxation time.

The present work aimed at exploring the spatial distribution of electroporation in apple tissue by combining computer vision system (CVS) analysis with magnetic resonance imaging (MRI) methods. PEF treatment parameters (60 pulses, 10 µs pulse width, 100 Hz, from 100 to 400 V/cm) were chosen according to earlier studies in apple (Dellarosa, Ragni, et al., 2016; Dellarosa, Tappi, et al., 2016) to obtain reversibly and irreversibly electroporated apple samples. MRI analysis was aided with the employment of a contrast agent solution which demonstrated to be unable to passively diffuse through the native intact plasma membranes, therefore until membranes electroporation took place (Dellarosa, Ragni, et al., 2016). A prior optimization step was required to establish suitable MRI sequences and parameters in order to both maximize the spatial resolution and simultaneously reducing the experimental time to few minutes. This led to observe kinetic alterations of apple tissue as function of the electroporation from 5 to 60 minutes after PEF treatments. Afterward, to finely understand the effects of pulsed electric fields on mass transfer mechanisms, two different MR images, based on both longitudinal and transverse relaxation time (T_1 and T_2), were acquired. Those were also compared to untreated dipped apple tissue and vacuum impregnated samples (Donker, Van As, Snijder, & Edzes, 1997) in order to clarify the tissue alterations induced by the application of PEF technologies.

2. Material and methods

2.1 Raw material

Apples (*Malus domestica*, cv Cripps Pink) were acquired at a local market and stored at 2 ± 1 °C for no longer than 6 weeks until utilization. The average moisture and soluble solid contents of apples were, respectively, 85.2 ± 0.3 g and 12.6 ± 0.3 g per 100 g of fresh product (g_{fw}). Parenchyma apple tissue was manually cut with a cork borer and a sharp knife to obtain cylindrical samples of 14 mm diameter and 25 mm length.

2.2 Pulsed electric field (PEF) treatments and samples processing

Pulsed electric field (PEF) treatments were applied to the samples by means of an in-house developed pulse generator based on MOSFET technology. The equipment provides monopolar pulses of near-rectangular shape at adjustable voltages, pulse width, frequency and treatment duration, thus resulting in a variable number of delivered pulses and energy input, consequentially. Treatments were run at 25 °C within a chamber equipped with two stainless steel electrodes with an active contact surface of 20 × 20 mm^2 and a distance between them fixed at 30 mm. Each treatment included the placement of an apple cylinder into the chamber with the two circle sides parallel to the electrodes. The chamber was filled up with tap water, with an electrical conductivity of 314 ± 4 µS/cm at 25 °C. The process parameters were chosen according to previous experiments (Dellarosa, Ragni, et al., 2016). Briefly, 300, 750 and 1200 V were applied to give rise to an average electric field strengths between the electrodes of 100, 250 and 400 V/cm, respectively. Pulse width was fixed at 100 ± 2 µS, repetition time at 10.0 ± 0.1 ms (100 Hz) and 60 pulses were delivered in each treatment. The current and voltage values were monitored using a digital oscilloscope (PicoScope 2204a, Pico Technology, UK) connected to the PEF generator and a personal computer.

After PEF treatments, samples were removed from the treatment chamber and immersed into an isotonic sucrose solution for 60 min, during which the analysis were carried out. Apple cylinders used for magnetic resonance imaging analysis were immersed into an isotonic sucrose solution containing also 0.01 M iron (III) chloride, as contrast agent. The total amount of iron was determined after 60 min from the immersion in apple samples using the method described by Adams (1995). Briefly, 0.1-0.5 g of freeze dried samples were dissolved in 10 mL of 2.0 M HCl. After 5 min, 1 mL of

filtered (0.45 µm) supernatant was collected, mixed with 1 mL of 1.5 M KSCN and the absorbance at 480 nm was obtained (UV-1601, Shimadzu, Japan) . A 5-points calibration curve was built using iron (III) chloride to obtain concentrations spanning from 0.1 to 1 mM, which resulted in a coefficient of determination R^2 = 0.997; the analysis was performed in triplicate.

2.3 Dipping and vacuum impregnation (VI) treatments, as references

Dipping into the isotonic solution (with the contrast agent for MRI analysis) up to 60 min was chosen as control for untreated apple cylinders. A vacuum impregnation treatment was used as further reference and compared to PEF treatments. According to Betoret et al. (2012), samples were immersed into an isotonic solution, containing the contrast agent, and a single vacuum step at 60 ± 10 mbar was applied for 10 min before restoring the atmospheric pressure for 60 min.

2.4 Computer vision system (CVS)

Apple cylinders were removed from the isotonic solution after 15, 30, 45 and 60 min from PEF treatments, split into two equal parts and directly acquired by the computer vision system. Digitalized images were obtained by introducing the samples inside a black box under controlled lighting condition with a digital camera D7000 (Nikon, Shinjuku, Japan) equipped with a 105-mm lens AF-S VR Micro-Nikkor (Nikon, Shinjuku, Japan). Images were acquired at 16.2 megapixels with fixed exposition time 1/8 s, F-stop f/8 and ISO 100. At least 18 apple cylinders for each electric field strength were sampled along with dipping, as control. Digitalized images were manually pre-elaborated by using GIMP 2.8 software to obtain a centred circular region of interest (ROI) of 500-pixels diameter. ImageJ was lately employed to understand the effect of electroporation on the browning kinetic by evaluating L, a, and b parameters of the CIELab colour space. A 16 colours Lookup table (LUT) was finally applied to each parameter of the colour space in order to illustrate the spatial distribution of L a b changes upon treatments through the tissue. Nevertheless, in this respect, it needed to be state that CIELab values calculated from the computer vision system can differ from those obtained by official methods based on tristimulus colorimeters due to the different acquisition tools. Variations of L, a and b values, in the present work, should be considered only in a relative scale by comparing PEF treated and untreated samples.

2.5 Magnetic resonance imaging (MRI)

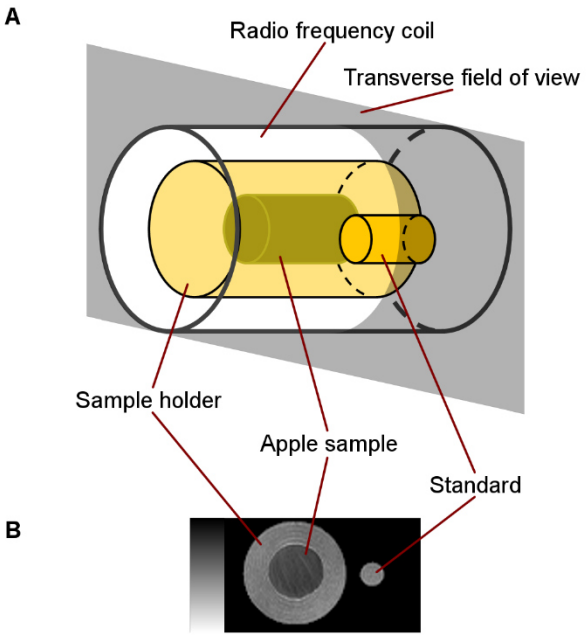

Fig. 1. Experimental setup: schematic layout (A) and example of a raw acquired MR image (B).

Apple samples that underwent to MRI analysis included PEF pre-treatment at 400 V/cm along with vacuum impregnation and dipping samples, as references. Fig. 1 displays the experimental setup used for the MRI trials and an example of acquired MR image. Briefly, each apple cylinder was fixed in the centre of a 50 mL falcon tube that was filled up with the isotonic solution containing the contrast agent. A 0.5 mL falcon tube filled up exclusively with the isotonic solution containing the contrast agent was placed aside, as external standard, in order to appear in the same field of view (FOV). MRI experiments were carried out using a 2.35 T (100 MHz proton frequency) MRI scanner (Bruker, Germany) equipped with a DOTY radio frequency birdcage coil with an internal diameter of 62 mm. An asymmetric 2D FOV of 125.7 × 31.4 mm^2 (256 × 64 pixels, i.e. spatial resolution = 0.491 mm/pixel) with 3 mm slice thickness was chosen to acquire MR images using a Multi Slice Multi Echo (MSME) pulse sequence. Such sequence gives rise to signal decays described by the equation (1):

$$S = \rho\left(1 - exp^{\frac{-TR}{T_1}}\right) exp^{\frac{-TE}{T_2}} \qquad (1)$$

where, ρ is the proton density, T_1 and T_2 are the longitudinal and transverse relaxation time, respectively, while TR and TE (repetition and echo time, respectively) are two adjustable MSME acquisition parameters. Each MR sequence included 52 equally spaced echoes with a fixed TE = 9.23 ms. Two TR values were chosen in order to acquire T_1-weigthed images (TR = 1,000 ms)

and, on the other hand, images where the effect of T_1 was negligible, i.e. governed by ρ and T_2 only (TR = 10,000 ms). The optimization of the two MRI analysis resulted in relatively short total time of acquisition: approximately 1 min for the former analysis and 8 min for the latter one. Finally, raw data, which was function of the 2D spatial coordinates and time, was fitted by means of in-house developed R script (R Foundation for Statistical Computing, Austria) based on the 'Levenberg–Marquardt nonlinear least-squares' algorithm. In order to compare apple samples treated with the different technologies, T_1-weigthed images were scaled by fixing the average intensity of the external standard at 0.5.

2.6 Statistical analysis

Significant differences between the treatments were studied by means of analysis of variance (ANOVA), followed by Tukey's multiple comparisons, implemented in R statistical software, at the significance level of 95% ($p < 0.05$). All the experiments were repeated at least three times and results were expressed as mean ± standard deviation of replications.

3. Results and discussion

3.1 Visual changes detected by computer vision system

Computer vision system analysis was focused on three electric fields strength levels which included PEF treatments at 100, 250 and 400 V/cm (60 pulses, 10 µs pulse width, 100 Hz) beside a control sample, i.e. dipped into an isotonic solution without pre-treatments. Fig. 2 illustrates kinetic results of the three CIELab parameters arisen from image analysis and examples of their spatial distribution throughout the 500-pixels region of interest. Untreated apple samples (time = 0) showed CIE values equal to L = 82.0 ± 0.2, a = -1,9 ± 0.1 and b = 25.8 ± 0.6. Dipping in isotonic solution did not affect those values significantly during 60 min after the immersion as well as PEF pre-treatment at 100 V/cm. At that electric field strength, previous works (Dellarosa, Ragni, et al., 2016; Dellarosa, Tappi, et al., 2016) demonstrated that electroporation occurred only in its reversible form. In that papers, the redistribution of water within subcellular organelles enhanced mass transfer, however, the present work highlighted no change in the visual quality. These two features promote the employment of low electric field strength levels whenever PEF is adopted to increase mass transfer in processes where any alteration of sensorial qualities is undesirable, as in the case of fresh-cut productions.

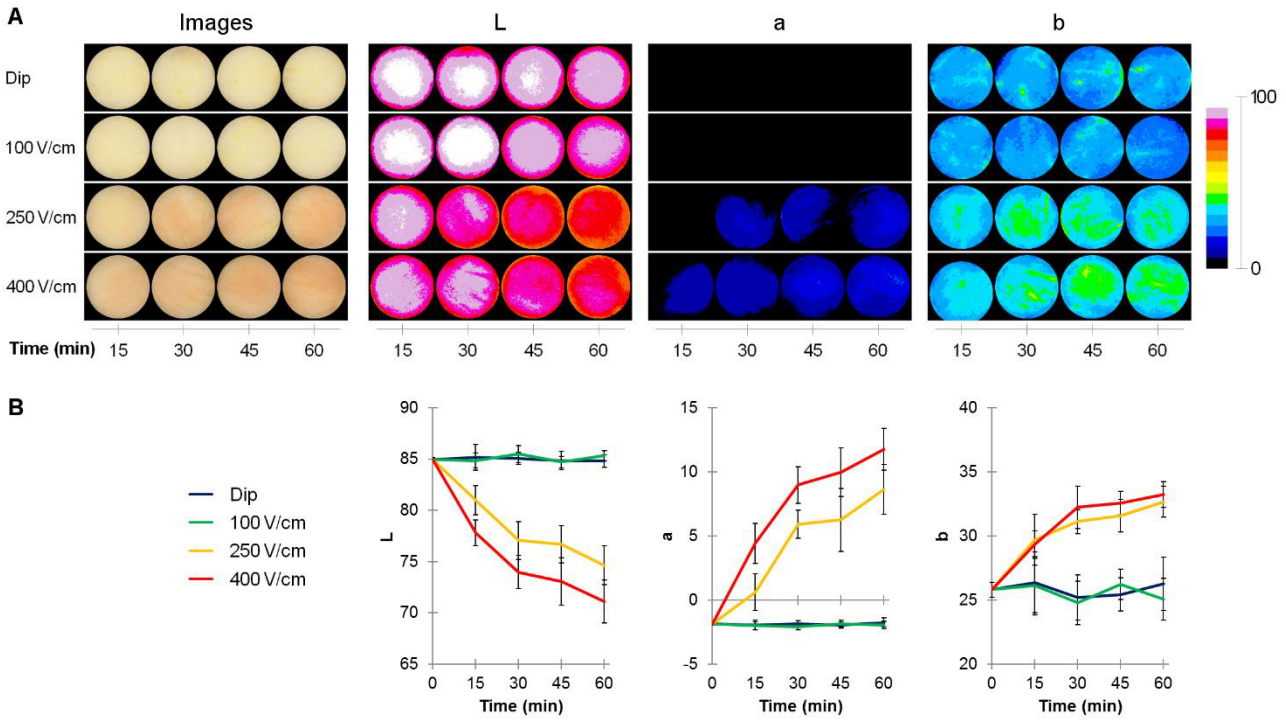

Fig. 2. Computer vision system analysis of dipping (Dip) and pulsed electric field (PEF) treatments sampled after 15, 30, 45 and 60 from treatments. Examples of digitalized images and L, a, b channels distributions through the apple tissue (A); mean values ± standard deviation (n=18) of L, a, b parameters (B).

On the contrary, a marked browning of the apple tissue was observed immediately after PEF treatments at 250 and 400 V/cm. Since the first sampling point, i.e. 15 min after PEF treatments, significant changes in all CIELab parameters were achieved, furthermore, kinetic behaviours were noticed throughout the observation time. The browning resulted in a lower luminosity (L value) while redness (a value) and yellowness (b value) simultaneously increased. Those PEF parameters induced irreversible electroporation of membranes with the consequent loss of compartmentalization and release of the intracellular content. This included the leakage of intracellular enzymes, i.e. polyphenol oxidase (PPO), which promoted the oxidation of phenolic molecules leading to the enzymatic browning (Rocha & Morais, 2003).

The two highest electric fields (250 and 400 V/cm) differentially influenced the browning kinetics taking into account both L and a values throughout the first hour after treatments. The different extent of the enzymatic process was a function of the applied energy, suggesting that colour changes can be considered as an index of the extent of irreversible electroporation. This confirmed previous findings which proved that mass transfer and metabolic response were significantly affected by the increasing of the electric field from 250 to 400 V/cm even though irreversible electroporation took place at both electric field strength levels (Dellarosa, Ragni, et al., 2016; Dellarosa, Tappi, et al., 2016). It worth highlighting that those PEF treatments gave rise to inhomogeneous colour changes spatially distributed through the apple tissue, especially monitored as a and b values distribution. The source of inhomogeneity can be ascribed to the different local conductivity of the apple parenchyma and the heterogeneous electric field distribution within the tissue. In fact, in a previous study Kranjk et al. (2016) found an asymmetric distribution of the electric field in potato tubers not predicted by the numerical simulation. In the present work, parallel plates were used instead of needle electrodes so that a homogeneous distribution was expected according to the literature (Raso et al., 2016). Moreover, the tissue pieces, which were cut and underwent to CSV analysis, laid in parallel within the two plate electrodes of the treatment chamber in order to prevent further field inhomogeneity during treatments. Consequentially, the main origin of the heterogeneous electric field distribution was ascribed to the local differences in conductivity of the material. According to Lebovka et al. (2002), conductivity usually increases upon irreversible PEF treatments due to the cell damage which induces the redistribution of water and solutes within apple tissue. This changes, however, were not uniformly distributed and the differences became more evident at the highest electric field strength applied. In order to clarify spatially distributed alterations of the tissue microstructure, the effect of the highest energy PEF pre-treatment (400 V/cm, 60 pulses, 10 µs pulse width, 100 Hz) in apple tissue was investigated by MRI analysis.

3.2 Distribution of electroporation explored by magnetic resonance imaging

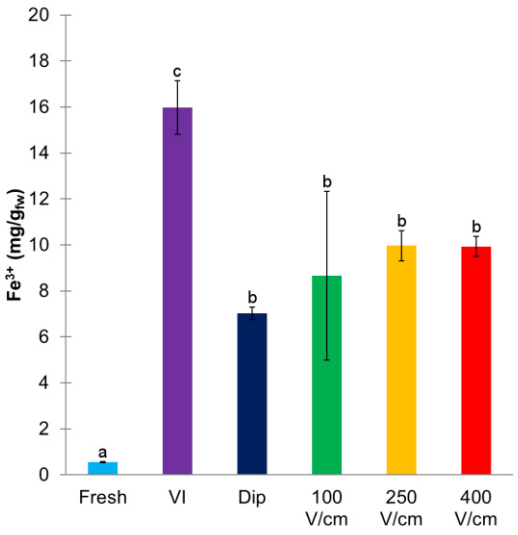

Fig. 3. Concentration of Fe3+ in apple cylinders after 60 minutes from vacuum impregnation (VI), dipping (Dip) and pulsed electric fields (PEF) treatments at various electric field strength along with fresh apple control (Fresh); results were expressed as mean values ± standard deviation (n=3).

Multiparametric magnetic resonance imaging provides an overview of the membranes breakage since longitudinal (T_1) and transverse (T_2) relaxation time values have been demonstrated to be directly affected by electroporation (Hjouj & Rubinsky, 2010). In the present work, a $FeCl_3$ rich contrast agent solution was adopted to enhance the differences of T_1 and T_2 values between apple samples and the surrounding solution. That solution was unable to passively diffuse through the tissue as confirmed by the spectrophotometric measurement of the Fe^{3+} concentration. Fig. 3 shows results of its concentration after 60 minutes from the treatments along with a fresh apple control. The Fe^{3+} concentration in apple samples dipped in the contrast solution, including those pre-treated by PEF at any electric field strength, spanned from 7 to 10 mg per g of sample with no significant differences among them. However, those values were far higher than the native concentration of the ion (< 1 mg per g of fresh apple) and significant lower than apple tissue subjects to prior vacuum impregnation (16.0 ± 1.2 mg per g of fresh apple). Indeed, vacuum impregnation is a recognized highly effective tool to enrich porous tissues by

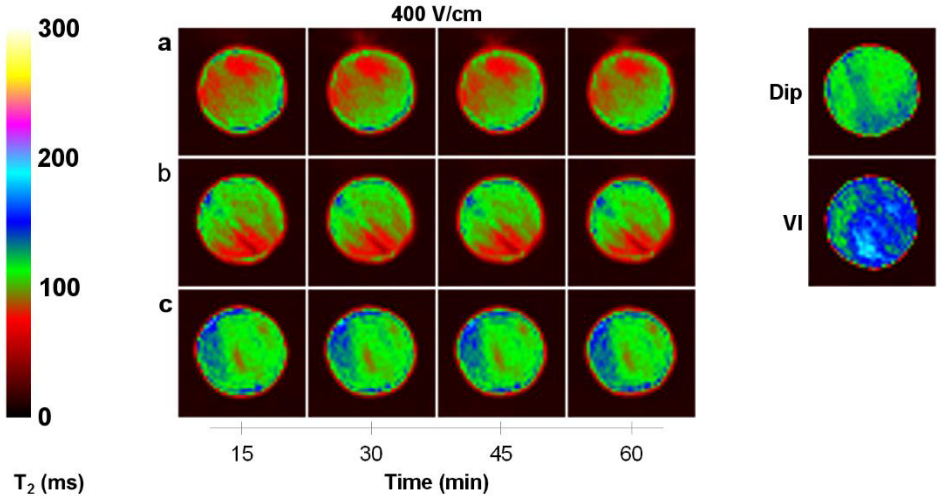

Fig. 4. T_2-maps of three apple cylinders treated with pulsed electric fields (PEF) at 400 V/cm (60 pulses, 10 µs pulse width, 100 Hz) and sampled 15, 30, 45 and 60 min after treatments; examples of dipping (Dip) and vacuum impregnation (VI) samples after 60 min from the treatments.

replacing the inner air with an external solution (Zhao & Xie, 2004). Conversely, within the observation time (60 min), PEF pre-treatment and dipping showed similar results. Such scores suggested that the entrance of the external solution was not eased by the application of external electric fields and the increase of the concentration of Fe^{3+} was probably ascribable to surface phenomena only.

The impact of electroporation in apple tissue was successfully detected by observing the modification of T_2 values. Fig. 4 illustrates the T_2-maps of three PEF-treated samples at 400 V/cm during 60 min after treatments and their immersion into the contrast solution. In general, T_2 decreased immediately after treatment, showing consistent values throughout the observation time, lately. On average, apple samples only dipped into the contrast solution showed a T_2 value equals to 125±10 ms. That value dropped when electroporation took place at 400 V/cm, according to previous results in the literature (Dellarosa, Ragni, et al., 2016).

This was due to the irreversible alteration of the tonoplast and plasma membranes which led to the collapse of the cell vacuole and cytoplasm. The loss of compartmentalization eased the diffusion of the intracellular water and solutes toward extracellular spaces and the external solution. That redistribution of water together with a lower water-to-solutes ratio resulted in a different interaction between water/solutes/biopolymers inside the tissue, i.e. a lower T_2 (Van Duynhoven, Voda, Witek, & Van As, 2010). Indeed, this finding was in agreement with previous investigations in apple tissue which proved that T_2 was systematically lowered by the application of other food process technologies which similarly affect the inner microstructure (Gonzalez et al., 2001; Hills & Remigereau, 1997; Mauro et al., 2016).

In the present experiment, a direct comparison with vacuum impregnation technology was also performed. VI guaranteed the complete replacement of air with the external solution without affecting the membrane integrity (Panarese et al., 2016). As expected and conversely to results obtained applying PEF treatments, a scattered generalized increase of T_2 and concurrently proton density (data not shown) were achieved. Thus, by comparing PEF with VI samples, the application of high voltage electric fields did not foster the diffusion of the external solution through the tissue pores but the breakage of cell membranes only provoked the redistribution of the inner solutions.

It worth observing that the reduction of T_2 was clearly heterogeneously distributed through the apple cylinders showing values around 80 ms in determinate areas and, at the same time, regions where T_2 was not influenced by PEF application. Moreover, the extension of the electroporated area markedly changed taking into account the three replicates. This was in perfect agreement with abovementioned CVS achievements and results previously obtained by Kranjk et al. (2016) that studied T_2 variations in potato tubers at similar electric field strength. Both T_2-maps analysis led to the conclusion that the heterogeneity of the raw material which undergoes to electroporation plays a non-negligible role in the effectiveness of the PEF treatment.

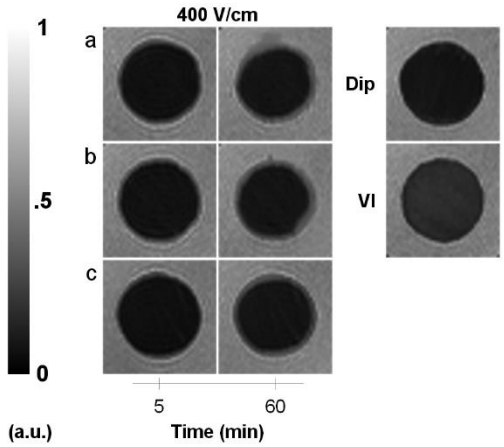

Fig. 5. T_1-weigthed images of three apple cylinders treated with pulsed electric fields (PEF) at 400 V/cm (60 pulses, 10 µs pulse width, 100 Hz) and sampled 5, 30 and 60 min after treatments; examples of dipping (Dip) and vacuum impregnation (VI) samples after 60 min from the treatments. Intensities were scaled by fixing the external standard intensity at 0.5 (a.u.).

T_2-maps images, displayed in Fig. 4, also directly reveals the percolation commonly induces by pulsed electric fields (Lebovka, Bazhal, & Vorobiev, 2001). In fact, this phenomenon was directly visible in sample 'a' of Fig. 4 after 30, 45 and 60 min. The average T_2 of the surrounding contrast solution was 11 ± 1 ms whereas higher values were remarkable in several pixels which surrounded the upper part of the MR images. Further evidences of water migration toward the external solution were provided by T_1-weigthed images, shown in Fig. 5. Interestingly, PEF pre-treated apple samples showed a surrounding ring with intermediate values between the apple tissue and the contrast solution after 30 and 60 min. Those values were weighted between the longitudinal relaxation time values of the contrast solution the apple tissue and, which were estimated in a parallel experiment around 30 and 2000 ms, respectively. However, that effect, which was not described either upon dipping or vacuum impregnation, was ascribed both to the percolation of the intracellular content and to the simultaneous shrinkage of the tissue. It is important to highlight that, once more, the phenomenon was not equally distributed around the cylinders and its extent varied among the different repetitions, confirming the inhomogeneous effects of PEF through the material.

Multiparametric MRI enabled highlighting the loss of membrane integrity and the migration of the intracellular content within few minutes from the application of pulsed electric fields. This promotes the employment of MRI analysis to estimate the extent of electroporation immediately after pulsation and predict possible macroscopic changes which may require long time to be apparent (Hjouj & Rubinsky, 2010; Kranjc et al., 2016). As a general rule, MRI techniques are not capable to distinguish a definite origin of field heterogeneity but it can provide an accurate snapshot of microstructural alterations of plant tissues. Nevertheless, tailored experimental plans can be designed to selectively monitor, as in the present work, a specific source of variability among many possible alternative ones.

4. Conclusions

The spatial distribution of electroporation induced by pulsed electric fields technology in apple tissue was accurately assessed by combining computer vision system and magnetic resonance imaging techniques. The loss of compartmentalization, as a consequence of the membranes breakage, resulted in a marked reduction of the transverse relaxation time, measured by MRI analysis and the simultaneous trigger of the enzymatic browning, which was kinetically evaluated by CVS analysis. However, both tools described a inhomogeneous distribution of electroporation through the tissues as a function of the probable different local conductivity within the apple parenchyma. Moreover, kinetic MRI analysis highlighted the migration of the intracellular content toward the external solution which led to the shrinkage of the apple samples. Those findings can affect the effectiveness of possible industrial applications of pulsed electric fields. Therefore, the present work provided useful powerful methods able to monitor within minutes, and backwardly optimize, novel mass transfer processes assisted by pulsed electric fields.

REFERENCES

Adams, P. E. (1995). Determining iron content in foods by spectrophotometry. *J. Chem. Educ, 72*(7), 649.

Barba, F. J., Parniakov, O., Pereira, S. A., Wiktor, A., Grimi, N., Boussetta, N., Witrowa-Rajchert, D. (2015). Current applications and new opportunities for the use of pulsed electric fields in food science and industry. *Food Research International, 77*, 773-798.

Betoret, E., Sentandreu, E., Betoret, N., Codoñer-Franch, P., Valls-Bellés, V., & Fito, P. (2012). Technological development and functional properties of an apple snack rich in flavonoid from mandarin juice. *Innovative Food Science & Emerging Technologies, 16*, 298-304.

Buckow, R., Schroeder, S., Berres, P., Baumann, P., & Knoerzer, K. (2010). Simulation and evaluation of pilot-scale pulsed electric field (PEF) processing. *Journal of Food Engineering, 101*(1), 67-77.

Dellarosa, N., Ragni, L., Laghi, L., Tylewicz, U., Rocculi, P., & Dalla Rosa, M. (2016). Time domain nuclear magnetic resonance to monitor mass transfer mechanisms in apple tissue promoted by osmotic dehydration combined with pulsed electric fields.

Innovative Food Science & Emerging Technologies, 37(C), 345-351.

Dellarosa, N., Tappi, S., Ragni, L., Laghi, L., Rocculi, P., & Dalla Rosa, M. (2016). Metabolic response of fresh-cut apples induced by pulsed electric fields. *Innovative Food Science & Emerging Technologies, 38*, 356-364.

Donker, H., Van As, H., Snijder, H., & Edzes, H. (1997). Quantitative 1H-NMR imaging of water in white button mushrooms (Agaricus bisporus). *Magnetic resonance imaging, 15*(1), 113-121.

Donsì, F., Ferrari, G., & Pataro, G. (2010). Applications of pulsed electric field treatments for the enhancement of mass transfer from vegetable tissue. *Food Engineering Reviews, 2*(2), 109-130.

Fincan, M., & Dejmek, P. (2002). In situ visualization of the effect of a pulsed electric field on plant tissue. *Journal of Food Engineering, 55*(3), 223-230.

Gonzalez, J. J., Valle, R. C., Bobroff, S., Biasi, W. V., Mitcham, E. J., & McCarthy, M. J. (2001). Detection and monitoring of internal browning development in 'Fuji'apples using MRI. *Postharvest biology and technology, 22*(2), 179-188.

Hills, B. P., & Remigereau, B. (1997). NMR studies of changes in subcellular water compartmentation in parenchyma apple tissue during drying and freezing. *International journal of food science & technology, 32*(1), 51-61.

Hjouj, M., & Rubinsky, B. (2010). Magnetic resonance imaging characteristics of nonthermal irreversible electroporation in vegetable tissue. *The Journal of membrane biology, 236*(1), 137-146.

Kranjc, M., Bajd, F., Serša, I., de Boevere, M., & Miklavčič, D. (2016). Electric field distribution in relation to cell membrane electroporation in potato tuber tissue studied by magnetic resonance techniques. *Innovative Food Science & Emerging Technologies, 37*, 384-390.

Lebovka, N., Bazhal, M., & Vorobiev, E. (2001). Pulsed electric field breakage of cellular tissues: visualisation of percolative properties. *Innovative Food Science & Emerging Technologies, 2*(2), 113-125.

Lebovka, N., Bazhal, M., & Vorobiev, E. (2002). Estimation of characteristic damage time of food materials in pulsed-electric fields. *Journal of Food Engineering, 54*(4), 337-346.

Lebovka, N. I., Praporscic, I., & Vorobiev, E. (2004). Effect of moderate thermal and pulsed electric field treatments on textural properties of carrots, potatoes and apples. *Innovative Food Science & Emerging Technologies, 5*(1), 9-16.

Luengo, E., Álvarez, I., & Raso, J. (2013). Improving the pressing extraction of polyphenols of orange peel by pulsed electric fields. *Innovative Food Science & Emerging Technologies, 17*, 79-84.

Luengo, E., Condón-Abanto, S., Condón, S., Álvarez, I., & Raso, J. (2014). Improving the extraction of carotenoids from tomato waste by application of ultrasound under pressure. *Separation and Purification Technology, 136*, 130-136.

Mauro, M. A., Dellarosa, N., Tylewicz, U., Tappi, S., Laghi, L., Rocculi, P., & Dalla Rosa, M. (2016). Calcium and ascorbic acid affect cellular structure and water mobility in apple tissue during osmotic dehydration in sucrose solutions. *Food chemistry, 195*, 19-28.

Panarese, V., Herremans, E., Cantre, D., Demir, E., Vicente, A., Galindo, F. G., Verboven, P. (2016). X-ray microtomography provides new insights into vacuum impregnation of spinach leaves. *Journal of Food Engineering, 188*, 50-57.

Parniakov, O., Barba, F. J., Grimi, N., Marchal, L., Jubeau, S., Lebovka, N., & Vorobiev, E. (2015). Pulsed electric field and pH assisted selective extraction of intracellular components from microalgae Nannochloropsis. *Algal Research, 8*, 128-134.

Praporscic, I., Lebovka, N., Vorobiev, E., & Mietton-Peuchot, M. (2007). Pulsed electric field enhanced expression and juice quality of white grapes. *Separation and Purification Technology, 52*(3), 520-526.

Raso, J., Frey, W., Ferrari, G., Pataro, G., Knorr, D., Teissie, J., & Miklavčič, D. (2016). Recommendations guidelines on the key information to be reported in studies of application of PEF technology in food and biotechnological processes. *Innovative Food Science & Emerging Technologies, 37*, 312-321.

Rocha, A., & Morais, A. (2003). Shelf life of minimally processed apple (cv. Jonagored) determined by colour changes. *Food Control, 14*(1), 13-20.

Traffano-Schiffo, M., Tylewicz, U., Castro-Giraldez, M., Fito, P., Ragni, L., & Dalla Rosa, M. (2016). Effect of pulsed electric fields pre-treatment on mass transport during the osmotic dehydration of organic kiwifruit. *Innovative Food Science & Emerging Technologies, 38*, 243-251.

Van Duynhoven, J., Voda, A., Witek, M., & Van As, H. (2010). Time-domain NMR applied to food products. *Annual reports on NMR spectroscopy, 69*, 145-197.

Wiktor, A., Iwaniuk, M., Śledź, M., Nowacka, M., Chudoba, T., & Witrowa-Rajchert, D. (2013). Drying kinetics of apple tissue treated by pulsed electric field. *Drying Technology, 31*(1), 112-119.

Wiktor, A., Sledz, M., Nowacka, M., Rybak, K., & Witrowa-Rajchert, D. (2016). The influence of immersion and contact ultrasound treatment on selected properties of the apple tissue. *Applied Acoustics, 103*, 136-142.

Zhao, Y., & Xie, J. (2004). Practical applications of vacuum impregnation in fruit and vegetable processing. *Trends in Food Science & Technology, 15*(9), 434-451.